COMPUTATIONAL AND IN VITRO MODELS TO ANALYZE THE INTERACTIONS OF VENTRICULAR ASSIST DEVICES AND THROMBOEMBOLI

A Dissertation

by

STACI LEANN JESSEN

Submitted to the Office of Graduate and Professional Studies of
Texas A&M University
in partial fulfillment of the requirements for the degree of

DOCTOR OF PHILOSOPHY

Chair of Committee,	Fred J. Clubb, Jr.
Co-Chair of Committee,	John C. Criscione
Committee Members,	Michael R. Moreno
	Brad R. Weeks
Head of Department,	Anthony Guiseppi-Elie

May 2016

Major Subject: Biomedical Engineering

ABSTRACT

Heart failure is consistently one of the top causes of death each year worldwide. Ventricular assist devices (VADs) have become common alternatives for patients with severe, end-stage heart failure; VADs take a significant load off of the heart and aid in perfusion of downstream organs by pumping blood from either or both ventricles to their corresponding great vessel. External VAD controllers track specific pump parameters such as estimated flow rates and device power consumption.

Suspected thrombosis is a common clinical adverse event in VAD therapy. In this condition, a VAD controller will indicate periods of low flow or high power; clinicians suspect that this indicates that a thrombus is increasing friction between the moving components and/or obstructing the inflow or outflow. Suspected thrombosis typically results in device exchange surgery. A pathology evaluation of the explanted VAD can reveal if materials inside the pump at explant originated within or upstream from the device.

VADs explanted after years of support often had an actively organizing thrombus along the inflow cannula or protruding from the insertion site in the ventricle. We hypothesize that these thrombi form over time due to regions of stagnation and recirculation of the blood in the ventricle. Moreover, as the VAD continues to take a load off of the heart, we suspect that the remodeling of the heart will change the flow dynamics within the ventricle and cause thrombi to dislodge and travel into the pump. As thrombi of different age and size pass into the device, we hypothesize that each VAD model will demonstrate a particular change in flow rate in response to the thrombus.

Through the research in this dissertation, we have investigated these phenomena by creating a computational model of the ventricular insertion site before and after cardiac

remodeling occurs, and an *in vitro* model that displays VAD response to thromboembolic particles. These computational and *in vitro* models show that over time, the presence of the VAD inflow cannula within the heart will change the potential for thrombi to form around the device, dislodge, and travel into the VAD, and result in changes of pump flow rate.

This research is beneficial to VAD manufacturers and clinicians in the development of devices that will limit opportunity for thromboembolic complications, and provide direction for treatment of patients currently undergoing VAD therapy.

DEDICATION

I dedicate my research to my family--especially those who have come and gone before me, whose lives were spent constantly pouring into my parents, making them who they are, who in turn made me the person I am today. All I am is because of them. I dedicate my research to you: Imogene and Curtis Jessen, Mary and Huey Sandell, Sue Sandell Smart, and Jerry Don Sandell.

ACKNOWLEDGEMENTS

A person's motivation speaks leaps and bounds of a person's character.

I would like to thank all of my colleagues in the Cardiovascular Pathology Laboratory, both past and present, for their continuous support, help and encouragement with my research. It is a privilege to work with others that are willing to share in your struggles as well as triumphs. I count it a blessing to have colleagues whose innate desire is to help others by improving their health, well-being, and quality of life.

I would also like to thank the staff and faculty of the Biomedical Engineering Department for helping me in my educational journey. Thanks to my advisors, Dr. Fidel Fernandez and Maria Lyons for helping me navigate the logistical hoops. I would like to acknowledge Carl Johnson in the machine shop for all of his help and advice on machining the parts necessary for my research. I could not have made any progress without the help of my advisory committee, Dr. Weeks, Dr. Criscione, Dr. Moreno, and my chair, Dr. Clubb.

I need to thank Mr. John Horn for his support, encouragement, and willingness to help me no matter how much work he had on his own plate. Additionally, I would like to acknowledge and thank Ms. Cara Martin for her consistent support and enthusiasm for this research. I'll always be grateful for their help.

Finally, I would like to acknowledge my family for loving me unconditionally and supporting me throughout this long journey. Their constant encouragement from the beginning has kept me going.

NOMENCLATURE

VAD	Ventricular Assist Device
LVAD	Left Ventricular Assist Device
RVAD	Right Ventricular Assist Device
Bi-VAD	Bi-Ventricular Assist Device
HF	Heart Failure
DCM	Dilated Cardiomyopathy
BTT	Bridge-to-Transplant
BTR	Bridge-to-Recovery
DT	Destination Therapy
BTD	Bridge-to-Decision
HCM	Hypertrophic Cardiomyopathy
GLP	Good Laboratory Practices
GCP	Good Clinical Practices
PMA	Premarket Approval
INTERMACS	Interagency Registry for Mechanically Assisted Circulatory Support
H&E	Hematoxylin and Eosin
PTAH	Phosphotungstic Acid Hematoxylin
CT	Computed Tomography
SEM	Scanning Electron Microscopy
TEM	Transmission Electron Microscopy
STEM	Scanning Transmission Electron Microscopy

EDX	Energy Dispersive X-Ray Spectroscopy
2D	Two-Dimensional
3D	Three-Dimensional
TF	Tissue Factor
LPM	Liters Per Minute
RPM	Rotations Per Minute
FDA	United States Food and Drug Administration
NYHA	New York Heart Association

TABLE OF CONTENTS

Page

LIST OF FIGURES

Page

LIST OF TABLES

Page

1. INTRODUCTION

Despite major technological and medical advancements made over the past century, heart failure continues to be a significant issue facing our nation. Heart failure (HF) accounts for over one million hospitalizations each year in the United States (US), with over three million secondary hospitalizations annually [1]. In 2007, HF was the underlying cause of 56,565 deaths in the US alone [2]. Although the number of patients who survive after being diagnosed with HF is increasing, the death rate remains high, keeping HF as one of the leading causes of death [3]. The outcome for patients diagnosed with HF remains grim: approximately 50% of patients diagnosed will die within five years [3].

In the US, the New York Heart Association (NYHA) classification system is clinically used to categorize HF based on the patient's symptoms and objective assessment [4]. The categories are labeled Class I-IV, with IV being the most severe. When the heart becomes enlarged and weakened, it cannot pump blood as efficiently as the body needs. As this decline in effective heart function continues, the downstream organs (i.e., kidney, brain, liver, lungs, etc.) will become ischemic. This condition can lead to a pathologic heart disease (cardiomyopathy) and eventually multi-organ system failure (NYHA Class IV). When patients are diagnosed with a cardiomyopathy, the optimal treatment is a heart transplant [5]. Depending on their HF classification and other symptoms, patients who are eligible to receive a heart transplant will be put on the heart transplant waiting list. In a large number of cases, patients die as a result of HF before a donor heart is found. As the population continues to increase, there is a growing disparity between the number of donor hearts and potential transplant recipients [6]; in the US, consistently only ~2,500 hearts are available for transplant each year [5, 7]. Furthermore, some patients' conditions are so severe they are ineligible to receive a transplant.

To combat these challenges in treating HF, specifically the lack of donor hearts available, researchers and clinicians have turned to mechanical circulatory assist devices to take the load off of the heart and provide adequate perfusion of body tissues. Ventricular assist devices (VADs) are surgically implanted pumps attached to either of the ventricles and corresponding great vessels to provide circulatory support. VADs are associated with four clinical applications: bridge-to-transplant (BTT), bridge-to-recovery (BTR), destination therapy (DT), or bridge-to-decision (BTD). VADs have proven to be successful in prolonging the lives of patients with refractory heart failure until a suitable donor heart can be found (BTT) [8-14]; there has been an increase in usage of VADs over the past few decades [15], resulting in fewer patients dying while on the heart transplant waiting list [7]. Additionally, VADs can provide long-term support for patients that are ineligible for a heart transplant (DT) [16]. VADs can also treat patients with potentially reversible HF (BTR) [17-20], or in the case of moribund patients, can be used to stabilize the patient giving doctors time to further evaluate the patient's condition (BTD) [21].

Since the 1960s, multiple generations of VADs have been developed and refined. VADs can be categorized based on patient-pump interface and flow type [22]. Accessory components that accompany each device include controllers, drivelines, grafts, and backup batteries. VAD controllers display pump parameters such as rotations per minute (RPM), flow rates, power consumption, etc. [23], and often store log files that clinicians can read to determine if the pump is functioning properly [24].

With each generation of assist devices and corresponding accessories, VAD developers and researchers are presented with new challenges to make these devices safer and more effective than the last. While each generation of VADs improves and meets higher standards

provided by advancements in technology, thrombosis has consistently been a concern hindering the effectiveness of VAD therapy [25-38].

Implanting a medical device inside the body inherently presents opportunities for thrombus formation. Patients most likely to be considered for VAD implantation have weak, dilated heart chambers, and are likely at risk for thrombus formation along the ventricle walls (mural thrombus). In addition, the atrial appendage is a common site for thrombus formation in diseased hearts. A thrombus may also form around the ventricular insertion site due to contact with a non-biological surface (i.e., the device), or within the ventricle/device as a result of stagnant regions or altered blood flow. Thrombi are dangerous because they may pass in to the device and cause mechanical failure, or travel through the device and cause ischemic damage downstream (e.g., stroke, renal infarct, etc.). Over time, as the VAD takes a significant workload off of the heart, the myocardium will likely remodel [39], which may change the flow dynamics within the ventricle and potentially dislodge organizing thrombi and send them into the device.

The Cardiovascular Pathology (CVP) Laboratory at Texas A&M University has performed pathology evaluations on 1,000+ VADs from various companies since 2008. Frequently, a pathology evaluation is requested by the manufacturer because the pump log files indicated periods of high power consumption or periods of low flow, due to presumed ingestion of biological material [24] (i.e., thrombus), or blockage of the outflow [40] or inflow cannulae. The increase of pump power consumption or low flow can cause a decrease in pump efficiency [24]; consequently, the patient may undergo device exchange surgery. VADs are also removed and sent for pathology evaluation (at the request of the device manufacturer) when patients receive a transplant, expire, or recover.

During the pathology evaluation of VADs, all external and internal surfaces are closely examined for any evidence of thrombi [22]. A histological analysis of material from explanted

VADs can reveal the origin of deposits found within VADs and differentiate ante- and post-mortem events. The morphology of the material can elucidate if a thrombus originated upstream from the device or developed *de novo* (i.e., within the device). In some cases, a gross and histological analysis reveal that upstream material may lodge inside a VAD and become a nidus for further thrombus formation along internal VAD components.

Pathology evaluations alone cannot reveal the full story, and clinical correlation is always recommended. Clinical information about the patient as well as pump data (power usage, flow rates, etc.) are also important and correlation with pathology findings will deliver the best account for the device/patient interaction, and provide the most useful information to improve VAD therapy.

VAD manufacturers often use computational modeling during the design phase to analyze flow patterns inside VADs. Computational modeling involving the ventricle (inflow insertion site) and aorta (outflow site) can also help with device design challenges, revealing more about device/patient interaction before pre-clinical trials [41-45]. Furthermore, VADs are typically tested prior to pre-clinical trials with *in vitro* circulatory loops [46, 47]; however, these are designed to specifically test the longevity of the device (i.e., how long the device lasts without mechanical failure) and testing VADs under hemodynamic conditions to reveal whether the device damages blood cells, produces sufficient flow rates, etc. [47-56].

Device testing can be expanded to include a computational model for determining how ventricular remodeling due to prolonged VAD support will change potential for thrombus formation and embolization in the device. In addition, *in vitro* models could be expanded to determine precise VAD response to thromboembolism. The research in this dissertation aims to present possible VAD testing protocols that can answer these questions and elucidate useful

information about the patient/VAD interaction without costly or dangerous pre-clinical and clinical trials.

This research will establish a basis for better understanding thrombus formation and embolization within VADs as the heart remodels due to long-term mechanical support. Additionally, data resulting from this research will be used to better understand the interaction between thrombi and VADs, specifically how to precisely detect and treat thromboembolism. This research will also make way for device design improvements for better tolerance of embolic particles. With better understanding of how thrombi form in the ventricle and how emboli interact with VAD components, future VAD designs will limit opportunity for thromboembolic complications, and hospitals can provide better clinical management of VAD patients by confidently assessing the risk of thrombus formation throughout duration of support. This will ultimately result in fewer high-risk, thrombus-related VAD exchange surgeries (thus reducing the cost associated with VADs), and reduce the overall risk of thrombosis in VADs.

The long-term goal of this research is to establish a need for periodic monitoring of pump orientation in the ventricle throughout duration of support for evidence of thrombus formation. The geometrical changes of the ventricle with an inflow cannula can potentially cause catastrophic thromboembolic damage after several years of successful VAD treatment, and periodic imaging of the device could prevent these occurrences. Secondarily, this research aims to establish VAD testing of thromboembolism as a recommendation for VAD manufacturers prior to beginning pre-clinical trials. This could help companies learn specific correlations for each individual VAD model, and add to the therapeutic value of receiving a VAD. Specifically, this bench-top test could reveal how clots of different strengths and sizes affect VADs and determine if there are correlations between the size/shear compliance of the thrombus and the magnitude of the power consumption/pressure changes indicated on the pump's controller log

when a thrombus is present. Physicians would have a better indication if thrombolytic agents alone could dissolve the thrombus or if an exchange surgery is necessary.

Overall, this research will add positively to the value of receiving a VAD as a destination therapy, bridge-to-transplant, bridge-to-decision, or bridge-to-recovery treatment option.

2. HEART FAILURE*

Heart Failure (HF) has been a leading cause of death worldwide for decades [2, 57]. HF is generically defined as a condition in which the heart is unable to pump blood at an adequate rate or an adequate volume. The mechanism of HF is explained using fundamental building block of the heart: the cardiac myocyte.

Cardiac myocytes stretch when blood enters the heart chambers and contract with a force great enough to expel blood to the body via the aorta. This is the Frank-Starling Law of the Heart: when there is an increase in venous return (blood returning to the heart), the cardiac myocytes respond with a greater force, thereby increasing stroke volume. When the body needs more oxygen and requires a greater demand from the heart, the myocytes respond by stretching more, generating more force, thus increasing cardiac output. This myocyte hyperfunction can lead to developmental hypertrophy (Figure 1). A sustained increase in heart function can lead to cardiomegaly: a normal, reversible, physiologic enlargement of the heart, involving myocyte adaptation. If the stress on the heart is maintained and pushed beyond what the myocytes can withstand, pathologic hypertrophy may develop, which involves the beginning of myocyte degeneration. At this point, if the stress on the heart is relieved, the heart can remodel to a state suitable for providing adequate perfusion of the body tissues. However, if the stress persists, and the myocytes continue to degenerate, the heart will progress to an irreversible state of HF. While heart transplantation is the optimal treatment for HF, other therapeutic interventions

---

*Part of this section is reprinted with permission from "Brief review of ventricular assist devices and a recommended protocol for pathology evaluations" by Carpenter BA, et. al., 2013. *Cardiovasc Pathol* 22: 408-415, 2013 by Elsevier.

(pharmaceutical treatments, medical devices, etc.) may help the heart remodel to a state suitable for adequate perfusion of the tissues.

The Law of Laplace states that the stress on the wall of the ventricle is directly proportional to both the internal pressure within the ventricle and the radius of the chamber, and indirectly proportional to the ventricular wall thickness. As the pressure within and the radius of the ventricle grows, the stress on the wall increases. Under normal conditions, the heart will respond with increased thickness (i.e., hypertrophy) to withstand this increase in wall stress.

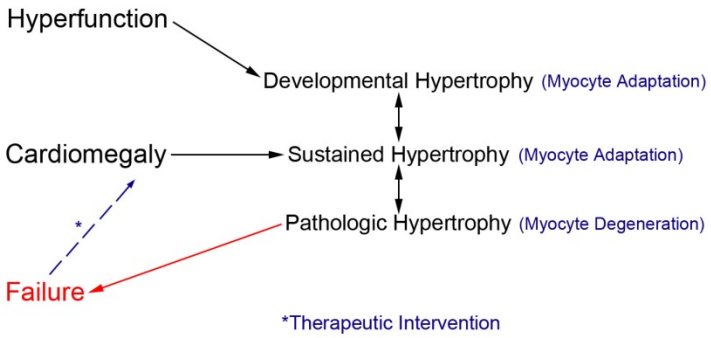

Figure 1. Cardiac myocyte response to stress. Hyperfunction of the heart muscle can lead to developmental hypertrophy. Sustained hypertrophy can lead to cardiomegaly, a normal reversible morphological enlargement of the heart. Application of stress greater than myocytes can adapt to leads to pathologic hypertrophy, which if sustained, will lead to irreversible heart failure.

The heart responds with different morphological changes according to the initial insult to homeostasis, which leads to two main classifications of morphological changes: eccentric (dilated) and concentric (hypertrophic). Eccentric or dilated cardiomyopathies (DCM) are generally associated with cardiac myocyte hypertrophy/remodeling in length, which leads to an increase in ventricle diameter with a thinner wall (i.e., increase in lumen volume). Concentric or hypertrophic cardiomyopathies (HCM) are associated with cardiac myocyte

hypertrophy/remodeling in width, which leads to an increased wall thickness and a decreased ventricle diameter (i.e., reduction in lumen volume).

While the primary cause of HF is idiopathic (unknown), there are several conditions that can lead to HF as a secondary problem. When there is residual blood in the ventricle after peak systole (indicating decreased cardiac output), the ventricle stretches over time due to the increased volume and remodels to a dilated state. This can arise secondarily from insufficient valve performance (regurgitation), or an increase in preload (venous return) without maintaining equal cardiac output. Additionally, if there is a stenotic vessel, valve, or increased systemic resistance, the ventricles must work harder to pump against an increased resistance. Over time the ventricular myocytes' adaptive response will be hypertrophy (increase in myocyte thickness), which can lead to a concentric or hypertrophic cardiomyopathy.

HF can also be divided in to functional classifications. Systolic disorders (forward HF) arise when the heart is not able to adequately eject enough blood, while diastolic disorders (backward HF) mean the heart cannot properly relax and is unable to fill completely. Disorders can also be classified based on which side of the heart is failing. Right-sided backward failure is a diastolic disorder in which the blood pools in the extremities because it cannot fill the right side of the heart properly. The venous return (blood returning to the right side of the heart) is increased and exceeds the right ventricle's performance capability; this increases hydrostatic pressure on the right side of the body (i.e., venous vasculature), and thus causes right-sided backward failure. Right-sided forward failure means that blood is not adequately going to the lungs, which is an immediately serious condition and the patient would become systemically

ischemic rather quickly and perish before this condition could develop beyond an acute state. Left-sided backward failure involves fluid accumulation in the lungs, which could potentially be fatal. The body has built-in mechanisms to keep the fluid from entering the lungs: the pulmonary vessels vasoconstrict when there is an increase in pulmonary pressure, which leads to an increase of fluid in the right ventricle. This is only a temporary solution, however, for pulmonary hypertension brings a new set of challenges to the body. Finally, left-sided forward failure can lead to decreased oxygenated blood reaching the entire body, which could acutely result in syncope (fainting), or chronically lead to increased activation of the renin-angiotensin system (RAS) and eventually hypertension.

HF is classified clinically according to the symptoms and objective assessments outlined in the New York Heart Association (NYHA) classification system in Table 1 [58]. Patients with Class I HF are asymptomatic, whereas Class IV HF patients are unable to perform everyday tasks without becoming out of breath, and for the most part are bedridden [4].

Table 1. New York Heart Association classification of heart failure [58]

Class	Patient Symptoms	Objective Assessment	
I	No limitation of physical activity. Ordinary physical activity does not cause undue fatigue, palpitation, shortness of breath.	A	No objective evidence of cardiovascular disease. No symptoms and no limitation in ordinary physical activity.
II	Slight limitation of physical activity. Comfortable at rest. Ordinary physical activity results in fatigue, palpitation, shortness of breath.	B	Objective evidence of minimal cardiovascular disease. Mild symptoms and slight limitation during ordinary activity. Comfortable at rest.
III	Marked limitation of physical activity. Comfortable at rest. Less than ordinary activity causes fatigue, palpitation, or shortness of breath.	C	Objective evidence of moderately severe cardiovascular disease. Marked limitation in activity due to symptoms, even during less-than-ordinary activity. Comfortable only at rest.
IV	Unable to carry on any physical activity without discomfort. Symptoms of heart failure at rest. If any physical activity is undertaken, discomfort increases.	D	Objective evidence of severe cardiovascular disease. Severe limitations. Experiences symptoms even while at rest.

Cardiac transplantation is the preferred treatment for end stage HF (Class IV). In the US, there are consistently between 2,000 and 2,500 hearts available for transplantation per year (Figure 2). Consistently, more hearts are needed, leading to people dying while on the waiting list. As a result, researchers started looking for alternative treatment methods to accommodate the growing disparity between HF patients and available donor hearts.

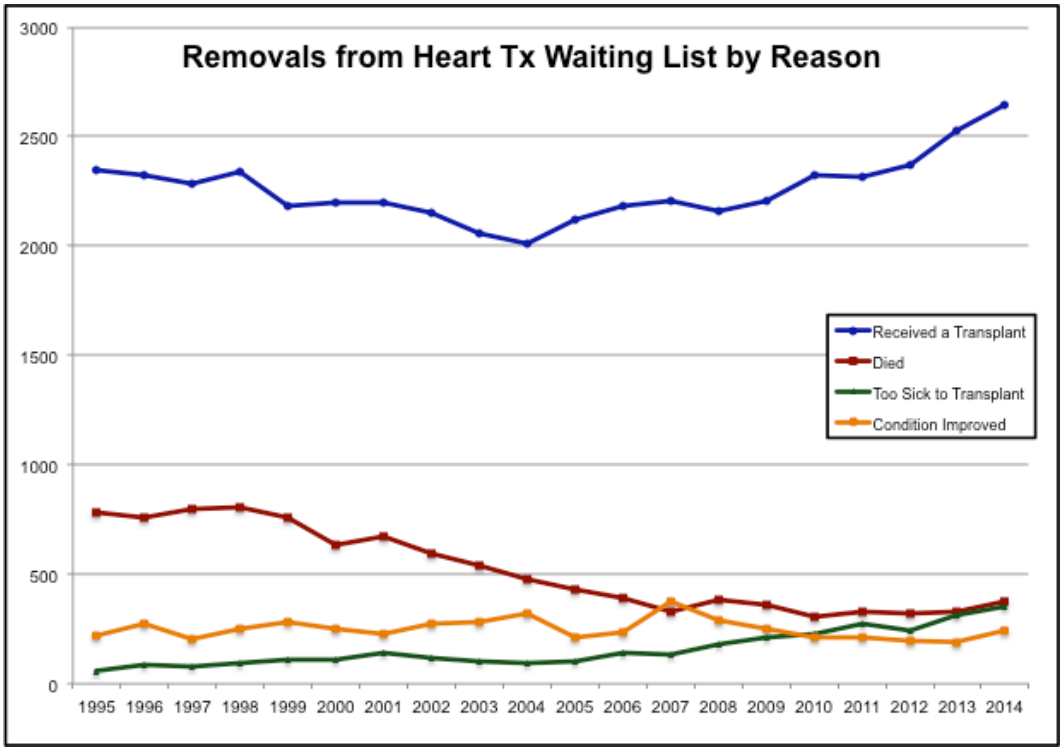

Figure 2. Data from the Organ Procurement and Transplant Network [7] concerning removal from the heart transplant waiting list by reason. The number of patients removed from the waitlist due to transplantation has stayed relatively consistent. However, since the use of mechanical circulatory support began, the number of patients removed due to expiration has decreased steadily in recent years.

The initiative to find an alternative to heart transplantation began in 1964 at the National Heart, Lung and Blood Institute [29]. A goal of the Institute was to find both long- and short-term circulatory support and ultimately an artificial heart for patients requiring heart transplants. Over the next decade, this goal evolved into a search for smaller implantable devices that would increase the quality of life for the users [29]. The Jarvik-7-100 was the first total artificial heart (TAH) developed and implanted in the 1980s by DeVries *et al.* [59]. Initially, this device was generally considered a success. However, the occurrence of thrombosis and infection in patients put a hold on the TAH device by 1991 [60]. Throughout this time, the medical device companies increasingly shifted their focus to developing devices to assist the heart rather than completely replace it. This shift in focus introduced ventricular assist devices (VADs) to augment heart

function. One of the first devices created was Thermo Cardiosystem's HeartMate, a pneumatically driven implantable left ventricular assist device (LVAD), which was first implanted in human patients starting in 1990 [61]. Over the past 2.5 decades, this industry has expanded vastly to include dozens of companies and device designs. Currently, companies worldwide are continuing to develop an array of VADs for various clinical indications that have proven to be successful in treating patients with HF, resulting in a steady decline of patients dying while on the heart transplant waiting list (Figure 2).

Several generations of VADs have been developed since the quest for alternate HF treatments began in the 1960s. While HF continues to be a widespread problem, VAD therapy has certainly brought relief to many and is definitely a growing industry that has peaked the interest of scientists, clinicians, and engineers worldwide.

3. VENTRICULAR ASSIST DEVICES*

Ventricular assist devices (VADs) are medical devices implanted in either the right or left ventricle to improve perfusion of downstream organs and tissues in patients with end-stage heart failure. VADs work in parallel with the ventricle to pump blood to the aorta (left VAD, or LVAD) or the pulmonary artery (right VAD, or RVAD) (Figure 3).

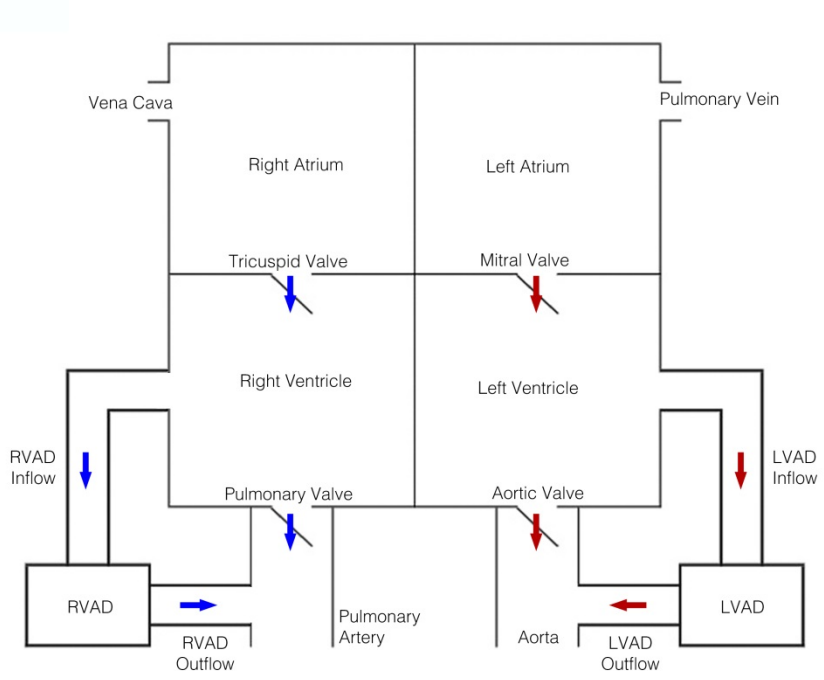

Figure 3. Diagram of heart with a bi-VAD (i.e., an LVAD and an RVAD). The LVAD receives oxygenated blood (red arrows) from the left ventricle and pumps it into the aorta. The RVAD receives unoxygenated blood (blue arrows) and delivers it to the pulmonary artery.

*Part of this section (including Figures 5-7) is reprinted with permission from "Brief review of ventricular assist devices and a recommended protocol for pathology evaluations" by Carpenter BA, et. al., 2013. *Cardiovasc Pathol* 22: 408-415, 2013 by Elsevier.

Numerous VAD designs have been developed, and currently FDA has approved three devices for use in the US: HeartMate II (Thoratec Corp.) [62], EXCOR (Berlin Heart) [63], and HVAS (HeartWare, Inc.) [64]. There are several types of VADs that are classified based on type of flow (pulsatile or continuous) and interface with patient (intracorporeal or extracorporeal).

3.1. Types of VADs

The two main varieties of VADs are pulsatile pumps and the more recent continuous flow pumps (Figure 4). Over the past decades, continuous flow pumps have gained precedence worldwide because of their smaller size and better performance. Furthermore, single center studies have shown little difference in survival rates of patients with the two types of pumps [65, 66].

3.1.1. Pulsatile flow pumps

The first generation of implantable VADs included pulsatile devices, which attempts to replicate the physiologic cardiac output. Examples of pulsatile devices include the Thermo Cardiosystems (TCI) HeartMate [61], Berlin Heart® Excor®, the Novacor® LVAS, the Abiomed® BVS 5000®, the Arrow LionHeart™, and the Syncardia Systems Inc. CardioWest™ [67]. These pulsatile devices mimic the pumping activity of the heart using a pressure membrane chamber

driven by a pneumatic motorized pump. Artificial valves prevent blood from flowing backward, which creates pulsation, replicating normal heart rhythm (Figure 4A). Pulsatile pumps normally function between 50 to 120 bpm [68].

Unfortunately, pulsatile pumps and associated equipment are typically bulky. Patients have to wear the pumps and external equipment with caution, thus their mobility is limited. Additionally, pulsatile pumps are subject to frequent exchanges due to a variety of complications such as suspected thrombi within the device, periods of high power, and adverse host response to the device. Fortunately, with pulsatile extracorporeal pumps, the VAD can be replaced quickly and efficiently; no additional major surgical procedures are required. These less-invasive exchanges are faster and induce less trauma to the body, thus minimizing post-exchange complications for patients. Furthermore, post-exchange recovery in pulsatile models has been shown in one study to preserve the physiological phenomenon of ventricular unloading unlike continuous flow pumps [67].

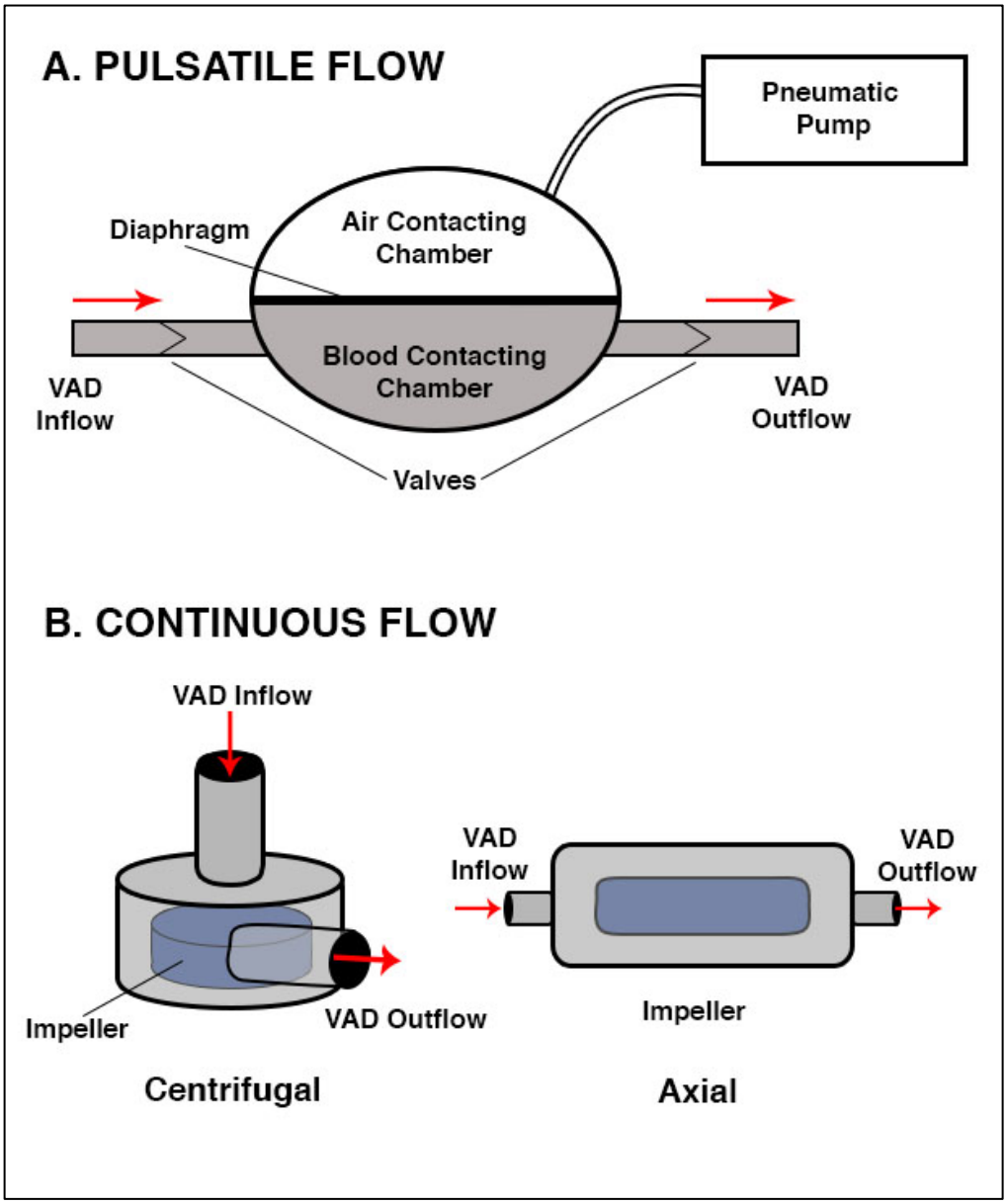

Figure 4. Diagrams of VADs. Based on flow, there are two main types of VADs: Pulsatile (A), and Continuous Flow (B). Continuous flow devices are further divided based on direction of flow: centrifugal (left) and axial (right). Direction of blood flow in each device type is indicated by red arrows.

3.1.2. Continuous flow pumps

The newer-generation VADs are often a continuous flow system designed around either axial or centrifugal flow (Figure 4B). Examples of continuous flow pumps include the Thoratec HeartMate II®, the MicroMed Cardiovascular Inc. HeartAssist 5®, the HeartWare Inc. HVAD™, and the Terumo Heart Inc. DuraHeart [69]. Continuous flow pumps have many advantages over pulsatile pumps, including smaller size, greater durability, higher energy efficiency, and lower thrombogenicity.

Continuous flow VADs are becoming more popular because they contain fewer moving parts, thereby increasing mechanical reliability and longevity of performance [70]. Additionally, continuous flow pumps consume less power, are powered by an electrical unit rather than pneumatic power, and have smaller drive accessories than pulsatile pumps. The design offers greater comfort and increased mobility for patients. The continuous flow method provides vascular perfusion equivalent to that provided by pulsatile pumps [70].

Rotary speeds of continuous flow pumps are typically adjusted by the power input delivered from an external controller. Speed varies depending on pump design; however most devices run at 8,000-12,000 rpm to provide optimal cardiac assist function [71].

3.2. Pump-patient interface

Ventricular assist devices are further classified based on the interface between the pump and the patient (Figure 5). The two types of interface are intracorporeal and extracorporeal/paracorporeal. For intracorporeal VADs, the VAD body is implanted entirely within the patient's body and the patient must wear the battery/controller connected to the VAD

via an indwelling driveline that exits through a small incision in the skin (Figure 5A). For extracorporeal/paracorporeal VADs, the VAD body is placed outside of the patient and inflow and outflow cannulae are connected to the heart through incisions in the skin (Figure 5B).

Surgical techniques for VAD implantation vary depending on the location of device placement, incision size, and need for cardiopulmonary bypass. The most common implant procedure consists of a median sternotomy to expose the patient's heart. If necessary, the patient is placed on cardiopulmonary bypass, and the surgeon excises a core of tissue at the base of the ventricle. The surgeon then makes an incision through the patient's abdominal wall and connects the ventricle to the inflow of the pump. The VAD either resides in a pouch worn by the patient or is placed within the thoracic cavity depending on the pump design. The pump connects to a system controller powering the device.

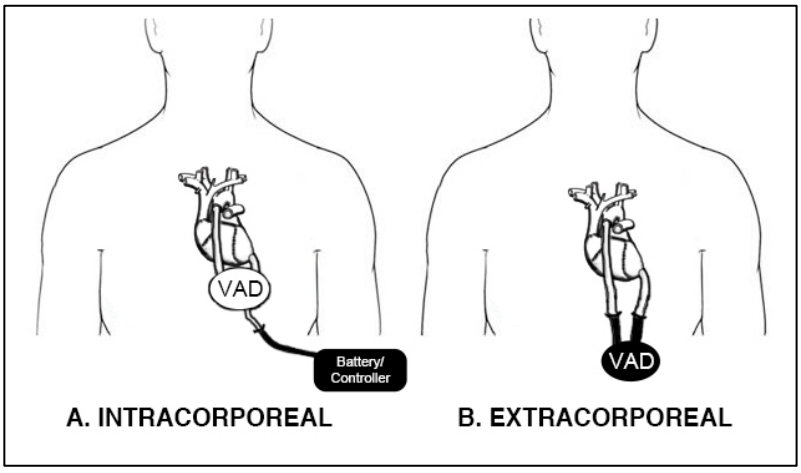

Figure 5. Types of VADs based on patient-pump interface: Intracorporeal (A) and Extracorporeal (B).

Implant procedures have become more standardized because of technological advancements and mastery of surgical techniques. Recently, surgical implantation has become less invasive, requiring smaller incisions. Surgeons are also becoming more efficient at

implanting VADs, thus reducing or eliminating the need for cardiopulmonary bypass. These newer techniques ultimately decrease post-operative recovery time and improve patient outcome.

3.2.1. Intracorporeal VADs

Intracorporeal VADs are so named because the pump body is placed within the patient's body. The main benefit of this placement is the presence of minimal transcutaneous hardware. Because most of this VAD type is within the body, the patient is safer after leaving the hospital, with fewer opportunities for daily activities to damage the pump. Intracorporeal VADs are further classified as intraventricular and extra cardiac devices. Intraventricular devices are surgically affixed into the patient's ventricle, whereas extra cardiac devices assist heart contraction but remain unattached to the heart wall.

The most common intracorporeal VADs are intraventricular. Examples of intraventricular VADs include the Thoratec HeartMate II®, the Jarvik 2000®, the MicroMed Cardiovascular Inc. Heart Assist 5®, and the Heartware Inc. HVAD™ [67, 69]. An important concern when implanting intraventricular VADs is the amount of time the patient must spend on cardiopulmonary bypass during surgery [69]. Prior to implantation, VAD components, including grafts, must be "pre-clotted," meaning the woven topography of the blood contact surfaces must be covered with adherent material to produce a smooth, essentially uniform surface [69]. The major immediate post-operative risk for any VAD implantation is hemorrhage, which can lead to right-sided heart failure and infection [69].

An example of an intracorporeal extra cardiac device is the Electro-Hydraulic Artificial Myocardium (EHAM) developed at Tohoku University, Japan [72]. This device is placed around the apex of the left ventricle on the epicardial surface and assists myocardial contraction by

creating a restrictive barrier, thus increasing myocardial tissue perfusion [72]. A benefit of extra cardiac VADs is the lack of contact between the device and the patient's circulatory system, which reduces the probability of thrombus formation. With the use of extra cardiac VADs, surgeons can avoid using cardiopulmonary bypass during implant surgery and lower the chance of post-operative bleeding. Extra cardiac VADs are currently in pre-clinical studies.

3.2.2. Extracorporeal/paracorporeal VADs

Extracorporeal or paracorporeal VADs are located mainly outside of the patient's body. This placement benefits both the patient and healthcare providers if the device must be exchanged because of suspected thrombus formation or other complication. However, the patient's overall quality of life may be decreased, because the patient must be careful to keep the VAD from catching on objects, particularly at home. Extracorporeal VADs, like some intracorporeal intraventricular VADs, require cardiopulmonary bypass during implantation and pose risk for cannula infection, thrombus formation, hemorrhage, and device failure [73]. Examples of extracorporeal VADs include Berlin Heart's Excor®, which has been approved by the United States Food and Drug Administration (FDA) for bridge-to-transplant use in pediatric patients, and Abiomed® BVS 5000® [67, 73].

3.2.3. Determining which VAD to use

It is up to the surgeon to determine which type of VAD to implant in each patient. Patient size can be a determining factor, for there are currently no FDA approved intracorporeal devices for pediatric use; therefore, infants and small children are most often implanted with

extracorporeal VADs. For non-infant patients with a more active lifestyle, an intracorporeal VAD is most often desired, because the driveline and connecting controller/battery pack are less cumbersome and easier to handle than both the inflow and outflow cannulae of an extracorporeal VAD.

3.3. Applications

There are three broad applications of VADs: bridge-to-transplant, destination therapy, and bridge-to-recovery. In the case of moribund patients, bridge-to-decision is also a short-term application of VADs. In these cases, when the patient has end-stage organ failure or their neurologic status is unclear, a doctor may decide to implant a VAD in order to stabilize the patient. This gives the physicians more time to further evaluate the patient's condition and make a decision [21].

3.3.1. Bridge-to-transplant

For younger or otherwise relatively healthy patients with a life-threatening, incurable heart condition, a heart transplant is the preferred solution. Patient eligibility criteria for heart transplant include age, histocompatibility, likelihood of organ acceptance, and overall health, aside from heart failure. If a patient meets the requirements for cardiac transplant surgery, he or she is placed on a wait list until a donor match becomes available. The donor heart must be of compatible size and tissue type. These requirements, coupled with the fact that fewer than 3,000 donor hearts are available each year worldwide [16], substantially lengthen the amount of time patients are on the wait list. The waiting time is often longer than the period for which the

patient's heart can adequately provide oxygenated blood to the body. VADs provide an option for assistance to the diseased heart while the patient awaits transplant. This application of VAD technology is known as bridge-to-transplant (BTT). Patients waiting for a transplant have an increased chance of surviving VAD implant surgery because non-cardiac organ function is maintained despite a failing heart [74].

Often a VAD can elevate a patient's eligibility status for a heart transplant. For example, pulmonary hypertension is a condition that prevents patients from being eligible for a heart transplant. Pulmonary hypertension can develop as heart failure progresses as a defense mechanism to decrease the amount of fluid going to the lungs. Acutely, this response will prevent pulmonary volume overload, which can cause patients to drown in their own fluids. As RVADs perfuse the lungs adequately and LVADs take a significant load off the heart, the decrease of blood volume in the heart allows the pulmonary vasculature to remodel, reversing instances of pulmonary hypertension and effectively elevating patient status.

3.3.2. Destination therapy

For patients with chronic, severe heart conditions who are not expected to recover and who are not eligible for heart transplants, VAD implantation is a viable option to improve quality of life and extend lifespan. When a patient receives a VAD for destination therapy (DT), the device is expected to support the patient for the rest of his or her life. DT patients are often of advanced age and/or have substantial comorbidities that preclude them from receiving heart transplants. If a patient survives the VAD implant surgery, he or she is likely to have a longer and more comfortable life than would have been possible without a VAD [74].

3.3.3. Bridge-to-recovery

Ventricular assist devices are also used in patients with potentially reversible heart conditions, such as women with post-partum cardiomyopathies. This application for VADs is commonly referred to as bridge-to-recovery (BTR). If a patient has a relatively good prognosis for recovery of myocardial function, temporary mechanical circulatory support is more suitable than cardiac transplantation. A VAD can assist an unhealthy heart during recovery. The VAD takes stress off the native heart, allowing it to recover while maintaining sufficient blood flow to other organs. An increasing number of patients are receiving temporary VAD support before transitioning back to natural heart function.

Some patients who are originally assigned to BTT or DT recover from their heart disease while receiving assistance from the VAD. In these patients, the VAD is subsequently removed without the patient going to transplant. For patients whose native hearts are able to recover, receiving a VAD for BTR is better than receiving a donor transplant or permanent VAD [75].

3.4. Approval and use of VADs in the United States

3.4.1. Bench-top testing

The development process for VADs begins with an initial design and systems testing. This process, much like that for other medical devices, is initiated by determining a need for the device and then determining the market size. To streamline the time to market, companies often set design goals based on previous VAD models and available performance data. After a

prototype is developed, initial testing and data collection begin. The results are compared with those obtained with current models.

Collection of benchmark data using research models allows engineers to fine-tune the design specifications until the design meets the desired specifications and the final prototype is developed. Once all officials in the company approve the VAD, the device enters a "design freeze" phase, in which the latest prototype can no longer undergo changes. This phase ends initial bench-top testing, and pre-clinical trials may be initiated.

3.4.2. Pre-clinical trials

Pre-clinical trials include data collection related to medical device performance in animal models. In the United States, pre-clinical studies are precursors to human trials. These studies are typical for a VAD application in the United States, because VADs are considered life-sustaining devices and thus classified as Class III devices by the FDA [76]. Therefore, in order for a company to obtain approval for a Class III VAD, a premarket approval (PMA) application must be submitted. Pre-clinical trial data collection is required for a PMA application to be considered complete.

Pre-clinical testing of a new VAD design is a critical step in evaluating safety and performance. The most common animal models for VADs are bovine, ovine, and caprine. In the US, pre-clinical studies can be divided into Good Laboratory Practices (GLP) and non-GLP studies. GLP is a federal policy that establishes the scientific benchmark for animal studies where standards and procedures are set in place to ensure consistency, reliability, and reproducibility of the results before FDA submission [77]. Device manufacturers use GLP standards to help transition to clinical trials.

3.4.3. Clinical trials

Clinical trials are the culmination of medical device development on the path to approval status. Data are collected from human patients in whom the devices have been implanted. The company determines the amount of clinical data sent to the FDA with the PMA application. However, only the clinical trial data sent to the FDA will be interpreted and used in determining whether or not the data constitutes valid scientific evidence for the medical device.

Gold standards similar to those in pre-clinical trials are also used in clinical trials. Good Clinical Practices (GCP) are the clinical trial counterpart to GLP. GCP standards are considered consistent and reliable, thus ensuring the accuracy and reproducibility of the data collected.

3.4.4. Control groups

In both pre-clinical and clinical trials, it is important to have a control group or an acceptable benchmark for comparing study results. For invasive medical devices with few or no predicate devices, as is the case for VADs, a control group is difficult to construct. For Thoratec's HeartMate II®, one of the first VADs reviewed by the FDA for BTT applications in adults, the only control group available consisted of patients who received drug therapy for heart disease without an assist device. The effectiveness of the device was determined based on the percentage of patients who survived long enough to receive a transplant or went 180 days with VAD support [62].

The Interagency Registry for Mechanically Assisted Circulatory Support (INTERMACS) is a registry established in 2005 by the National Heart, Lung and Blood Institute, the Centers for Medicare and Medicaid Services, FDA, and the University of Alabama

at Birmingham. In recent clinical trials, INTERMACS has been used as a control group. The registry was used in the clinical trials for HeartWare Inc. HVAD^{TM}, which was reviewed by a FDA advisory panel in April 2012 [64]. The effectiveness of INTERMACS as a control group is being evaluated.

3.5. Pathology evaluation of VADs

According to the FDA PMA application, pathology evaluation of VADs is not currently a specific element required for submission. Although biocompatibility, stress, wear, and shelf life are examined during non-clinical laboratory studies and/or clinical investigations, pathology evaluation is not mandated [76]. However, establishing that a device is safe and effective without pathology analysis is challenging. The Cardiovascular Pathology Laboratory at Texas A&M University believes complete pathology workup (as outlined below) should be performed for both the pre-clinical and clinical portions of any FDA submission, especially PMA submissions. These recommendations arise from many years of experience with pathology of VADs at various testing stages including pre-clinical trials, clinical trials, and post-market surveillance.

Pathology data are most credible when an independent pathologist with experience in cardiovascular medical device evaluations performs the post-explant examination of a VAD focusing on:

1. Characterizing components of the VAD:
    a. Blood-contact surfaces
    b. Housings, diaphragms, conduits, grafts, sewing rings, etc.
2. Determining the type of device complication (if applicable) and the physiologic or pathologic basis for any device related complications [78].

To achieve these two goals, pathologists should use many diagnostic tools and data analysis techniques (outlined below). The pathology data gathered from these analyses can aid VAD manufacturers in improving pump designs and ultimately producing safer and more effective devices.

A complete pathology analysis involves two tiers of analyses, depending on the situation presented in each case. The first set of analyses (Tier 1) should be conducted on any explanted VAD, regardless of the reason for explant (death, transplant, exchange, or recovery). These procedures constitute a baseline analysis necessary to evaluate the performance of the device and the effects it had on the patient. The second set (Tier 2) includes an array of analyses that supplement Tier 1 procedures. Tier 2 contains investigative or confirmatory analyses used at the pathologist's discretion. Tier 2 procedures are more time consuming, more expensive, and more specialized. The pathologist must be cognizant of specimen retention for Tier 2 analyses while performing Tier 1 procedures in order for the additional investigation to augment the pathology analysis. Table 2 summarizes analyses in Tiers 1 and 2 [78].

3.5.1. Tier 1 analyses

Tier 1 analyses are typically the only procedures performed for a routine VAD evaluation. They entail both gross and microscopic analyses. For cardiac devices in general, and especially VADs, the pathologist should evaluate both the device and the host response. For a post-mortem VAD analysis, performing a(n) necropsy or autopsy yields vital details about the performance of the VAD, especially the host response to the device (i.e., biocompatibility). A preferred technique during the necropsy/autopsy is perfusion-fixation of the patient's heart and VAD. This technique allows superior sections to be made for histological processing one to

fourteen days after fixation of the heart and VAD, depending on the amount of tissue present. Small amounts of tissue present on the VAD and associated components are adequately fixed after 1-2 days, whereas substantial amounts of tissue require longer fixation periods. During the necropsy/autopsy, photographic documentation of the following is performed to ensure quality data when generating a post-evaluation report: device *in situ*, key end organs (heart, brain, kidneys, intestines, and lungs), and any host or device abnormalities. Additionally, the key end organs and samples of any documented lesions are collected for histological preparation. In many cases, the pump is removed and submitted independently for evaluation. However, in cases where the heart and pump are received and evaluated *en bloc*, important landmarks to examine are: 1) remodeling with possible change in orientation of the inflow conduit; 2) endocardial/pump interface healing; 3) signs of ascending infection (via driveline) or seeding secondary from the implant insertion (i.e., sewing ring). In the downstream organs, the major lesions to look for are infarcts (which could be indicative of thrombosis) and any infection related effects. The pathologist evaluates the VAD after device explant and perfusion fixation/post-fixation, if applicable.

The analysis commences with the pathologist and technicians assisting in the evaluation verifying the contents received for evaluation (VAD [serial number], attachment device, graft, driveline connections, cannulae, etc.). Serial numbers are documented and photographed. The pathologist performs an evaluation of the external surfaces, and the technician documents any abnormalities. External surfaces include the electrical unit, inflow and outflow cannulae, driveline connections, de-airing ports, etc. Throughout the external evaluation, the pathologist removes and evaluates the pump accessories (outflow graft, sewing ring, cannula tubing, driveline). All aspects of the graft are photographed. First, the external surfaces of the graft are photographed, as well as the proximal and distal openings. Then, the graft is cut open, and the

entire lumen is photographed. The pathologist evaluates both the superior and inferior surfaces of the attachment device, paying close attention to any attached myocardium and/or connective tissue for thrombus or pannus formation. The cannulae are evaluated as another blood-contacting surface and are examined for any abnormalities. The driveline is observed for contamination by blood components, stretching or heating damage of its external surfaces, and contamination within the connector.

After a thorough examination of the external surfaces and VAD accessories, the pathologist disassembles the VAD. The inflow and outflow ostia are assessed during the disassembly. The pathologist evaluates the opened unit, focusing on the blood contacting surfaces, noting and collecting any unusual materials or deposits for histological examination (formalin-fixed, paraffin-embedded tissues; hematoxylin and eosin [H&E] and phosphotungstic acid hematoxylin [PTAH] stains). These deposits are characterized in a standardized manner by appearance, size, color, and location within the pump. The pump is examined for any non-biologic abnormalities (surface abrasions or imperfections, insufficient valvular response, wear, etc.). These abnormalities are documented both photographically and in the written report. Once all internal lesions and abnormalities are documented, the evaluation is complete. Figure 6 and Figure 7 represent a selection from a 22-24 photograph montage for a Berlin Heart® Excor® (Figure 6) and HeartWare Inc. HVAD™ (Figure 7) evaluation.

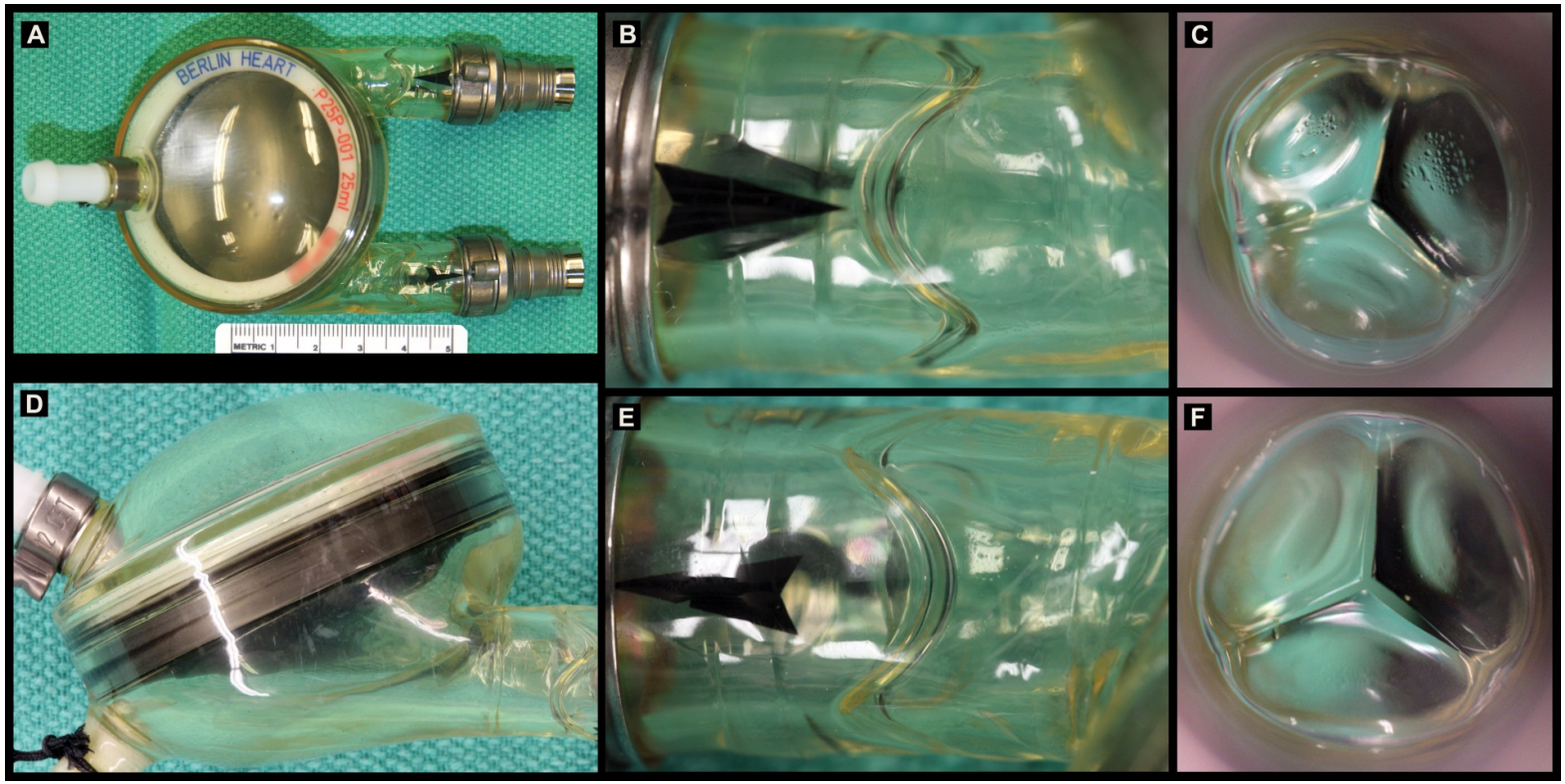

Figure 6. A representative subset of photos to be included in montage accompanying the final pathology report for a Berlin Heart EXCOR. A) Superior view of pump. B) Pump inflow. C) Inflow valve leaflet. D) Lateral view. E) Pump outflow. F) Outflow valve leaflet.

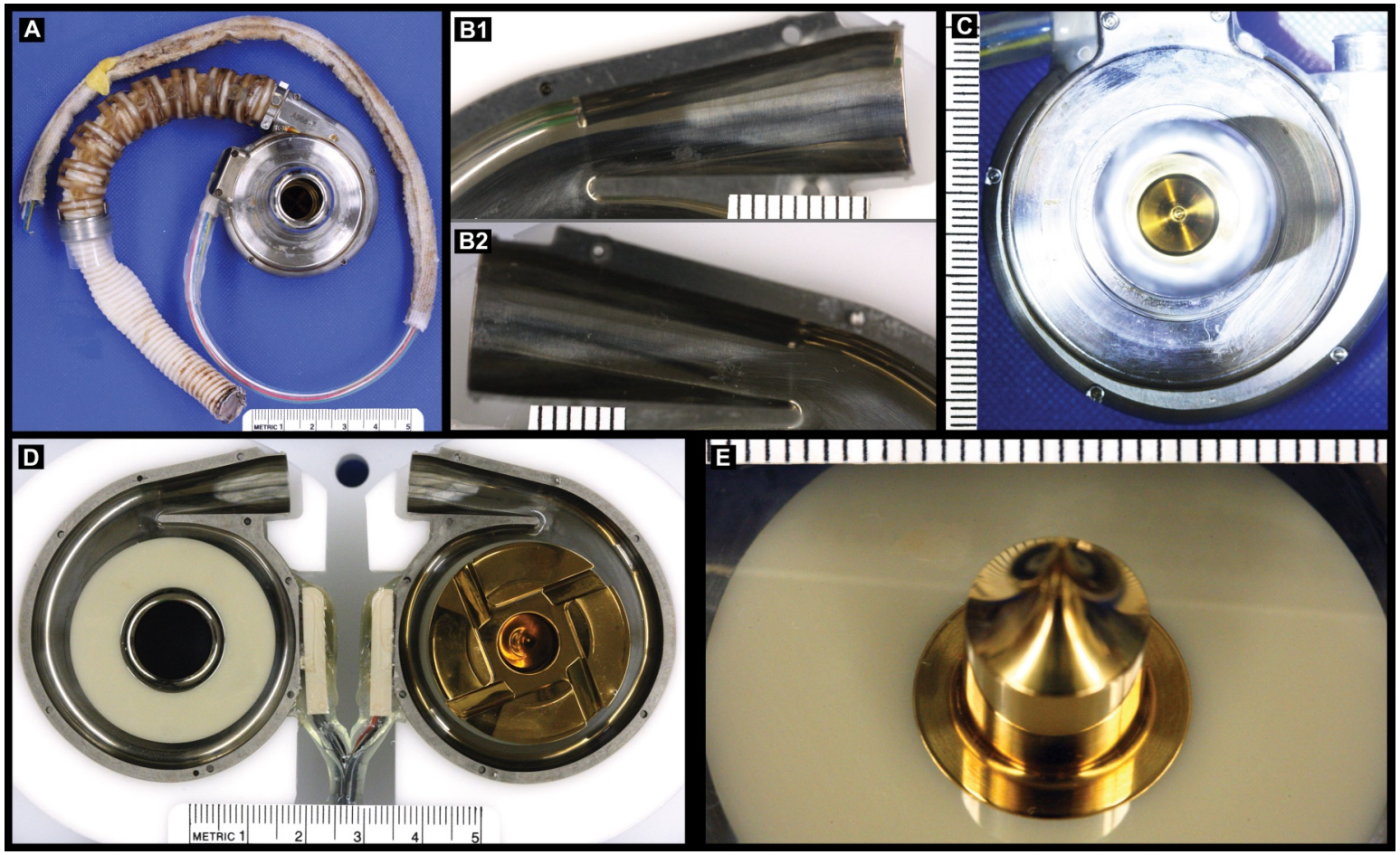

Figure 7. A representative subset of photos from several pump evaluations to be included in montages accompanying the final pathology report for a HeartWare HVAD. A) Superior view of all contents received (status post op (s/p) 17 days). B1) Upper housing outflow (s/p 31 days). B2) Lower housing outflow (s/p 31 days). C) Inflow (s/p 46 days). D) Opened unit with impeller *in situ* (s/p 722 days). E) Impeller post (s/p 592 days).

Next, the pathologist generates a report of the gross findings from both the necropsy/autopsy, if applicable, and the VAD evaluation. The technician selects a subset of the photographs taken during the evaluation to create a photographical representation of the findings during the gross evaluation, referring to the figures by number in the generated report. The pathologist supplements the report with his or her findings from light microscopy, including for each deposit the etiology (i.e. "pass through" or *de novo*), morphology, approximate age, if possible, and the effect on device performance. Additionally, the pathologist takes photomicrographs to visually support the light microscopic findings. Finally, the pathologist draws conclusions from the gross and microscopic findings and comments on the overall device performance relative to that of idealized or similar devices. Correlation with the clinical findings in the patient is always recommended. Report submission to the VAD company is the culmination of Tier 1 analyses as performed for every VAD evaluation.

Microscopic evaluation of deposits found within VADs elucidates more information than can be obtained with gross evaluation alone. In VADs that have not been properly rinsed immediately following explant, it can be difficult to assess whether the internal components contain thrombi or simply post-explant clotted blood. Microscopic evaluation is necessary to confirm material composition. Sometimes blood coagulates and settles to the gravity-dependent side of a VAD and forms a clot with the heavier blood components (i.e., cellular) gathering at the bottom and the lighter components (i.e., fibrin) rising to the top. This is indicative of a post-mortem blood clot, and can help the pathologist determine the position the patient was laying in at time of death. Microscopic evaluation of these deposits will reveal abundant erythrocytes with little to no fibrin and no evidence of organization; there are usually loose, randomly oriented eosinophilic strands with scattered enmeshed leukocytes. In VADs with rotating surfaces, ante-mortem/ante-explant thrombi are characterized by an eosinophilic dense matrix arranged in

layers that typically show variations of platelet/fibrin layers, fibrin enmeshed erythrocytes and/or leukocyte sheets within fibrin enmeshed erythrocytes. These laminar areas are flow dependent. For example, high flow shows more compacted cellular elements and lower flow or turbulence shows greater accumulations of cellular elements.

3.5.2. Tier 2 analyses

Tier 2 analyses should supplement Tier 1 analyses in specific cases at the discretion of the pathologist. This level of analysis requires a more specialized laboratory with specialized capabilities. This includes but is not limited to one or more of the following: radiographs (2-5μm resolution), computed tomography (CT) analysis (2-10μm resolution), and scanning and transmission electron microscopic analysis.

Radiographs and CT are used to evaluate entire VADs or individual components. These are useful resources to determine stress fractures or points of fatigue on moving parts. These imaging modalities are used to determine the extent of mineralization within the VAD, which correlates with a foreign body response [78]. CT is used to identify device abnormalities that a two-dimensional (2D) image cannot display and is performed before device evaluation to prevent the movement of particles. Device irregularities are further evaluated using CT after injection of a contrast agent (for example, barium).

Electron microscopy provides a more detailed analysis of the surface of tissues or devices. Scanning electron microscopy (SEM) is used to identify the surface topography of devices, including degree of fibrin and platelet deposition, abrasion scoring, degree of pitting on a device, neointimal growth, and thrombus formation. Transmission electron microscopy (TEM) provides comprehensive images of the ultrastructure of the sampled tissue. This information

allows the pathologist to provide a detailed description of the biological response to the VAD. Scanning transmission electron microscopy (STEM) allows the ultrastructure of samples to be visualized without the use of stains common in TEM, thus STEM is effective at imaging tissues that cannot be stained.

In conjunction with SEM, electron dispersive X-ray spectroscopy (EDX) provides an elemental analysis of the surface composition of a device or tissue. This technology is used to determine the elemental identity of contaminants in medical devices. EDX also supplements light microscopy by determining the identity of unstained areas on a slide through the isolation of unstained areas within the paraffin block.

3.5.3. Executive summaries

At the conclusion of the VAD studies, the pathologist creates an executive summary report to present the major conclusions. The executive summary is a finely detailed report that summarizes the methods used to evaluate the device both grossly and histologically, as well as the gross and histologic findings. Review of pathology executive summary reports is an important step for regulatory agencies in deciding whether a device is safe and effective or not. Executive summaries are also extremely useful for studies with large numbers of pump specimens, as they enable the pathologist to draw overall conclusions about pump functionality and host response. As with all pre-clinical and clinical studies, QAUs are crucial and should audit all reports before submission to a regulatory agency.

3.6. Discussion

The risk to benefit assessment represents a delicate balance between introducing life-saving medical devices to market as soon as possible and preventing unsafe devices from being implanted in patients. With VAD technology constantly changing, it is difficult to properly assess the safety of such devices in a timely manner. Clinical data alone provide only a small portion of information about patient interaction with the device. This narrow view could result in the implantation of unsafe devices.

A thorough device study involves both clinical data and a pathology evaluation. Pathology, in conjunction with clinical correlation, lets investigators and regulatory agencies evaluate VADs of various designs by the same criteria. For example, finding thrombus formation grossly and confirming the diagnosis microscopically may reveal potential problems with the device, sometimes before clinical symptoms are apparent. All VADs need a pathology evaluation with at least the Tier 1 analyses, which includes a gross evaluation, photographic documentation, and, if the gross evaluation reveals abnormal deposits, light microscopy. For cases with unique or unusual findings, Tier 2 analyses, such as radiography or electron microscopy, can aid in identifying abnormal or foreign material.

A pathologist familiar with comparative anatomy should perform pathology analyses in pre-clinical trials. Many of the host responses observed in humans are similar in animals; thus, if a complete pathology analysis is performed in pre-clinical trials, unsafe devices are less likely to be implanted in humans. However, comparative anatomy has limitations and must be treated cautiously so that data are not misinterpreted or overlooked.

Whereas clinical data elucidate past problems with medical devices, pathology findings show past and future problems through the use of integrative techniques that provide a more

thorough understanding of the effect of the device on the patient. To accurately indicate VAD safety, comprehensive pathology analyses are essential for all VADs, in both pre-clinical and clinical trials, and the findings should be correlated with clinical data. This correlation allows for a more complete determination of long-term safety and is more useful to medical device reviewers.

3.6.1. Rationale for subsequent sections

A wholesome review of pathology evaluations performed throughout the course of pre-clinical and clinical trials for multiple types of VADs can be useful for comparing different VAD models and determining trends seen in each. For example, a classification system for categorizing deposits collected from VADs could be developed to learn more about each VAD model and how certain pump parameters (flow type, implant duration, speed, etc.) correlate to the type of deposits found post-explant. The Cardiovascular Pathology Laboratory at Texas A&M University has developed a classification system after 1,000+ VAD pathology evaluations; however clinical correlation and correlation with pump log files is necessary to reveal more information specific to each pump. The remaining sections of this dissertation provide a comprehensive review of blood coagulation as related to VADs, and a computational and bench-top model that can reveal information specific to each VAD model before pre-clinical trials commence. The ultimate goal of these models is to decrease instances of thrombotic complications in VADs.

4. HEMOSTASIS, CLOTTING, AND THROMBUS FORMATION

The body has built-in mechanisms to maintain homeostasis within the vasculature to continue sufficient oxygen delivery and waste removal necessary for life. Blood, as a body tissue, is complex and constantly changing its dynamic to provide for the body's needs [79]. Hemostasis, the cessation of blood flow, is an important defense mechanism against vascular injury. The mechanism of hemostasis involves clotting of blood at areas of tissue or vessel damage. The goal of hemostasis is two-fold: 1) prevent oxygen carrying erythrocytes from leaking out into the tissue after vascular injury, and 2) re-establish vessel wall integrity [80]. Implanting a VAD causes a disruption in the normal body mechanisms, and the right balance between hemorrhage and VAD thrombosis is a difficult and challenging task for manufacturers and clinicians. This section provides a general overview of the hemodynamic process and discusses the multitude of ways that implantation of a VAD might alter normal physiologic hemodynamics.

Clotting and thrombosis are common terms used in the medical community with related

but different meanings. Clotting can have a negative connotation; however, it is a normal physiologic process that prevents injured tissues from hemorrhaging. Thrombosis is pathological in nature and can be defined as intravascular blood clotting in an undesirable area [81, 82]. A thrombus can disrupt blood flow or become an embolus (moving thrombus). Emboli, depending on their size, can occlude blood flow in a downstream vessel potentially limiting oxygen delivery and causing ischemic damage.

4.1 Coagulation in vivo

In general, blood coagulation (clotting) begins after an initial insult to tissue, and involves primary hemostasis, the coagulation cascade (intrinsic, extrinsic and common pathways), and fibrinolysis (Figure 8). This complex process and can be initiated by multiple stimuli and many components often overlap.

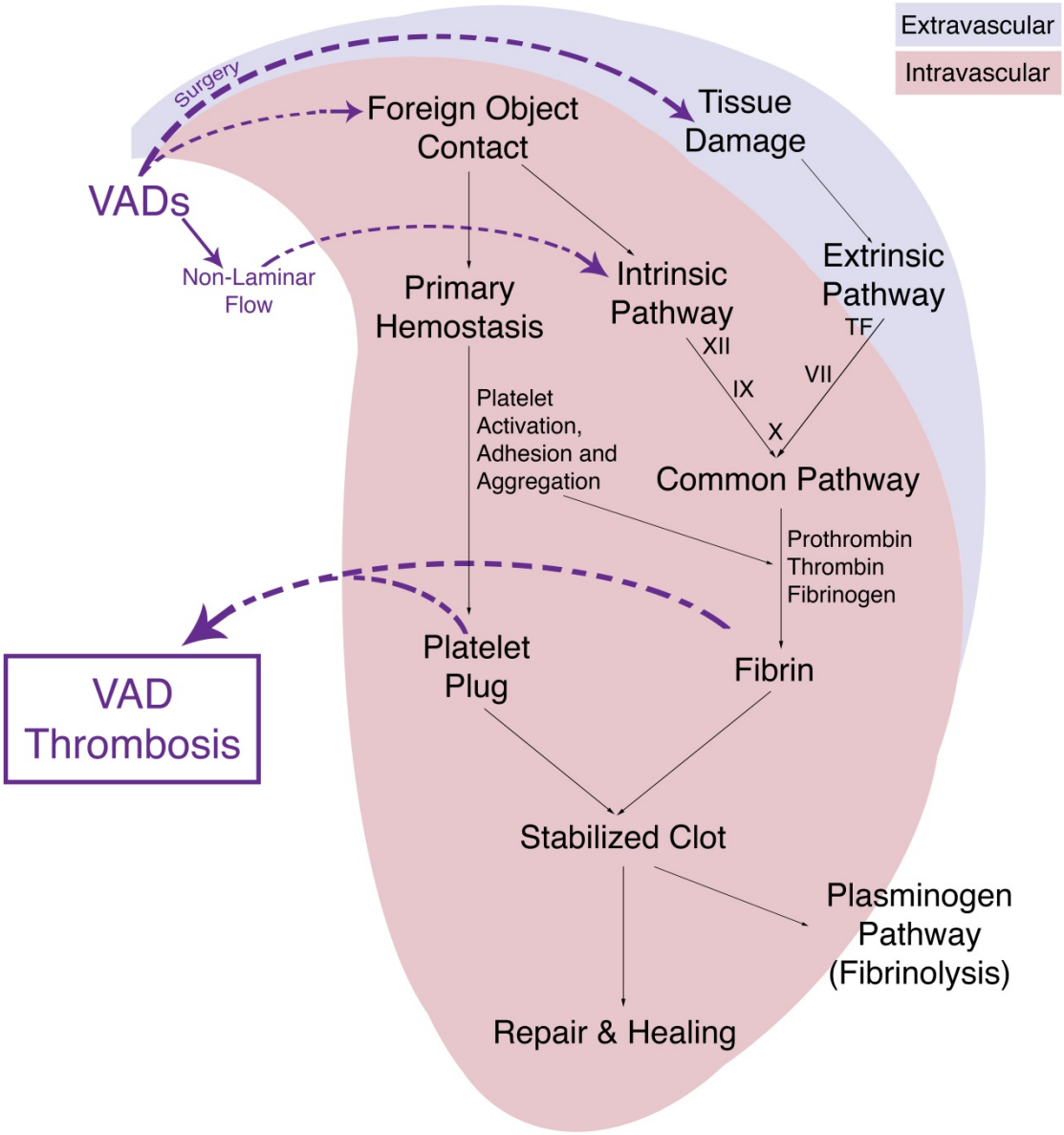

Figure 8. Overview of physiologic coagulation *in vivo* and changes associated with VAD implantation. Coagulation is initiated by two mechanisms: contact with a foreign object (i.e., exposed basement membrane, collagen fibers, etc.), and tissue damage. These mechanisms initiate primary hemostasis (platelet activation, adhesion and aggregation), and the coagulation cascade (intrinsic, extrinsic and common pathways [clotting factors noted in Roman numerals]), which ultimately results in formation of a stabilized, fibrin clot. The clot is maintained in size by various mechanisms, including fibrinolysis, and eventually the wound is healed. Inserting a VAD into the body changes the coagulation process indicated by the dotted purple lines, and may result in the inappropriate formation of a thrombus.

4.1.1 Primary hemostasis

Primary hemostasis is initiated when the basement membrane of vessels are exposed during tissue injury (e.g., from surgery, trauma, etc.), and begins with activation of platelets, a cellular component crucial in coagulation. Activated platelets adhere to connective tissue fibers (i.e., exposed basement membrane), as well as glass and metal, within a few seconds after contact [80]. Adhered platelets change shape and recruit platelet aggregates to form an initial "platelet plug" that seals off the injury. This "platelet plug" is sufficient to prevent major loss of blood, but is not a permanent solution.

4.1.2 Coagulation cascade

The coagulation cascade is an amplifying series of enzymatic conversions that ultimately results in the formation of fibrin [81], which will fortify the platelet plug created during primary hemostasis and increase the likelihood that the clot will heal the injury. Clotting factors derived from plasma are denoted by Roman numerals I-XIII. (Refer to Appendix I for a list of all tissue factors and detailed description of the coagulation cascade). The coagulation cascade includes intrinsic and extrinsic pathways each initiated by separate mechanisms, which eventually combine to form the common pathway. The extrinsic pathway begins when tissue damage provides a tissue factor (TF) that acts as a catalyst in the activation of factor X [83]. In the intrinsic pathway, surface contact with a foreign (non-endothelial) substance (i.e., exposed basement membrane, medical device, etc.) acts as a catalyst for activation of factor XII, which ultimately joins the extrinsic pathway with the activation of factor X [80]. The common pathway involves the conversion of prothrombin to thrombin, which leads to the formation of fibrin

monomers. Fibrin is a major part of coagulation because it fortifies and stabilizes the clot to adequately heal the injury.

4.2 Coagulation related to VADs – Virchow's triad

The main goal of blood coagulation is to heal vascular injury. However, when a medical device is implanted and in contact with blood, the normal body response may lead to thrombosis, a dangerous condition with potentially fatal results. Figure 8 shows how VAD implantation can change the normal hemostatic mechanisms to lead to VAD thrombosis (noted in purple dotted lines).

Virchow's triad has become a focus in the study of physiologic thrombosis [81], and describes three major contributing phenomena: alterations in blood coagulability, alterations in blood flow, and introduction of non-endothelial surfaces [84] (Figure 9). VAD implantation is linked with all of these phenomena, making thrombosis a serious complication associated with VAD therapy [26-34].

Ventricular assist device implantation disrupts the vascular homeostatic environment through multiple mechanisms beginning with surgery, following through to long-term post-operative management. During implantation procedures, patients' blood coagulability is altered due to anticoagulation therapy (heparin, warfarin sodium, etc.), which decreases the risk of clotting during and immediately following the surgical procedure [85]. Additionally, the introduction of the device will cause alterations of blood flow, introduce new areas of stasis and turbulence, and introduce a non-endothelial surface. The rotating components in these devices provide a shear force on the blood components [86], and the device itself provides a surface for platelets to adhere and aggregate on [87]. Additional factors such as altered endothelial surfaces,

infections, and other patient variables [27] may contribute to thrombosis. Regardless of thrombus size or origin, if embolized to the pump, the brain or other down-stream organs, the outcomes could include pump failure, disability, or death [27].

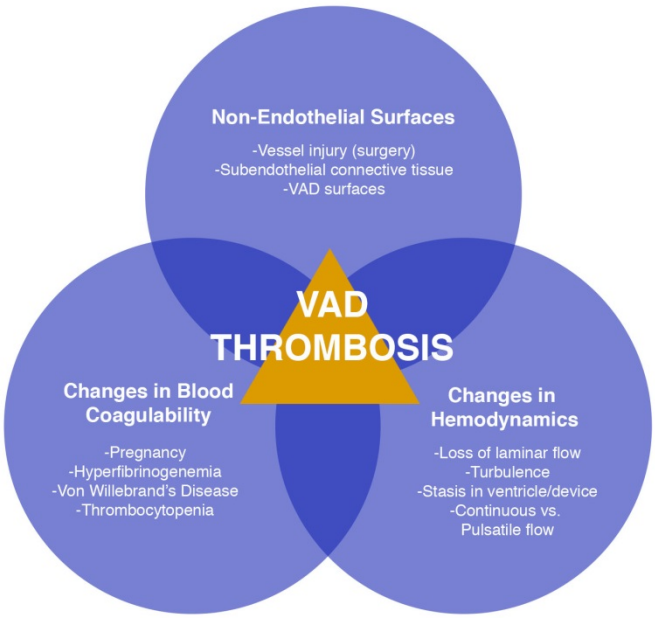

Figure 9. Virchow's Triad with emphasis on how each branch relates to VADs. Changes in blood coagulability includes patient conditions that may lead to an increase in clot formation. Non-endothelial surfaces can include exposed basement membrane and subendothelial connective tissue from tissue injury that occurs during surgery or the surface of the implanted device. Hemodynamic changes mostly refer to the changes in laminar flow due to the implant of the device.

4.2.1 Alterations in blood coagulability

Alteration of blood constituents is one component of Virchow's triad that may lead to thrombosis. Conditions such as pregnancy, thrombocytopenia, Von Willebrand's disease, and many others can change blood coagulability and increase risk of thrombus formation. In fact, any

change of levels in blood constituents (platelets, fibrinogen, etc.) may cause undesired clotting, requiring that preventative measures be taken during surgical procedures.

Anticoagulation protocols during VAD implantation are necessary to keep blood from clotting within the device before it can begin operating. Aspirin, warfarin, and heparin are common drugs known to inhibit coagulation and are used in anticoagulation protocols during surgery (Figure 10). Warfarin (brand name Coumadin) interferes with oxidation of vitamin K, which then induces liver production of clotting factors (II [prothrombin], VII, IX and X) with reduced clotting function [88]. Heparin indirectly prevents coagulation by accelerating the rate at which antithrombin (a protein in the blood) offsets thrombin activity [89]; heparin acts by increasing the binding of antithrombin to prothrombin and factor X, ultimately preventing fibrin formation. Finally, aspirin is effective at decreasing platelet activity by indirectly reducing the production of thromboxane in platelets, which leads to diminished platelet aggregation [90]. Although these three drugs are the most common anticoagulants, specific doses of each for anticoagulation protocols vary between physicians and hospitals, and are sometimes patient- or device-specific.

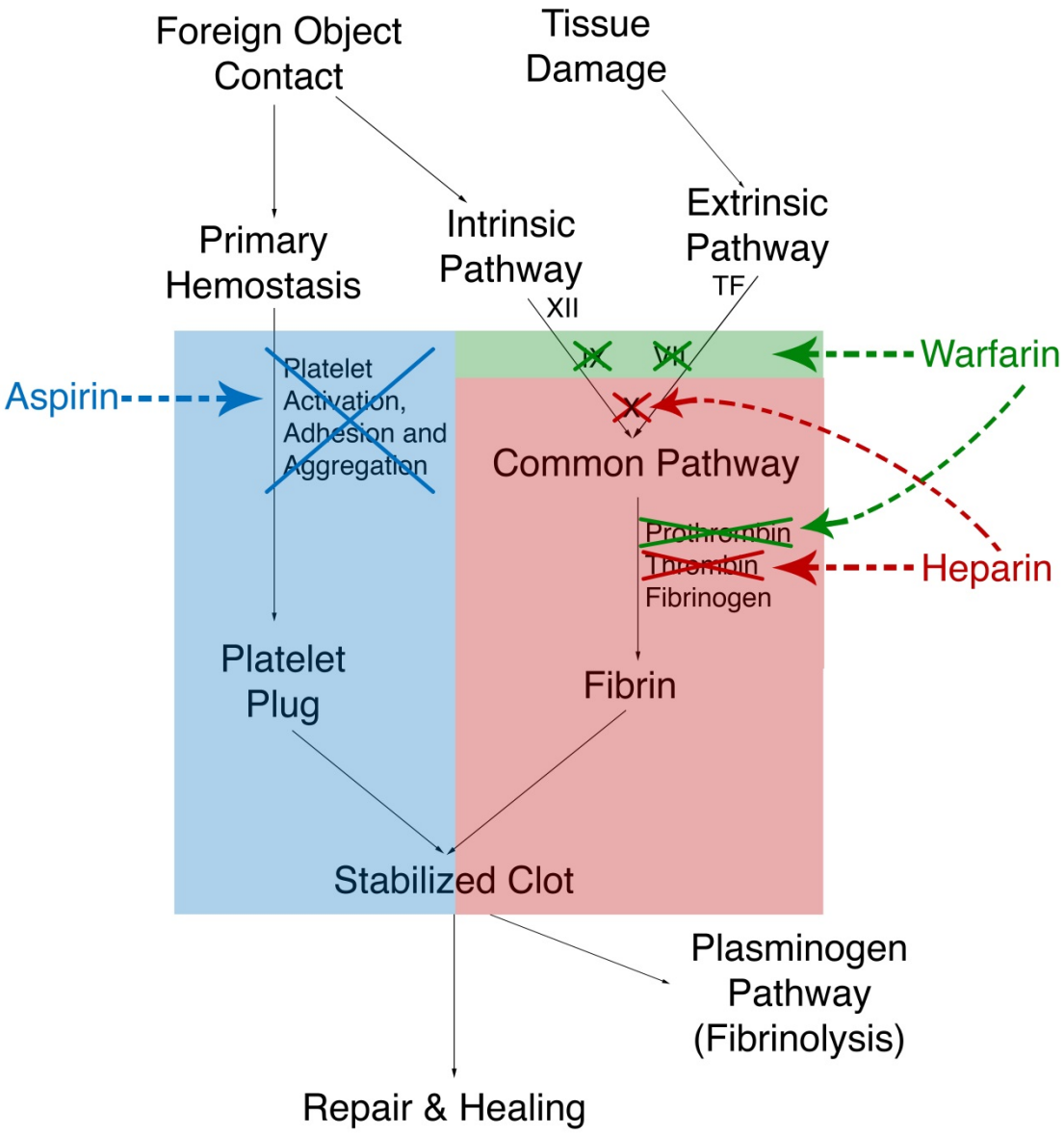

Figure 10. Mechanisms of anticoagulation therapy used during surgery. Aspirin, warfarin, and heparin are common drugs administered to prevent clotting during surgery. For the duration of a cardiovascular implant, such as a VAD, stent, or pacemaker, a combination of these drugs might be prescribed to prevent thrombosis within or around the device.

A unique balance of anticoagulants must be administered post-operatively to prevent both hemorrhage and excessive thrombus formation. Patients are typically administered warfarin or aspirin after VAD implantation to help maintain this balance. Shortly after surgery, protamine is often used to counteract the effects of heparin [91]. Long-term anticoagulation protocols must be revisited for each patient, however, for conditions such as hemorrhage and thrombocytopenia [10] might develop that require alternative treatment options.

4.2.2 Alterations in blood flow patterns

Altering blood flow patterns is another aspect of Virchow's triad that may lead to thrombosis. The presence of the VAD inflow cannula in the ventricle changes the flow patterns of blood, introducing areas of stasis and recirculation [92]. Areas of stasis allow accumulation of thrombogenic substances such as activated thrombin, platelets, etc. In normal circumstances these thrombogenic molecules flow downstream and become deactivated once crossing capillary beds [93]. However, in areas of stasis, platelets and other trapped molecules initiate coagulation and form a thrombus. Additionally, in areas of low blood flow or stasis, rapid desaturation of erythrocytes occurs as a result of the inability to exchange oxygen within tissue. This causes the area of stasis to become hypoxic, thereby activating the endothelium [93], which exacerbates the inappropriate formation of a thrombus. In patients with dilated cardiomyopathy (patients most likely to receive a VAD), this mechanism of blood coagulation is common due to the geometry of the ventricle and amount of residual blood in the chamber after each stroke, which leads to mural thrombus formation. Mural thrombi, if detached from the wall, may easily enter the pump and cause mechanical failure or pass-through the device and cause devastating ischemia.

While VAD implantations mostly serve as a temporary solution until a donor heart is found, in some cases VADs can become a long-term treatment. Over time, as the VAD implant duration increases and a significant load is taken off of the heart, the heart will begin to remodel to its previously non-dilated state. As the heart remodels, the flow around the cannula in the ventricle may change, which can disrupt mural thrombi or any thrombi formed around the device. Consequently, it is possible to see complications from VAD thrombosis after several years of successful VAD function.

4.2.3 Non-endothelial surfaces

Finally, introduction of foreign objects, the last branch of Virchow's triad, may lead to thrombus formation. Normally, blood is in contact with endothelium, which is the lining all vessels, tissues and organs. Any foreign, non-endothelialized object will cause the blood to clot in an effort to shield the body from this object. As shown in Figure 8, contact with a foreign substance will initiate the intrinsic pathway and platelet activation. In the case of VAD implantation, this could happen in response to the device itself. If the patient is not on anticoagulants, a thrombus will form.

The surface texture of the device can initiate clot formation around and within the device. Historically, smooth surfaces have been thought to reduce thromboembolic occurrences [94]. However, more recently, in both VADs and grafts, textured surfaces have been shown to promote deposition of a pseudointimal layer along the surface of the device to create a biological barrier between the device and the blood contact surface [95, 96]. On smooth surfaces, any microscopic imperfections can become a nidus for platelet aggregation and/or thrombus generation. Additionally, if the pseudointimal layer covering textured surfaces is disrupted,

thrombi can readily form at the site of the disruption. The constant movement of the heart can cause these fragile thrombi to easily break off and travel downstream to cause infarcts or device malfunction.

4.3 Summary

Coagulation is a natural response to maintain adequate blood volume following vascular injury. Throughout history, Virchow's Triad has been used to explain physiologic and environmental changes that can cause coagulation without first having vascular injury. Implantation of a VAD inherently allows each component of Virchow's Triad to manifest: changes in blood coagulability and flow patterns, as well as introduction of non-endothelial surfaces. These environmental and physiological changes can result in VAD thrombosis. The Cardiovascular Pathology Laboratory at Texas A&M University has performed a pathology evaluation of over 1,000 VADs with and without clinical adverse events, and developed a classification system for categorizing deposits and findings within multiple VAD models. This system can be correlated with clinical data to learn more about the condition of VAD thrombosis and eventually limit the opportunity for thromboembolic complications in future designs.

5. THROMBOSIS OF VENTRICULAR ASSIST DEVICES

Thrombosis in ventricular assist devices is a common concern facing VAD manufacturers and clinicians. Clinically, a thrombus is suspected to be within the pump when the controller log associated with the device indicates high power consumption or periods of low flow, at which time the device is typically exchanged. A pathology evaluation of the device can aid in determining what caused the irregularities noted on the controller log. A gross and histological evaluation of specimens found within the device can determine the etiology of the clot/thrombus, and provide a timeline for when the thrombus developed [22]. Over the course of several years, the Cardiovascular Pathology Laboratory at Texas A&M University has categorized the types of deposits found within VADs (Figure 11 and Table 2), which are outlined below.

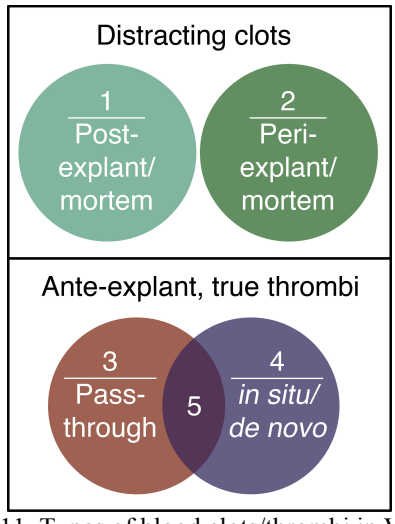

Figure 11. Types of blood clots/thrombi in VADs.

Table 2. Classification of clots & thrombi within VADs.

Classification Name	Description
Low impact/distracting deposits	
1. Post-mortem/explant clots	Clots formed after death or after device explant
2. Peri-mortem/explant fibrin deposits	Fibrin deposits formed at the time of death or explant
Ante-mortem, true thrombi	
3. Pass-through thrombi	Thrombi formed outside of the device that traveled into the device
4. *In situ*/*de novo* thrombi	Thrombi formed within the device
5. Combination thrombi	Thrombi that originally formed outside device, traveled inside the VAD and became a nidus for further *in situ* thrombus formation

5.1 Distracting clots

Post- or peri-explant/mortem clotting of residual blood inside VADs will lead to a low impact and distracting blood clot. Clots that form quickly after death or explant are dark red "currant jelly" clots (Figure 12A). These clots are regionally homogenous and lack organization. Histologically, post-explant clots are characterized by loose, randomly oriented, eosinophilic strands with abundant enmeshed erythrocytes (Figure 12B). Other times, when the clot forms slowly, the cellular components gravitate toward the bottom of the vessel or device, creating a "chicken fat" clot with a gray-yellow plasma layer on top (Figure 12C) [97].

Mild peri-explant fibrin deposits were formed at the time of explant. These deposits have started to develop but do not have the same level of organization as ante-explant thrombi (Figure 12D,E). Excess post- and peri-mortem deposits often complicate pathology evaluation of VADs, making it more difficult to see any possible ante-mortem deposits. These clots can, however, give indication of the time of death and/or orientation of the specimen at time of death based on the way the erythrocytes settle in the "chicken fat" clot.

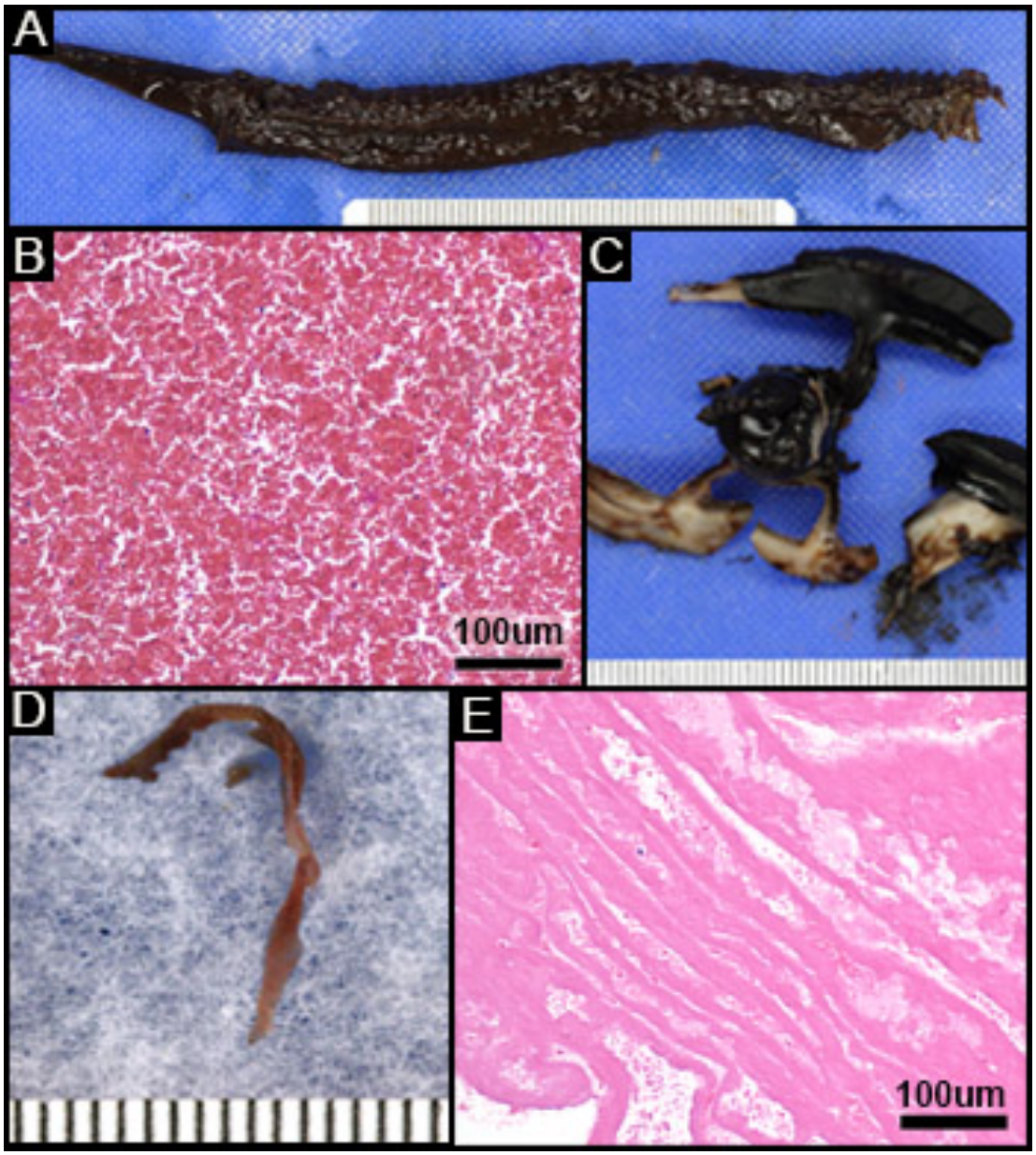

Figure 12. Post- and peri-explant clots. A,B) Post-explant “red currant jelly” clot found within an outflow graft. C) Post-explant chicken fat clot. D,E) Peri-explant fibrin deposit.

5.2 Pass-through, ante-mortem thrombi

Prior to patient death or explantation of device, thrombi may form outside the device, possibly in the atrial appendage, along the ventricle wall (mural thrombus), around the sewing ring (inflow insertion site), or elsewhere in the vasculature. If a thrombus dislodges from its origin and embolizes into the VAD, it may lodge between pump components and hinder device performance, or create micro-emboli to send out the pump outflow. This type of thrombus is referred to a "pass-through" thrombus, because it originated outside the pump and traveled into or through the pump. The gross and histologic appearances of these thrombi are largely dependent on their origin. If a thrombus developed next to high velocity blood flow, there are distinct layers alternating between fibrin and erythrocytes, usually with a fragile tip pointing downstream (Figure 13A). If a thrombus forms in regions of stagnation, perhaps near the sewing ring/apex after incomplete clearing of blood with each contraction, the thrombus will be irregularly shaped with pockets of trapped erythrocytes (Figure 13B,C).

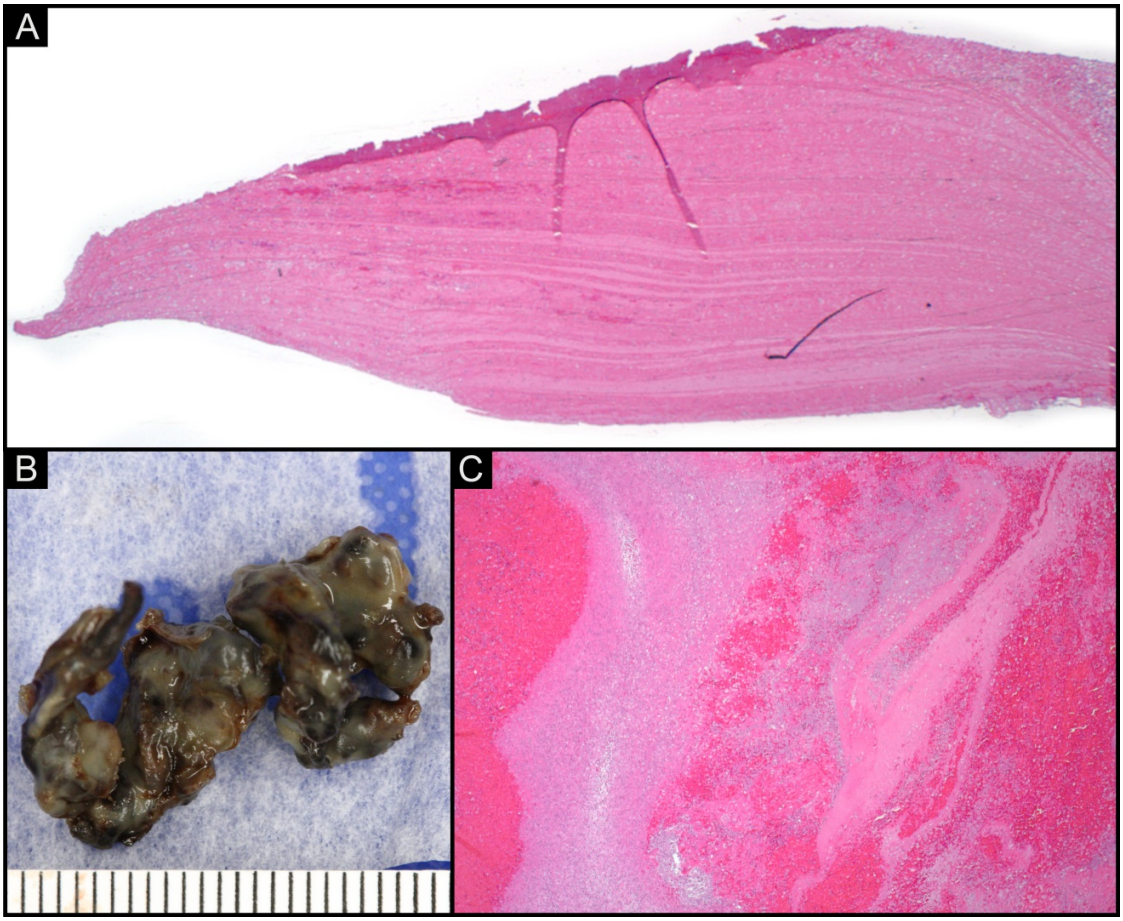

Figure 13. Pass-through thrombi. A) Organized thrombus formed along sewing ring with a fragile tip and distinct laminations from the high flow of blood passed the device. B,C) Organized thrombus found in the inflow of an explanted VAD.

5.3 In situ/de novo*, ante-mortem thrombi*

Thrombi may also develop inside the device prior to device explant/patient death. These thrombi may form due to stasis/recirculation of blood within the device, shear forces acting on the blood, or in reaction to device surfaces. These thrombi are grossly and histologically different from post-explant clots: rather than appearing as a dark red "currant jelly" clot or a "chicken fat" clot, *de novo* thrombi are smaller, usually brittle specimens with clear organization (Figure 14). The color varies from transparent and white to alternating layers of dark and bright red. When thrombi form on flat surfaces (e.g., vane of a centrifugal flow impeller), they are usually transparent, and often firmly adhered to the device surface. Histologically, these thrombi are characterized by a homogeneous to slightly stranded pale eosinophilic material with occasionally enmeshed platelets and erythrocytes. Ante-mortem thrombi formed within the VAD are mostly influenced by the high velocity of blood flow. As the blood continues to flow past the thrombus, layers form, altering the thrombus morphology. If a thrombus developing on the impeller increases in size, it will impede device function, especially if proper device function requires a precisely balanced, axially symmetric impeller, or if the geometry provides small tolerances (i.e., <1mm) between rotating and stationary components. This may lead to increased friction within the device, which would be indicated on the VAD controller log as an increase in power. Thrombi formed where two components meet, such as a stator/impeller interface in an axial flow device, are typically composed of cellular components with alternating layers of dark and light brown regions. The origin of these thrombi is not fully known. Shear forces from the rotation of the impeller has shown to activate platelets, and the heat at the component interfaces may or may not contribute to the formation of thrombi *de novo*.

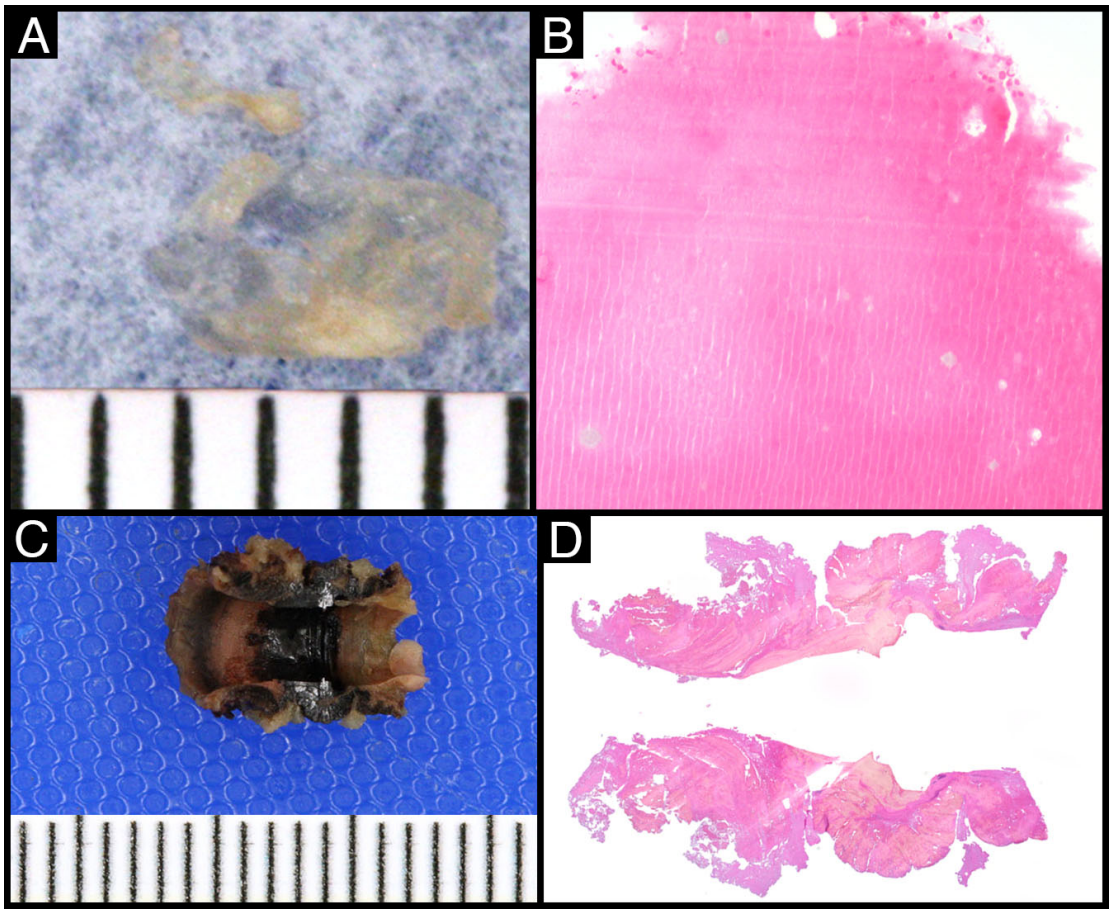

Figure 14. *De novo* style thrombi. A,B) Thrombus collected from the internal flat surface of a centrifugal flow device. C,D) Cross section of thrombus collected from a mechanical joint inside an axial flow device.

5.4 Combination of pass-through and de novo

Finally, thrombi may form as a combination of the pass-through and *de novo* style thrombi. Some thrombi of origin proximal to VAD inflow that travel into the device become a nidus for further thrombus development within the VAD. These deposits grow onto the internal pump components, thus hindering performance of the device. Combination-style deposits are grossly characterized by two distinct regions: the first (of upstream origin) is grossly similar to pass-through thrombi described before. The second is an area of irregular, fragile, semi-transparent material similar to *de novo* thrombi (Figure 15).

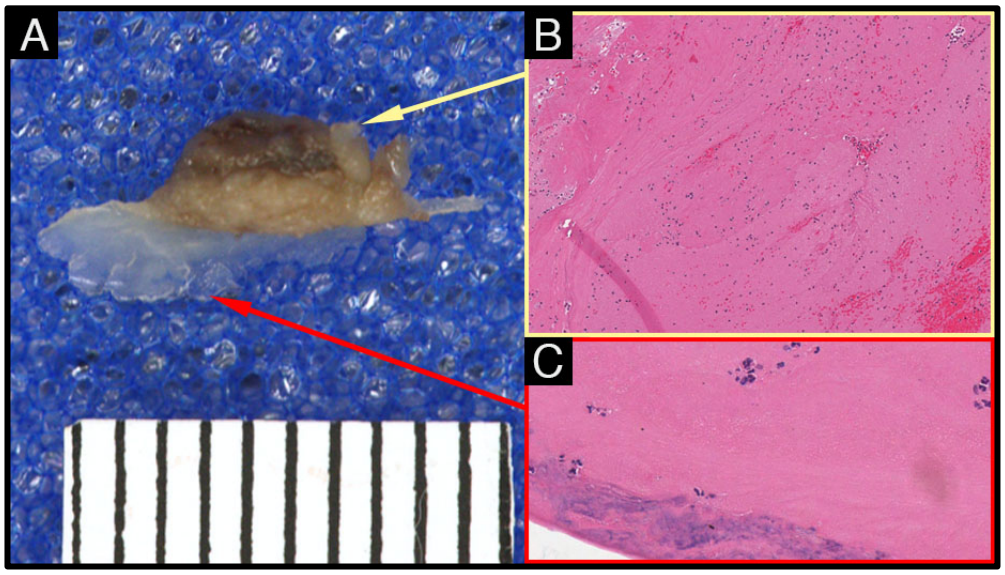

Figure 15. Combination of pass-through and *de novo* style thrombus. This specimen was recovered from an explanted VAD. A) Grossly, this specimen has two distinct regions: a light to dark brown area of upstream origin (yellow arrow), with a thin, semi-transparent vegetative segments extending from the base (red arrow). B) H&E stained section of region of upstream origin. This section is composed of alternating layers of fibrin/platelets and fibrin/erythrocytes with scattered leukocytes. C) H&E stained section of vegetative region developed *de novo* on the internal surface of the VAD. This section is composed of a dense acellular substrate made up of a fibrin base with alternating layer of fibrin and fibrin enmeshed platelets and wispy basophilic material.

5.5 Ventricular insertion site – potential source of pass-through thrombi

After numerous VAD evaluations with increasingly lengthened implant durations, the inflow cannula insertion site has become a potential source for pass-through thromboemboli that needs further investigation. Inflow cannula position and orientation within the ventricle can play an important role in VAD thrombosis, for the presence of the inflow cannula can change the flow dynamics inside the ventricle, causing areas of stasis or recirculation that can lead to thrombus formation. To further understand VAD thrombosis, it is important to also look at potential sources of thromboemboli, learn how and where they are forming, and determine if there is a way to prevent them from forming at all.

Patients with dilated cardiomyopathy inherently have increased chances of mural thrombi formation (with or without VAD implantation) due to large regions of stagnant flow caused by decreased contraction strength and increased ventricular volume. In patients with VADs, a thrombus may develop initially due to platelet activation upon contact with the VAD surface or because of geometry-induced blood stasis (i.e., around the inflow cannula). As time goes on and the thrombus continues to develop, cellular components will collect within the thrombus. Normally, inflammatory cells will replace the thrombus with collagen during the tissue repair process. However, in the case of VAD implants, the constant high flow of blood passing by the thrombus prevents any inflammatory cells from "healing" the thrombus. Thus the thrombus continues to develop in alternating layers of fibrin and erythrocytes (Figure 16) extending off of the sewing ring or along the inflow cannula. The thrombi in Figure 16 are from VADs used in a clinical setting that were removed after 900 days of implantation.

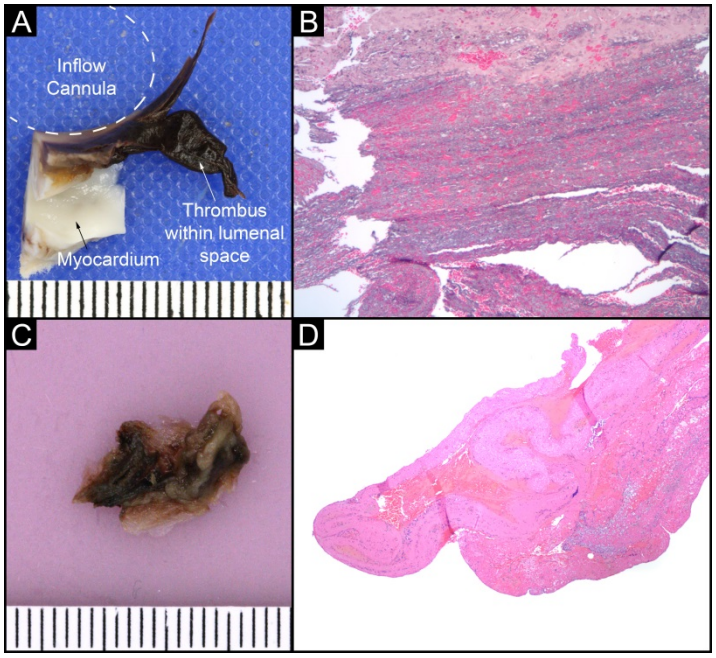

Figure 16. Gross and histologic views of organizing thrombi retrieved from explanted VADs. Dark brown material extending from the sewing ring and attached myocardium removed from the VAD at time of explant (A) was histological composed of layers of fibrin and fibrin-enmeshed erythrocytes indicating that this material is an organizing thrombus. Material removed from the exterior of an explanted inflow cannula (C) was histologically determined (D) to be an organizing thrombus arranged in laminations similar to the thrombus in B. Each of these devices had been implanted for over 990 days.

During pre-clinical studies, VADs are implanted into healthy specimens, as pre-clinical trials are often used to determine the safety of a device. The tissue response to an implanted VAD (Figure 17A,B) after 8 days showed a light brown tissue protruding into the ventricle in two areas. This tissue is mostly tan with circular areas of dark brown and lighter brown edges. Histologically, the tip of the tissue extending into the lumen of the ventricle is arranged into distinct layers with incomplete endothelialization at the tip (Figure 17C). Grossly and histologically, this is an area of active thromboegenesis.

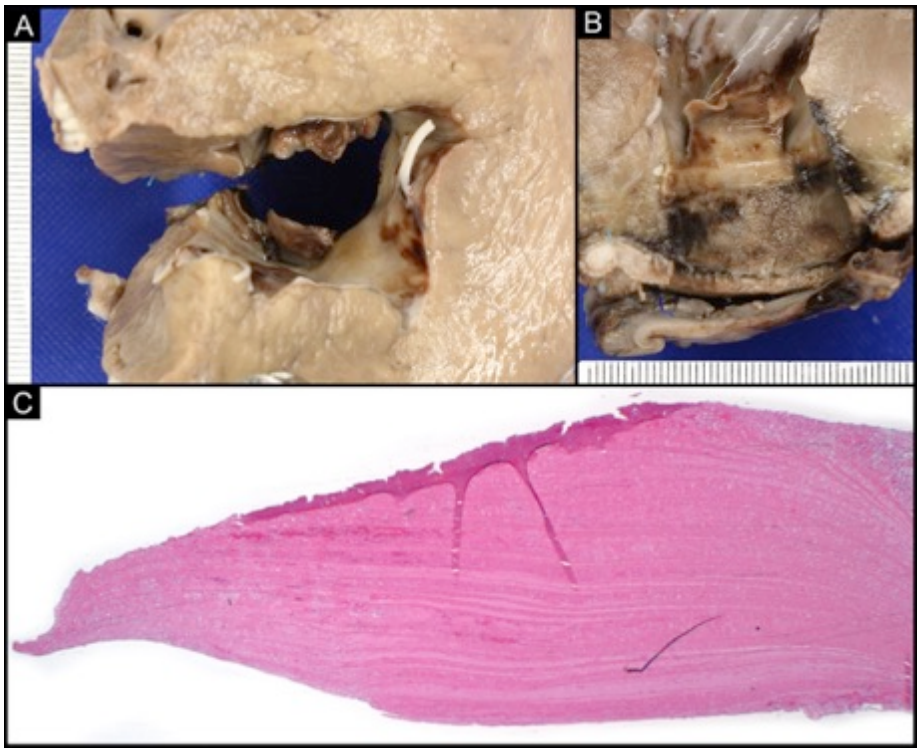

Figure 17. Pre-clinical heart specimen (calf) after VAD removal. A) Cross-section of transected ventricle with inflow cannula removed. B) Lateral view of ventricle with inflow cannula removed. C) H&E stained sections of thrombus collected from inflow region.

5.6 Discussion

5.6.1 Clinical significance

Post-explant blood clots have no clinical significance and often inhibit the pathology evaluation of VADs, making it difficult for the pathologist to distinguish between what happened before and after the pump was explanted. Post-mortem clots, however, may be useful in autopsies for indicating orientation of the device at time of death. The greatest concerns to the pathologist and device manufacturer are ante-mortem thrombi. Thrombi have the potential to disrupt device function, or send emboli downstream that cause life-threatening or debilitating areas of ischemia.

Thrombi inside the pump can lead to increased areas of friction, which causes an increase in power consumption indicated on the VAD controller log [24, 40]. Occlusion of the inflow/outflow cannula will cause low flow. Most VAD companies have algorithms to sound alarms when logs show either increase in power or a decrease in flow rate, which alerts medical professionals to either administer thrombolytics, or in extreme cases, perform a VAD exchange surgery. VAD exchange surgeries can be risky depending on the stability of the patient, and may provide new physical (and monetary) burdens on the patient.

The rigidity and elasticity of the thrombus may change the clinical significance [98] of VAD thrombosis. Different concentrations of viscoelastic components cause the thrombus to react differently to stresses and strains present in the body [99]. Thrombus rigidity and elasticity can also depend on age; older thrombi have had more time for the fibrin strands to cross-link, thus are more compact but are often brittle and prone to fragmenting [98]. The rigidity and elasticity of thrombi will impact how the device or organs sustain thromboembolism; softer

thrombi may be broken up small enough to not cause noticeable clinical changes, but more brittle thrombi will fragment and provide a higher risk of infarct. In the case of axial flow pumps, the upstream thromboemboli can undergo shear and create microemboli to send downstream [98].

5.6.2 Thrombus age

The precise age of a thrombus is difficult to ascertain histologically. As explained previously, a thrombus may develop initially due to platelet activation upon contact with the VAD surface or from shear forces, or may be initiated because of geometry-related blood stasis. As time goes on and the thrombus continues to develop, cellular components (mostly erythrocytes) will collect within the thrombus. In the case of vascular injury, leukocytes will infiltrate the area, eventually replace the clot with new collagen, and effectively heal the injury. However in the case of VAD thrombosis, the constant high flow of blood passing by the thrombus prevents any leukocyte activity from clearing out the thrombus. Consequently, the age of the thrombus is difficult to determine histologically, for active growth (thrombogenesis) at the tip of the thrombus indicates a newly developed (or developing) thrombus, but in fact this thrombus may have been initiated at any time after implant.

5.6.3 Inflow cannula surface

In recent generations of VADs, a textured surface has been added to the inflow surface to decrease the risk of thrombus formation. The textured surface promotes development of a

"pseudointima" along the surface of the device, thus removing the direct connection between the device and the blood [85]. However, this smooth "pseudointima" is not always a perfect solution for eliminating thrombogenesis, and sometimes a thrombus will extend across the sintered surface and on to the smooth surface of the device.

Due to the constant movement of the heart and the circulating blood, active, organizing thrombi around the inflow cannula that protrude into the ventricle present a significant risk for the patient. At the right time they could break off, travel through the pump, and cause damage to the device or become lodged in a downstream organ, causing an ischemic stroke or infarct.

5.6.4 Remodeling of the heart

VADs can be long-term or short-term treatments for HF. With all VADs, the perioperative period presents a significant challenge for clinical management of the patient. Initial interactions between the native heart/cardiovascular system and device can have an effect on device performance [100]; therefore, the patient is carefully monitored for suspected thrombus and other adverse events. After an inclusive review of the VADs evaluated in the Cardiovascular Pathology Laboratory, some long-term implants have organizing thrombi in the ventricle that could easily cause device malfunction or ischemic damage if dislodged. In addition, it is worth re-mentioning that the intended recipients for VADs are patients with dilated cardiomyopathies, patients with enlarged ventricles. In long-term implants, as the VAD takes a significant load off of the heart, the ventricle may remodel [101] which will change the lumen size of the ventricle and alter the flow dynamics within the chamber. The healthy pre-clinical specimen in Figure 17 produced similar changes as those seen from patients with long implant

duration. The re-shaping of the ventricle may be a source for thrombus development putting otherwise long-term successful implants at risk for failure.

5.6.5 Reducing instances of VAD thrombosis

Pathology evaluations alone cannot elucidate more information about the formation of thrombi, for all examinations are post-explant; clinical information about the patient is usually missing and pump data (power usage, flow rates, etc.) are typically unknown to the pathologist at time of evaluation. Understanding VAD thrombosis fully has become a focus in VAD research, and will continue to be a crucial component in expanding the impact of VADs worldwide.

The ventricular insertion site offers a unique opportunity for thrombus formation and potential origin of thromboemboli that requires further research. Depending on the length of implant duration in human cases, the tissue response varies from mild deposition of fibrin along the inflow cannula, to areas of active thrombogenesis.

Therefore, it is important to study the angle and depth of the inflow cannula into dilated and normal sized ventricles to determine if this change can produce thrombus formation. This research could also determine an optimal inflow cannula orientation for decreasing recirculation and stasis of blood, thereby decreasing thrombus formation both during the perioperative period and after the heart remodels. Most computational models of VADs are used during development stages, and show the operation of the device separate from the vasculature. A computational model of VADs *in vivo* (in a ventricle) could help improve pump design and provide physicians with more information about how thrombi form in the ventricle as the implant duration increases [102].

6. EFFECT OF MYOCARDIAL REMODELING ON VENTRICULAR THROMBOSIS DURING LONG-TERM MECHANICAL SUPPORT

Ventricular assist device implantation procedures begin by determining the insertion site of the device. A sewing ring is sewn into either the right ventricle (for a right-VAD [RVAD]) or the left ventricle (for a left-VAD [LVAD]) around the desired position. The myocardium within the center of the sewing ring is removed, and the VAD is then mechanically fastened to the sewing ring. LVAD inflow cannulae are placed within the left ventricle most commonly in either of two positions: on the anterior surface lateral to the apex [103, 104] or on the posterior diaphragmatic surface [105] (Figure 18). The specific insertion site for each VAD model is chosen depending on the surgeon's preference. Despite the varied implantation techniques, a main goal of VAD implantation is to have an unobstructed inflow cannula. If the inflow cannula opening is too close to the septum or the free wall, the inflow may be occluded which will result in device malfunction [91]. Some surgeons recommend orienting the cannula toward the aortic valve [91], while others recommend that the cannula be parallel to the axis of the ventricle chamber (i.e., septal wall) [106]. Inflow cannula placement and orientation are monitored during surgery via transesophageal echocardiography while simultaneously observing pump function (i.e., flow rate) [91]. Before the patient leaves the operating room, if VAD flow rate is not optimal, the inflow cannula may be adjusted by rotating the device [106] or re-entering the pericardial pocket and adjusting the device.

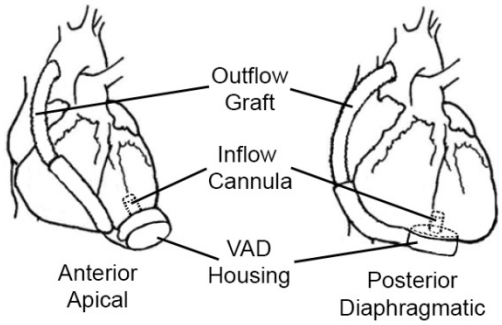

Figure 18. Anterior apical (A) and posterior diaphragmatic (B) options for surgical placement of the VAD inflow cannula within the thoracic cavity.

Inflow cannula position and orientation can also play an important role in thrombosis, a condition with potentially fatal consequences. VAD thrombosis has historically been a concern in VAD therapy, but the incidence of thrombosis has unexpectedly increased since 2011 [36, 107]. VAD thrombosis can significantly increase patient morbidity and mortality unless the pump is replaced or the patient receives a transplant [36]. Thrombi can either pass into the device and cause malfunction, or travel through the pump and cause ischemia-related problems downstream. The presence of the inflow cannula changes the flow dynamics inside the ventricle, and creates new areas of stasis or recirculation of blood around the inflow cannula, which can lead to thrombus formation. In a recent retroactive study performed by Taghavi et al., surgical placement of the HeartMate II (Thoratec Corporation, Pleasanton, CA) inflow cannula less than 55° relative to the center of the device rotor was associated with higher incidence of post-operative pump thrombosis [108]. In this study, the inflow cannula orientation remained constant throughout duration of support. Another study by Truong et al. showed that although a shift in inflow cannula orientation in long-term implants is possible, most patients do not experience a significant shift that would impact VAD function (i.e., obstruct the inflow and cause low flow

rate) [109]. However, instances of cannula misalignment despite correct initial pump placement have been documented for several pump models [101, 110-112].

As discussed in Section 5, patients with dilated cardiomyopathy inherently have increased chances of mural thrombi formation (with or without VAD implantation). After a VAD is implanted, a thrombus may develop initially due to the presence of the device initiating primary hemostasis. Over time, a thrombus may develop in alternating layers of fibrin and erythrocytes extending off of the sewing ring or along the inflow cannula (recall Figure 16). The remodeling of the ventricle throughout sustained VAD support [39] may change the blood flow patterns in the ventricle, which may cause these organizing thrombi to break off, travel into the device, and put otherwise successful long-term implants at a greater risk for failure.

Computational modeling is a beneficial technique for analyzing the effect on flow patterns of inflow and outflow cannulae orientation relative to the shape of the ventricle and aorta [41, 42, 45], as well as analyzing potential designs of new inflow cannula geometries [43, 44]. Computational modeling can also be used to study the areas of stagnation and recirculation inside the ventricle lumen with an attached cannula as the heart remodels from a dilated to a healthy size. This could be used to determine how remodeling of the heart after long-term VAD support will affect thrombus formation and embolization within the ventricle.

In this section, a computational model is described and utilized for determining how a tubular inflow cannula at varied depths and angles in the ventricle affects areas of stasis and recirculation in healthy and dilated sized human hearts. If the VAD implant duration is sustained for several years, cardiac remodeling from a dilated to a smaller shape will change the blood flow patterns within the ventricle and change the potential for organized ventricular thrombi to dislodge and pass into the device. Overall, the goal of this study is to provide information that

will help VAD developers and physicians decrease the amount of blood clotting in and around the inflow cannula to decrease clinical adverse events related to thrombosis.

6.1 Materials and methods

To analyze the effects of cardiac remodeling on blood flow patterns inside the ventricle, healthy and dilated heart geometries were created in a 3D CAD software based off of measurements from human CT data obtained from The Visible Heart Laboratory (University of Minnesota, Twin Cities, MN) and measurements from the literature [113-115]. A simple, tubular inflow cannula similar in size to the HVAD (HeartWare, Inc.) and the HeartMate II (Thoratec Corporation, Pleasanton, CA) was added to the heart geometry in the anterior apical and posterior diaphragmatic positions at three different depths into the ventricle (Figure 19). Commercially available computational fluid dynamics (CFD) software (StarCCM+, CD-adapco) was used to predict the flow patterns present within each geometry.

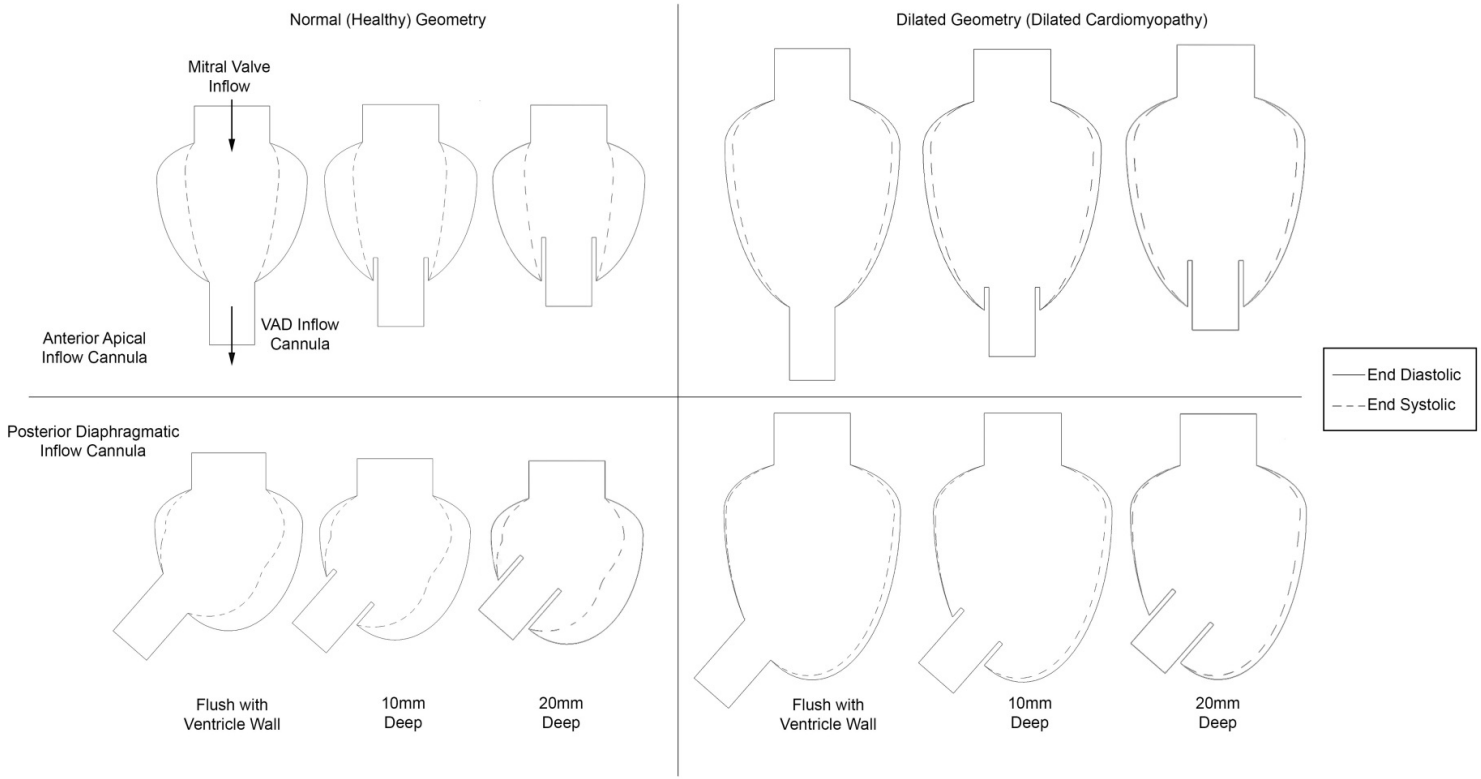

Figure 19. Geometries used for Computational Fluid Dynamics Study.

6.1.1 Geometry

DICOM (digital imaging and communication in medicine) files of a healthy human heart and a heart with dilated cardiomyopathy were imported into a free CT analysis software (OsiriX Imaging Software, Geneva, Switzerland). The following measurements were taken of each left ventricle: longest ventricle depth parallel to the septum measured from the bottom of the mitral valve, length of the septum when the ventricle was the longest, widest internal diameter, and mitral valve width (Table 3). These patient-specific measurements were used to generate idealized geometries of both an average and a dilated adult male left ventricle in a 3D CAD software (SOLIDWORKS, Dassault Systèmes SolidWorks Corporation, Waltham, MA) with the inflow cannula at different depths in anterior apical and posterior diaphragmatic orientations. A 2D slice was taken across the midline of the inflow cannula in each model (Figure 19) for CFD modeling.

Table 3. Measurements of healthy and dilated heart

	End Diastole		End Systole	
Measurements from Literature/CT Data	"Healthy" Heart	Dilated Cardiomyopathy	"Healthy" Heart	Dilated Cardiomyopathy
Longest ventricle depth (parallel to the septum)	6.88cm	7.75cm	N/A	N/A
Length of septum	N/A	8.3 +/- 1.2cm**	N/A	8.3 +/- 1.2cm**
Widest internal diameter	6.83	7.1 +/- 1.1cm**	3.37 +/- 3.7cm***	6.4 +/- 1.2cm**
Mitral valve width	3.0-3.5cm[+]	3.37cm	3.0-3.5cm[+]	N/A
Generalized Measurements for Model Geometry				
Maximum diameter	6.7cm	7.7cm	4.7cm	7.2cm
Maximum length	6.6cm	9.6cm	6.0cm*	9.4cm*
Mitral valve width	3.3cm	3.3cm	3.3cm	3.3cm
Inflow cannula inner diameter	2cm	2cm	2cm	2cm

*These measurements are for geometries involving the posterior diaphragmatic cannula placement only. For the anterior apical placement, the length of the ventricle did not change.
**Measurements from Douglas et al., Table 1. [113]
***Measurements from Semelka et al., Table 3. [114]
[+]Measurements taken from e-Echochardiography, An Echocardiography and Ultrasound Learning Resource [115]

6.1.2 CFD modeling

CFD was used to determine the regions of stasis and recirculation for each 2D geometry. The 2D mesh for each geometry had a base cell size of 0.375mm, and a 6-cell deep prism layer at each boundary. Each simulation incorporated laminar flow of a Newtonian fluid with a constant density of 1060 kg/m^3 [116] and constant viscosity of 3.5E-3 Pa-S (common value for blood analogs when assuming a Newtonian fluid at high shear rates, such as those present in the heart [117]). The inlet condition was uniform across the mitral valve boundary and set at a constant rate of 0.11489 m/s, which corresponds to a flow rate of 6 LPM (typical cardiac output) through a tube with diameter of 3.3cm. The motion of the ventricle walls was prescribed with mesh morphing. The initial geometry represented end diastole; then the walls contracted toward the center (end systole) and expanded back to the original geometry in a periodic fashion according to a sinusoidal waveform (time step of 0.01s, period of 1s). The motion of each wall was defined by equations in Appendix II. For the dilated hearts, the ejection fraction ranged from approximately 9-17%, while the ejection fraction for remodeled hearts ranged from approximately 40-56%. Each simulation ran for 17s (i.e., 17 contractions).

6.1.3 Data analysis

Each simulation ran for five complete ventricular contractions before data collection began to allow the solution to stabilize. Areas of stagnation were analyzed by collecting residence time values: at each time step, each cell within the mesh was given a value for length

of time the fluid had been in that cell. The residence time values were exported into a spreadsheet and then processed in MATLAB.

The ability of the ventricle to clear the blood from the chamber was measured by virtually injecting a dye uniformly across the mitral valve opening for 2 complete cycles. The dye highlighted areas of recirculation and stagnation inside the ventricle. Additionally, vorticity values within the chamber were analyzed to further identify recirculation zones.

6.2 Results

6.2.1 Stagnation – residence times

Overall, the ventricles with inflow cannula flush with the apex and in-line with the mitral valve had the least areas with residence times greater than 10 seconds (i.e., smaller areas of stagnation) after 12 seconds of simulation (Figure 20, indicated by areas of orange-red). Only

a thin layer of blood remained along the wall of the dilated ventricle throughout the simulation (Figure 20A.1); in the remodeled, smaller sized ventricle (Figure 20A.2) the stagnant areas were smaller and limited to the wall region on either side of the mitral valve. The inflow cannulae implanted at greater depths into the ventricle yielded increasing areas of stagnation around the inflow cannula (Figure 20B.1-C.2).

Overall, the dilated ventricle with inflow cannula flush with the wall and at an angle to the mitral valve showed the greatest areas of stagnation (after 12 seconds) (Figure 21). In this geometry, the area of stagnation was opposite the VAD inflow cannula, next to the mitral valve (Figure 21A.1). Deeper cannula depths resulted in a reduced area of stagnation near the mitral valve, but also resulted in areas of stagnation surrounding the cannula (Figure 21C.1). When comparing the remodeled to the dilated ventricles, the areas of stagnation decreased when the cannula was flush with the lumen and was at a depth of 10mm (Figure 21A.2, B.2), but the overall area of stationary blood increased slightly in the remodeled ventricle when the cannula was inserted 20mm into the lumen (Figure 21C.2).

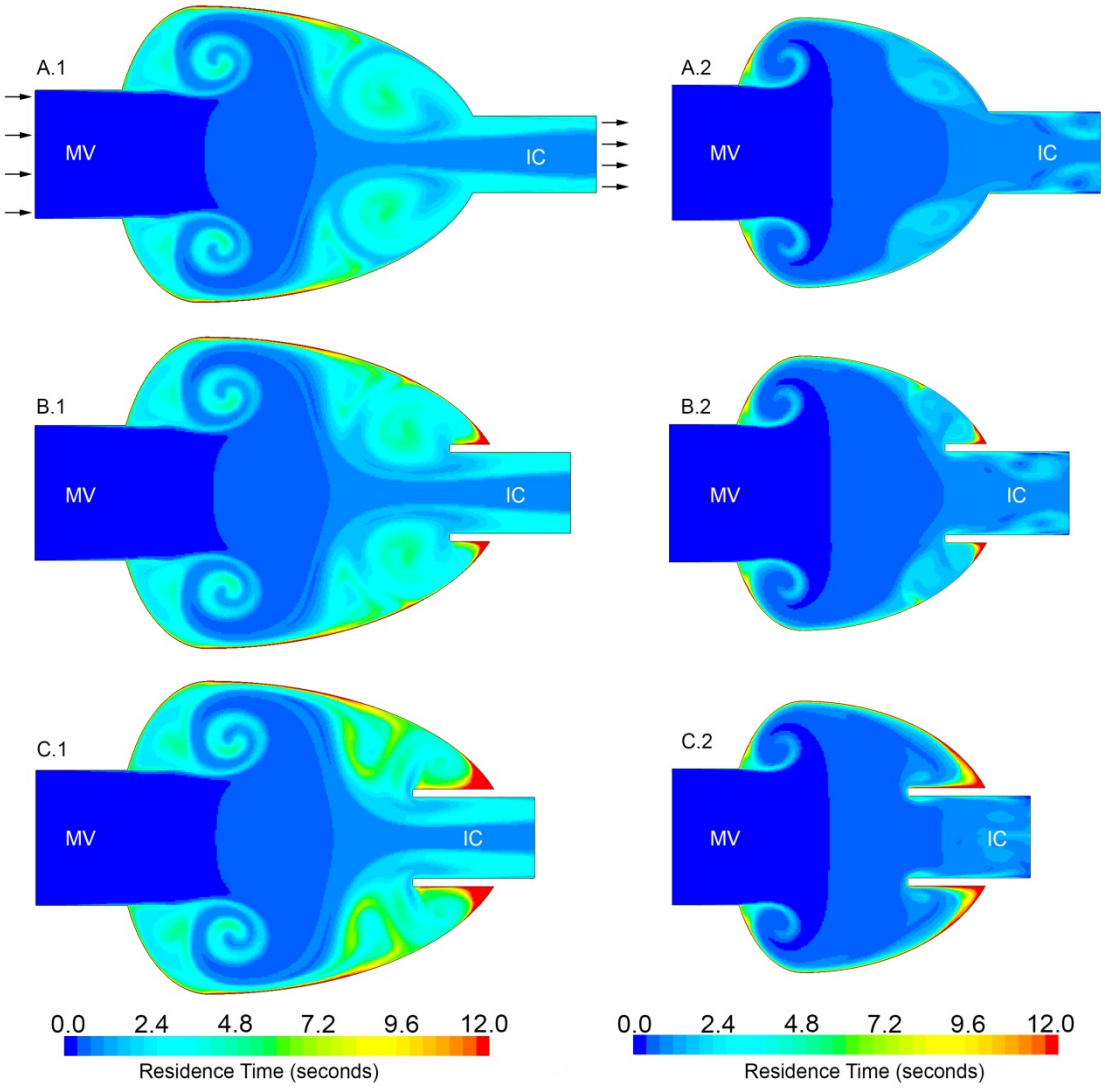

Figure 20. Residence times values (at end diastole) after 12 contractions for dilated and remodeled ventricles with inflow cannula in-line with the mitral valve. The inflow is uniform across the mitral valve (MV) boundary and outflow passively flowing out of the VAD inflow cannula (IC). Dilated (1) and remodeled ventricles (2) with IC in the anterior apical placement flush with the wall (A), protruding 10mm into the lumen (B), and protruding 20mm (C).

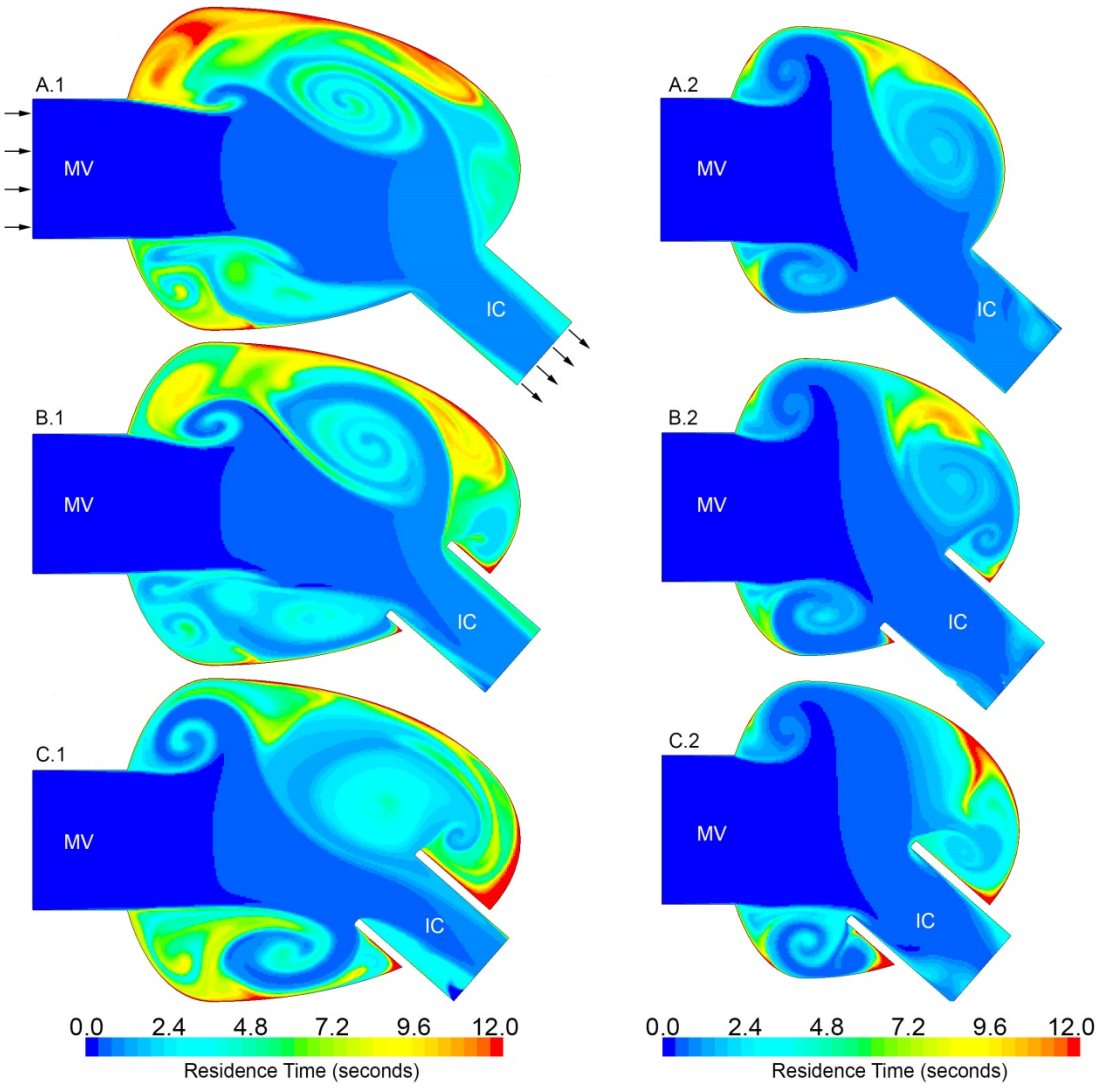

Figure 21. Residence times values (at end diastole) after 12 contractions for dilated and remodeled ventricles with inflow cannula at an angle to the mitral valve. The inflow is uniform across the mitral valve (MV) boundary and outflow passively flowing out of the VAD inflow cannula (IC). Dilated (1) and remodeled ventricles (2) with IC in the posterior diaphragmatic placement flush with the wall (A), protruding 10mm into the lumen (B), and protruding 20mm (C).

To quantify and compare the residence time for each of the geometries, the total area within the chamber with residence times exceeding a certain threshold at each time step was analyzed. This area-sum was normalized by the total area across the entire domain. These values, when plotted against time (in seconds), remained zero until the threshold was reached, then increased to a certain area value, where it remained asymptotic around a certain area. This asymptotic area value was obtained for each threshold and displayed in Figure 22. A threshold of 3 to 7s was chosen to make sure that each data point contained at least 5 cardiac cycles worth of data.

The anterior apical (straight) cannula placement (Figure 22A) showed a large difference between the dilated and remodeled geometries at a threshold of 3-5s. The average residence time values for both the dilated and remodeled ventricles did not change much between the flush and 10mm depth, but significantly increased when the cannula depth changed from 10mm to 20mm. After the 5s threshold, the cannula in-line with the mitral valve at a depth of 20mm into the lumen has the greatest residence time values regardless of dilated or remodeled geometry.

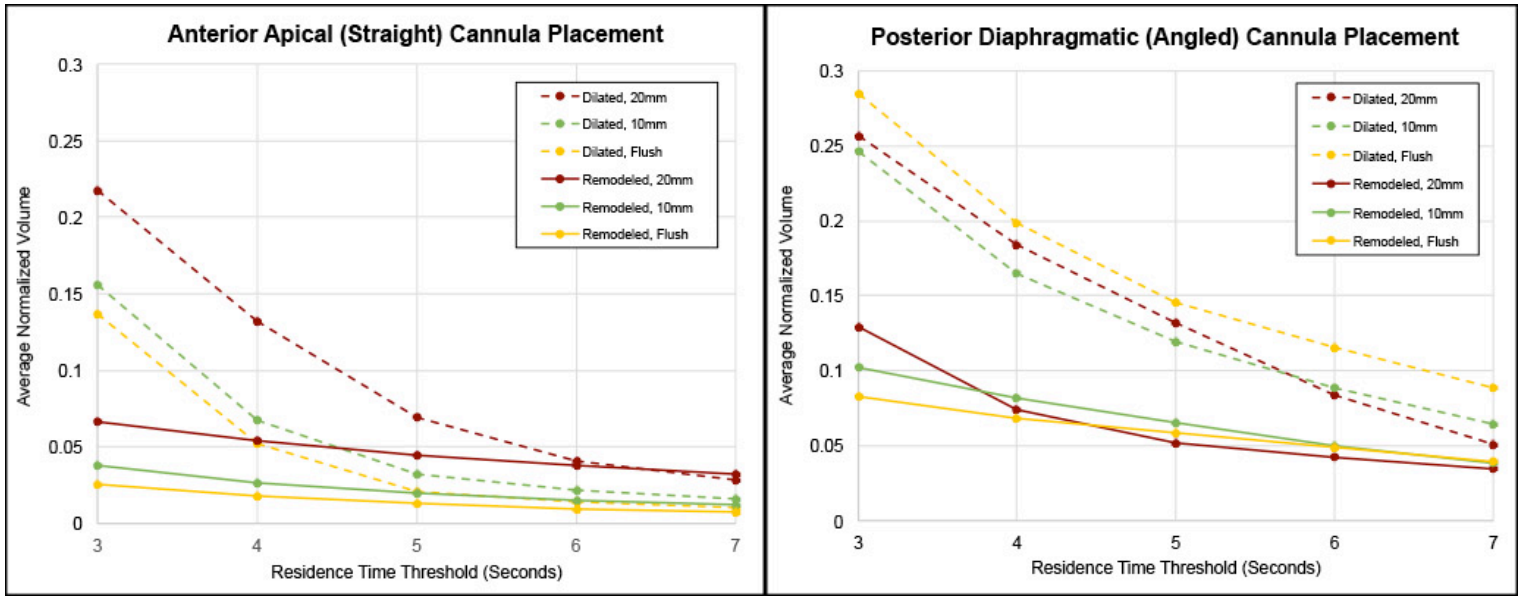

Figure 22. Average normalized volume with residence times that exceeded thresholds ranging from 3-7 seconds. The horizontal axis shows the residence times (in seconds) and the vertical axis shows the normalized volume.

For the posterior diaphragmatic cannula placement (Figure 22B), the dilated geometries consistently showed greater areas with longest residence time values. Within the same lumen size, there was not a significant difference in residence time values when the depth of the cannula increased. The dilated ventricle with cannula flush with the wall had the greatest areas with increased residence times when compared to the other cannula depths in dilated ventricles.

6.2.2 Ventricular washout

When the inflow cannula was in-line with the mitral valve, as the ventricle contracted toward the center, the majority of the fluid moved in a straight line directly from the mitral valve to the cannula (Figure 23A). As the walls relaxed, the dye that remained circled around in the pockets along the upper and lower boundary walls (Figure 23A). When the inflow cannula was at an angle to the mitral valve, the dye entering the chamber that did not directly go out of the

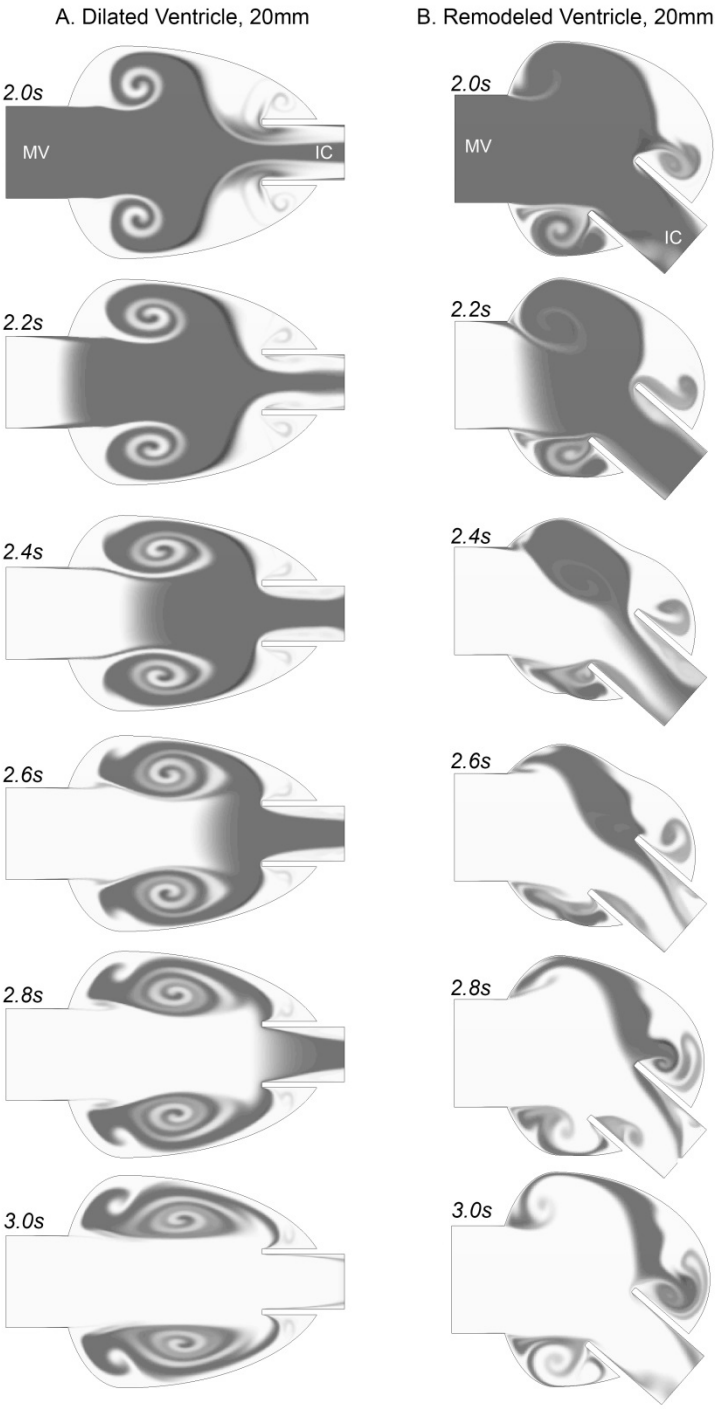

Figure 23. Snapshots of dye washing through dilated (left) and remodeled (right) ventricles throughout one cardiac cycle.

cannula swirled around in a large pocket near the upper boundary and a smaller pocket near the lower boundary (Figure 23B).

After each contraction there was less remnant dye until most had been cleared out after 12 contractions (Figure 24-Figure 25). In the ventricles with inflow cannula in-line with the mitral valve, the dye cleared the remodeled chamber (Figure 24B) faster than the dilated ventricle (Figure 24A). The dilated heart with inflow cannula at an angle to the mitral valve (Figure 25A) had the most residual dye remaining in the ventricle after 12 contraction. The remodeled geometry with cannula at an angle to the mitral valve (Figure 25B) also showed increased residual dye after each contraction when compared to the simulations with cannula in line with the mitral valve, but not as much as the dilated geometry.

Figure 26 shows the extent to which the dye had washed out of each ventricle after 12 contractions. The remodeled heart with the straight cannula was the only geometry where the dye had completely washed out within this time frame. The dilated heart with angled cannula had the greatest amount of residual dye in the ventricle within this time frame.

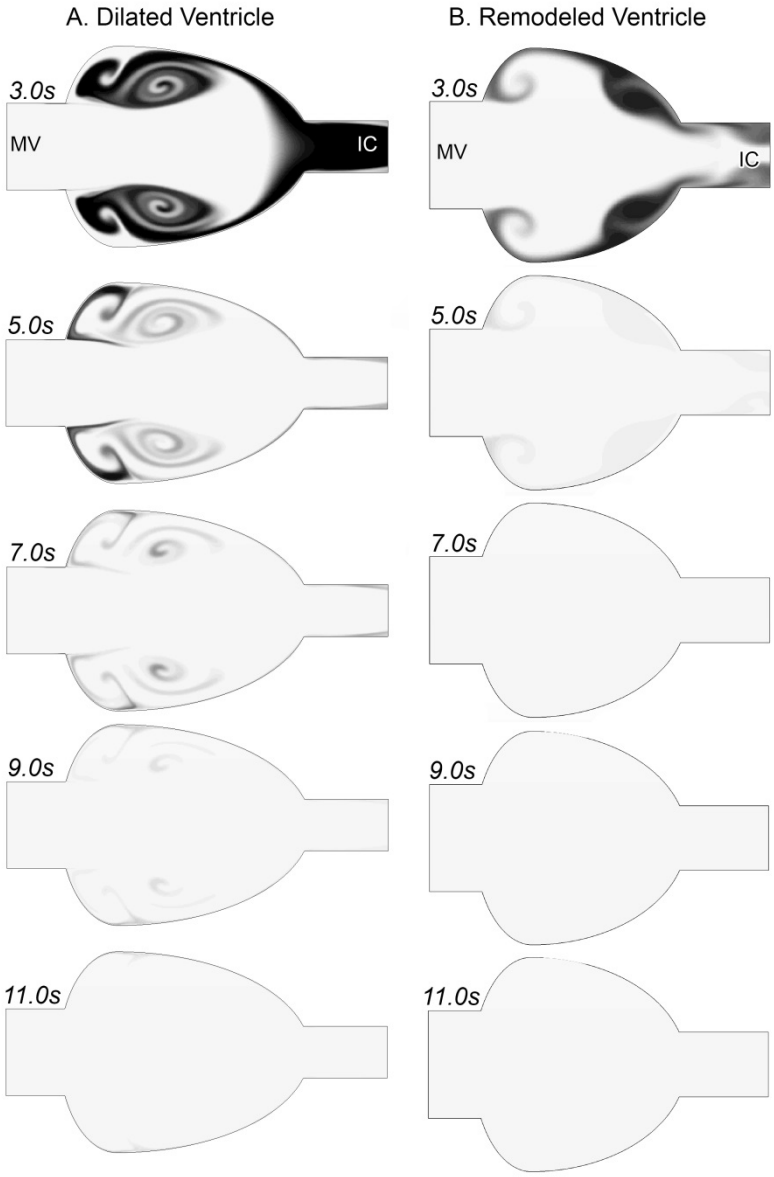

Figure 24. Snapshots of dye washing through dilated (left) and remodeled (right) ventricles with inflow cannula placed in the anterior apical placement.

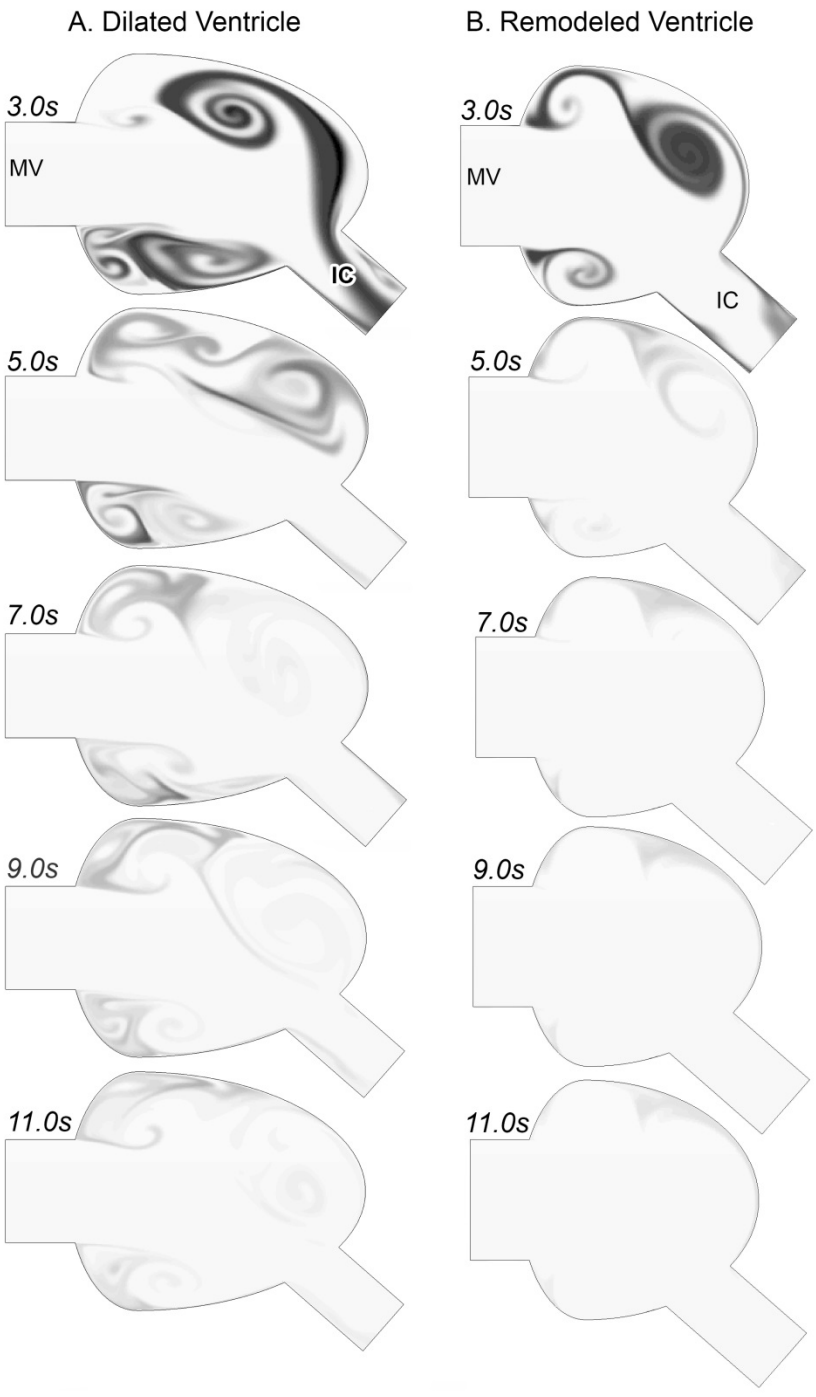

Figure 25. Snapshots of dye washing through dilated (left) and remodeled (right) ventricles with inflow cannula placed in the posterior diaphragmatic placement.

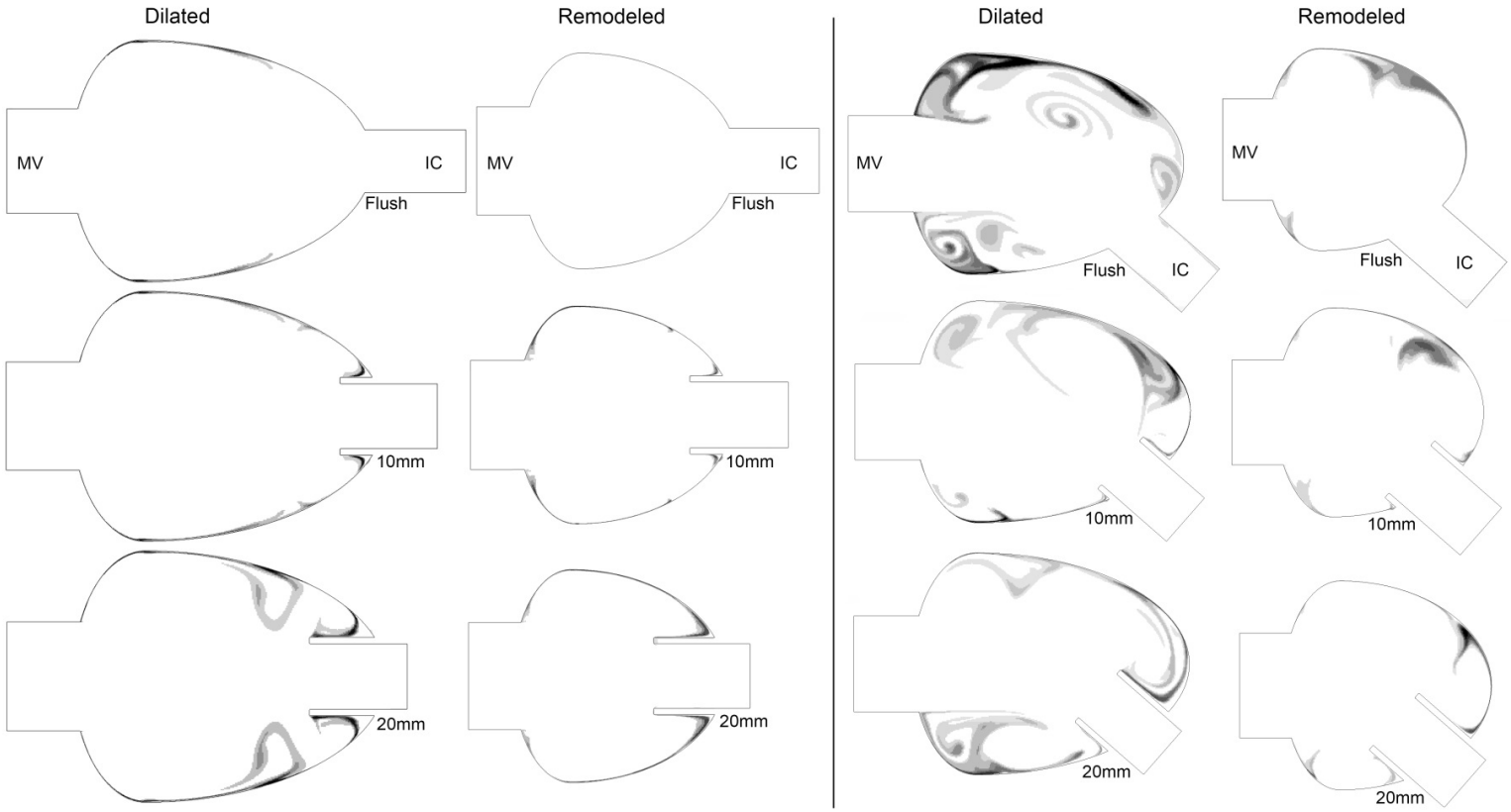

Figure 26. Residual dye in the ventricle after 12 contractions.

6.2.3 Recirculation zones – vorticity

Ventricles with a cannula implanted in the anterior apical placement had vorticity values mostly symmetric across the midline (Figure 27A). When the cannula was implanted in the remodeled ventricle at a depth of 20mm, the recirculation zone in the mitral valve pocket was pushed through the cannula with each contraction, whereas when the cannula was either flush with the wall or at a depth of 10mm, this pocket of recirculation did not leave the ventricle until after two contractions. When the cannula protrudes into the ventricle, a small recirculation zone appears at the cannula/apex interface. The dilated hearts had larger pockets of recirculation toward the periphery of the chamber. These pockets moved across the lumen slower than in the remodeled hearts, throughout the duration of three or four contractions. Deeper cannula insertion in the lumen created larger recirculation zones at the apex/cannula interface than appeared in the remodeled ventricles.

The ventricles with cannula at an angle to the mitral valve had three main regions that developed recirculation zones: along the top wall near the mitral valve, along the apex near the cannula, and along the bottom wall between the mitral valve and the cannula (Figure 27B). When the ventricle was relaxing, a small recirculation zone was created next to the wall of the cannula (arrow); this zone was circulating in the opposite direction as the zones along the top wall created from the mitral valve inlet. In the dilated hearts, the zones of recirculation were larger and took three or four cycles to leave the chamber, whereas the remodeled hearts had smaller recirculation zones that moved through the cannula after two contractions.

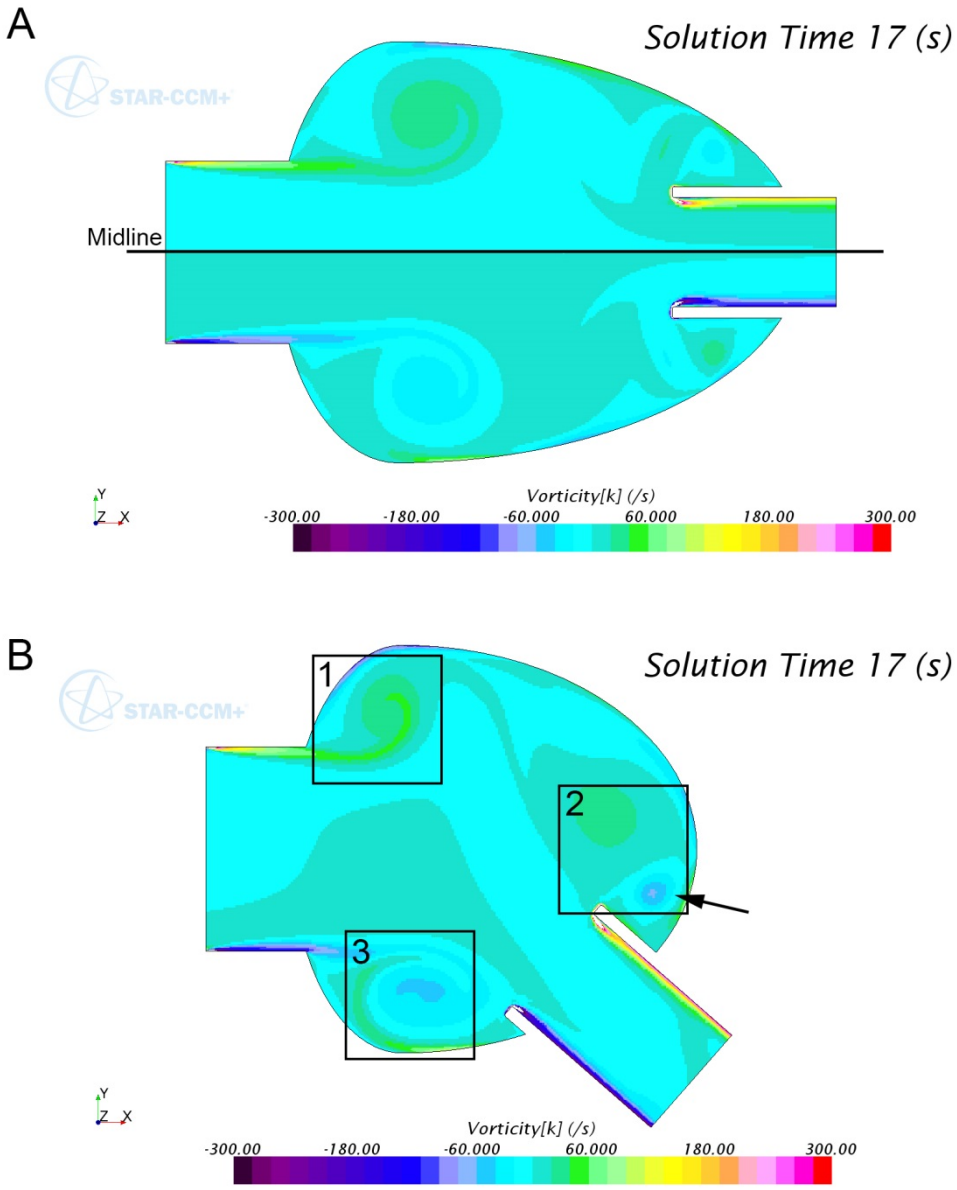

Figure 27. The z-component of vorticity values for dilated ventricle with inflow cannula in line with the mitral valve inflow (A) and at an angle to the mitral valve (B). The black squares indicate areas of interest within the chamber: 1) Upper boundary near the mitral valve inlet; 2) Apex/cannula interface; arrow indicates the recirculation zone created as the ventricle relaxes; 3) Lower boundary between mitral valve and cannula.

6.3 Discussion

Because VADs are mostly implanted in patients with dilated cardiomyopathy, the purpose of this study was to first determine an optimal VAD inflow cannula orientation and depth that will reduce areas of stagnation and recirculation inside dilated ventricles. Secondarily, as sustained mechanical support is likely to lead to myocardial remodeling, a second focus of this study was to highlight the change in flow patterns of ventricles after remodeling occurs. A complete review of the study results has revealed a possible clinical application and design recommendation that could reduce risk of thromboembolic complications in future VAD patients.

6.3.1 Inflow cannula placement in DCM patients

In a heart with dilated cardiomyopathy, the ventricular wall is thin, and the lumen has expanded in volume due to prolonged stretching of cardiomyocytes. These morphological changes arise over time after an initial insult to the myocardium renders it weak, preventing the ventricular contraction from generating the ejection fraction necessary for adequate downstream organ perfusion, leading to blood pooling in the heart. Over time, this buildup of blood causes the myocardium to dilate further and become weaker. The main goal of VAD implantation is to take the load off of the heart and to bring the heart back to the proper ejection fraction the body needs.

In dilated hearts, when the inflow cannula is flush with the lumen and in-line with the mitral valve inflow, there are fewer places for the blood to pool in the ventricle. Out of all the geometries studied, this orientation (anterior apical placement) had the smallest regions of

stagnation throughout the chamber after 12 heart contractions. As the inflow cannula depth increases further into the lumen of the ventricle, the areas of "trapped" blood at the apex/cannula interface increases in size (see areas of orange-red in Figure 20B.1, Figure 20C.1). In contrast, when a dilated heart has a VAD implanted at an angle to the mitral valve (posterior diaphragmatic placement), a depth of 10mm into the lumen is more optimal than flush alignment with the ventricle wall. When there is some protrusion into the lumen (10mm), as the wall contracts it pushes blood against the cannula and provides a greater force to flush the blood out of the crevice between the apex and the cannula (Figure 21B.1). When the cannula is too deep into the lumen (20mm), it is easier for the fluid to get trapped into recirculation zones near the apex/cannula crevice (Figure 21C.1). When the cannula is flush with the wall and at an angle to the mitral valve (Figure 21A.1), the blood entering the ventricle is more likely to get trapped in the pocket along the upper boundary near the mitral valve because the contraction is not strong enough to push the blood toward the cannula inlet, which is now further away. In this configuration, the area of stagnation near the mitral valve is larger in size than the stagnant region created by inserting the inflow cannula into the ventricle at either depth.

All of the dilated ventricles tested in this study had pockets next to the mitral valve and around the inflow cannula with higher levels of recirculation, vorticity, and greater residence times, furthering the hypothesis that dilated hearts are more susceptible to the formation of mural thrombi, as well as thrombus formation along the base of the inflow cannula. Over time, the thrombus will continue to organize and, if it dislodges, will increase the chances of causing greater mechanical failure.

6.3.2 Ventricular remodeling with VADs

As myocardial offloading persists, the volume of blood inside the ventricle decreases, and the myocytes will remodel to their shorter length, effectively decreasing the lumen size. Throughout ventricular remodeling, it is possible that the inflow cannula will change its orientation; however, as mentioned previously, most patients do not experience a significant shift in inflow cannula orientation over time [109]. According to the results of the current study, if there is not a significant shift in inflow cannula orientation but the heart itself remodels to a smaller shape, the flow patterns will be different in the remodeled heart than those present immediately post-implant.

As expected, for each geometry tested, the smaller, healthy-sized ventricles had improved washout compared to their dilated counterparts after fewer contractions. If a thrombus began organizing while the heart was in a dilated state, as the heart remodels, the increased washout combined with the greater force of contraction will increase the risk of dislodging the thrombus and sending it into the pump.

6.3.3 Clinical application

Myocardial remodeling in long-term VAD implants is not currently monitored or tracked for each patient while undergoing VAD therapy. VAD function is closely monitored during and immediately after implantation; throughout the duration of support, controllers accompanying the device monitor parameters such as flow rate, impeller RPM, and wattage, and will sound alarms if these parameters exceed an acceptable range. VAD position and orientation are investigated only if the controller indicates low flow or high power consumption, which may

mean a material is obstructing the inflow/outflow, or a thrombus may be inside the pump. Based on the results of this study, for long-term implants it could prove beneficial to periodically determine the degree to which the heart has remodeled and thus how much the change in lumen size and strength of contraction is likely to displace existing thrombi. Administering thrombolytics could be beneficial at certain times of the implant duration to decrease risk of thromboembolic related complications.

6.3.4 VAD design

The results of this study show that inserting the inflow cannula into the ventricle lumen creates areas for stagnation immediately surrounding the cannula. In the simplified motion modeled in this study, these regions are never fully washed out with each heartbeat, providing opportunity for thrombus formation. It may be possible that decreasing the cannula length can decrease the regions of stagnation in the chamber and increase the washout after each ventricular contraction. Further research is needed to determine if decreasing the length of the inflow cannula is a probable design change to proactively prevent inflow cannula thrombus formation.

6.3.5 Study limitations and future applications

This study only incorporated a 2D representation of a left ventricle with mitral valve inlet and a VAD cannula, where the flow out of the cannula was passive and did not have the suction effect as it would *in vivo*. This model did not include the aortic valve outflow. Although flow through the aortic valve is limited during VAD support [118], aortic valve output should to

be added in a 3D model. Additionally, the movement of the ventricle was simplified and did not represent the physiologic wringing motion of the heart. The flow into the mitral valve opening was constant across the length of the wall, and not pulsatile as it is *in vivo*. The inflow cannula remained stationary throughout the simulation, whereas in reality there should be minor movements with each heartbeat. Finally, the clotting factors and platelet activity were not factored into the simulation; however, this may not be an issue because patients are typically put on anticoagulants to decrease the function of these clotting components. Although this study has physiologic limitations, this model can be used to draw comparisons between the inflow cannula orientations and depths in dilated and remodeled sizes as the same limitations are applied to all models. This model will serve as a preliminary study to build upon in order to expand its clinical accuracy and significance. This model can be expanded to incorporate more complex geometries and motions of a 3D representation. Ideally, this computational model can be personalized for each patient to determine which orientation of the inflow cannula is best for his or her specific heart geometry. This personalized treatment option could incorporate a 3D model derived from patient CT data.

6.4 Conclusion

As VADs transition from a temporary to long-term treatment option for heart failure, new questions are arising surrounding how cardiac remodeling affects VAD function. The study described in this section serves as a preliminary platform for investigating the risk of thrombus formation inside a dilated left ventricle after VAD implantation, and possible thrombus dislodgement after the myocardium undergoes remodeling. The study showed that there might be an optimal cannula depth that minimizes the risk of thromboembolism. This study involving a

simplified geometry and simplified motion revealed that placing the VAD inflow cannula in-line with the mitral valve inlet (anterior apical placement) and flush with the ventricle wall will result in the shortest residence times and greatest washout of dilated ventricles. Placing the cannula at an angle to the mitral valve (posterior diaphragmatic placement) results in greater areas of stagnation; however, if patient anatomy prevents flexibility in choosing VAD cannula insertion site and only allows for posterior diaphragmatic placement, a cannula depth between flush and 20mm may be optimal for providing the best washout and shortest residence times within the ventricle.

The remodeled ventricles in this study showed improved washout and smaller recirculation zones compared to their dilated versions. The increased washout may change the possibility of thrombi that formed and developed when the heart was in its dilated state to dislodge and travel into the pump. In clinical management of patients with VADs, the orientation of the inflow cannula and ventricular lumen size are only monitored if a period of low flow or high power consumption is noted on the VAD controller; the results of this study suggest that monitoring myocardial remodeling periodically as the patient receives mechanical support could improve the value of VAD therapy by decreasing the risk of thromboembolic complications. Additional investigation as to how the length of the cannula can affect thrombus formation inside the ventricle may also prove beneficial to VAD therapy. Overall, these considerations in VAD development and clinical application may decrease the amount of clinical adverse events related to thrombus formation and embolization.

While these considerations may reduce thromboembolic events, thromboembolism is still possible any time a VAD is implanted, and VADs should be tested during bench-top design concept testing for toleration of embolic particles. Current *in vitro* testing of VADs includes durability and hemocompatibility testing; these tests answer questions such as: how long will the

device last under normal working conditions? Will this device lyse red blood cells? Does this device produce sufficient flow rates to keep up with required cardiac output? These tests are crucial and should not missed in the development process. However, *in vitro* testing could be taken a step further to answer questions about VAD thrombosis. How does the VAD controller log respond to pass-through thrombi? How does the size of the thrombus change the VAD response? The remaining sections introduce a method for creating artificial thrombi and a controlled environment for testing VAD thrombosis. We believe this research, together with the computational model in this section, will translate to clinical VADs used worldwide and will overall add to the therapeutic value of receiving a VAD for heart failure treatment.

7. CREATING ARTIFICIAL THROMBI*

Clot and thrombus formation have been studied *in vitro* with both continuous and pulsatile flow conditions [51, 52, 119]. These studies characterize the thrombus formation morphology in specific locations and geometries based on length, speed, and type of flow and material surface. Taylor et al. demonstrated areas of high wall shear stresses leads to larger thrombus formation, and multiple studies have shown areas of low flow are more likely to cause platelet activation leading to formation of loosely adhered thrombi [52, 86, 87, 120]. Loosely adhered thrombi *in vivo* have a greater potential to dislodge and introduce thromboembolism. Introducing a textured surface in the blood has been shown to reduce platelet adhesion and thus reduce thrombus formation, however thrombus formation is not completely diminished [52, 87].

VADs are typically tested prior to pre-clinical trials with *in vitro* circulatory loops [46, 47]; however, these are designed to specifically test the hemodynamic conditions of the device. Precise VAD response to thromboembolism needs to be studied in a controlled *in vitro* setting where specific pump parameters (i.e., power consumption, flow rates, impeller RPM) can be monitored while various types of thrombi are introduced. This section describes a novel method for creating standardized fibrin thrombi that could be introduced into a mock circulatory loop for testing VAD response to pass-through thromboembolism. Complete results from experiments pertaining to this section are detailed in Appendix III.

---

*This section's text and figures are reprinted with permission from "A method for creating artificial thrombi *in vitro* using a rotating mechanical surface" by Jessen SL, et. al., 2016. *ASAIO J*, Publish-ahead-of-print (DOI: 10.1097/MAT.0000000000000332) by Wolters Kluwer Health Lippincott Williams & Wilkins©.

7.1 Materials and methods

Normal equine blood was originally collected for transfusion in commercial 450mL blood storage bags containing sodium citrate and stored at 5°C. Blood stored beyond its usable date for transfusions was made available to this experiment. The blood in all experiments mentioned in this paper was collected from the same donor approximately three months prior to use.

Approximately half of the citrated whole blood was collected into 5mL aliquots. The remaining blood was transferred from the blood bag to a plastic container with a screw-top lid and stored at 5°C. Due to the high sedimentation rate of equine blood [121, 122], the cells collected at the bottom of the container and the cell-free plasma top layer was collected using pipettes and stored in 5mL aliquots. For superior red blood cell sedimentation, it is best to let the blood sit undisturbed for approximately 24 hours before removing the plasma layer [123]. To preserve the blood components and ensure success of creating consistent thrombi, 5mL volumes of whole blood and plasma were put into separate vials and stored in a 5°C refrigerator and -20°C freezer, respectively. Approximately 24 hours before plasma clot creation, the plasma was transferred to the 5°C refrigerator and allowed to thaw.

7.1.1 Titration of $CaCl_2$

To initiate clotting by counteracting the sodium citrate effect, calcium chloride ($CaCl_2$) was added to the blood. Approximately 5mL each of either equine whole blood or plasma were collected into separate test tubes. Granular, dihydrate $CaCl_2$ (Macron Fine Chemicals^{TM}) was dissolved in distilled water at a concentration of 12mg/mL [124]. Approximately 50μL of the

$CaCl_2$ solution was added to each test tube, once per minute starting at time t = 0. After each drop was added, the test tube was tilted to test the coagulation of the blood and plasma. Once the test tube could be tilted at a 45° angle without disruption of the liquid, the titration was complete and the time and total volume of $CaCl_2$ added were recorded and used for the following experiments.

7.1.2 Adding the rotational component

To mimic the forces and conditions inside a VAD *in vivo*, small plastic petri dishes (Corning, Inc., 38mm diameter) were affixed to the shafts of electric and gear motors (four total) with 3M™ Dual Lock Reclosable Fastener. This apparatus was arranged so the petri dish rotated inside a larger stationary petri dish (Corning, Inc., 50mm diameter) with an adjustable gap between the dishes (Figure 28). Each motor was powered by a variable power supply ranging from 0–12V and produced speeds ranging from 75–300 RPM.

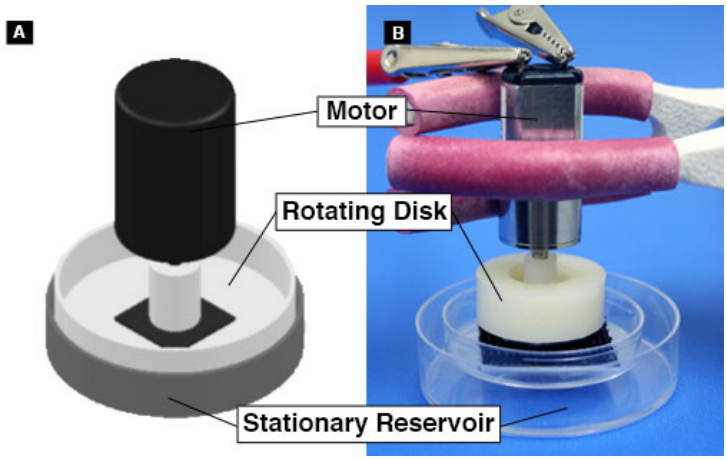

Figure 28. Diagram (A) and photograph (B) of the device used to create thrombi.

7.1.3 Creation of thrombi

Multiple clots were created with the setup shown in Figure 28 testing the following parameters: 1) $CaCl_2$ concentration, 2) gap size between rotating disk and stationary reservoir, 3) RPM, and 4) duration of rotation. For all experiments, both the rotating and stationary petri dishes were lined with disposable aluminum foil. After each experiment, clots remained stationary for approximately 18 hours to maximize clot condensation. Clots were then carefully removed from the aluminum foil and placed in formalin for at least 24 hours. Formalin-fixed clots were then sectioned to fit in a 2.5x2.5cm cassette and processed for traditional paraffin histology and scanning electron microscopy (SEM) to characterize the microstructure [125]. Histology sections were stained with Hematoxylin and Eosin (H&E). Clots examined by SEM were dehydrated in progressively increasing concentrations of alcohol (following 24 hour formalin fixation), coated with gold using a Ted Pella 108 Manual Sputter Coater, and finally imaged using a Tabletop Hitachi TM3000 Scanning Electron Microscope.

7.1.3.1 Adjusting the concentration of $CaCl_2$

In order to determine the optimal volume and concentration of $CaCl_2$ necessary for clotting of citrated whole blood and plasma, thrombi were created using two concentrations of $CaCl_2$: 12 and 24mg $CaCl_2$/mL distilled water. This will also reveal if different concentrations of $CaCl_2$ introduce artifactual histologic differences in the morphology of the clots. Approximately 5mL of whole blood and plasma were collected in stationary test tubes; 0.15mL of $CaCl_2$ was added every 3 minutes until clotting was observed. The clotting blood and plasma remained stationary for approximately 18 hours to maximize clot condensation before collection and formalin fixation.

7.1.3.2 Adjusting the gap height

The distance between the rotating disk and stationary reservoir was set at approximately 6mm (+/- 1mm) and 4mm (+/- 0.2mm). The distance was set by raising the rotating component and measured with calipers. The motors ran for approximately 6 hours then the resulting thrombi were collected and fixed in formalin.

7.1.3.3 Adjusting the speed and duration of rotation

In this set of experiments, the motor speed and total time rotating were varied. For this set, all four motors were attached to power sources with similar distances between the rotating disk and stationary reservoir (4mm +/- 0.2mm). Motors were set to 75, 225, 240 and 300 RPM

and ran for approximately 6-48 hours. After the allotted time period, the clots were left undisturbed for approximately 4-6 hours before collection and formalin fixation.

7.1.3.4 Clot image analysis

H&E stained sections of clot were photographed using a microscope camera and images were read by a program in MATLAB (MathWorks, Inc., Natick, MA) to analyze the clot density by determining the percentage of the pixels in the picture that contained clot. Each image analyzed contained a consistent square area of clot. Additionally, area and length measurements were collected using open-source imaging software (ImageJ, National Institute of Health).

7.2 Results

7.2.1 $CaCl_2$ concentration

The volumes and concentrations of $CaCl_2$ needed to initiate clotting in whole blood and plasma are represented in Table 4.

Table 4. Volumes and concentrations of $CaCl_2$ necessary for clotting

	12 mg $CaCl_2$/mL	24 mg $CaCl_2$/mL
5 mL whole blood	1.2mL	0.6mL
5 mL plasma	2.2mL	1.1mL

Using a relatively dilute $CaCl_2$ solution required the addition of a greater volume of solution to the blood and plasma to facilitate clotting. The liquid completely clotted in the test tube after addition of $CaCl_2$. Grossly, the clots were cylindrically shaped gelatinous, either yellow (plasma) or dark red (whole blood) material. Figure 29 shows the H&E stained sections of each clot (whole blood and plasma) at different concentrations of $CaCl_2$. Figure 29A and Figure 29B (whole blood) show a dominance of red blood cells, while Figure 29C and Figure 29D (plasma) show primarily a uniform network of fibrin. Histologically, there are no apparent differences between the clots created from different $CaCl_2$ concentrations. Computational image analysis in MATLAB also reveals no significant differences between the two clotting methods; images of randomly select areas of each clot had a density (measured as the percentage of colored pixels) that only varied by less than 3.10% for both plasma and whole blood clots. Thus, a higher concentration of $CaCl_2$ was used for the remaining experiments because the smaller stationary reservoirs limited the amount of liquid that could be added.

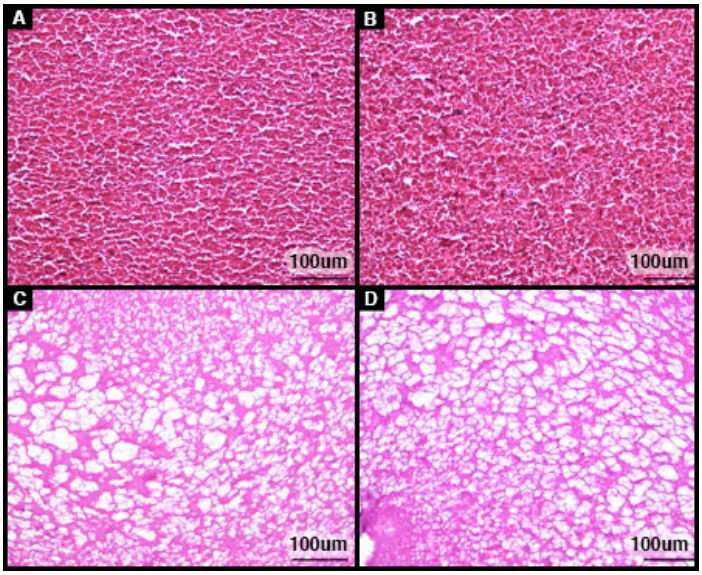

Figure 29. H&E stained histological samples of thrombi created from whole blood and plasma at different concentrations of calcium chloride. Whole blood titrated with 12mg $CaCl_2$/mL distilled water (A) and 24mg $CaCl_2$/mL distilled water (B); Plasma titrated with 12mg $CaCl_2$/mL distilled water (C) and 24mg $CaCl_2$/mL distilled water (D). Scale bar in each image is 100um.

7.2.2 Gap height

When using whole blood in the setup shown in Figure 28, the blood tended to clot in separate sections loose within the stationary reservoir. The largest clot section created in each trial ranged in size from 6-7mm x 10-14mm regardless of height of the rotating component. Figure 30 shows the resulting histology of whole blood clots created with varied distances between the rotating and stationary components. Figure 30A (6mm gap) and Figure 30B (4mm gap) show two distinct areas, one consisting of abundant erythrocytes, and the other of fibrin enmeshed erythrocytes and leukocytes. These clots, formed at low shear stresses (75 RPM), are relatively isotropic, and there are no apparent differences between the two gap widths. Figure 30C (6mm gap) shows a more uniform section of a fibrin mesh with embedded erythrocytes, while Figure 30D (4mm gap) shows fibrin strands arranged into compact layers of common

directionality with scattered erythrocytes. These clots, formed at higher shear stresses (225 RPM), indicates a smaller clearance between the rotating surfaces will create greater morphological changes that more closely resemble ante-explant thrombi found in clinically used VADs.

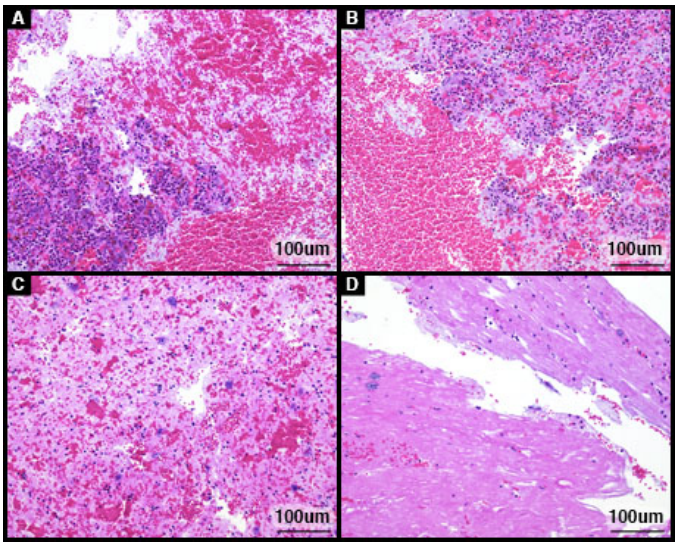

Figure 30. H&E stained histological samples of thrombi created from whole blood with different gap heights between the rotation and stationary dish. Thrombus created from whole blood at 75 RPM with a 6mm gap (A) and a 4mm gap (B) between the rotating disk and stationary reservoir; Thrombus created from whole blood at 225 RPM with a 6mm gap (C) and 4mm gap (D) between the rotating disk and stationary reservoir. Scale bar in each image is 100um.

7.2.3 Speed and duration of rotation

When using plasma in the setup shown in Figure 28, the blood tended to clot as two pieces: one circular gelatinous yellow clot loose within the stationary reservoir and one or more sections adhered to the rim of the stationary reservoir. In rare cases the clot adhered to the rotating component. As the speed of the rotating component increased, the size of the clot created decreased from approximately 40mm to 20mm in largest dimension. As the time of rotation increased, the gross appearance of the clot changed from a gelatinous, glistening material of larger size to a dry, brittle, dull material smaller in size.

Figure 31 shows H&E stained histology sections of plasma clots created with varied speeds of the rotating component and increasing lengths of duration. As the motors' run-time and speed increased, the resulting thrombi became more layered and compact. When the motor ran less than 10 hours, the shear forces from the motor at low RPMs did not have a great effect on the thrombi, which resulted in layers spread further apart (maximum width of 33 microns) (Figure 31A, D, G). However, as the device rotated for extended periods of time, the layers of the thrombi were compacted. This resulted in a tight, more uniform and acellular appearance as seen in the 24 hour (Figure 31B, E, H) and 48 hour runs (Figure 31C, F, I). By increasing the time of rotation from 24 to 48 hours at 225 RPM, the clot density increased by 3.45% (measured by percentage of colored pixels). The gaps between the layers of fibrin strands decreased from an average length of 11 microns (Figure 31B) to 5-8 microns (Figure 31H, C) until they were essentially nonexistent (Figure 31F, I).

Figure 32 shows SEM images of plasma clots created from slow speeds with short duration (Figure 32A, B) and faster speeds with longer duration (Figure 32C, D). In thrombi created at lower speeds and in shorter lengths of time (Figure 32A, B), fibrin strands begin to

align into layers. As the motor speed and length of time increased (Figure 32C, D), these layers became more compact.

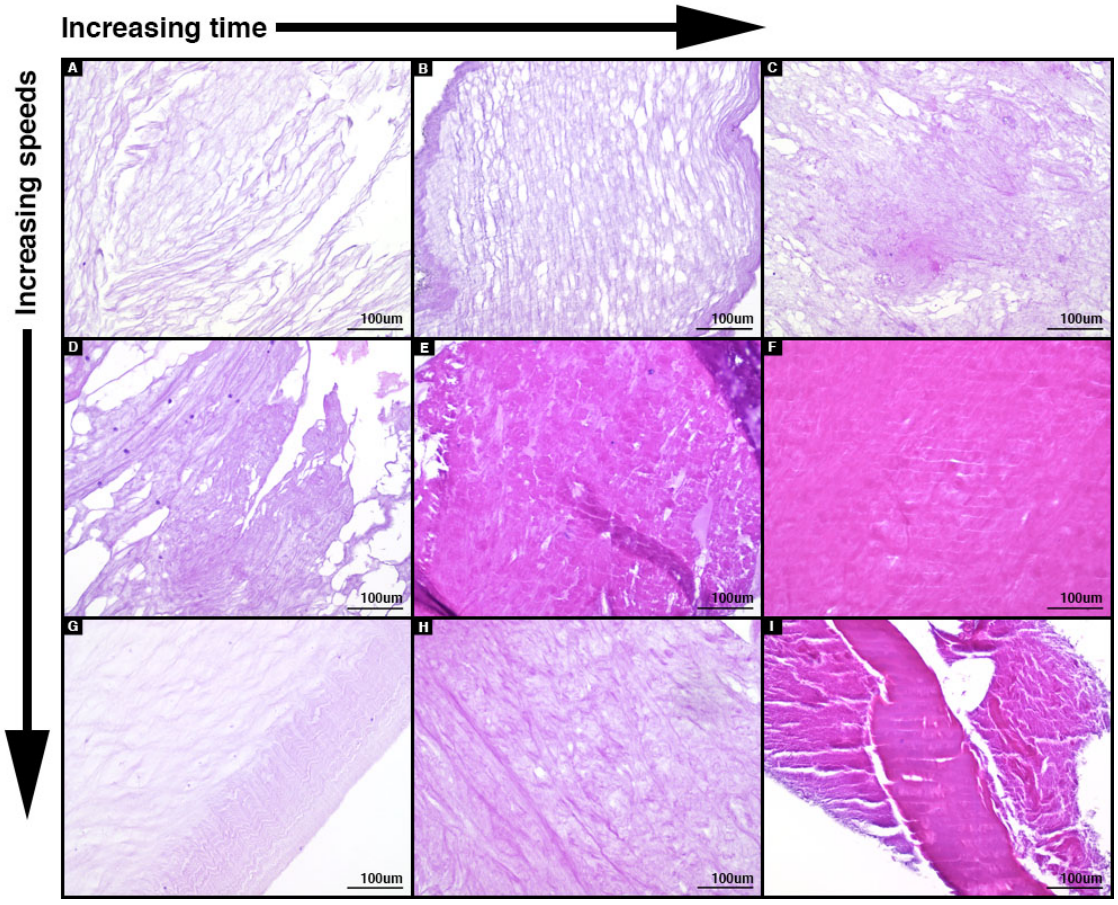

Figure 31. H&E stained histological samples of thrombi created from plasma with varying motor speeds and lengths of time. 75 RPM at 6 hours (A); 75 RPM at 24 hours (B); 75 RPM at 48 hours (C); 225 RPM at 6 hours (D); 225 RPM at 24 hours (E); 225 RPM at 48 hours (F); 300 RPM at 6 hours (G); 300 RPM at 24 hours (H); 300 RPM at 48 hours (I). Scale bar in each image is 100um.

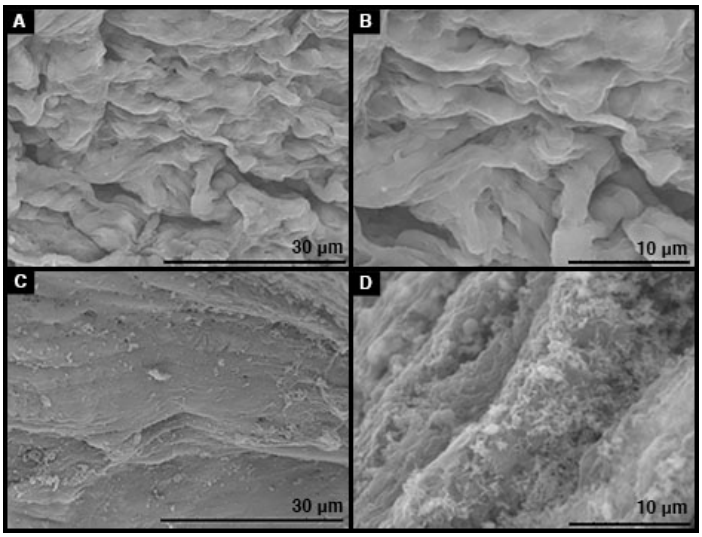

Figure 32. SEM images of thrombi created from plasma with varying motor speeds and lengths of time. 75 RPM at 6 hours (A,B); 300 RPM at 48 hours (C,D). Scale bar in image (A) and (C) is 30um. Scale bar in image (B) and (D) is 10um.

7.3 Discussion

7.3.1 In vivo *thrombi versus* in vitro *clots*

The implantation of a VAD inherently poses a risk for thrombus formation. Because thrombi can damage the pump and/or cause infarction, when a VAD controller log indicates a suspected thrombus [24, 28, 38], the physician must pursue either anti-coagulation therapy or VAD exchange surgery.

Thrombi may form inside the VAD due to a combination of shear forces from the moving components, areas of stasis within the device, or the blood-device interaction. Additionally, thrombi may form outside the VAD, such as around the sewing ring, along the ventricular wall, in the atrial appendage, etc. In some cases, thrombi developed outside the

device may travel into the VAD and become a nidus for further thrombus formation inside the VAD. Regardless of origin, if a thrombus adheres to some part of the VAD, it will cause an increase in friction, which leads to the increase in power consumption denoted on the controller log. A histological analysis of the material within the device can distinguish post-explant from ante- and peri-explant materials and, based on the morphology, determine the potential origin of the material [22]. Typically in post-explant VAD evaluations, the thrombi discovered are clots that either originated upstream from and traveled through the device, or formed inside the device (or some combination of the two). The creation of artificial thrombi with similar features and morphologies of *in vivo* thrombi as discussed in this section will help elucidate the interaction of VADs and "pass-through" thromboemboli, which will potentially help VAD manufacturers and physicians create and implement devices that can reduce the risks associated with VAD therapy.

Many histological similarities are observed when comparing the clots produced using the technique discussed in this paper to the thrombi seen *in vivo*. The two most influential factors for recreating thrombi with abundant layers were time and speed of rotation. No rotation applied to the blood while it was clotting resulted in a post-explant blood clot (Figure 33A-B). The greatest difference between these two clots is the amount of erythrocytes per 243mm^2 area, which differs by less than 10%; this variation is expected because of the innate differences between equine and human blood. A small duration of rotation resulted in a clot that resembled the peri-explant fibrin thrombus with similar fibrinous layers (Figure 33C-D) that varied in density by less than 7%. A faster rotational speed resulted in a clot with dense layers, which resembled the organized thrombus seen *in vivo* (Figure 33E-F). These specimens are histologically similar; the only noticeable difference is that the eosinophilic material in the *in vitro* clot (Figure 33E) stained more vividly than the *in vivo* thrombus (Figure 33F).

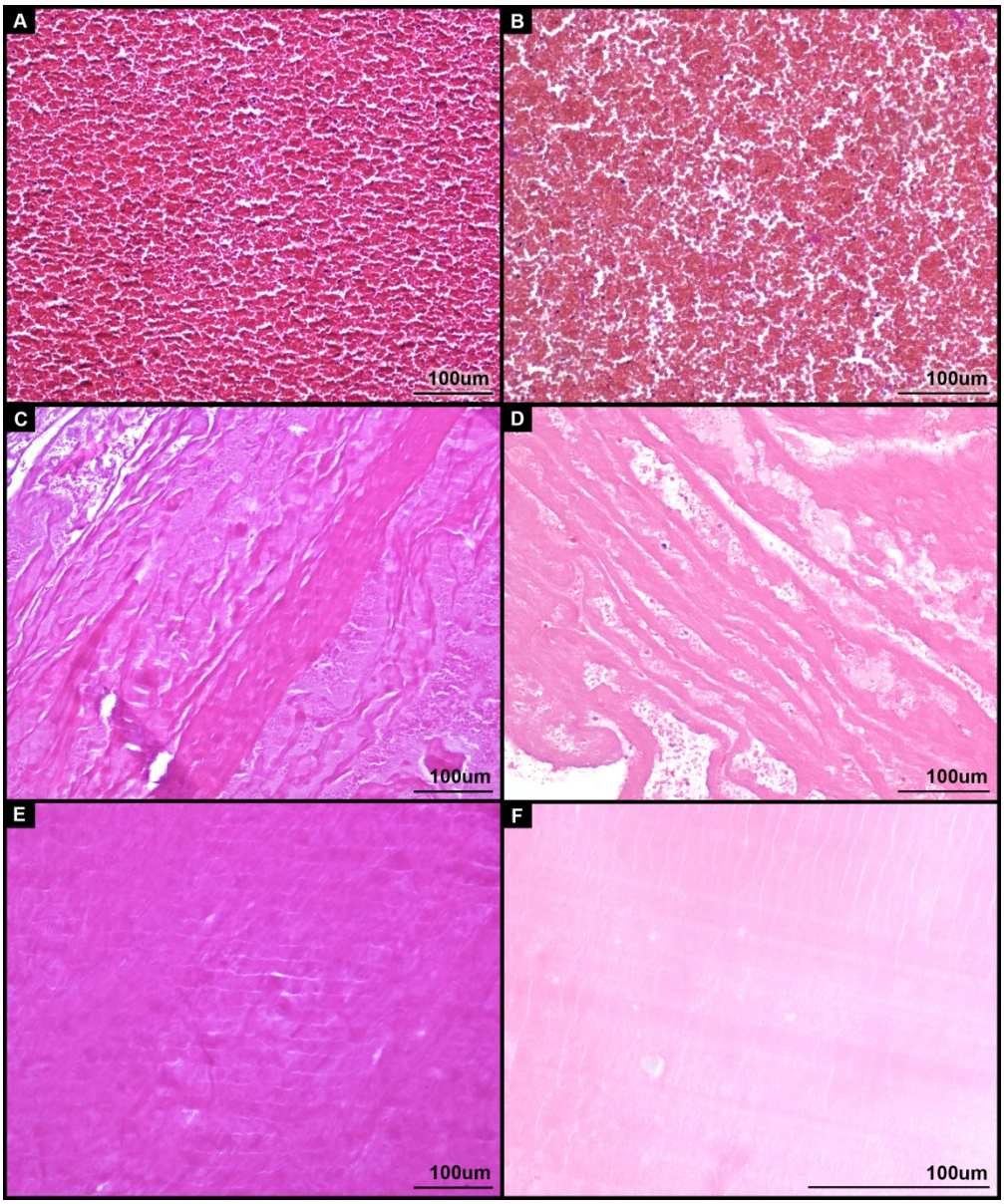

Figure 33. H&E stained histological comparison of specimens collected from explanted VADs to artificial clots created *in vitro*. Post explant clot *in vitro* (A) and *in vivo* (B). Peri-explant fibrin thrombus *in vitro* (C) and *in vivo* (D). Organized thrombus *in vitro* (E) and *in vivo* (F). Scale bar in each image is 100um.

7.3.2 Plasma versus whole blood

In this section, we described a method to create both plasma and whole blood derived clots. Although it would be ideal to use whole blood exclusively, plasma has benefits that might make *in vitro* experiments more attainable. Plasma, as opposed to whole blood, created clots that showed greater histological uniformity and were more consistently reproducible. Plasma also allowed for better visualization of the fibrin strands in comparison to whole blood (i.e., lacked enmeshed erythrocytes). Additionally, due to plasma's ability to be frozen without losing its utility, it is much easier to preserve long-term, which readily allows for future experiments without acquiring and titrating new blood samples. However, for *in vitro* experiments that study biochemical reactions between the device and the blood, whole blood clots would be necessary to ascertain the reaction of blood components (i.e., platelets, leukocytes, and erythrocytes).

Platelets play an important role in coagulation, particularly inside a VAD. The shear stress from device-induced flow activates platelets, which leads to aggregation of platelets, and eventually a thrombus. The plasma used in these experiments contained little to no platelets, meaning the coagulation came from the plasma proteins. The lack of platelets caused the clot that formed to be mostly gelatinous in a flat circular shape mostly formed between the two plates. However in the whole blood samples, the platelets were activated and the resulting clot was irregular in shape and formed in clumps rather than flat disks.

7.3.3 This method versus others

The Chandler Loop is a historic method for creating thrombi *in vitro* [119]. This method uses an inclined rotating closed loop that circulates blood until it coagulates, thus producing a

thrombus. These thrombi are grossly and histologically comparable to vascular thrombi [119], whereas the method described in this paper focuses on creating clots similar to what would be seen within a medical device that has a rotating component. The rotating mechanism within the device applies different forces to the blood components not seen in the body naturally.

Other previous studies that created clots *in vitro* studied the adhesion characteristics of certain materials used in medical devices [52], the potential for thrombi to form on these surfaces, how the shear rates applied by the rotating component affected the thrombus formation [52, 87], and how certain geometries created a potential for thrombus formation [86]. In the method described in this paper, the end goal is to have an artificial clot that can be introduced into a mock circulatory loop for the purposes of studying thromboembolism in medical devices, specifically VADs.

7.3.4 Study limitations

Only equine blood was made available for this experiment, while bovine, porcine, and ovine blood is typically used for VAD development. Equine blood has a higher sedimentation rate[23-24] compared to that of humans, however a high sedimentation rate in humans can be indicative of an inflammatory reaction in the body, which might be possible in VAD patients. Porcine blood is most similar to human blood in adhesive forces [126] while bovine, ovine and porcine specimens are most often used for VAD testing due to of size and other physiologic similarities. Although equine blood has differences to human blood, the authors believe same experiments using blood from different species would yield similar results, with potential differences in the titration curve.

The parallel plates used in these experiments had a limited clearance of 4-6mm (+/- 1mm), whereas distances between the impeller and adjacent VAD housing can be much smaller (<1mm). Additionally, the parallel plate setup described in this manuscript most closely resembles a centrifugal-flow device (as opposed to an axial-flow VAD orientation). The goal of this experiment was to add a rotational force to the blood while it was clotting to show the morphological changes compared to a clot formed under static conditions. Future testing could be performed with real VAD-like conditions (closer gap sizes, and multiple orientations of the rotating component) to further describe thrombus formation in an environment with rotational forces.

7.3.5 Future applications

Future applications of this method include testing "pass-through" thromboembolism in VADs. Such a study would include a mock circulatory system incorporating a VAD, pressure transducers and a flow meter. Previously citrated blood specimens would be titrated with $CaCl_2$ as described here, and then clots created in a static environment would then be introduced to the system proximal to the VAD. The resulting clots would then be compared histologically to the clots created with a rotating component as described in this paper, as well as those seen *in vivo*. This test would determine the pressure changes and changes in flow rate as a clot travels into the VAD and potentially correlate the size/age of the clot to magnitude of the power-spike seen on a VAD controller log. This flow loop would require a clear liquid, such as water or a water/glycerin mixture, in order to be able to visualize the clot as it travels into the device. See Section 8 for more information about a bench-top model for testing VAD response to thromboembolism.

Furthermore, future studies could also be performed to learn more about thrombus formation inside of VADs as well. In this case the flow loop would need to be filled with previously citrated whole blood (or an appropriate blood analog), and varying amounts of $CaCl_2$ could be added to the system (as blood is flowing) to allow blood to clot as it would *in vivo* according to shear forces inside the VAD and geometrical constraints. Furthermore, *in vivo* studies could be performed where real-time VAD parameters are monitored while inducing instances of thromboembolism by inserting previously formed clots into the ventricle.

7.4 Conclusions

Based on the numerous variables tested, we were able to optimize a method to create artificial thrombi similar to those seen in blood-contacting devices with rotating surfaces. In all experiments, the rotating disk and the stationary reservoir were similar in size, with the rotating disk slightly smaller. We believe this caused the thrombi to form almost completely under the rotating disk where they experienced the most shear force and allowed minimal stagnation. A smaller distance between the rotating dish and stationary reservoir (approximately 4mm) allowed formation of a clot large enough to withstand processing and handling with histologic evidence of lamination. Due to sample size constraints, 24mg $CaCl_2$/mL distilled water was used because less volume could be added to achieve the same amount of clotting for whole blood and plasma.

This standardized method for creating *in vitro* whole blood and plasma clots will be used for additional studies involving physiologic flow loops to further elucidate the interaction of VADs with fibrin thromboemboli (further explained in Section 8). These experiments will establish a basis for better understanding of blood flow, thrombus formation and embolization within VADs, which will help future VAD designs in limiting thromboembolic complications.

8. MODELING VAD RESPONSE TO THROMBOEMBOLISM

Understanding and limiting thromboembolic events is critical to expanding the clinical indication for existing devices to other patient populations, as well as introducing new life-saving devices to the market. Current *in vitro* testing of VADs includes testing longevity of the device (i.e., how long the device lasts without mechanical failure) and testing VADs under hemodynamic conditions to reveal whether the device damages blood cells, produces sufficient flow rates, *etc.* [46, 47, 49-56, 127]. *In vitro* testing could be expanded to reveal the specific VAD response to "pass-through" thromboembolism, resulting when thrombi formed outside the VAD are transported into the device. If physiologic flow loops used for testing VADs incorporated a port for introducing thrombi upstream from the device, VAD researchers could ascertain specific patterns for individual VAD models, such as correlations between clot size or structure and flow pattern response to "pass-through" thromboembolism. This type of flow loop could improve the diagnostic capabilities of thrombosis by retroactively comparing VAD controller response in the *in vitro* model to recorded clinical events. Overall, such a model would add to the therapeutic value of receiving a VAD by providing valuable insight to VAD manufacturers about how specific VAD models respond to thromboembolic events. Complete results from experiments pertaining to this section are detailed in Appendix IV.

8.1 Materials and methods

In an effort to model VAD response to "pass-through" thromboembolism, a mock circulation environment was created that included mock-VADs with a proximal port for inserting artificial thrombi. Two mock intracorporeal, intraventricular VADs were created to simulate

centrifugal and axial flow pumps. Fibrin clots of various ages ranging from 14 to 70 days were introduced into each device to determine how structural changes brought about with age (i.e., stiffness) elicited different responses inside the VAD. The VAD response was characterized by monitoring flow rate and pressure drop across the pump before and after the clot entered the VAD. Clots were then collected from the device or flow loop for histological comparison to thrombi collected from explanted clinical VADs.

8.1.1 Artificial thrombi

Artificial thrombi were created using the method outlined in Section 7. Briefly, equine and bovine blood collected with sodium citrate for transfusion was stored beyond its clinically usable date and made available for this experiment. Plasma was collected after erythrocytes were precipitated by standing in refrigerator or by gentle centrifugation. Bovine and equine blood have similar clotting factors in the plasma, and the artificial clots created from both had similar gross and histologic appearances. To counteract the calcium-chelating effect of citrate, calcium chloride was added to each specimen to activate clotting. Resulting clots were stored at 5°C for different lengths of time to produce clots of varied stiffness. Clots were created using 5mL aliquots of plasma in individual glass test tubes. Next, clots were divided into multiple pieces for introduction into the test system. One section from each clot was not introduced into the flow loop but retained for analysis as a control.

8.1.2 Flow loop setup

The flow loop was designed to replicate the physiologic environment of an implanted left ventricular assist device (Figure 34). Reservoirs were created to simulate systemic resistance and venous return, and were connected with ½" plastic tubing. To maintain bovine and equine physiologic temperature (38-43°C), the reservoirs were placed in heated water baths. The systemic reservoir was placed on a shelf approximately 60cm above the venous return reservoir, and the mock-VAD was placed approximately 30cm below the venous return reservoir. The heights of the reservoirs added pressure differences in the system; the mock-VAD pumping against gravity to the elevated reservoir simulated systemic resistance. Fluid from the lower reservoir passively flowed into the mock-VAD to simulate flow into the heart from venous return. Because VADs are implanted in functioning ventricles, a peristaltic pump (Masterflex I/P, Cole-Parmer, Vernon Hills, IL) was placed in parallel with the mock-VAD to simulate a beating ventricle. A one-way valve was placed immediately distal to the mock-VAD to prevent retrograde flow into the VAD from the peristaltic pump, and a port for inserting clots was placed immediately proximal to the mock-VAD inflow. Pressure transducers (Model A-10, WIKA Instrument, LP, Lawrenceville, GA) were placed at the inflow and outflow of the mock-VAD/peristaltic pump system to determine the pressure drop across the ventricle, and an electromagnetic flow meter (IFM SM6000, IFM Efector, Inc., Malvern, PA) measured ventricular output.

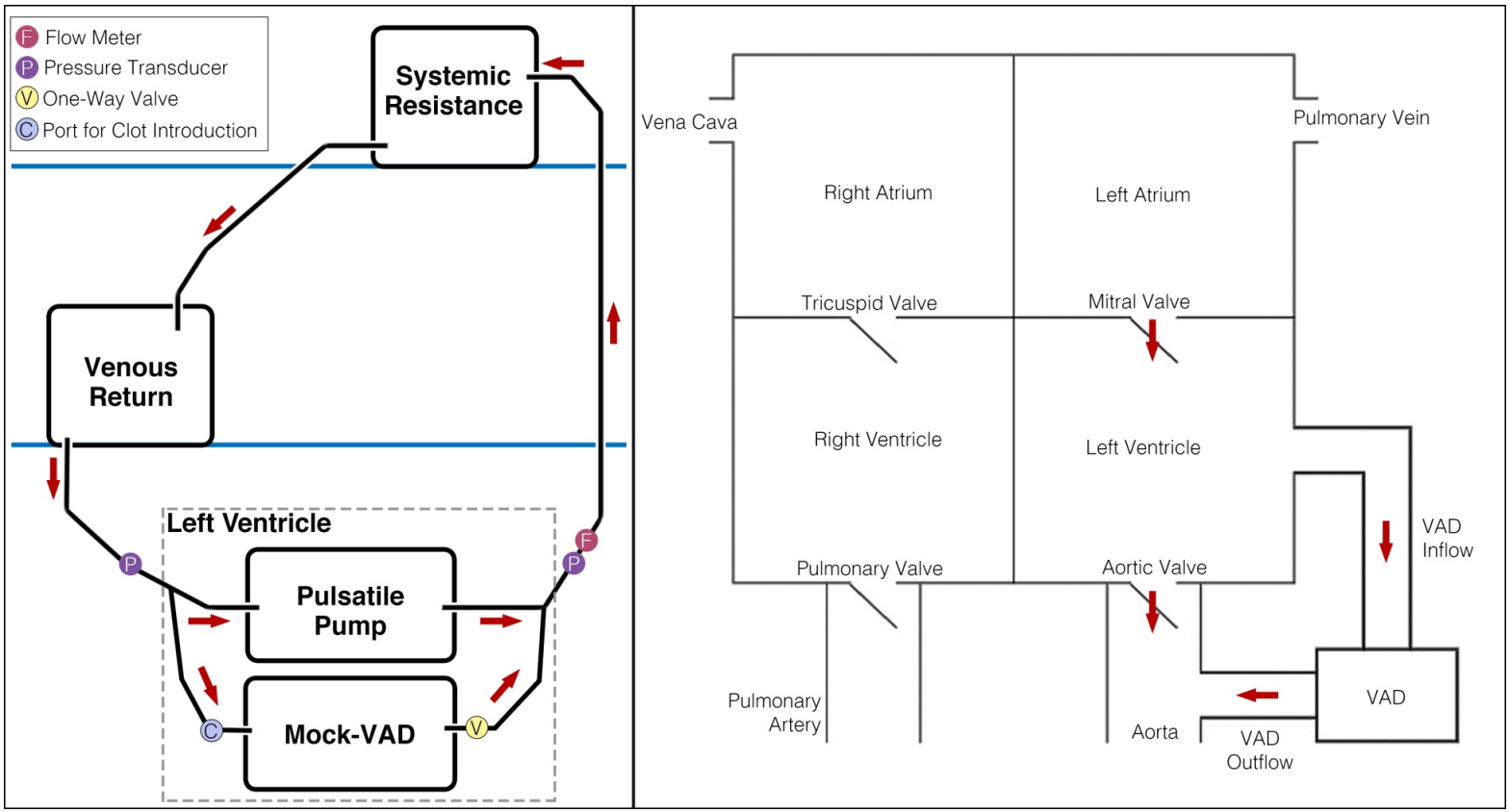

Figure 34. Diagram (left) and rationale (right) of mock-circulatory system. Systemic resistance and venous return were modeled with reservoirs placed at different heights. A peristaltic pump was placed in parallel with a mock-VAD to simulate a beating left ventricle with implanted device. Pressure across the pumps was measured, and flow was measured distal to the mock-VAD. A port proximal to the mock-VAD inflow allowed for clot insertion into the system.

8.1.3 Mock VADs

The centrifugal and axial flow mock-VADs were designed for testing the system's ability to characterize VAD response to "pass-through" thromboembolism (Figure 35). These generic, non-specific pump designs replicate the centrifugal and axial flow configurations of intracorporeal devices on the market. The casing for the axial pump and lid of the centrifugal pump were machined from a 2.5" diameter polycarbonate rod, and the lower housing for the centrifugal pump was machined from an acrylic block. These materials were chosen for the pump casing for their workability and transparency. The centrifugal flow impeller was machined from aluminum, and the axial flow impeller and stator were printed in Acrylonitrile Butadiene Styrene (ABS) plastic with a Flashforge Creator 3D Printer (Zhejiang Flashforge 3D Technology, Co. Ltd., Jinhua, China). The axial flow impeller design had a low-carbon steel sphere (1/8" diameter) glued to the tip to create a ball-bearing interface with the 3D-printed stator (Figure 35E). The shaft connected to the impeller of both designs was affixed to a 12V DC motor capable of rotating at 2900 RPM. Table 5 lists the specifications for each mock-VAD design, including maximum diameter of impeller, inner diameter of pump casing, and clearance between impeller and pump housing.

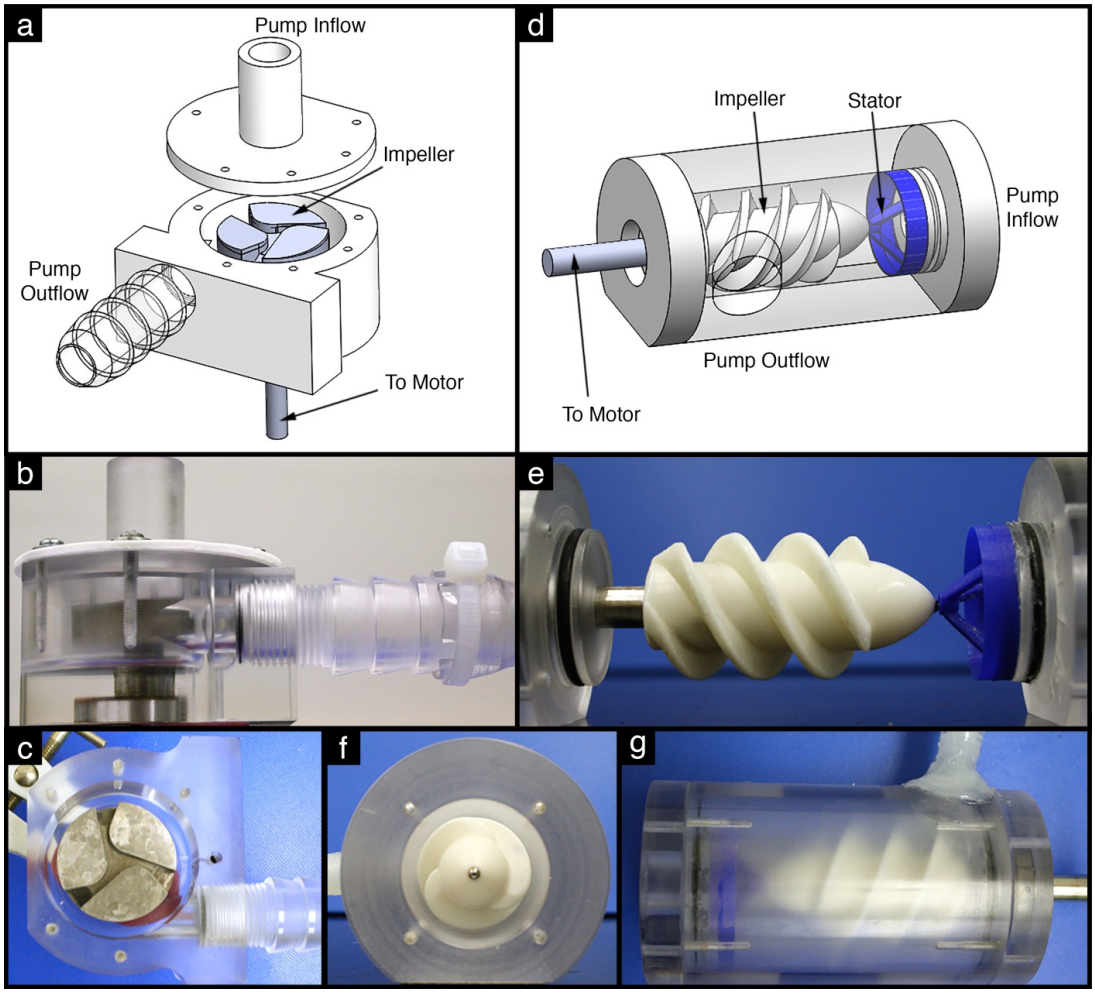

Figure 35. Mock-VADs designed in SOLIDWORKS. The impeller in each design was connected to an external motor through a rotating seal. A) Centrifugal flow pump design diagram. B) Front view of centrifugal flow device. C) Top view of centrifugal flow device with inflow removed. D) Axial flow design. E) Impeller/stator interface of axial flow device with outer casing removed. F) Lateral view of axial flow device with stator removed (inflow view). G) Top view of axial flow device with inflow on left.

Table 5. Specifications for mock-VAD designs

	Centrifugal Flow Design	Axial Flow Design
Maximum diameter of impeller	33.92mm	32.68mm
Inner diameter of pump housing	44.33mm	34.82mm
Clearance between impeller and pump housing	5.21mm	1.07mm
Pitch / revolutions of impeller vanes	N/A	1.717 / 1.115

8.1.4 Data acquisition

VAD response to thromboembolism was characterized by monitoring the flow and pressure across the VAD/ventricle system. The pressure transducers and flow meter were connected to a data acquisition system (NI ELVIS II, National Instruments Corp., Austin, TX). Voltage measurements from the pressure transducers and flow meter were collected and exported in spreadsheet form using a custom LabVIEW (National Instruments Corp., Austin, TX) program.

Fibrin clots were introduced into the mock-VAD while the peristaltic pump produced pulsatile flow. Pulsatile flow rate was set at a different value for each clot. Higher flow rates (1.5-2 LPM) simulated a normal heart; lower flow rates (1.0-1.5 LPM) were used to simulate heart failure conditions. The flow rates were scaled down from physiologic values (6 LPM for a healthy heart) because the mock-VAD motor allowed for ~2000 RPM (<0.5 LPM), whereas clinical VADs operate around 3000-12000 RPM [128, 129] (~6 LPM). During each experiment, the loop was filled with approximately 3.2L of either water or a glycerin/water mixture (40/60 mix) to simulate blood viscosity [130]. Experiments were run at room temperature (21°C), and elevated (43°C) and normal (38°C) values for bovine/equine specimens.

Baseline flow rate and pressure data were collected separately for each experiment before introducing each clot to the system. The peristaltic pump first ran alone and then in parallel with the mock-VAD. A stopwatch was started when pressure and flow rate data collection began; the clot was introduced to the system via the proximal port, and the time at which the clot first entered the VAD was recorded in order to divide data into pre-clot and post-clot segments. Each clot was observed in the pump for times ranging from 30s to 2min, after which the pumps were disconnected from power and clot fragments were collected from within the system.

8.1.5 Data analysis

Clots were analyzed histologically for microscopic comparison to thrombi collected during pathology evaluation of post-explanted clinical VADs [22]. Clots were processed for conventional paraffin-embedded histology, stained with Hematoxylin and Eosin (H&E), and scanned with an Olympus VS120 Virtual Microscopy Slide Scanning System (Olympus, Corp., Center Valley, PA). Pressure and flow rate data were processed in Microsoft Excel and MATLAB (MathWorks, Inc., Natick, MA). High frequency noise was removed from pressure and flow data using a digital low-pass filter. The pressure drop across the pump was calculated, and the mean of the baseline (i.e., flow and pressure data from the peristaltic pump and VAD before a clot was inserted) was subtracted from each data set to display variance from the normal.

8.2 Results

8.2.1 Centrifugal flow mock-VAD

Fibrin clots stored for approximately 30 days were a transparent, white to yellow, gelatinous substance less than 2.5cm in diameter with a slightly firm outer layer (Figure 36A). Before being subjected to the mock-VAD, sections of clot (approximately 3mm thick) were circular and retained their structural integrity during dissection (Figure 36B). During separate experiments that simulated normal heart function and heart failure (i.e., higher vs. lower flow rates), clots divided into multiple irregularly shaped pieces when interacting with the centrifugal flow impeller. The more gelatinous clot sections went into flow loop circulation (Figure 36C), while the firmer pieces remained within the device housing loosely adhered to the impeller or the housing wall (Figure 36D-G).

Fibrin clots stored for >30 days (Figure 36H-I) had a gross appearance and interaction with the device similar to those of the clots stored for 30 days for both normal and heart failure conditions. The gelatinous material broke into fragments that were collected via filtration for histological evaluation (Figure 36J). Larger pieces remained in the device housing or the one-way valve distal to the mock-VAD after the loop was drained (Figure 36K).

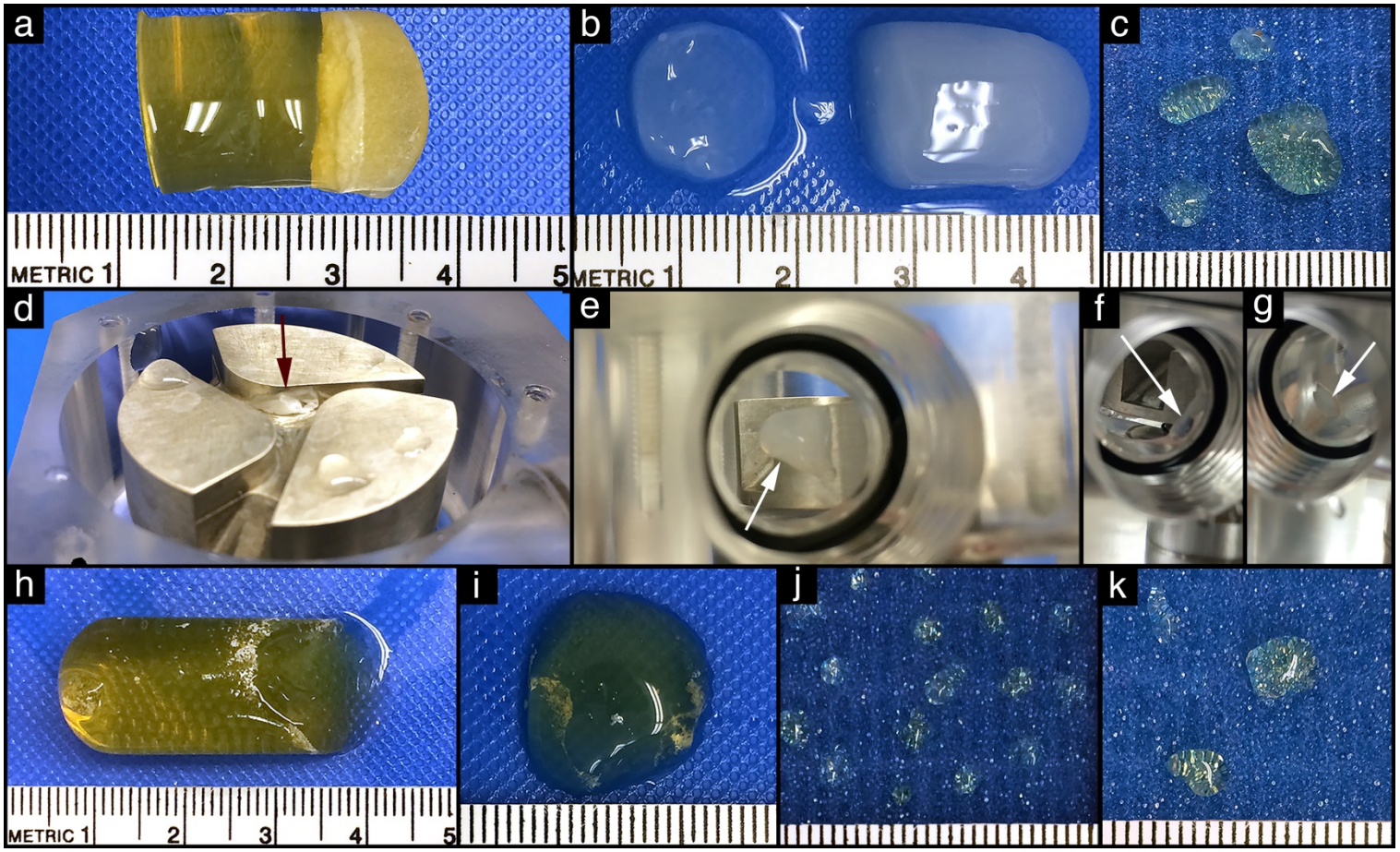

Figure 36. Plasma clots pre- and post- mock-VAD ingestion. A-G) Plasma clots <30 days old. A,B) Clots created in test tubes. C) Gelatinous sections of clots filtered out of flow loop after clot was subjected to rotational forces inside VAD. D-G) Fibrinous parts of clots loosely adhered to the impeller (D,E) and device casing (F,G) after the clot was subjected to the VAD. H-K) Older plasma clots (>30 days old). H,I) Clots created in test tubes. J) Smaller pieces of clot after contact with the impeller. K) Larger pieces in device casing after VAD was turned off.

The fibrin clots altered the flow rate as shown in Figure 37 (experiments simulating normal heart function). At room temperature, smaller gelatinous pieces of clot that entered the flow loop circulation after breaking off of the initial clot caused negative spikes in flow rate as they traveled through the flow meter (artifact; Figure 37A, red arrows). Inserting the clot caused an initial 0.5-1 LPM increase in the flow rate (Figure 37, blue arrows). Figure 37C shows an adjusted flow rate, in which the average of the baseline measurements (peristaltic pump and VAD flow rate before the clot was introduced) was subtracted from the experimental flow rate. In Figure 37C, normal heart flow was simulated (~1.5-1.6 LPM, 38°C); flow was relatively similar to the baseline (+/- 0.5 LPM) until approximately 6.5s after a large circular clot (15mm diameter, 5mm thick) entered the VAD (indicated by the vertical black line at 6.55s), after which the flow increased (blue arrow) and then decreased by ~0.5 LPM. Experiments simulating heart failure conditions (~1.0-1.5 LPM) produced similar responses in flow rate adjustments: after approximately 6-8s, there was a large increase in flow rate followed by a decrease in flow rate (similar profile as in Figure 37C). After the pumps were disconnected from power, loose clot particles were noted in the tubing and reservoirs. Additionally, clot fragments were observed in the pump housing, which had become loosely adhered to the pump components. These fragments were gently removed and placed in formalin for histological evaluation.

Histologically, the artificial clots were composed of an acellular eosinophilic matrix similar to the control specimen (Figure 37). The control clot (Figure 37A.1) had a uniform, amorphous, sponge-like appearance with small circular gaps scattered throughout. The clot that was subjected to the VAD (Figure 37A.2) exhibited a more compact eosinophilic matrix with

minimal gaps. In the experiment outlined in Figure 37B (normal heart flow and room temperature solution), the deposit collected from the inferior surface of the impeller (Figure 37B.2) had scattered black punctate material along the specimen, presumed to be grease from the rod connecting the impeller to the motor. Compared to the control (Figure 37B.1), the clot subjected to the VAD had visible layers of more dense material (i.e., dark vs. light-pink areas). The clot shown in Figure 37C traveled through the mock-VAD rather quickly and was exposed to the rotating component for less time than previous samples. Thus, these samples (Figure 37C.2) were histologically similar to the controls (Figure 37C.1). Clots in experiments simulating heart failure conditions had histology results similar to those from normal heart flow experiments.

When a larger, firmer section of the clot (Figure 38) entered the mock-VAD, the clot remained in the grooves of the impeller (Figure 38A) and initially decreased the flow rate (Figure 38B); however, over time, the flow rate gradually increased (Figure 38B). Histologically, this clot had more compact layers (Figure 38C) than the control (the clot section not subjected to the device, Figure 38D).

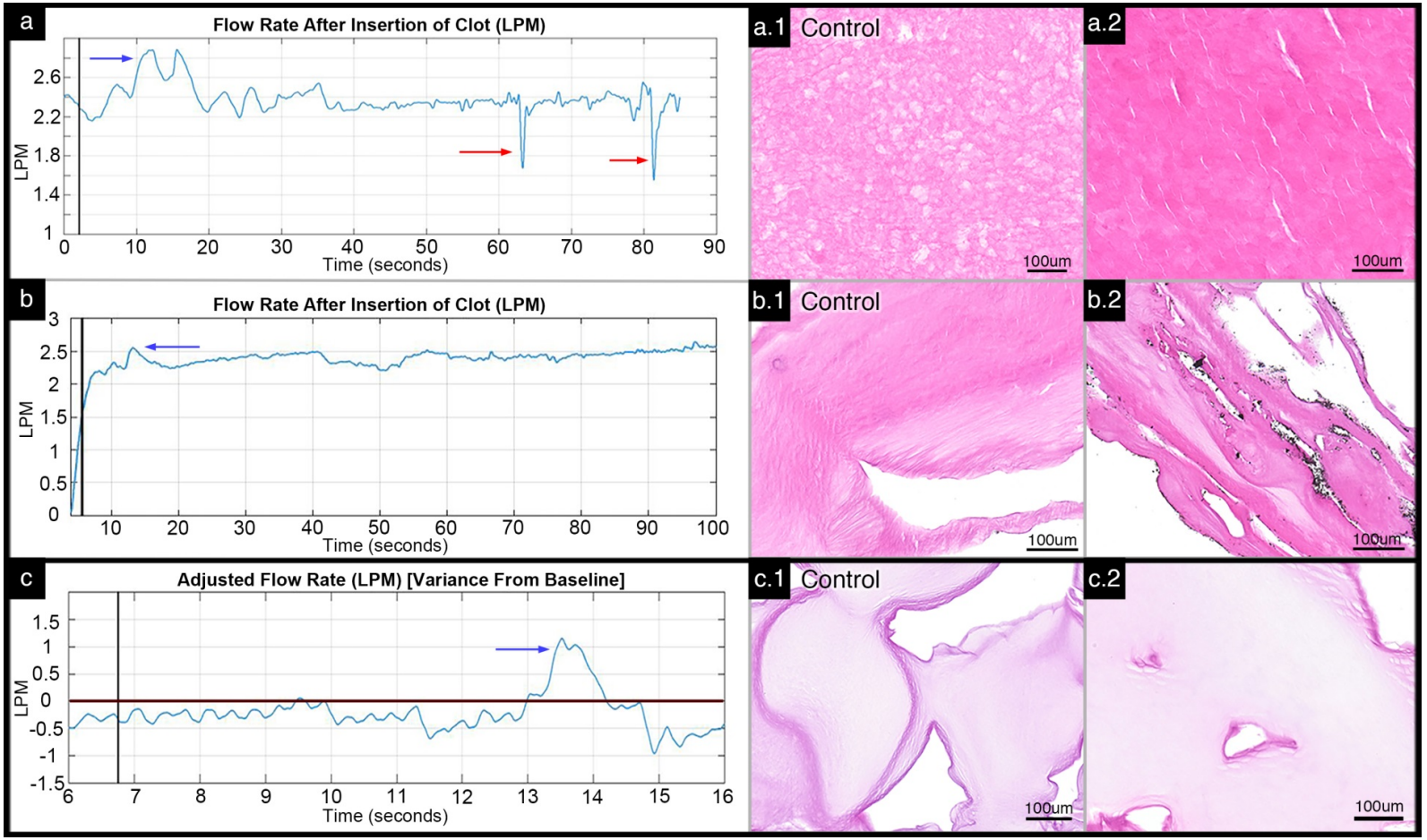

Figure 37. Results for centrifugal flow experiments. A,B) Flow rates monitored from an electromagnetic flow meter distal to the peristaltic pump and centrifugal flow mock-VAD. C) Adjusted flow rate of flow loop (flow rate observed throughout duration of experiment minus the average flow rate prior to insertion of clot). Vertical black line indicates time that the clot entered the mock-VAD. Horizontal axis indicates time in seconds, and vertical axis indicates flow rate in liters per minute (LPM). Blue arrows indicate initial spike in flow rate; red arrows indicate artifact due to clot pieces passing through the flow meter. A.1-C.2) H&E stained histology sections of control clots (1) and clots subjected to the devices (2). Scale bar in each histology image is 100 microns (um).

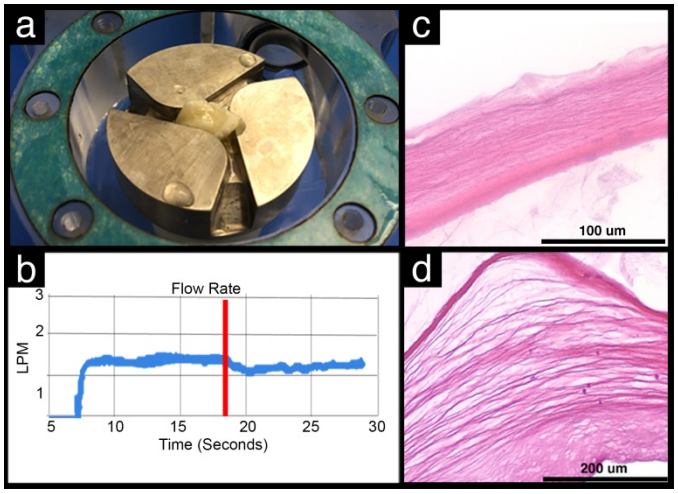

Figure 38. Plasma clot with fibrinous gross morphology (17 days old). A) Clot was introduced into device and remained in impeller grooves throughout duration of rotation. B) Flow rate data collected and displayed in LabVIEW program. The red vertical line indicates the time the clot entered the pump. C) H&E stained histology section of clot ingested by mock-VAD. D) H&E stained histology section of control.

8.2.2 Axial flow mock-VAD

Clots used for the axial flow mock-VAD experiments were grossly similar to those used for the centrifugal flow. This specific pump design allowed clots to stay intact and remain mostly in the pump housing throughout each experiment. The stator provided an added barrier for clots upon entering the pump. In most cases, the clot adhered to the impeller vanes (Figure 39A), stator struts (Figure 39C,G), or casing wall (Figure 39E).

When the peristaltic pump was set to higher flow rates to simulate normal heart function, the adjusted flow rate after the clot entered was shifted above the horizontal axis (Figure 39B,D), with occasional spikes in flow (red arrows in Figure 39D). For heart failure conditions (i.e., lower flow rates), the flow rates remained relatively similar to the baseline flow (Figure 39F,H),

with an occasional spike in flow (red arrows in Figure 39H). The temperature of the solution had no appreciable effect on adjusted flow rate or clot behavior, and the pressure drop across the peristaltic pump and mock-VAD remained relatively constant throughout the duration of each experiment for both axial and centrifugal flow devices (Figure 40).

Histologically, clots from axial flow VAD experiments had minimal changes from control clots (Figure 41). Control clots were microscopically uniform in all directions and composed of a loose eosinophilic matrix (Figure 41A,D). The test clots, approximately 2 months old, had similar histologic changes after being exposed to higher and lower flow rates (Figure 41B,C, higher flow rates; Figure 41E-G, lower flow rates). Each clot was histologically composed of two distinct regions. Near the center, the eosinophilic matrix is similar to the controls, but toward the edges, the matrix was much denser and had distinct laminations. In one experiment with pulsatile flow set to a lower flow rate, a piece of the clot broke off of the stator and was collected via filtration (Figure 41G); this clot was histologically composed of faint regions of eosinophilic material with various larger gaps in the tissue.

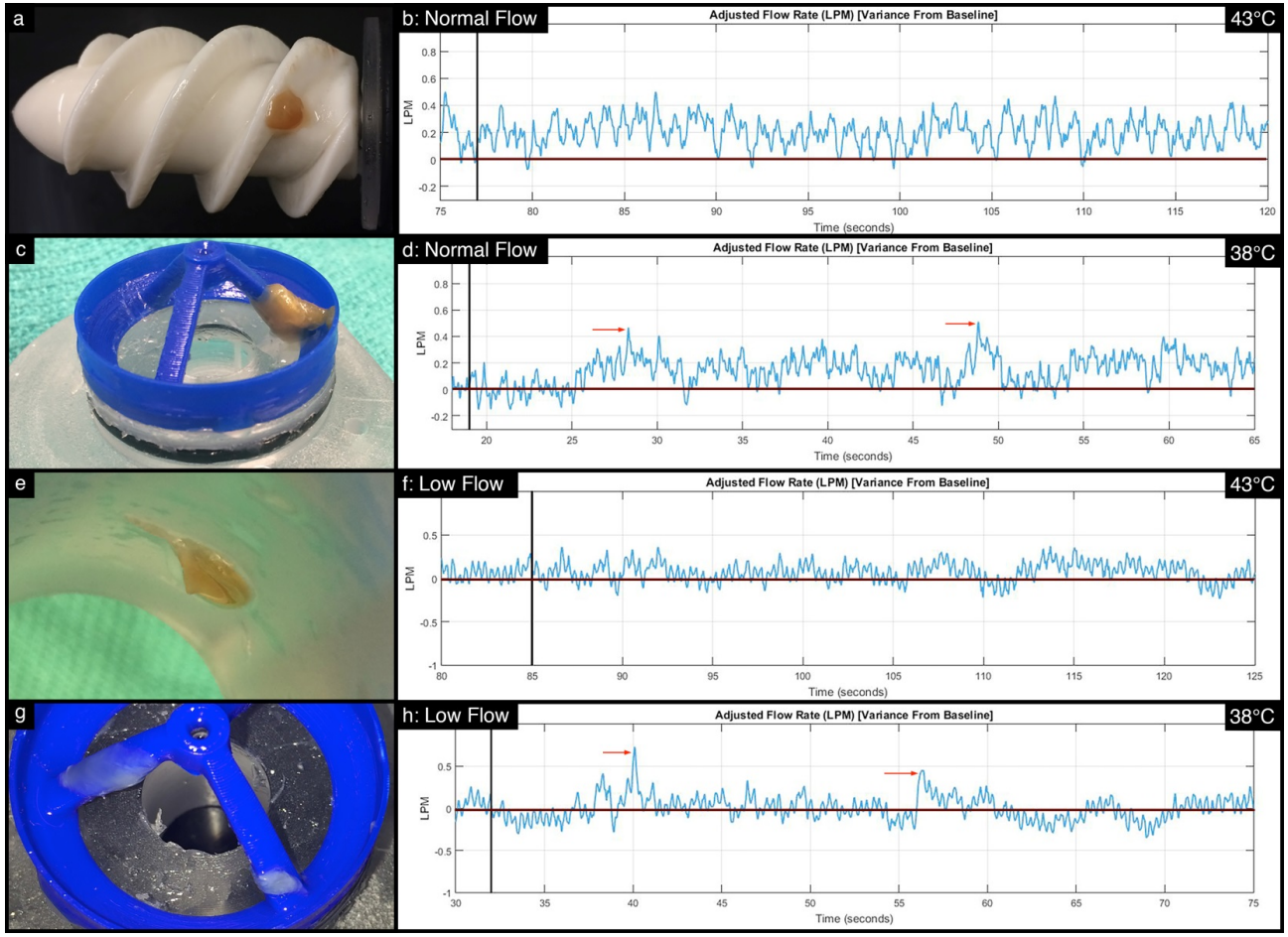

Figure 39. Results for axial flow experiments. A,B) 3D printed impeller with clot loosely adhered to the impeller vane and corresponding adjusted flow rate data. Clot entered the VAD at t = 76s. C,D) Clot loosely adhered to 3D printed stator and corresponding adjusted flow rate data. Clot entered the VAD at t = 19s. E,F) Clot loosely adhered to the wall of the pump housing and corresponding adjusted flow rate data. Clot entered the VAD at t = 84s. G,H) Two clot pieces loosely adhered to the stator and corresponding adjusted flow rate data. Clot entered the VAD at t = 32s.

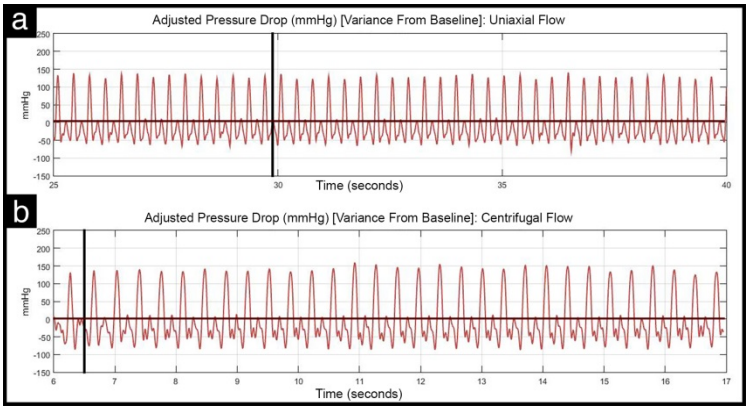

Figure 40. Adjusted pressure readings across the peristaltic pump and mock-VAD. The mean baseline pressure was subtracted from the pressure drop across the axial flow (A) and centrifugal flow (B) mock-VADs. Vertical black line indicates time that the clot entered the mock-VAD. Horizontal axis indicates time in seconds, and vertical axis indicates pressure in millimeters of Mercury (mmHg).

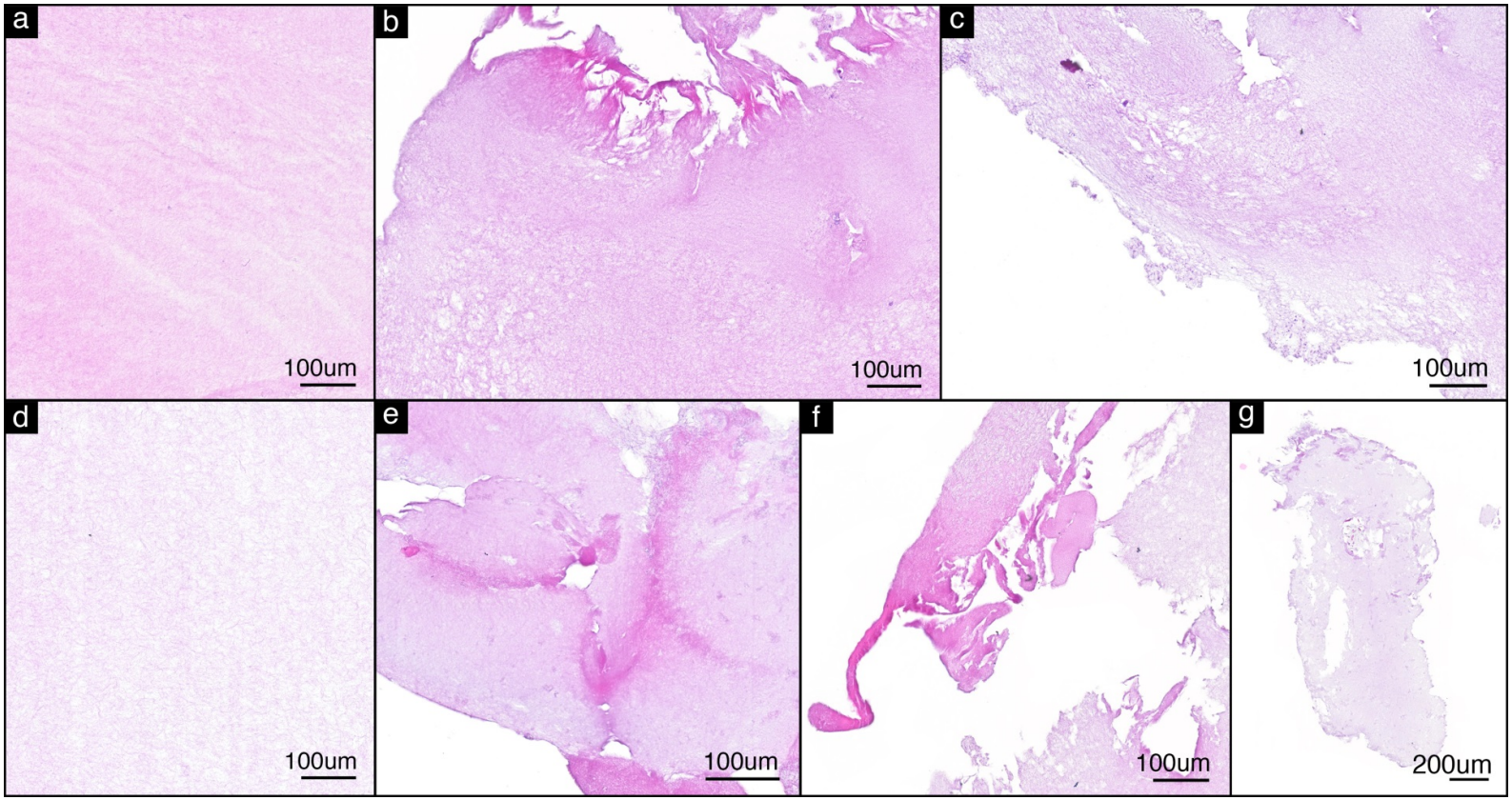

Figure 41. H&E stained sections of clots from axial flow experiments. Top Row: Clots from normal flow simulations (i.e., higher flow rates; See Figure 39A-D). Bottom Row: Clots from heart failure flow simulations (i.e., lower flow rates; See Figure 39E-H).
Top Row: A) Control clot B) Clot subjected to the mock-VAD at higher flow rates that was recovered from the vanes of the impeller (Figure 39A). C) Clot subjected to the mock-VAD at higher flow rates that was recovered from the stator (Figure 39C).
Bottom Row: D) Control clot. E) Clot subjected to the mock-VAD at lower flow rates that was recovered from the wall of the pump housing (Figure 39E). F) Clot subjected to the mock-VAD at lower flow rates that was recovered from the stator (Figure 39G). G) Clot subjected to the mock-VAD at lower flow rates that was recovered from the flow loop via filtration.

8.3 Discussion

The purpose of this study was to model VAD response to thromboembolism by monitoring pressure drop and flow rate across mock-VADs as artificial thrombi were introduced proximally to the device. Overall, this flow loop revealed specific flow patterns for both the centrifugal flow and the axial mock-VAD models. Softer, more gelatinous clots that fragmented when ingested by the centrifugal flow device caused an initial increase in flow rate followed by a flow rate decrease, while firmer clots that remained in the impeller caused an initial decrease in flow rate. After the clot was inserted in the axial flow device, the average flow rate was increased from the baseline when the flow loop ran under normal heart conditions (higher flow rates). When the flow loop ran under heart failure conditions (lower flow rates), the average flow rate did not vary much from the baseline except for sporadic spikes. Histologically, for both mock-VAD designs, differences in clot morphology before and after exposure to the VAD are observed, indicating that the VAD does have an impact on clot morphology. Changing the temperature of the solution did not affect the flow rate or pressure patterns in either of the mock-VAD models studied. This indicates that elevation in temperature from an infection (often seen in VAD patients at the driveline insertion site) or other sickness may not change the reaction of VADs to thromboembolism.

8.3.1 What does this study tell us about VAD/controller design?

The results of this study show that pump design markedly affects consequences of a VAD's ingestion of a thrombus. The stator of the axial flow mock-VAD served as an initial barrier for clots, and in many cases the clots remained on the stator regardless of the flow and

temperature settings. The centrifugal flow mock-VAD had fewer components and a much greater clearance between the impeller and the casing wall. This allowed the "pass-through" clot to move beyond the VAD more easily than it did in the axial flow model. Additionally, the conical shape and soft material composition of the axial flow impeller allowed the clot to stay mostly intact, whereas the metal impeller of the centrifugal flow device disrupted clot integrity more and caused most clots to divide into multiple pieces and enter flow loop circulation.

The range of changes noted over time as clots were introduced to the mock-VADs suggests that it may be difficult to know that a thrombus is in the device based solely on flow and pressure data; in some of the axial flow experiments the flow remained steady (except for a few small spikes in flow rate) while the clot remained inside the VAD chamber. However, subtracting the average baseline data from experimental values may aid in determining when the flow rate is deviating from normal. This information could be translated into the clinical use of VADs, where baseline information for each VAD model could be incorporated into algorithms (based on VAD RPM, heart rate, body size, *etc.*) used to generate data captured in controller logs and sound alarms when there is a deviation from normal. The loop discussed here could be used to test this algorithm for each VAD model and determine the magnitude of flow irregularity at which surgical intervention is necessary.

8.3.2 How does this study relate to clinical VADs?

The clots created for these experiments were made from platelet poor-plasma. These clots are comprised principally fibrin and lack platelets, which are normally present in clinical thrombi. However, the histological results in these experiments strongly resemble those from thrombi from clinical VADs (see Section 7). Often, thrombi that develop *in vivo* in the high-

velocity regions within the ventricle have a distinct appearance; the flow causes the thrombus to form in layers alternating between fibrin and entrapped erythrocytes, usually with a fragile tip pointing downstream. The artificial clots had similar velocity-induced laminations of fibrin, although they lacked enmeshed erythrocytes.

These mock-VADs were designed as nonspecific devices using generic components for centrifugal and axial flow devices. Therefore, results seen with these two mock-VADs are not necessarily expected for any particular centrifugal or axial flow VAD models currently on the market or undergoing investigation. Additionally, the flow rates produced by the mock-VADs and peristaltic pump were not at human physiologic or clinical values. However, this *in vitro* system was designed to easily incorporate actual VADs and accessory components (e.g., controllers) from various sources to examine specific correlations for each model. In particular, this bench-top test could reveal how clots of different sizes and firmness affect VADs. It could also determine whether the size or consistency of the thrombus correlates with the magnitude and duration of power consumption or pressure changes indicated on the pump's controller log. Results could be retroactively compared to clinical experiences with those specific devices and correlated with resulting pathology evaluations. Additionally, this flow loop setup could potentially allow for testing of thrombolytic treatments *in vitro* before clinical testing. Thus, physicians could better determine whether thrombolytic agents alone could dissolve a thrombus or if an exchange surgery is necessary.

8.3.3 Future applications

The system developed in this paper solely measured the pressure drop across and the flow rate distal to the mock-VAD/peristaltic pump system. For future studies, the data

acquisition system will be expanded to incorporate VAD power consumption data and measure VAD RPM throughout thrombus ingestion. This study modeled the interaction of VADs with thrombi that formed outside the VAD (around the sewing ring, in the atrium, atrial appendage, *etc.*). This *in vitro* model could be adapted to study thrombus formation within VADs (*de novo* thrombi). Whole blood could be used as opposed to the glycerin/water mixture to simulate blood viscosity, or various blood components (thrombin, fibrinogen, factor XIII, platelets, *etc.*) could be added to the existing system to induce thrombus formation [131]. This type of *in vitro* testing could be useful throughout the development of VADs as well, because there are many device-blood interactions that should be considered in thrombus formation. All iterations of the VAD design could be tested to see which geometries most limit opportunities for thromboembolic showers and resulting downstream ischemia. This system could prove to be beneficial for VAD manufacturers by providing insight into pump design and flow rates at a lower cost than performing pre-clinical *in vivo* studies.

8.3.4 Thromboembolism in pulsatile VADs

This section focused on pass-through thromboembolism in continuous flow, intracorporeal VADs; however, a pulsatile VAD design, such as the Berlin Heart EXCOR, is also currently on the market for use in the US. One major benefit to using the Berlin Heart EXCOR VAD is that it is easily exchangeable [132]. The instructions for use manual requires that the pump be visually inspected every four hours for evidence of thrombi inside the device with the aid of a flashlight [133]. If a thrombus is discovered anywhere in the device chamber, the device may be replaced [133]. The *in vitro* model discussed in this paper would be useful for testing new device designs and the potential for thromboemboli to develop, but *in vivo* testing of

extracorporeal VADs is significantly less cumbersome than intracorporeal devices, due to the external placement of the device and ease of exchange.

8.4 Conclusion

In the development of VADs, *in vitro* testing is crucial for determining the lifetime of the device and assessing whether the device inherently damages the tissues and blood (e.g., hemolysis). However, there is currently not an *in vitro* testing protocol for determining the device response to thromboembolism, which is a significant and common clinical concern in VAD therapy. The *in vitro* system developed in this study has proven successful at demonstrating VAD response to "pass-through" thromboembolism by characterizing the flow rate and pressure drop across mock-VADs as artificial clots were introduced. This system has the potential to be an effective tool for testing VAD controller log response to and indication of thromboembolism. The authors recommend that all existing and new VAD designs use an *in vitro* testing system similar to that described here to analyze the interaction of the device and various types of thromboemboli. The correlations between clot size or structure and flow profile, power consumption or impeller RPM could be retroactively compared with controller log data from previously implanted devices to increase understanding of clinical events and help limit chances of thromboembolic complications in future designs. Understanding the relationship between the thrombus and the device response is one of the keys to creating, improving, and implementing devices that will help more patients living with heart failure.

9. SUMMARY

Ventricular assist devices have been widely documented as successful alternatives to heart transplantation for treating patients with end-stage heart failure. Thrombosis in VADs is a major complication associated with VAD therapy that can put otherwise successful implants at risk for mechanical failure or cause patient death.

As more VADs become approved for use in the United States, the overall usage of VADs has increased. With increased use, more frequently VADs are providing cardiac assistance for increasing lengths of time. As such, the idea of studying ventricular remodeling due to sustained mechanical circulatory support is still relatively new and thus not much data relating late-stage VAD thrombosis with myocardial remodeling has been presented in the literature.

In an effort to investigate this phenomenon, a computational model was made to simulate the VAD inflow cannula insertion site in dilated, diseased ventricles with weak movements, and remodeled, smaller-sized ventricles with a decreased lumen volume and increased contraction strength.

The computational model was used to compare anterior apical placement of the inflow cannula (in-line with the mitral valve) to the posterior diaphragmatic insertion site (at an angle to the mitral valve). Additionally, each insertion site was examined with the cannula placed at various depths into the lumen. At all depths, the anterior apical placement of the cannula was superior in terms of decreased regions of recirculation and stagnation. For this orientation, inserting the cannula deeper into the lumen increased the areas of trapped blood around the inflow cannula.

When the cannula is at an angle to the mitral valve, a depth in between the extremes of flush with the wall and deep into the lumen provided the best ventricle performance (for dilated hearts) in terms of recirculation and stagnation. This depth decreased the overall distance blood entering the chamber must travel to reach the cannula inflow, without creating large pockets of recirculation between the inflow cannula and the apex of the heart.

In the computational model described, the ventricles consistent with dilated cardiomyopathy (DCM) had greater stagnant regions along the ventricular walls, as well as around the inflow cannula. This corroborates the hypothesis that patients with DCM are more susceptible to mural thrombus formation. The ventricles consistent with a remodeled geometry had increased washout and decreased regions of stagnation. This supports the hypothesis that ventricular insertion site is a potential source for thrombus formation and sustained VAD support may increase chances of dislodging thrombi thus sending them into VADs that had clinically been adverse-event free for multiple years.

In a clinical setting, when a thrombus travels into the pump, it is suspected that the presence of the thrombus increases the friction within the device, and causes periods of high power consumption. Depending on the thrombus size, the inflow or outflow may be obstructed, resulting in low flow through the device. Either way, a thrombus may decrease pump efficiency, damage the device, or create micro-emboli that cause areas of ischemia downstream (e.g., stroke, renal infarct, etc.). When a thrombus is suspected, thrombolytic drugs may be administered to break up the clot; if thrombolytics are unsuccessful, a VAD exchange procedure is required.

In an effort to understand what is seen clinically, an *in vitro* model was created that can be used for testing specific VAD models' response to thromboembolism. This model involved creating artificial thrombi and introducing them into a flow loop that incorporated a VAD working in parallel with a pulsatile pump, thus simulating a VAD operating in parallel with the

ventricle *in vivo*. Although this model was only used to test mock-VADs, this model did reveal that it is possible to determine specific VAD response to thromboembolism. A model such as the one described here could be used to define correlations between size or age of a thrombus and the magnitude of changes experienced within the pump as displayed on the unit's controller.

This model revealed that the pump design and materials used for each component markedly affects consequences of a VAD's ingestion of a thrombus. Additionally, this model revealed the importance of establishing a baseline of normal activities within the pump, so it is easier to determine when the VAD operation is deviating from normal.

9.1 Conclusions and final remarks

The research in this dissertation set out to investigate the phenomenon of thrombosis in ventricular assist devices. The motivation for this research began after performing pathology evaluations on hundreds of explanted VADs revealed similar thrombi in pumps that had been operating in the body for several years. These thrombi were organizing and extending from the ventricular insertion site, along the inflow cannula. This phenomenon was investigated by creating a computational model of a ventricle with an implanted inflow cannula before and after sustained mechanical support.

Secondarily, hundreds of pathology evaluations of explanted VADs revealed that many deposits found within the device originated outside the device, possibly in the atrial appendage, along the ventricle wall (mural thrombus), or around the inflow cannula insertion site. This type of thrombus (termed "pass-through" thrombus) was investigated further by creating an *in vitro* mock-circulatory loop used to reveal specific VAD response to thromboembolism.

Based on this research, several changes can be recommended that will overall reduce instances of VAD thromboembolism and thus increase the value of VAD therapy. First, evaluating the geometry of patients' hearts as duration of mechanical support increases will provide physicians with a better indication of how the heart is remodeling, and if there is a chance for thrombus formation or dislodgment that would put the patient at risk for mechanical failure or thrombus-related ischemic damage. Second, prior to pre-clinical studies, testing the VAD response to thromboembolism in a bench-top setting (i.e., *in vitro*) will give a better idea of what is going on inside the device when certain parameters are displayed on the controller, which will ultimately provide better indication of how to treat the patient (i.e., device exchange versus thrombolytics).

Overall, this research has helped in understanding the relationship between thrombi and VADs, which will aid in creating and improving devices for treating patients with heart failure worldwide.

REFERENCES

[1] Blecker S, Paul M, Taksler G, Ogedegbe G, Katz S: Heart failure-associated hospitalizations in the United States. *J Am Coll Cardiol* 61: 1259-1267, 2013.

[2] Roger VL, Go AS, Lloyd-Jones DM, Adams RJ, Berry JD, et al.: Heart disease and stroke statistics-2011 update: a report from the American Heart Association. *Circulation* 123: e18-e209, 2011.

[3] Levy D, Kenchaiah S, Larson MG, Benjamin EJ, Kupka MJ, et al.: Long-term trends in the incidence of and survival with heart failure. *New Engl J Med* 347: 1397-1402, 2002.

[4] Mosterd A, Hoes AW: Clinical epidemiology of heart failure. *Heart* 93: 1137-1146, 2007.

[5] Baran GR, Kiani MF, Pravee S: Cardiovascular devices: getting to the heart of the matter. In: *Healthcare and biomedical technology in the 21st century: an introduction for non-science majors*. Springer Science+Business Media, New York, NY, 2014. DOI 10.1007/978-1-4614-8541-4_9.

[6] Orians CE, Evans RW, Ascher NL: Estimates of organ-specific donor availability for the United States. *Transpl P* 25: 1541-1542, 1993.

[7] Department of Health and Human Services, Health Resources and Services Administration, Healthcare Systems Bureau, Division of Transplantation, Rockville, MD; United Network for Organ Sharing, Richmond, VA; University Renal Research and Education Association, Ann Arbor, MI: 2015 annual report of the U.S. Organ Procurement and Transplantation Network and the scientific registry of transplant recipients: transplant data 1995-2014. Available at: http://optn.transplant.hrsa.gov. Accessed 5 Jan 2015.

[8] Sun BC, Catanese KA, Spanier TB, Flannery MR, Gardocki MT, et al.: 100 long-term implantable left ventricular assist devices: the Columbia Presbyterian interim experience. *Ann Thorac Surg* 68: 688-694, 1999.

[9] Gandhi SK, Huddelston CB, Balzer DT, Epstein DJ, Boschert TA, Canter CE: Biventricular assist devices as a bridge to heart transplantation in small children. *Circulation* 118: S89-S93, 2008.

[10] John R, Kamdar F, Liao K, Colvin-Adams M, Boyle A, Joyce L: Improved survival and decreasing incidence of adverse events with the HeartMate II left ventricular assist device as bridge-to-transplant-therapy. *Ann Thorac Surg* 86: 1227-1235, 2008.

[11] Sharma MS, Webber SA, Morell VO, Gandhi SK, Wearden PD, et al.: Ventricular assist device support in children and adolescents as a bridge to heart transplantation. *Ann Thorac Surg* 82: 926-933, 2006.

[12] Almond CS, Morales DL, Blackstone EH, Turrentine M, Imamura M, et al.: The Berlin Heart EXCOR pediatric ventricular assist device for bridge to heart transplantation in US children. *Circulation* 127: 1702-1711, 2013.

[13] Humpl T, Furness S, Gruenwald C, Hyslop C, Arsdell GV: The Berlin Heart EXCOR pediatrics-the SickKids experience 2004-2008. *Artif Organs* 34: 1082-1086, 2010.

[14] Rockett SR, Bryant JC, Morrow R, Frazier EA, Fiser WP, et al.: Preliminary single center North American experience with the Berlin Heart pediatric EXCOR device. *ASAIO J* 54: 479-482, 2008.

[15] Slater JP, Rose EA, Levin HR, Frazier OH, Roberts JK, et al.: Low thromboembolic risk without anticoagulation using advanced-design left ventricular assist devices. *Ann Thorac Surg* 62: 1321-1328, 1996.

[16] Rose EA, Gelijns AC, Moskowitz AJ, Heitjan DF, Stevenson LW, et al.: Long-term use of a left ventricular assist device for end-stage heart failure. *New Engl J Med* 345: 1435-1443, 2001.

[17] Drakos SG, Wever-Pinzon O, Selzman CH, Gilbert EM, Alharethi R, et al.: Magnitude and time course of changes induced by continuous-flow left ventricular assist device unloading in chronic heart failure. *J Am Coll Cardiol* 61: 1985-1994, 2013.

[18] Lang SA, O'Neill B, Waterworth P, Bilal H: Can the temporary use of right ventricular assist devices bridge patients with acute right ventricular failure after cardiac surgery to recovery? *Interac Cardiovas Thorac Surg* 18: 499-510, 2014.

[19] George CLS, Ameduri RK, Reed RC, Dummer KB, Overman DM, St. Louis JD: Long-term use of ventricular assist device as a bridge to recovery in acute fulminant myocarditis. *Ann Thorac Surg* 95: e59-e60, 2013.

[20] McCarthy PM, Nakatani S, Vargo R, Kottke-Marchant K, Harasaki H, et al.: Structural and left ventricular histologic changes after implantable LVAD insertion. *Ann Thorac Surg* 59: 609-613, 1995.

[21] Robertis FD, Rogers P, Amrani M, Petrou M, Pepper JR, et al.: Bridge to decision using the Levitronix CentriMag short term ventricular assist device. *J Heart Lung Transplant* 27: 474-478, 2008.

[22] Carpenter BA, Gonzalez CG, Jessen SL, Moore EJ, Thrapp AN, et al.: Brief review of ventricular assist devices and a recommended protocol for pathology evaluations. *Cardiovasc Pathol* 22: 408-415, 2013.

[23] Lund LH, Gabrielsen A, Tiren L, Hallberg A, Karlsson KEL, Eriksson MJ: Derived and displayed power consumption, flow, and pulsatility over a range of HeartMate II left ventricular assist device settings. *ASAIO J* 58: 183-190, 2012.

[24] Chorpenning K, Brown MC, Voskoboynikov N, Reyes C, Dierlam AE, Tamez D: HeartWare controller logs a diagnostic tool and clinical management aid for the HVAD pump. *ASAIO J* 60: 115-118, 2014.

[25] United States Food and Drug Administration, Center of Devices and Radiological Health Division of Industry Communication and Education: Serious adverse events with implantable

left ventricular assist devices (LVADs): FDA safety communication. 5 Aug 2015. Available at: http://www.fda.gov/MedicalDevices/Safety/AlertsandNotices/ucm457327.htm?source=govdelivery&utm_medium=email&utm_source=govdelivery. Accessed 5 Aug 2015.

[26] Levinson MM, Smith RG, Cork RC, Gallo J, Emery RW, et al.: Thromboembolic complications of the Jarvik-7 total artificial heart: case report. *Artif Organs* 10: 236-244, 1986.

[27] Icenogle TB, Smith RG, Cleavinger M, Vasu MA, Williams RJ, et al.: Thromboembolic complications of the Symbion AVAD system. *Artif Organs* 13: 532-538, 1989.

[28] Eckman PM, John R: Bleeding and thrombosis in patients with continuous-flow ventricular assist devices. *Circulation* 125: 3038-3047, 2012.

[29] Goldstein DJ, John R, Salerno C, Silvestry S, Moazami N, et al.: Algorithm for the diagnosis and management of suspected pump thrombus. *J Heart Lung Transpl* 32: 667-670, 2013.

[30] Muthiah K, Robson D, Macdonald PS, Keogh AM, Kotlyar E, et al.: Thrombolysis for suspected intrapump thrombosis in patients with continuous flow centrifugal left ventricular assist device. *Artif Organs* 37: 313-322, 2013.

[31] Najjar SS, Slaughter MS, Pagani FD, Starling RC, McGee EC, et al.: An analysis of pump thrombus events in patients in the HeartWare ADVANCE bridge to transplant and continued access protocol trial. *J Heart Lung Transpl* 33: 23-34, 2014.

[32] Pratt AK, Shah NS, Boyce SW: Left ventricular assist device management in the ICU. *Crit Care Med* 42: 158-168, 2014.

[33] Uriel N, Han J, Morrison KA, Nahumi N, Yuzefpolskaya M, et al.: Device thrombosis in HeartMate II continuous-flow left ventricular assist device: a multifactorial phenomenon. *J Heart Lung Transpl* 33: 53-59, 2014.

[34] Hasin T, Deo S, Maleszewski JJ, Topilsky Y, Edwards BS, et al.: The role of medical management for acute intravascular hemolysis in patients supported on axial flow LVAD. *ASAIO J* 60: 9-14, 2014.

[35] McBride LR, Naunheim KS, Fiore AC, Moroney DA, Swartz MT: Clinical experience with 111 Thoratec ventricular assist devices. *Ann Thorac Surg* 67: 1233-1239, 1999.

[36] Starling RC, Moazami N, Silvestry SC, Ewald G, Rogers JG, et al.: Unexpected abrupt increase in left ventricular assist device thrombosis. *New Engl J Med* 370: 33-40, 2013.

[37] Fyfe B, Schoen FJ: Pathologic analysis of 34 explanted Symbion ventricular assist devices and 10 explanted Jarvik-7 total artificial hearts. *Cardiovasc Patholo* 2: 187-197, 1993.

[38] Bashir J, Cheung A, Kaan A, Kearns M, Ibey A, Ignaszewski A: Thrombosis and failure of a HeartMate II device in the absence of alarms. *J Heart Lung Transpl* 30: 1197-1199, 2011.

[39] Levin HR, Oz MC, Chen JM, Packer M, Rose EA, Burkhoff D: Reversal of chronic ventricular dilation in patients with end-stage cardiomyopathy by prolonged mechanical unloading. *Circulation* 91: 2717-2720, 1995.

[40] Ferns J, Dowling R, Bhat G: Evaluation of a patient with left ventricular assist device dysfunction. *ASAIO J* 47: 696-698, 2001.

[41] Ong C, Dokos S, Chan B, Lim E, Al Abed A, et al.: Numerical investigation of the effect of cannula placement on thrombosis. *Theor Biol Med Model* 10: 1-14, 2013.

[42] Laumen M, Kaufmann T, Timms D, Schlanstein P, Jansen S, et al.: Flow analysis of ventricular assist device inflow and outflow cannula positioning using a naturally shaped ventricle and aortic branch. *Artif Organs* 34: 798-806, 2010.

[43] Sumikura H, Toda K, Takewa Y, Tsukiya T, Ohnuma K, et al.: Development and hydrodynamic evaluation of a novel inflow cannula in a mechanical circulatory support system for bridge to decision. *Artif Organs* 35: 756-764, 2011.

[44] Tsukiya T, Toda K, Sumikura H, Takewa Y, Watanabe F, et al.: Computational fluid dynamic analysis of the flow field in the newly developed inflow cannula for a bridge-to-decision mechanical circulatory support. *Artif Organs* 14: 381-384, 2011.

[45] Karmonik C, Partovi S, Loebe M, Schmack B, Ghodsizad A, et al.: Influence of LVAD cannula outflow tract location on hemodynamics in the ascending aorta: a patient-specific computational fluid dynamics approach. *ASAIO J* 58: 562-567, 2012.

[46] Timms D, Hayne M, McNeil K, Galbraith A: A complete mock circulation loop for the evaluation of left, right, and biventricular assist devices. *Artif Organs* 29: 564-572, 2005.

[47] Pantalos GM, Koenig SC, Gillars JK, Giriharan GA, Ewert DL: Characterization of an adult mock circulation for testing cardiac support devices. *ASAIO J* 50: 37-46, 2004.

[48] Birks EJ, Tansley PD, Yacoub MH, Bowles CT, Hipkin M, et al.: Incidence and clinical management of life-threatening left ventricular assist device failure. *J Heart Lung Transpl* 23: 964-969, 2004.

[49] Baloa LA, Boston JR, Antaki JF: Elastance-based control of a mock circulatory system. *Ann Biomed Eng* 29: 244-251, 2001.

[50] Ferrari G, Lazzari CD, Kozarski M, Clemente F, Gorczynska K, et al.: A hybrid mock circulatory system: testing a prototype under physiologic and pathological conditions. *ASAIO J* 48: 487-494, 2002.

[51] Taylor JO, Witmer KP, Neuberger T, Craven BA, Meyer RS, et al.: *In vitro* quantification of time dependent size using magnetic resonance imaging and computational simulations of thrombus near surface shear stresses. *J Biomech Eng* 136: 1-11, 2014.

[52] Navitsky MA, Taylor JO, Smith AB, Slattery MJ, Deutsch S, et al.: Platelet adhesion to polyurethane urea under pulsatile flow conditions. *Artif Organs* 38: 1046-1053, 2014.

[53] Koenig SC, Pantalos GM, Gillars KJ, Ewert DL, Litwak KN, Etoch SW: Hemodynamic and pressure-volume responses to continuous and pulsatile ventricular assist in an adult mock circulation. *ASAIO J* 50: 15-24, 2004.

[54] Schima H, Baumgartner H, Spitaler F, Kuhn P, Wolner E: A modular mock circulation for hydromechanical studies on valves, stenosis, vascular grafts and cardiac assist devices. *Int J Artif Organs* 15: 417-421, 1992.

[55] Vandenberghe S, Segers B, Meyns B, Verdonck P: Hydrodynamic characterization of ventricular assist devices. *Int J Artif Organs* 24: 470-477, 2001.

[56] Vermette P, Thibault J, Laroche G: A continuous and pulsatile flow circulation system for evaluation of cardiovascular devices. *Artif Organs* 22: 746-752, 1998.

[57] Esper SA, Subramaniam K: Heart failure and mechanical circulatory support. *Best Pract Res Cl Anaesthesiol* 26: 91-104, 2012.

[58] American Heart Association: Classes of heart failure. Available at: http://www.heart.org/HEARTORG/Conditions/HeartFailure/AboutHeartFailure/Classes-of-Heart-Failure_UCM_306328_Article.jsp#.VvRJmuIrLIU. Accessed 5 Jan 2014.

[59] DeVries WC, Anderson JL, Joyce LD, Anderson FL, Hammond EH, et al.: Clinical use of the total artificial heart. *New Engl J Med* 310: 273-278, 1984.

[60] Johnson KE, Prieto M, Joyce LD, Pritzker M, Emery RW: Summary of the clinical use of the Symbion total artificial heart: a registry report. *J Heart Lung Transpl* 11: 103-116, 1992.

[61] Burton NA, Lefrak EA, Macmanus Q, Hill A, Marino JA, et al.: A reliable bridge to cardiac transplantation: the TCI left ventricular assist device. *Ann Thorac Surg* 55: 1425-1431, 1993.

[62] United States Food and Drug Administration, Center for Devices and Radiological Health: Summary of safety and effectiveness data for Thoratec HeartMate® II left ventricular assist system (LVAS). 21 Apr 2008. Available at: http://www.accessdata.fda.gov/cdrh_docs/pdf6/P060040b.pdf. Accessed 3 June 2013.

[63] United States Food and Drug Administration, Center for Devices and Radiological Health: Summary of safety and probable benefit for EXCOR® pediatric ventricular assist device (EXCOR). 16 Dec 2011. Available at: http://www.accessdata.fda.gov/cdrh_docs/pdf10/h100004b.pdf. Accessed 3 June 2013.

[64] United States Food and Drug Administration, Center for Devices and Radiological Health: Summary of safety and effectiveness data for HeartWare® ventricular assist system. 20 Nov 2012. Available at: http://www.accessdata.fda.gov/cdrh_docs/pdf10/p100047b.pdf. Accessed 3 June 2013.

[65] Nativi JN, Drakos SG, Kucheryavaya AY, Edwards LB, Selzman CH, et al.: Changing outcomes in patients bridged to heart transplantation with continuous- versus pulsatile-flow ventricular assist devices: an analysis of the registry of the International Society for Heart and Lung Transplantation. *J Heart Lung Transpl* 30: 854-861, 2011.

[66] Kato TS, Chokshi A, Singh P, Khawaja T, Cheema F, et al.: Effects of continuous-flow versus pulsatile-flow left ventricular assist devices on myocardial unloading and remodeling. *Circ Heart Fail* 4: 546-553, 2011.

[67] Potapov EV, Loforte A, Weng Y, Jurmann M, Pasic M, et al.: Experience with over 1000 implanted ventricular assist devices. *J Card Surg* 23: 185-194, 2008.

[68] Garbade J, Bittner HB, Barten MJ, Mohr FW: Current trends in implantable left ventricular assist devices. *Cardiol Res Pract* 2011: 1-9 (Article ID 290561), 2011.

[69] Slaughter MS., Pagani FD, Rogers JG, Miller LW, Sun B, et al.: Clinical management of continuous-flow left ventricular assist devices in advanced heart failure. *J Heart Lung Transpl* 29: S1-S39, 2010.

[70] Travis AR, Giridharan GA, Pantalos GM, Dowling RD, Prabhu SD, et al.: Vascular pulsatility in patients with a pulsatile- or continuous-flow ventricular assist device. *J Thorac Cardiov Sur* 133: 517-524. 2007.

[71] Tuzun E, Rutten M, Dat M, van de Voss F, Kadipasaoglu C, de Mol B: Continuous-flow cardiac assistance: effects on aortic valve function in a mock loop. *J Surg Res* 171: 443-447, 2011.

[72] Wang Q, Yambe T, Shiraishi Y, Duan X, Yoshizawa M, et al.: Non-blood contacting electro-hydraulic artificial myocardium (EHAM) improves the myocardial tissue perfusion. *Technol Health Care* 13: 229-234, 2005.

[73] Fragasso T, Ricci Z, Grutter G, Albanese S, Varano C, et al.: Incidence of healthcare-associated infections in a pediatric population with an extracorporeal ventricular assist device. *Artif Organs* 35: 1110-1114, 2011.

[74] Felker GM, Rogers JG: Same bridge, new destinations – rethinking paradigms for mechanical cardiac support in heart failure. *J Am Coll Cardiol* 47: 930-932, 2006.

[75] Stevenson LW, Pagani FD, Yount JB, Dessup M, Miller L, et al.: INTERMACS profiles of advanced heart failure: the current picture. *J Heart Lung Transpl* 28: 535-541, 2009.

[76] United States Food and Drug Administration, Center for Devices and Radiological Health: Guidance for industry and FDA staff: premarket approval application filing review. 3 Nov 2003. Available at: http://www.fda.gov/downloads/medicaldevices/deviceregulationandguidance/guidancedocuments/ucm089767.pdf Accessed 6 June 2013.

[77] United States Food and Drug Administration, Center for Devices and Radiological Health: Code of Federal Regulation: Title 21, Part 58. Available at: http://www.accessdata.fda.gov/scripts/cdrh/cfdocs/cfcfr/CFRsearch.cfm?CFRPart=58 Accessed 6 June 2013.

[78] Schoen FJ, Anderson JM, Didisheim P, Dobbins JJ, Gristina AG, et al.: Ventricular assist device (VAD) pathology analyses: guidelines for clinical studies. *J Appl Biomater* 1: 49-56, 1990.

[79] Gilbert EF, Huntington RW: Diseases of the blood. In: *An introduction to pathology*. Oxford University Press, New York, NY, 1978.

[80] Taussig MJ: The circulation. In: *Processes in pathology.* Blackwell Scientific Publications, London, England, 1979.

[81] Kumar V, Abbas AK, Fausto N, Mitchell RN: Hemodynamic disorders, thrombosis, and shock. In: *Robbins basic pathology, 8th edition*. Saunders Elsevier, Philadelphia, PA, 2007.

[82] Boron WF, Boulpaep EL: The cardiovascular system. In: *Medical physiology, 2nd edition*. Saunders Elsevier, Philadelphia, PA, 2012.

[83] Butenas S, Mann KG: Blood coagulation. *Biochemistry (Moscow)* 67: 3-12, 2002.

[84] Dickson BC: Venous thrombosis: on the history of Virchow's triad. *U Toronto Med J* 81: 166-171, 2004.

[85] Spanier T, Oz M, Levin H, Weinberg A, Stamatis K, et al.: Activation of coagulation and fibrinolytic pathways in patients with left ventricular assist devices. *J Thorac Cardiov Sur* 112: 1090-1097, 1996.

[86] Hochareon P, Manning KB, Fontaine AA, Tarbell JM, Deutsch S: Correlation of *in vivo* clot deposition with the flow characteristics in the 50 cc Penn State artificial heart: a preliminary study. *ASAIO J* 50: 537-542, 2004.

[87] Milner KR, Snyder AJ, Siedlecki CA: Sub-micron texturing for reducing platelet adhesion to polyurethane biomaterials. *J Biomed Mater Res* 76A: 561-570, 2006.

[88] Hirsh J, Fletcher AP, Sherry S: Effect of fibrin and fibrinogen proteolysis products on clot physical properties. *Am J Physiol* 209: 415-424, 1965.

[89] Rosenberg RD: Biochemistry of heparin antithrombin interactions, and the physiologic role of this natural anticoagulant mechanism. *Am J Med* 87: 1-8, 1989.

[90] Plumb DC: *Plumb's veterinary drug handbook pocket, 7th edition*. PharmaVet Press, Stockholm, Sweden, 2011. pp. 112-113, 661-662, 1393-139.

[91] Noon GP, Morley DL, Irwin S, Abdelsayed SV, Benkowski RJ, Lynch BE: Clinical experience with the MicroMed DeBakey ventricular assist device. *Ann Thorac Surg* 71: S133-S138, 2001.

[92] Long CC, Marsden AL, Bazilevs Y: Shape optimization of pulsatile ventricular assist devices using FSI to minimize thrombotic risk. *Comput Mech* 54: 921-932, 2014.

[93] Lopez JA, Chen J: Pathophysiology of venous thrombosis. *Thromb Res* 123: S30-S34, 2009.

[94] Olsen DB, Unger F, Oster H, Lawson J, Kessler T, et al.: Thrombus generation within the artificial heart. *J Thorac Cardiov Sur* 70: 248-255, 1975.

[95] Dasse KA, Chipman SD, Sherman CN, Levine AH, Frazier OH: Clinical experience with textured blood contacting surfaces in ventricular assist devices. *T Am Soc Artif Intern Organs* 33: 418-425, 1987.

[96] McGee E, Chorpenning K, Brown MC, Breznock E, LaRose JA, Tamez D: *In vivo* evaluation of the Heartware MVAD pump. *J Heart Lung Transpl* 33: 366-371, 2014.

[97] Anderson JM: Cardiovascular device retrieval and evaluation. *Cardiovas Patholo* 2: 199S-208S, 1993.

[98] Chueh JY, Wakhloo AK, Hendricks GH, Silva CF, Weaver JP, Gounis MJ: Mechanical characterization of thromboemboli in acute ischemic stroke and laboratory embolus analogs. *Am J Neuroradiol* 32: 1237-1244, 2011.

[99] Ryan EA, Mockros LF, Weisel JW, Lorand L: Structural origins of fibrin clot rheology. *Biophys J* 77: 2813-2826, 1999.

[100] Fraser KH, Taskin ME, Griffith BP, Wu ZJ: The use of computational fluid dynamics in the development of ventricular assist devices. *Med Eng Phys* 33: 263-280, 2011.

[101] Sakaguchi T, Matsumiya G, Yoshioka D, Miyagawa S, Nishi H, et al.: DuraHeart™ magnetically levitated left ventricular assist device: Osaka University experience. *Circ J* 77: 1736-1741, 2013.

[102] Fraser KH, Zhang T, Taskin E, Griffith BP, Wu ZJ: Computational fluid dynamics analysis of thrombosis potential in left ventricular assist device drainage cannulae. *ASAIO J* 56: 157-163, 2010.

[103] Radovancevic B, Frazier OH, Duncan JM: Implantation technique for the Heartmate® left ventricular assist device. *J Cardiac Surg* 7: 203-207, 1992.

[104] Westaby S, Frazier OH, Pigott DW, Saito S, Jarvik RK: Implant technique for the Jarvik 2000 Heart. *Ann Thorac Surg* 73: 1337-1340, 2002.

[105] Gregoric ID, Cohn WE, Frazier OH: Diaphragmatic implantation of the Heartware ventricular assist device. *J Heart Lung Transpl* 30: 467-470, 2011.

[106] Komoda T, Weng Y, Nojiri C, Hetzer R: Implantation technique for the DuraHeart left ventricular assist system. *Artif Organs* 10: 124-127, 2007.

[107] Kirklin JK, Naftel DC, Kormos RL, Pagani FD, Myers SL, et al.: Interagency registry for mechanically assisted circulatory support (INTERMACS) analysis of pump thrombosis in the HeartMate II left ventricular assist device. *J Heart Lung Transpl* 33: 12-22, 2014.

[108] Taghavi S, Ward C, Jayaranjan SN, Gaughan J, Wilson LM, Mangi AA: Surgical technique influences HeartMate II left ventricular assist device thrombosis. *Ann Thorac Surg* 96: 1259-1265, 2013.

[109] Truong TV, Stanfield R, Chaffin JS, Elkins CC, Kanaly PJ, et al.: Postimplant left ventricular assist device fit analysis using three-dimensional reconstruction. *ASAIO J* 59: 586-592, 2013.

[110] Milano CA, Simeone AA, Blue LJ, Rogers JG: Presentation and management of left ventricular assist device inflow cannula malposition. *J Heart Lung Transpl* 30: 838-840, 2011.

[111] Bolen MA, Popovic ZB, Gonzalez-Stawinski G, Schoenhagen P: Left ventricular assist device malposition interrogated by 4-D cine computed tomography. *J Cardiovasc Comput Tomogr* 5:186-188, 2011.

[112] Paluszkiewicz L, Schulte-Eistrup S, Gummert J, Koertke H: Asymptomatic displacement of the inflow cannula of a patient 18 months after implantation of a DuraHeart left ventricular assist device. *J Am Coll Cardiol* 58: 1, 2011.

[113] Douglas PA, Morrow R, Ioli A, Reichek N: Left ventricular shape, afterload and survival in idiopathic dilated cardiomyopathy. *J Am Coll Cardiol* 13: 311-315, 1989.

[114] Semelka RC, Tomei E, Wagner S, Mayo J, Caputo G, et al.: Interstudy reproducibility of dimensional and functional measurements between cine magnetic resonance studies in the morphologically abnormal left ventricle. *Am Heart J* 119: 1367-1373, 1990.

[115] Shernan SK: e-Echocardiography, an echocardiography and ultrasound learning resource: normal mitral valve measurements. Available at: https://e-echocardiography.com/page/page.php?UID=1867001. Accessed 5 Jan 2016.

[116] Wang SH, Lee LP, Lee JS: A linear relation between the compressibility and density of blood. *J Acoust Soc Am* 109: 390-396, 2001.

[117] Gijsen FJH, van de Vosse FN, Janssen JD: The influence of the non-Newtonian properties of blood on the flow in large arteries: steady flow in a carotid bifurcation model. *J Biomech* 32: 601-608, 1999.

[118] John R, Mantz K, Eckman P, Rose A, May-Newman K: Aortic valve pathophysiology during left ventricular assist device support. *J Heart Lung Transpl* 29: 1321-1329, 2010.

[119] Chandler AB: *In vitro* thrombotic coagulation of the blood – a method for producing a thrombus. *Lab Invest* 7: 110-114, 1958.

[120] Topper SR, Navitsky MA, Medivtz RB, Paterson EC, Siedlecki CA, et al.: The use of fluid mechanics to predict regions of microscopic thrombus formation in pulsatile VADs. *Cardiovasc Eng Technol* 5: 54-69, 2014.

[121] Geddes LA, Sadler C: The specific resistance of blood at body temperature. *Med Biol Eng Comput* 11: 336-339, 1973.

[122] Knisely MH, Bloch EH, Brooks F, Warner L: Microscopic observations of the circulating blood of nine healthy normal horses, all of which had unagglutinated circulating blood cells and high *in vitro* erythrocyte sedimentation rates: a contribution to the theory and general understanding of the pathologic circulatory physiology of sludged blood. *Am J Med Sci* 219: 249-267, 1950.

[123] Eicker SW, Ainsworth DM: Equine plasma banking: collection by exsanguination. *J Am Vet Med Assoc* 185: 772-774, 1984.

[124] Roessler FC, Ohlrich M, Marxsen JH, Stellmacher F, Sprenger A, et al.: The platelet-rich plasma clot: a standardized *in-vitro* clot formation protocol for investigations of sonothrombolysis under physiological flows. *Blood Coagul Fibrinolysis* 22: 407-415, 2011.

[125] Joy DC: Scanning electron microscopy. In: *Materials science and technology*. Wiley-VCH Verlag GmbH & Co KGaA. Weinheim, Germany, 2006. DOI 10.1002/9783527603978.mst0012.

[126] Weng X, Cloutier G, Pibarot P, Durand LG: Comparison and simulation of different levels of erythrocyte aggregation with pig, horse, sheep, calf, and normal human blood. *Biorheology* 33: 365-377, 1996.

[127] Colacino FM, Arabia M, Moscato F, Danieli GA: Modeling, analysis, and validation of a pneumatically driven left ventricle for use in mock circulatory systems. *Med Eng Phys* 29: 829-839, 2007.

[128] Tuzun E, Roberts K, Cohn WE, Sargin M, Gemmato C, et al.: *In vivo* evaluation of the HeartWare centrifugal ventricular assist device. *Tex Heart Inst J* 34: 406-411, 2007.

[129] Chiu WC, Girdhar G, Xenos M, Alemu Y, Soares JS, et al.: Thromboresistance comparison of the HeartMate II ventricular assist device with the device thromboenicity emulation-optimized HeartAssist 5 VAD. *J Biomech Eng* 136: 1-9, 2014.

[130] Stevens MC, Gregory SD, Nestler F, Thomson B, Choudhary J, et al.: *In vitro* and *in vivo* characterization of three different modes of pump operation when using a left ventricular assist device as a right ventricular assist device. *Artif Organs* 38: 931-939, 2014.

[131] Sherwood L: *Human physiology: from cells to systems, 8th edition*. Brooks/Cole, Cengage Lerning, Belmont, CA, 2013. pp. 404-410.

[132] Malaisrie SC, Pelletier MP, Yun JJ, Sharma K, Timek TA, et al.: Pneumatic paracorporeal ventricular assist device in infants and children: initial Stanford experience. *J Heart Lung Transpl* 27: 173-177, 2008.

[133] Berlin Heart: EXCOR® VAD with stationary driving unit Ikus instructions for use. Jan 2008. Available online at: http://www.berlinheart.de/UserFiles/Downloaddokumente/Medical_Professionals_Distributoren/Non_US/EXCOR_Parakorporales_Herzunterstuetzungssystem/Gebrauchsanweisungen/EXCOR_VAD_Ikus_Antrieb/Ikus_Rev_2_1_Software_3_40/Gebrau3.40AMRev80en.pdf. Accessed 10 Oct 2015.

APPENDIX I

COAGULATION CASCADE

The figure below displays creation of a stabilized fibrin clot originating from tissue injury, negatively charged surfaces, and non-laminar flow. Tissue injury involves injury of endothelial cells (EC) and exposure of subendothelial collagen. Injured EC release von Willebrand factor (vWf), which activates when bound to subendothelial collagen. Mammalian platelets are activated once they bind to activated vWf. Platelets contain secretory vesicles that release adenosine diphosphate (ADP), platelet factors, thromboxane A_2, vWf, vasoconstrictors, and several others once activated within the plasma [1]. The activation of platelets initiates a second messenger signaling pathway (IP3/DAG) that causes the release of cytosolic calcium from intracellular stores within the endoplasmic reticulum of platelets [2]. Intracellular and extracellular calcium play an important role in mediating the release of secretory vesicles [3]. ADP and thromboxane A_2 released from the vesicles of activated platelets attract additional circulating platelets to aggregate and form a platelet plug. Thrombin helps to further activate platelets, thereby intensifying aggregation. ADP released from platelets stimulates the healthy surrounding endothelium to secrete nitric oxide and prostacyclin, which prevents the clot from extending to the normal tissue.

Injured tissue, in addition to activating platelets, also activates the extrinsic pathway by releasing Tissue Factor (TF) [4]. TF binds with clotting factor VII, which is normally present in its inactive form in the bloodstream. TF activates factor VII to become factor VIIa, which activates clotting factor X in the presence of calcium and additional TF, thereby completing the extrinsic clotting cascade and initiating the common pathway.

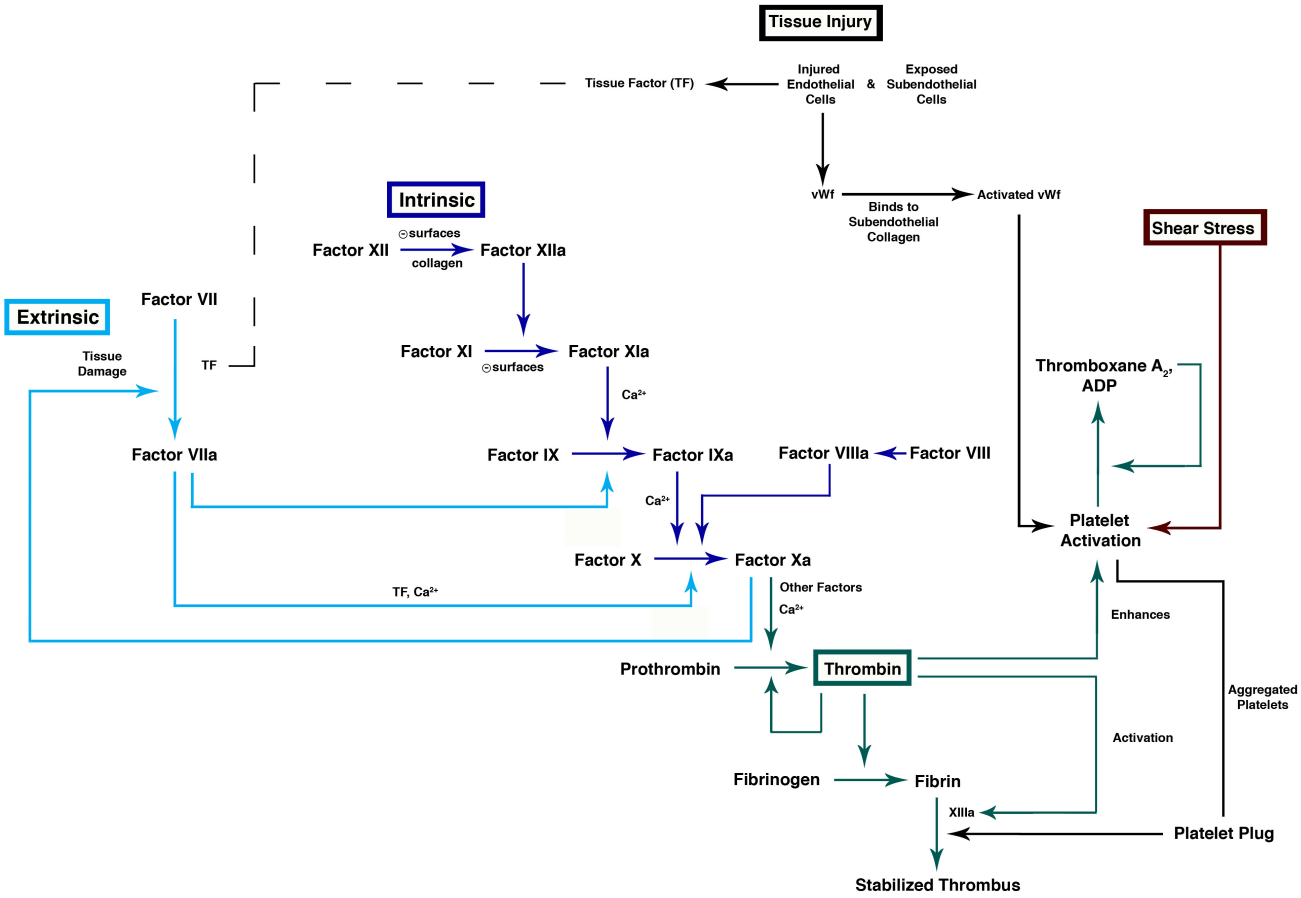
Tissue Injury
Tissue Factor (TF)
Injured Endothelial Cells
&
Exposed Subendothelial Cells
vWf
Activated vWf
Binds to Subendothelial Collagen
Intrinsic
surfaces
Factor XII
collagen
Factor XIIa
Shear Stress
Extrinsic
Factor VII
Factor XI
surfaces
Factor XIa
Tissue Damage
TF
Thromboxane A2, ADP
Ca2+
Factor VIIa
Factor IX
Factor IXa
Factor VIIIa
Factor VIII
Ca2+
Platelet Activation
Factor X
Factor Xa
TF, Ca2+
Other Factors
Ca2+
Enhances
Prothrombin
Thrombin
Aggregated Platelets
Activation
Fibrinogen
Fibrin
XIIIa
Platelet Plug
Stabilized Thrombus

References:

[1] Sherwood L. Human Physiology: From Cells to Systems, 8th Edition. Belmont, CA, Brooks/Cole, Cengage Learning, 2013, pp. 404-410.

[2] Boon GD. Overview of Hemostasis. Toxicologic Pathology 21: 170-176, 1993.

[3] Varga-Szabo D, Braun A, Nieswandt B. Calcium Signaling in Platelets. Journal of Thrombosis and Haemostasis 7: 1057-1066, 2009.

[4] Kierszenbaum AL, Tres LL. Histology and Cell Biology: An Introduction to Pathology, 3rd Edition. Philadelphia, PA, Elsevier Press, 2012, pp. 180-181.

APPENDIX II

CFD MOTION EQUATIONS

Equations for movement of ventricle wall with cannula in anterior apical placement:

(1.1) $$\frac{dy}{dt} = (y_1 - line) * \frac{a\pi}{T} * \sin(\frac{2\pi}{T} t)$$

(1.2) $$\frac{dx}{dt} = 0$$

Where

$$line = y_1 - (mx_1 + y_{int})$$

$$x_1 \text{ and } y_1 \text{ are coordinates of the ventricle wall at end diastole}$$

$$y_{int} \text{ and } m \text{ are the } y \text{ intercept and slope values of the line created by connecting the end points of the moving wall}$$

$$T = period$$

$$t = time$$

$$a = average\ y_{value}\ of\ "line"$$

Equations for movement of ventricle wall with cannula in posterior diaphragmatic placement:

(2.1) $$\frac{dx}{dt} = \frac{-\pi r a}{T} * \sin\frac{2\pi t}{T} * [\cos(2(\pi - \theta_c)) + \theta_c] \quad for \quad y_0 - y_c < 0$$

(2.2) $$\frac{dx}{dt} = \frac{-\pi r a}{T} * \sin\frac{2\pi t}{T} * \cos(2(\pi - \theta_c)) \quad for \quad y_0 - y_c \geq 0$$

(2.3) $$\frac{dy}{dt} = \frac{-\pi r a}{T} * \sin\frac{2\pi t}{T} * [\sin(2(\pi - \theta_c)) + \theta_c] \quad for \quad y_0 - y_c < 0$$

(2.4) $$\frac{dy}{dt} = \frac{-\pi r a}{T} * \sin\frac{2\pi t}{T} * \sin(2(\pi - \theta_c)) \quad for \quad y_0 - y_c \geq 0$$

Where

$$a = a_{max} * \sin\frac{\pi}{(a_1 - a_2)} * (2(\pi - \theta_c) + \theta_c \quad for \quad y_0 - y_c < 0$$

$$a = a_{max} * \sin\frac{\pi}{(a_1 - a_2)} * (2(\pi - \theta_c) \qquad for \qquad y_0 - y_c \geq 0$$

$$r = radius = \sqrt{(x_0 - x_c)^2 - (y_0 - y_c)^2}$$

$$T = Period = 1$$

$$t = time$$

$$\theta_c = \cos^{-1}((x_0 - x_c)/r)$$

$$x_0 \text{ and } y_0 = original\ x \text{ and } y\ coordinates\ of\ the\ moving\ walls$$

$$x_c \text{ and } y_c = x \text{ and } y\ coordinates\ of\ the\ center\ of\ the\ ventricle$$

$$a_{max} = constant$$

$$a_1 = min\ \theta_c$$

$$a_2 = max\ \theta_c$$

APPENDIX III

COMPLETE ARTIFICIAL CLOT DATA

Forty-eight clots were created to determine the best method for producing artificial clots (outlined in Section 7 of above work). This appendix contains specific information for each clot including date of creation, blood component(s) used, species of blood, concentration of Calcium Chloride ($CaCl_2$) used to make the blood clot, and a brief description of the method used to create the clot.

Clot Name: Clot 1

Date Created: 4/22/13

Blood Component: Whole Blood

Species: Porcine

$CaCl_2$ Concentration: 12mg $CaCl_2$ / mL distilled H_2O

Method: Approximately 5mL of porcine blood collected for transfusion was placed into a 50mL Erlenmeyer flask. Ten drops of the $CaCl_2$ solution at 3 separate times, each 2 minutes apart. The blood began to have a noticeable clot after 6 minutes since the first drops of $CaCl_2$ were added. The blood clot was photographed and transferred to a conical vial and stored at room temperature overnight.

Gross Evaluation: The clot is malleable (but shape retentive), bright red, and measured 16mm x 31mm. Clot is transferred to formalin and sectioned after 44.8 hours (since time of formation).

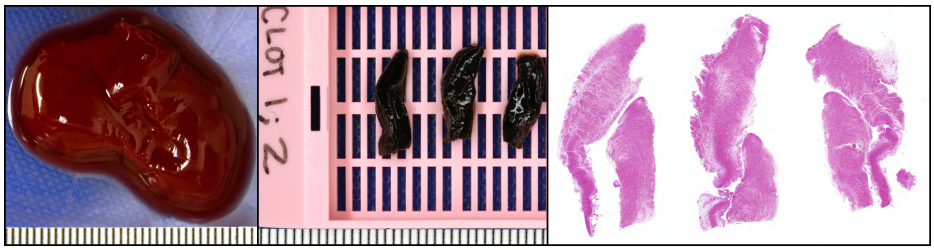

Clot Name: Clot 2

Date Created: 4/22/13

Blood Component: Whole Blood

Species: Porcine

$CaCl_2$ Concentration: 12mg $CaCl_2$ / mL distilled H_2O

Method: 5mL of porcine whole blood and the $CaCl_2$ solution were placed in a petri dish (50mm diameter). A second petri dish (38mm diameter) applied a rotational force on the blood while it was clotting.

RPM: 60

Gap Thickness: 4mm

Total Time Rotating: 2.87 hours

Gross Evaluation: Clot formed on the inferior surface of the rotating petri dish. Stationary dish also had a small deposit. Both deposits were collected for histology.

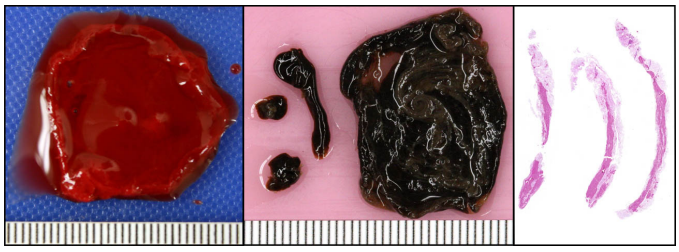

Clot Name: Clot 3

Date Created: 4/23/13

Blood Component: Whole Blood

Species: Porcine

$CaCl_2$ Concentration: 12mg $CaCl_2$ / mL distilled H_2O

Method: 5mL of porcine whole blood and the $CaCl_2$ solution were placed in a petri dish (50mm diameter). A second petri dish (38mm diameter) applied a rotational force on the blood while it was clotting.

RPM: 60

Gap Thickness: 2mm

Total Time Rotating: 5.05 hours

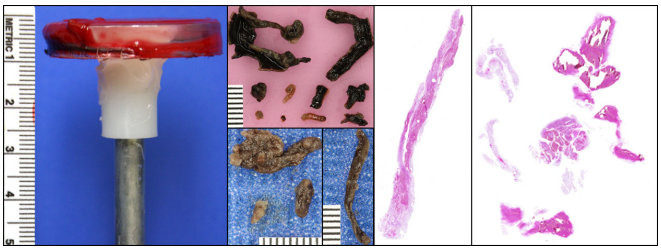

Clot Name: Clot 4

Date Created: 5/20/13

Blood Component: Whole Blood

Species: Equine

$CaCl_2$ Concentration: 24mg $CaCl_2$ / mL distilled H_2O

Method: Whole blood and $CaCl_2$ solution allowed to clot in a stationary glass test tube.

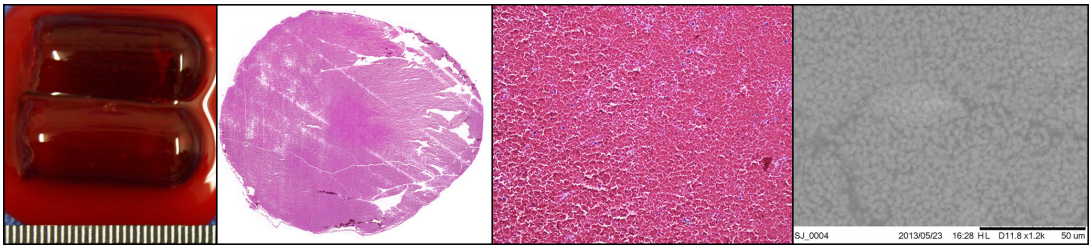

Clot Name: Clot 5

Date Created: 5/20/13

Blood Component: Plasma

Species: Equine

$CaCl_2$ Concentration: 24mg $CaCl_2$ / mL distilled H_2O

Method: Plasma and $CaCl_2$ solution allowed to clot in a stationary glass test tube.

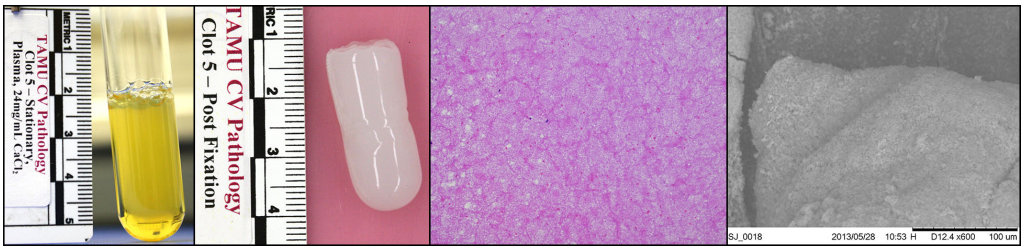

Clot Name: Clot 6

Date Created: 5/20/13

Blood Component: Plasma

Species: Equine

$CaCl_2$ Concentration: 24mg $CaCl_2$ / mL distilled H_2O

Method: Equine plasma and the $CaCl_2$ solution were placed in a petri dish (84mm diameter). A second petri dish (38mm diameter) applied a rotational force on the plasma while it was clotting.

RPM: 60

Gap Thickness: 5mm

Total Time Rotating: 8.58 hours

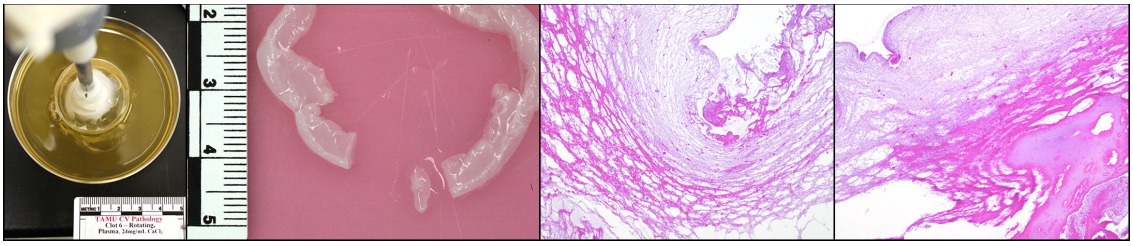

Clot Name: Clot 7

Date Created: 5/20/13

Blood Component: Plasma

Species: Equine

$CaCl_2$ Concentration: 12mg $CaCl_2$ / mL distilled H_2O

Method: Plasma and $CaCl_2$ solution allowed to clot in a stationary glass test tube.

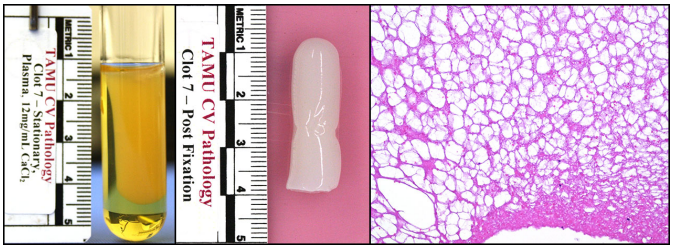

Clot Name: Clot 8

Date Created: 5/20/13

Blood Component: Whole Blood

Species: Equine

$CaCl_2$ Concentration: 24mg $CaCl_2$ / mL distilled H_2O

Method: Whole blood and $CaCl_2$ solution allowed to clot in a stationary glass test tube.

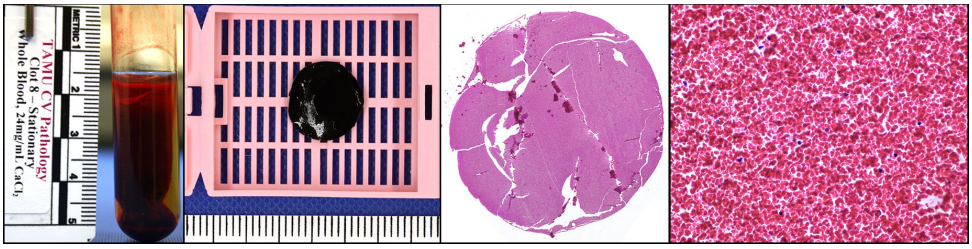

Clot Name: Clot 9

Date Created: 5/20/13

Blood Component: Plasma

Species: Equine

$CaCl_2$ Concentration: 24mg $CaCl_2$ / mL distilled H_2O

Method: Plasma and $CaCl_2$ solution allowed to clot in a stationary glass test tube.

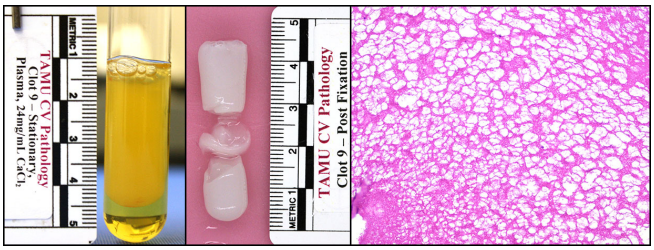

Clot Name: Clot 10

Date Created: 5/21/13

Blood Component: Whole Blood

Species: Equine

$CaCl_2$ Concentration: 24mg $CaCl_2$ / mL distilled H_2O

Method: Equine whole blood and the $CaCl_2$ solution were placed in a petri dish (50mm diameter) l. A second petri dish (38mm diameter) applied a rotational force on the blood while it was clotting.

RPM: 60

Gap Thickness: 7.5mm

Total Time Rotating: 7.55 hours

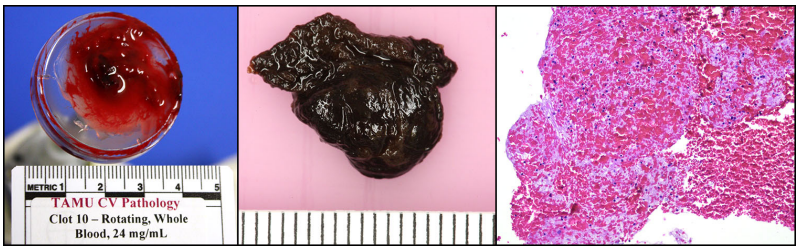

Clot Name: Clot 11

Date Created: 5/21/13

Blood Component: Whole Blood

Species: Equine

$CaCl_2$ Concentration: 12mg $CaCl_2$ / mL distilled H_2O

Method: Whole blood and $CaCl_2$ solution allowed to clot in a stationary glass test tube.

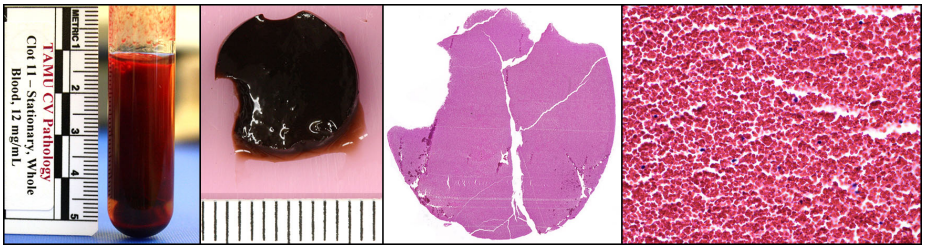

Clot Name: Clot 12

Date Created: 5/21/13

Blood Component: Plasma

Species: Equine

$CaCl_2$ Concentration: 12mg $CaCl_2$ / mL distilled H_2O

Method: Plasma and $CaCl_2$ solution allowed to clot in a stationary glass test tube.

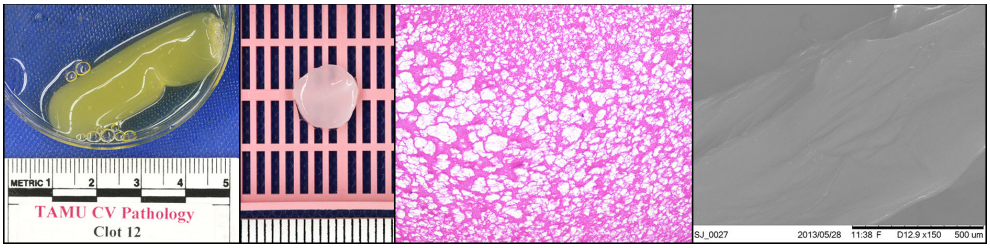

Clot Name: Clot 13

Date Created: 5/22/13

Blood Component: Whole Blood

Species: Equine

$CaCl_2$ Concentration: 24mg $CaCl_2$ / mL distilled H_2O

Method: Equine whole blood and the $CaCl_2$ solution were placed in a petri dish (55mm diameter). A second petri dish (38mm diameter) lined with aluminum foil applied a rotational force on the blood while it was clotting.

RPM: 60

Gap Thickness: 4 mm

Total Time Rotating: 6.35 hours

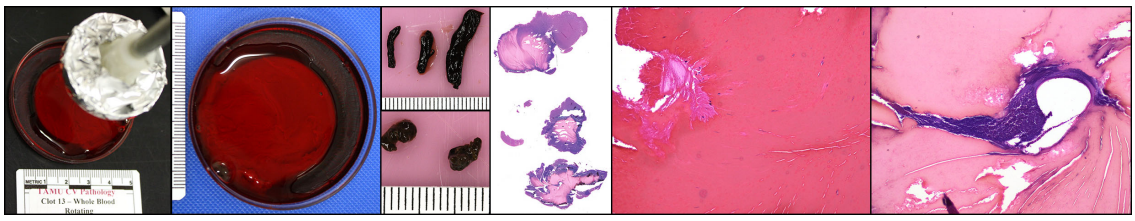

Clot Name: Clot 14

Date Created: 5/23/13

Blood Component: Whole Blood

Species: Equine

$CaCl_2$ Concentration: 24mg $CaCl_2$ / mL distilled H_2O

Method: Equine whole blood and the $CaCl_2$ solution were placed in a petri dish (55mm diameter). A second petri dish (38mm diameter) lined with aluminum foil that had been scratched with sand paper applied a rotational force on the blood while it was clotting.

RPM: 60

Gap Thickness: 5.5mm

Total Time Rotating: 9.15 hours

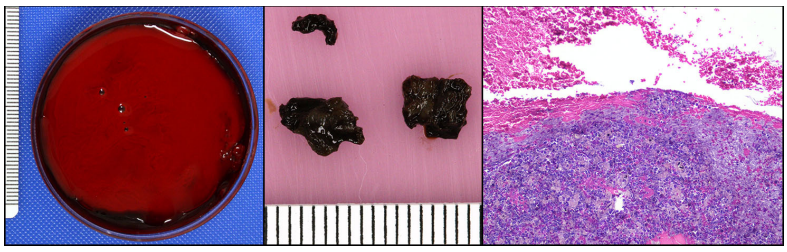

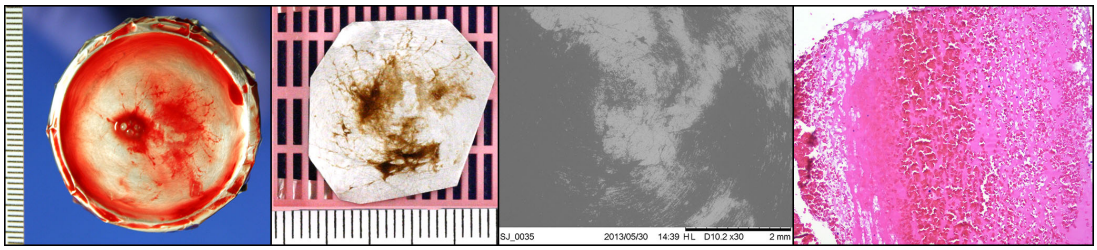

Clot Name: Clot 15

Date Created: 5/28/13

Blood Component: Whole Blood

Species: Equine

$CaCl_2$ Concentration: 24mg $CaCl_2$ / mL distilled H_2O

Method: Equine whole blood and the $CaCl_2$ solution were placed in a petri dish (50mm diameter) lined with aluminum foil. A second petri dish (38mm diameter) lined with aluminum foil applied a rotational force on the blood while it was clotting.

RPM: 60

Gap Thickness: 5mm

Total Time Rotating: 6.62 hours

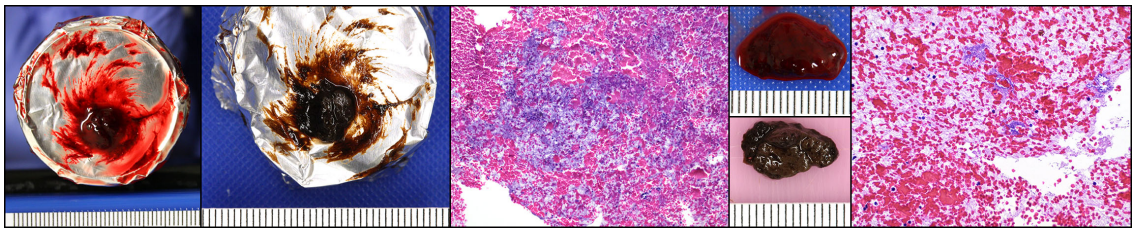

Clot Name: Clot 16

Date Created: 5/29/13

Blood Component: Plasma

Species: Equine

$CaCl_2$ Concentration: 24mg $CaCl_2$ / mL distilled H_2O

Method: Equine plasma and the $CaCl_2$ solution were placed in a petri dish (50 mm diameter) lined with aluminum foil. A second petri dish (38mm diameter) lined with aluminum foil applied a rotational force on the plasma while it was clotting.

RPM: 60

Gap Thickness: Unknown

Total Time Rotating: 6.82 hours

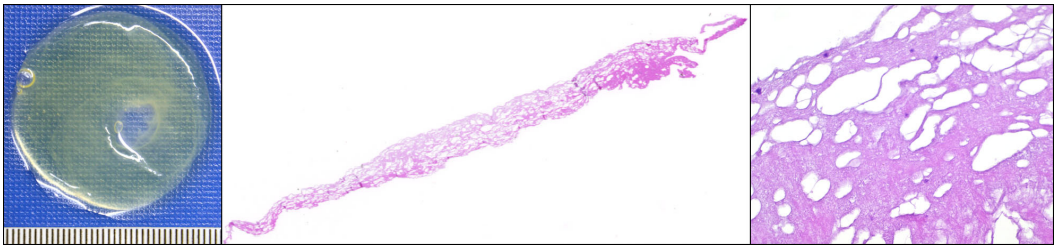

Clot Name: Clot 17

Date Created: 6/3/13

Blood Component: Plasma

Species: Equine

$CaCl_2$ Concentration: 24mg $CaCl_2$ / mL distilled H_2O

Method: Equine plasma and the $CaCl_2$ solution were placed in a petri dish (50mm diameter) lined with aluminum foil. A second petri dish (38mm diameter) lined with aluminum foil applied a rotational force on the plasma while it was clotting.

RPM: 60

Gap Thickness: 4.5mm

Total Time Rotating: 6.55 hours

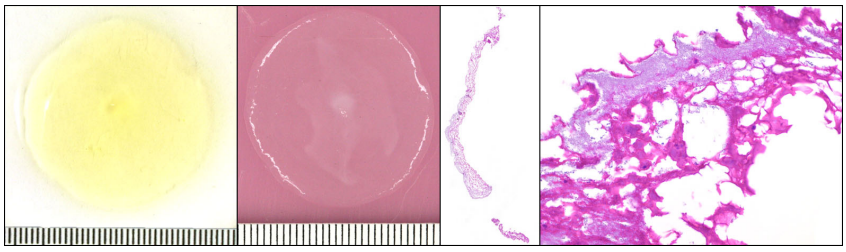

Clot Name: Clot 18

Date Created: 6/11/13

Blood Component: Plasma

Species: Equine

$CaCl_2$ Concentration: 24mg $CaCl_2$ / mL distilled H_2O

Method: Plasma and $CaCl_2$ solution allowed to clot in a stationary glass test tube.

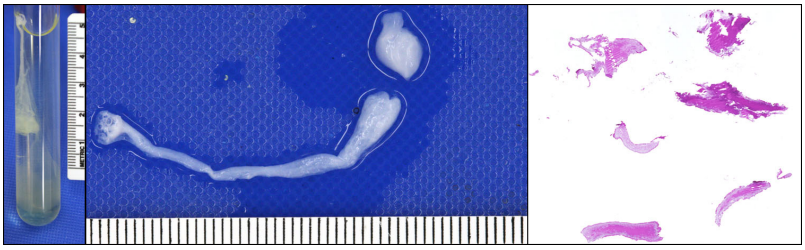

Clot Name: Clot 19

Date Created: 6/11/13

Blood Component: Plasma

Species: Equine

$CaCl_2$ Concentration: 48mg $CaCl_2$ / mL distilled H_2O

Method: Equine plasma diluted with distilled water was placed in a plastic jar with two openings in the bottom that were connected to a continuous flow pump. The $CaCl_2$ solution as added as the diluted plasma was moved by the pump; a rotational force was applied to the plasma as it pumped throughout the reservoir by a petri dish lined with aluminum foil that was connected to a rotational motor.

RPM: 60

Gap Thickness: 9mm

Total Time Rotating: 5.75 hours

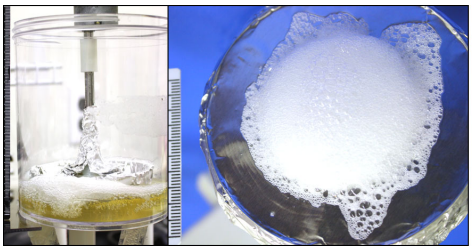

Clot Name: Clot 20 – Failed to clot

Clot Name: Clot 21

Date Created: 6/17/13

Blood Component: Plasma

Species: Equine

$CaCl_2$ Concentration: 48mg $CaCl_2$ / mL distilled H_2O

Method: Equine plasma diluted with distilled water was placed in a plastic jar with two openings in the bottom that were connected to a continuous flow pump. The $CaCl_2$ solution as added as the diluted plasma was moved by the pump; a rotational force was applied to the plasma as it pumped throughout the reservoir by a petri dish lined with aluminum foil that was connected to a rotational motor.

RPM: 60

Gap Thickness: 7mm

Total Time Rotating: 6.83 hours

Clot Name: Clot 22

Date Created: 6/18/13

Blood Component: Whole Blood

Species: Equine

$CaCl_2$ Concentration: 24mg $CaCl_2$ / mL distilled H_2O

Method: Equine whole blood the $CaCl_2$ solution were placed in a petri dish (84mm diameter) lined with aluminum foil. A second petri dish (38mm diameter) also lined with aluminum foil applied a rotational force on the blood while it was clotting.

RPM: 60

Gap Thickness:

Total Time Rotating: 5.5 hours

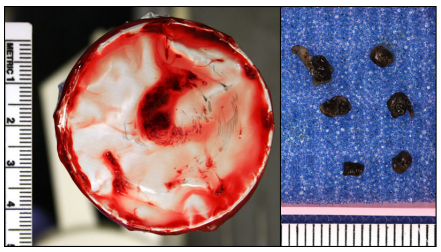

Clot Name: Clot 23

Date Created: 6/20/13

Blood Component: Plasma

Species: Equine

$CaCl_2$ Concentration: 24mg $CaCl_2$ / mL distilled H_2O

Method: Equine plasma and the $CaCl_2$ solution were placed in a petri dish (50mm diameter) lined with aluminum foil. A second petri dish (38mm diameter) also lined with aluminum foil applied a rotational force on the plasma while it was clotting.

RPM: 60

Gap Thickness: 8mm

Total Time Rotating: 5.85 hours

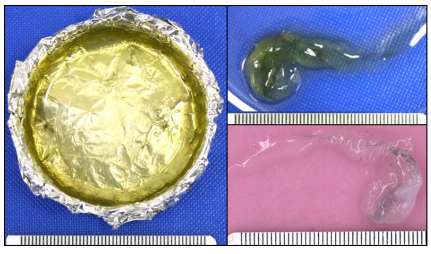

Clot Name: Clot 24

Date Created: 6/24/13

Blood Component: Whole Blood

Species: Equine

$CaCl_2$ Concentration: 24mg $CaCl_2$ / mL distilled H_2O

Method: 5mL of equine whole blood and 12 drops of $CaCl_2$ solution were placed in a petri dish (50mm diameter) lined with aluminum foil. A second petri dish (38mm diameter) also lined with aluminum foil applied a rotational force on the blood while it was clotting.

RPM: 225

Gap Thickness: 5.56mm

Total Time Rotating: 5.68 hours

Gross Evaluation: Rotating surface had a large bubble in the middle, but was otherwise clean and free of deposits. Stationary surface had one larger deposit and five smaller deposits collected for histology.

Clot Name: Clot 25

Date Created: 6/24/13

Blood Component: Whole Blood

Species: Equine

$CaCl_2$ Concentration: 24mg $CaCl_2$ / mL distilled H_2O

Method: 5mL of equine whole blood and 12 drops of $CaCl_2$ solution were placed in a petri dish (50mm diameter) lined with aluminum foil. A second petri dish (38mm diameter) also lined with aluminum foil applied a rotational force on the blood while it was clotting.

RPM: 75

Gap Thickness: 3.95mm

Total Time Rotating: 5.67 hours

Gross Evaluation: Rotating surface had a large deposit off center and radiating off of that are several smaller deposits in a spiral like pattern. The stationary surface had a filmy like substance on the aluminum foil that came off in four pieces. There were two deposits that remained when the blood was drained. Five deposits from stationary surface and the aluminum foil from the rotating surface collected for histology.

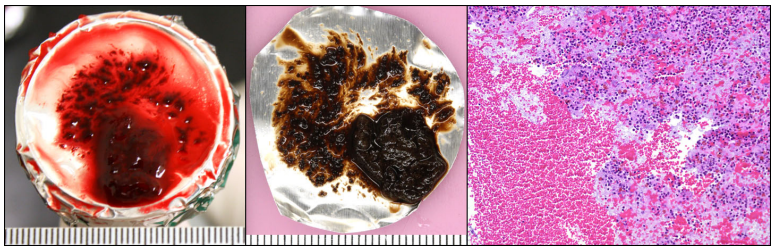

Clot Name: Clot 26

Date Created: 6/25/13

Blood Component: Whole Blood

Species: Equine

$CaCl_2$ Concentration: 24mg $CaCl_2$ / mL distilled H_2O

Method: 5mL of equine whole blood and 12 drops of $CaCl_2$ solution were placed in a petri dish (50mm diameter) lined with aluminum foil. A second petri dish (38mm diameter) also lined with aluminum foil applied a rotational force on the blood while it was clotting.

RPM: 225

Gap Thickness: 4mm

Total Time Rotating: 6 hours

Gross Evaluation: Rotating surface was clean. Stationary surface had one large and three small deposits. All four deposits were collected for histology.

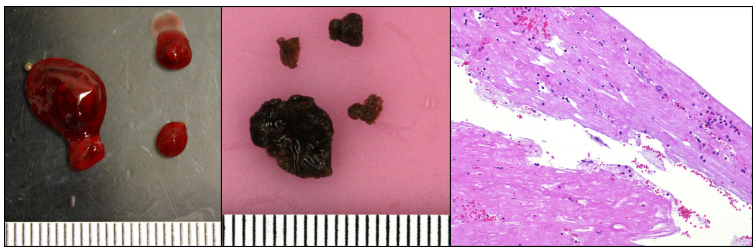

Clot Name: Clot 27

Date Created: 6/25/13

Blood Component: Whole Blood

Species: Equine

$CaCl_2$ Concentration: 24mg $CaCl_2$ / mL distilled H_2O

Method: 5mL of equine whole blood and 12 drops of $CaCl_2$ solution were placed in a petri dish (50mm diameter) lined with aluminum foil. A second petri dish (38mm diameter) also lined with aluminum foil applied a rotational force on the blood while it was clotting.

RPM: 75

Gap Thickness: 6.05mm

Total Time Rotating: 6 hours

Gross Evaluation: Rotating surface had a large deposit in the center with a spiral pattern radiating out from it. The stationary surface had two medium sized, and 2 small red-brown to black deposits. Top aluminum foil piece and four bottom deposits collected for histology.

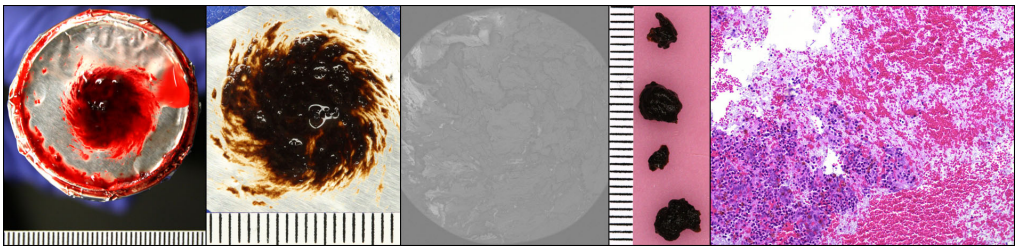

Clot Name: Clot 28

Date Created: 6/26/13

Blood Component: Plasma

Species: Equine

$CaCl_2$ Concentration: 24mg $CaCl_2$ / mL distilled H_2O

Method: 5mL of equine plasma and 22 drops of $CaCl_2$ solution were placed in a petri dish (50mm diameter) lined with aluminum foil. A second petri dish (38mm diameter) also lined with aluminum foil applied a rotational force on the plasma while it was clotting.

RPM: 75

Gap Thickness: 3.96mm

Total Time Rotating: 6 hours

Gross Evaluation: Rotating surface has a gel-like deposit firmly adhered to the entire flat surface. This circular deposit was removed in one piece and collected for histology. The stationary surface had a thin film along the outer rim of dish (donut shaped) that was collected for histology.

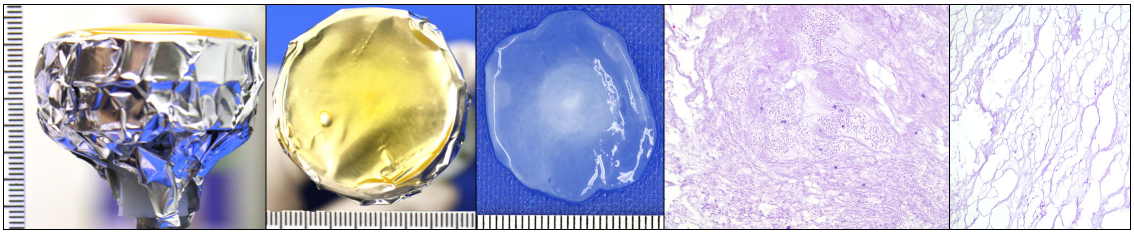

Clot Name: Clot 29

Date Created: 6/26/13

Blood Component: Plasma

Species: Equine

$CaCl_2$ Concentration: 24mg $CaCl_2$ / mL distilled H_2O

Method: 5mL of equine plasma and 22 drops of $CaCl_2$ solution were placed in a petri dish (50mm diameter) lined with aluminum foil. A second petri dish (38mm diameter) also lined with aluminum foil applied a rotational force on the plasma while it was clotting.

RPM: 225

Gap Thickness: 3.88mm

Total Time Rotating: 6 hours

Gross Evaluation: Rotating surface had a gelatinous material along outer rim of aluminum foil that measured ~7.9cm x 1-3mm. The stationary surface had a circular shaped deposit, and another deposit along the outer rim that measured ~5cm x 2-6mm. All three deposits were collected for histology.

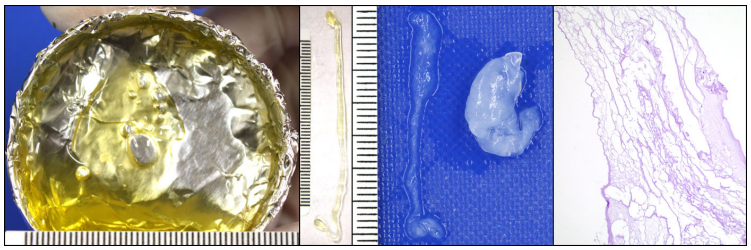

Clot Name: Clot 30

Date Created: 6/26/13

Blood Component: Plasma

Species: Equine

$CaCl_2$ Concentration: 24mg $CaCl_2$ / mL distilled H_2O

Method: 5mL of equine plasma and 22 drops of $CaCl_2$ solution were placed in a petri dish (50mm diameter) lined with aluminum foil. A second petri dish (38mm diameter) also lined with aluminum foil applied a rotational force on the plasma while it was clotting.

RPM: 240

Gap Thickness: 4.14mm

Total Time Rotating: 6 hours

Gross Evaluation: Rotating surface had several bubbles grouped together on the outer edge. The outer edge had a thin film that came off in four small pieces. Stationary surface had a large circular deposit. Five deposits were collected for histology.

Clot Name: Clot 31

Date Created: 6/26/13

Blood Component: Plasma

Species: Equine

$CaCl_2$ Concentration: 24mg $CaCl_2$ / mL distilled H_2O

Method: 5mL of equine plasma and 22 drops of $CaCl_2$ solution were placed in a petri dish (50mm diameter) lined with aluminum foil. A second petri dish (38mm diameter) also lined with aluminum foil applied a rotational force on the plasma while it was clotting.

RPM: 300

Gap Thickness: 3.98mm

Total Time Rotating: Approximately 2 hours

Gross Evaluation: Stationary surface adhered to the rotating surface throughout experiment. Plasma splashed around counter in 4-5cm radius. The motor stopped at two hours in. On 6/27/13, the rotating surface was clean and free of deposits. Stationary surface had a gelatinous material that came off in several small pieces.

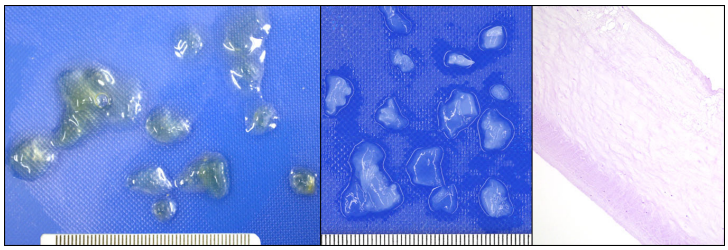

Clot Name: Clot 32

Date Created: 6/27/13

Blood Component: Plasma

Species: Equine

$CaCl_2$ Concentration: 24mg $CaCl_2$ / mL distilled H_2O

Method: 5mL of equine plasma and 18 drops of $CaCl_2$ solution were placed in a petri dish (50mm diameter) lined with aluminum foil. A second petri dish (38mm diameter) also lined with aluminum foil applied a rotational force on the plasma while it was clotting.

RPM: 75

Gap Thickness: 5.68mm

Total Time Rotating: 10.2 hours

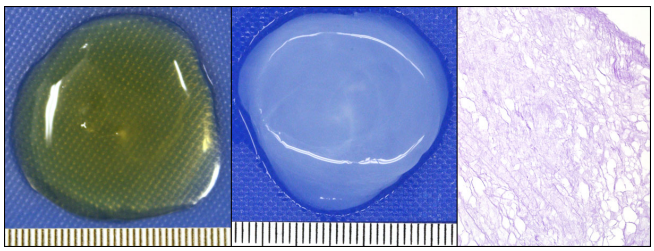

Clot Name: Clot 33

Date Created: 6/27/13

Blood Component: Plasma

Species: Equine

$CaCl_2$ Concentration: 24mg $CaCl_2$ / mL distilled H_2O

Method: 5mL of equine plasma and 18 drops of $CaCl_2$ solution were placed in a petri dish (50mm diameter) lined with aluminum foil. A second petri dish (38mm diameter) also lined with aluminum foil applied a rotational force on the plasma while it was clotting.

RPM: 225

Gap Thickness: 6.08mm

Total Time Rotating: 10.2 hours

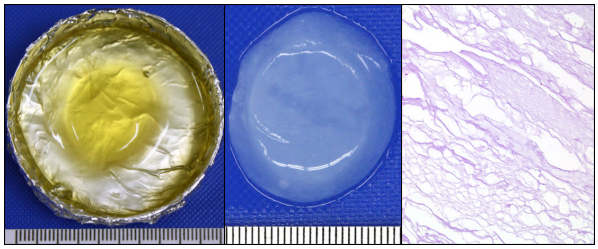

Clot Name: Clot 34

Date Created: 6/27/13

Blood Component: Plasma

Species: Equine

$CaCl_2$ Concentration: 24mg $CaCl_2$ / mL distilled H_2O

Method: 5mL of equine plasma and 18 drops of $CaCl_2$ solution were placed in a petri dish (50mm diameter) lined with aluminum foil. A second petri dish (38mm diameter) also lined with aluminum foil applied a rotational force on the plasma while it was clotting.

RPM: 240

Gap Thickness: 6.16mm

Total Time Rotating: 10.2 hours

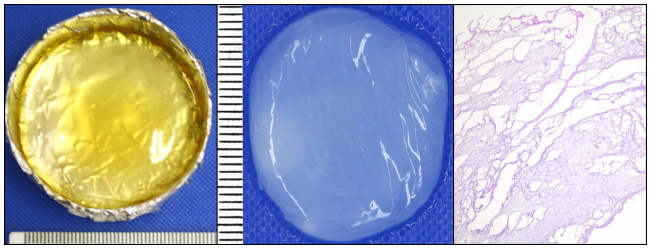

Clot Name: Clot 35

Date Created: 6/27/13

Blood Component: Plasma

Species: Equine

$CaCl_2$ Concentration: 24mg $CaCl_2$ / mL distilled H_2O

Method: 5mL of equine plasma and 18 drops of $CaCl_2$ solution were placed in a petri dish (50mm diameter) lined with aluminum foil. A second petri dish (38mm diameter) also lined with aluminum foil applied a rotational force on the plasma while it was clotting.

RPM: 300

Gap Thickness: 6.14mm

Total Time Rotating: 10.2 hours

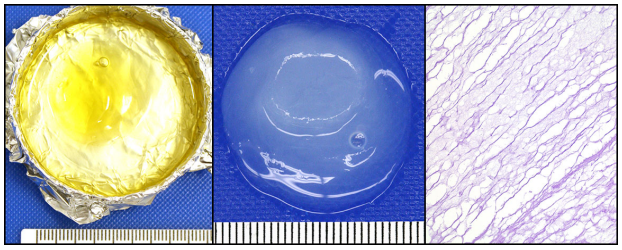

Clot Name: Clot 36

Date Created: 7/1/13

Blood Component: Whole Blood

Species: Equine

$CaCl_2$ Concentration: 24mg $CaCl_2$ / mL distilled H_2O

Method: 7.5mL of equine whole blood and 18 drops of $CaCl_2$ solution were placed in a petri dish (50mm diameter) lined with aluminum foil. A second petri dish (38mm diameter) also lined with aluminum foil applied a rotational force on the blood while it was clotting.

RPM: 75

Gap Thickness: 4.13mm

Total Time Rotating: 23 hours

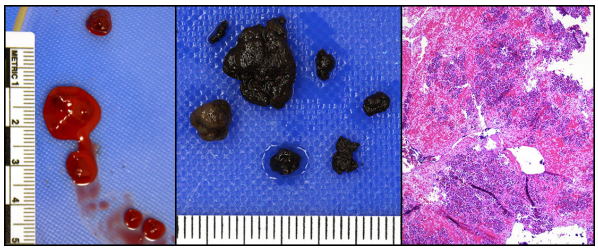

Clot Name: Clot 37

Date Created: 7/1/13

Blood Component: Whole Blood

Species: Equine

$CaCl_2$ Concentration: 24mg $CaCl_2$ / mL distilled H_2O

Method: 7.5mL of equine whole blood and 18 drops of $CaCl_2$ solution were placed in a petri dish (50mm diameter) lined with aluminum foil. A second petri dish (38mm diameter) also lined with aluminum foil applied a rotational force on the blood while it was clotting.

RPM: 225

Gap Thickness: 4.13mm

Total Time Rotating: 23 hours

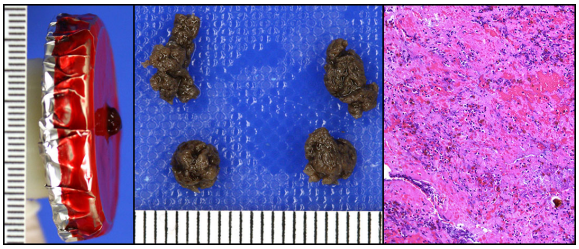

Clot Name: Clot 38

Date Created: 7/1/13

Blood Component: Whole Blood

Species: Equine

$CaCl_2$ Concentration: 24mg $CaCl_2$ / mL distilled H_2O

Method: 7.5mL of equine whole blood and 18 drops of $CaCl_2$ solution were placed in a petri dish (50mm diameter) lined with aluminum foil. A second petri dish (38mm diameter) also lined with aluminum foil applied a rotational force on the blood while it was clotting.

RPM: 240

Gap Thickness: 3.98mm

Total Time Rotating: 23 hours

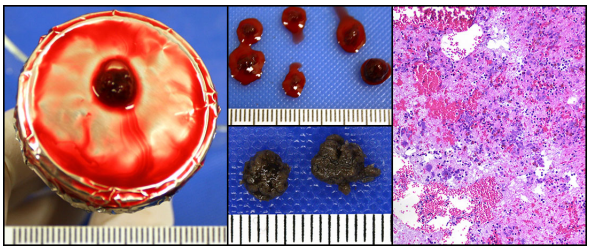

Clot Name: Clot 39

Date Created: 7/1/13

Blood Component: Whole Blood

Species: Equine

$CaCl_2$ Concentration: 24mg $CaCl_2$ / mL distilled H_2O

Method: 7.5mL of equine whole blood and 18 drops of $CaCl_2$ solution were placed in a petri dish (50mm diameter) lined with aluminum foil. A second petri dish (38mm diameter) also lined with aluminum foil applied a rotational force on the blood while it was clotting.

RPM: 300

Gap Thickness: 4.07

Total Time Rotating: 23 hours

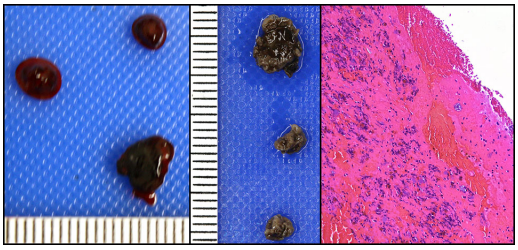

Clot Name: Clot 40

Date Created: 7/7/13

Blood Component: Plasma

Species: Equine

$CaCl_2$ Concentration: 24mg $CaCl_2$ / mL distilled H_2O

Method: 7.5mL equine plasma and 33 drops of $CaCl_2$ solution were placed in a petri dish (50mm diameter) lined with aluminum foil. A second petri dish (38mm diameter) also lined with aluminum foil applied a rotational force on the plasma while it was clotting.

RPM: 75

Gap Thickness: 3.99mm

Total Time Rotating: 45.5 hours

Gross Evaluation: Gelatinous clot lightly adhered to the rotating dish. Stationary dish contained a donut shaped gelatinous material.

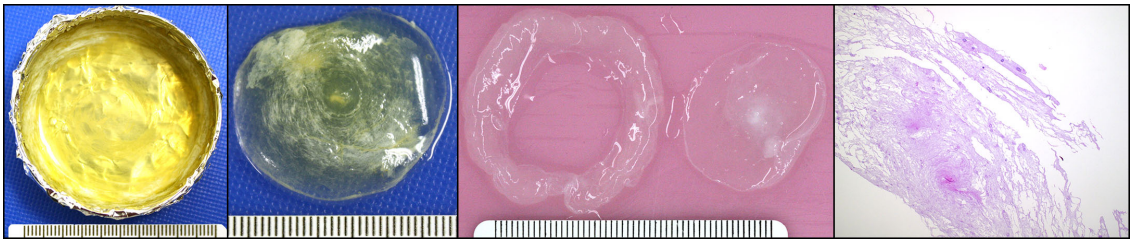

Clot Name: Clot 41

Date Created: 7/7/13

Blood Component: Plasma

Species: Equine

$CaCl_2$ Concentration: 24mg $CaCl_2$ / mL distilled H_2O

Method: 7.5mL of equine plasma and 33 drops of $CaCl_2$ solution were placed in a petri dish (50mm diameter) lined with aluminum foil. A second petri dish (38mm diameter) also lined with aluminum foil applied a rotational force on the plasma while it was clotting.

RPM: 225

Gap Thickness: 3.92mm

Total Time Rotating: 45.5 hours

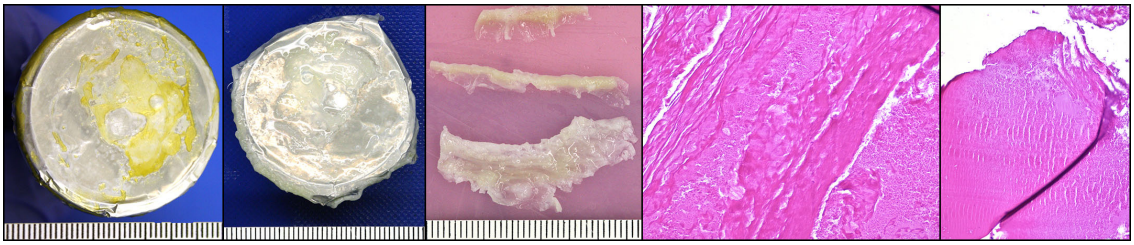

Clot Name: Clot 42

Date Created: 7/7/13

Blood Component: Plasma

Species: Equine

$CaCl_2$ Concentration: 24mg $CaCl_2$ / mL distilled H_2O

Method: 7.5mL of equine plasma and 33 drops of $CaCl_2$ solution were placed in a petri dish (50mm diameter) lined with aluminum foil. A second petri dish (38mm diameter) also lined with aluminum foil applied a rotational force on the plasma while it was clotting.

RPM: 240

Gap Thickness: 4.13mm

Total Time Rotating: 45.5 hours

Gross Evaluation: Brittle, fragile, greenish-yellow (with gray to black center) discolored deposit adhered to the outer rim of the rotating dish and the stationary dish.

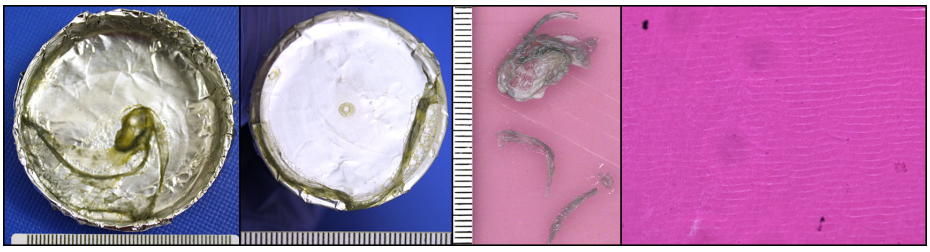

Clot Name: Clot 43

Date Created: 7/7/13

Blood Component: Plasma

Species: Equine

$CaCl_2$ Concentration: 24mg $CaCl_2$ / mL distilled H_2O

Method: 7.5mL of equine plasma and 33 drops of $CaCl_2$ solution were placed in a petri dish (50mm diameter) lined with aluminum foil. A second petri dish (38mm diameter) also lined with aluminum foil applied a rotational force on the plasma while it was clotting.

RPM: 300

Gap Thickness: 3.9mm

Total Time Rotating: 45.5 hours

Gross Evaluation: Brittle, fragile, greenish-yellow pieces along the outer rim of the rotating dish. In the center of the rotating dish, there is an approximately 4mm diameter circular deposit firmly adhered to the aluminum foil.

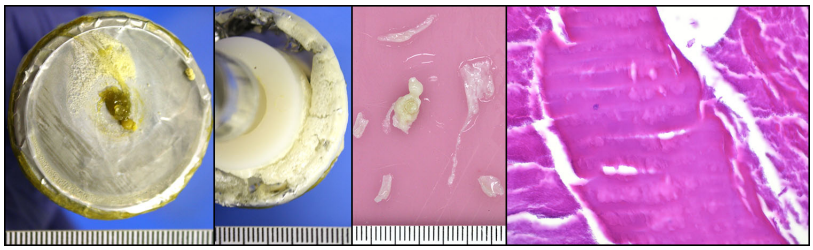

Clot Name: Clot 44

Date Created: 7/10/13

Blood Component: Plasma

Species: Equine

$CaCl_2$ Concentration: 24mg $CaCl_2$ / mL distilled H_2O

Method: 7.5mL of equine plasma and 33 drops of $CaCl_2$ solution were placed in a petri dish (50mm diameter) lined with aluminum foil. A second petri dish (38mm diameter) also lined with aluminum foil applied a rotational force on the plasma while it was clotting.

RPM: 75

Gap Thickness: 4.08mm

Total Time Rotating: 24 hours

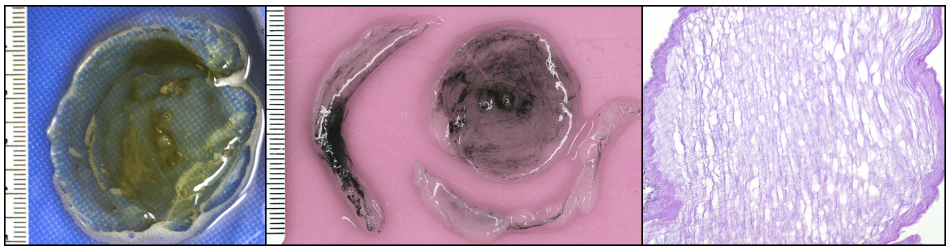

Clot Name: Clot 45

Date Created: 7/10/13

Blood Component: Plasma

Species: Equine

$CaCl_2$ Concentration: 24mg $CaCl_2$ / mL distilled H_2O

Method: 7.5mL of equine plasma and 33 drops of $CaCl_2$ solution were placed in a petri dish (50mm diameter) lined with aluminum foil. A second petri dish (38mm diameter) also lined with aluminum foil applied a rotational force on the plasma while it was clotting.

RPM: 225

Gap Thickness: 4.03mm

Total Time Rotating: 24 hours

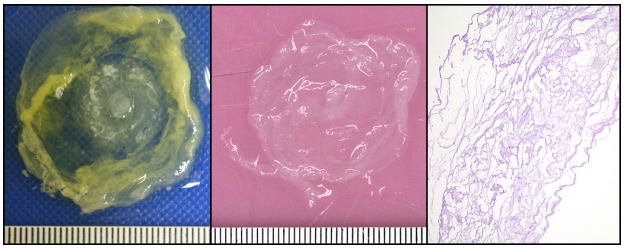

Clot Name: Clot 46

Date Created: 7/10/13

Blood Component: Plasma

Species: Equine

$CaCl_2$ Concentration: 24mg $CaCl_2$ / mL distilled H_2O

Method: 7.5mL of equine plasma and 33 drops of $CaCl_2$ solution were placed in a petri dish (50mm diameter) lined with aluminum foil. A second petri dish (38mm diameter) also lined with aluminum foil applied a rotational force on the plasma while it was clotting.

RPM: 240

Gap Thickness: 4mm

Total Time Rotating: 24 hours

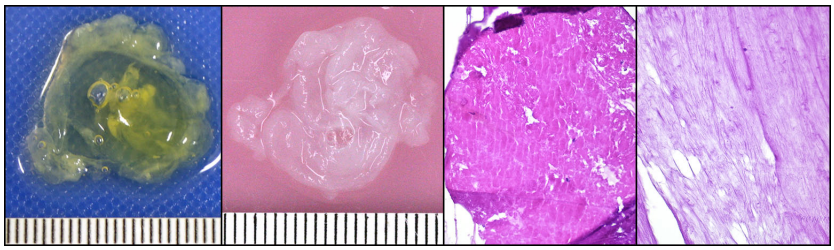

Clot Name: Clot 47

Date Created: 7/10/13

Blood Component: Plasma

Species: Equine

$CaCl_2$ Concentration: 24mg $CaCl_2$ / mL distilled H_2O

Method: 7.5mL of equine plasma and 33 drops of $CaCl_2$ solution were placed in a petri dish (50mm diameter) lined with aluminum foil. A second petri dish (38mm diameter) also lined with aluminum foil applied a rotational force on the plasma while it was clotting.

RPM: 300

Gap Thickness: 4.01mm

Total Time Rotating: 24 hours

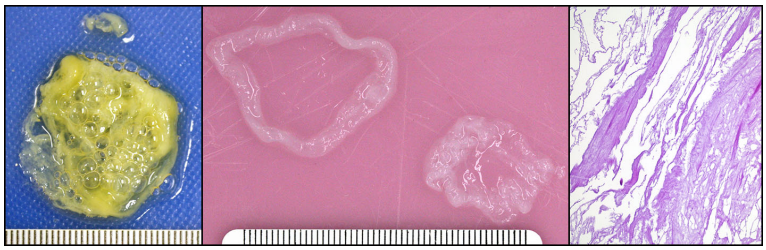

Clot Name: Clot 48

Date Created: 5/14/14

Blood Component: Plasma

Species: Bovine

$CaCl_2$ Concentration: 24mg $CaCl_2$ / mL distilled H_2O

Method: Plasma and $CaCl_2$ solution allowed to clot in a stationary glass test tube.

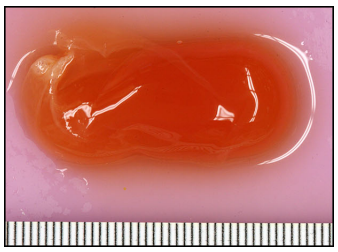

APPENDIX IV

COMPLETE IN VITRO ANALYSIS

Experiments to analyze the interaction of ventricular assist devices and thromboemboli (outlined in Section 8 of above work) are detailed below.

Centrifugal Flow Experiments

Setup for experiments 1-11:

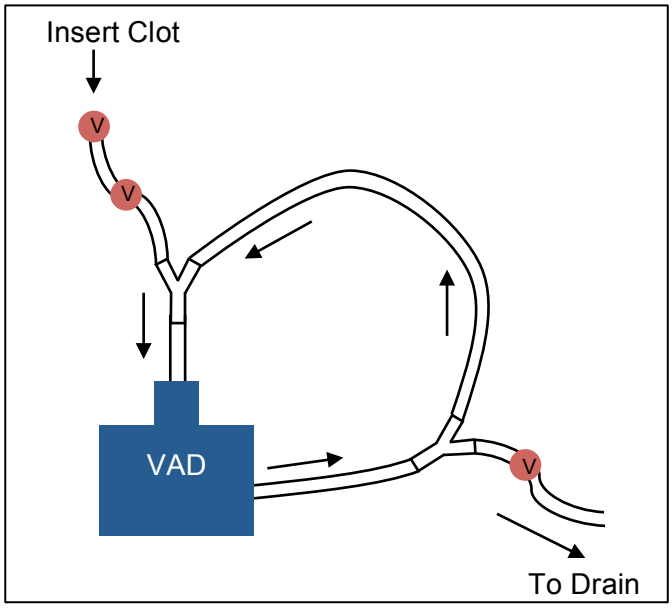

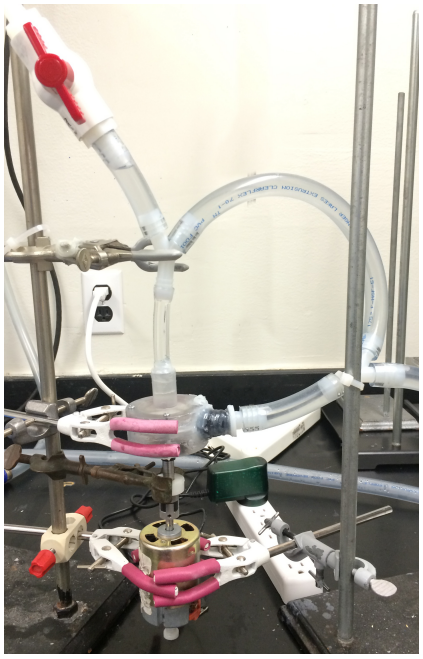

Centrifugal Flow Mock-VAD Design Version 1.0 (used in experiments 1-6):

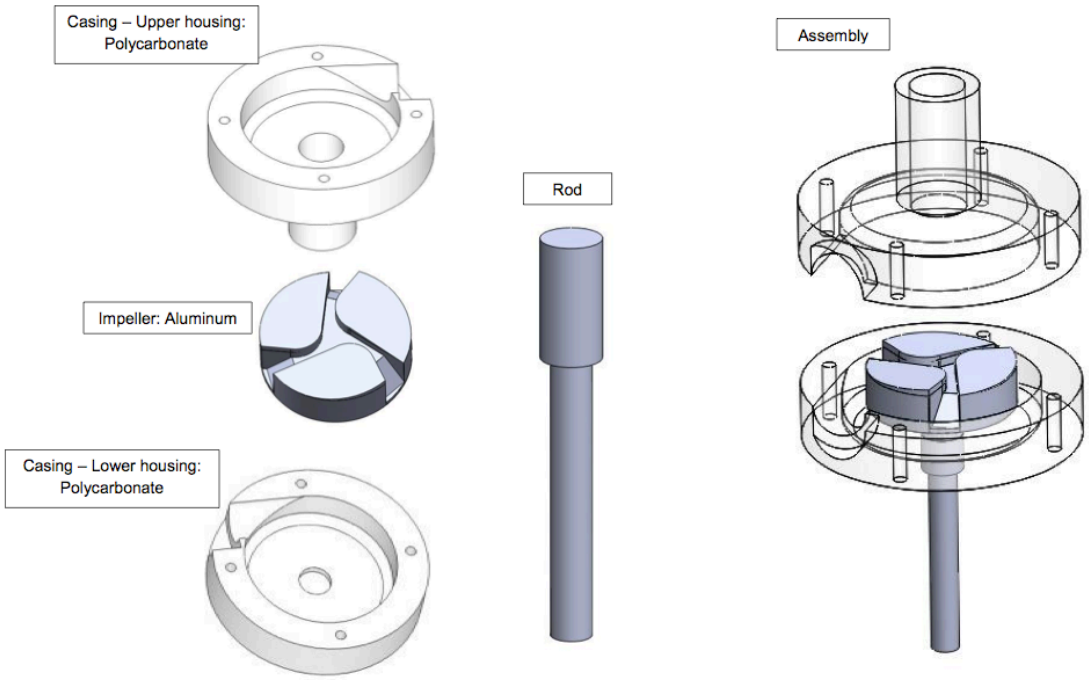

List of Experiments:

1. Experiment 1 (Clot 50)
    a. Experiment Description: 5mL of equine plasma and the $CaCl_2$ solution were added to a petri dish (50mm diameter) lined with aluminum foil. A second petri dish (38mm diameter) was affixed to a rotational motor capable of 75 RPM. The petri dish applied a rotational force to the plasma as it clotted. The clot formed in a circular shape under the rotating surface as the motor ran for 6 hours. The clot was then sectioned into 4 pieces of equal size. One piece was collected as a control and the other was administered to the mock-VAD. The VAD ran for approximately 20 seconds. VAD disassembly revealed that the clot was stuck inside the VAD near the outflow.
    b. Data Collected:
        i. Cassette 1: Control (one section of clot that was not subjected to the VAD)

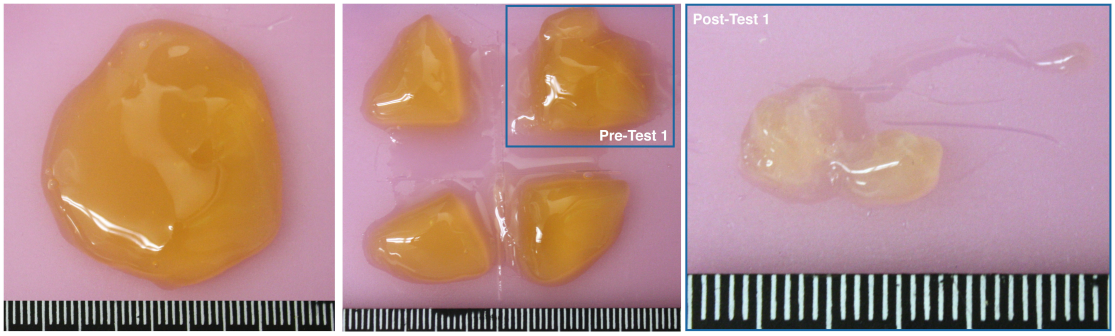

Whole Clot. Clot Sectioned into 4 pieces. Section of Clot collected from VAD

        ii. Cassette 2: One section of clot that was subjected to the VAD.

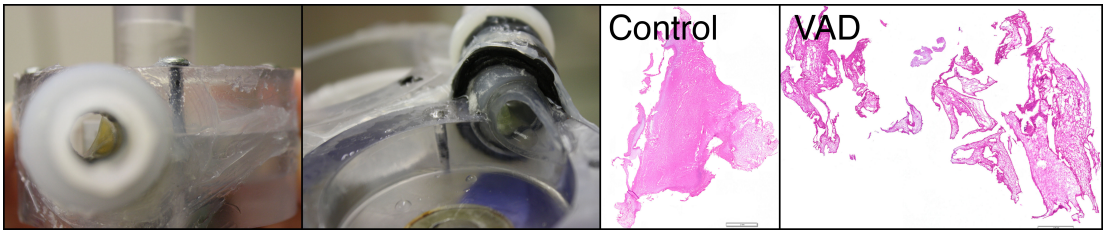

---

2. Experiment 2 (Clot 50)
    a. Experiment Description: Remaining two sections of Clot 50 were stored in the refrigerator for 2 days before subjected to the mock-VAD. The VAD ran for approximately 3 minutes. Clot appeared to be in the outflow. The VAD was turned off, and the clot floated into the loop distal to the outflow. The VAD was

turned back on and the clot appeared to break into smaller pieces. When the VAD was turned off, deposits were seen in the outflow track and in the central section of the impeller.

b. Data Collected:
    i. Cassette 3: Control
    ii. Cassette 4: Specimens collected from the outflow and impeller.

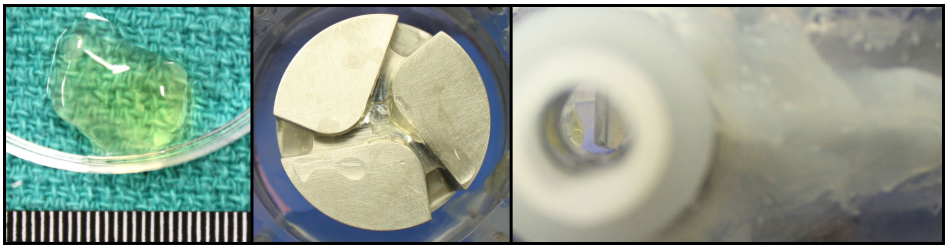

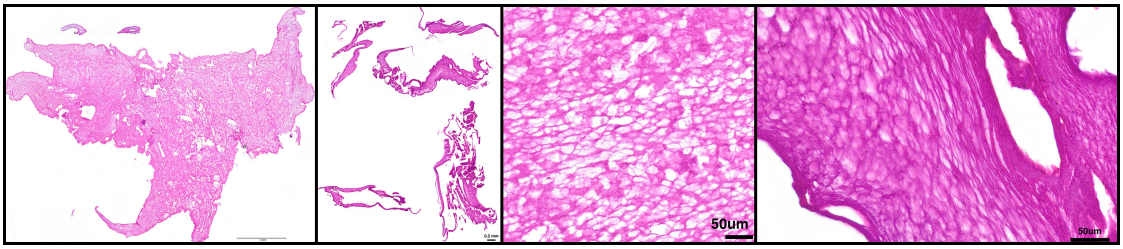

---

3. Experiment 3 (Clot 52)
    a. Experiment Description: 5mL of equine plasma and the $CaCl_2$ solution were added to a petri dish (50mm diameter) lined with aluminum foil. A second petri dish (38mm diameter) was affixed to a rotational motor capable of 225 RPM. The petri dish applied a rotational force to the plasma as it clotted. The clot formed in a circular shape under the rotating surface as the motor ran for 30 hours. There were also pieces of clot around the rim of the stationary petri dish. The circular clot was sectioned into 4 pieces of equal size. One piece of the circular clot and one section of the clot along the rim of the stationary dish were collected as controls. A piece from the rim of the stationary dish was administered to the flow loop along with a piece from the circular clot. The VAD motor was turned on several times. The clot got stuck and then traveled through the loop several times. The clot eventually got stuck in the outflow track.
    b. Data Collected:
        i. Cassette 1: Control from circular clot
        ii. Cassette 2: Control from rim of stationary dish
        iii. Cassette 3: Specimens from the outflow track

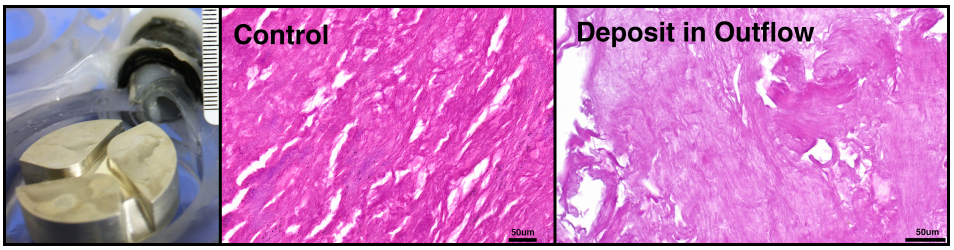

---

4. Experiment 4 (Clot 52)
    a. Experiment Description: The remaining sections of Clot 52 were stored in water for less than 24 hours. One section was collected as a control to be dehydrated and analyzed with scanning electron microscopy. The remaining sections were administered to the VAD. The clot appeared to be stuck in the outflow track. Specimens were collected for analysis with scanning electron microscopy.
    b. Data Collected:
        i. Cassette 4: Control
        ii. Cassette 5: Specimen from the outflow track

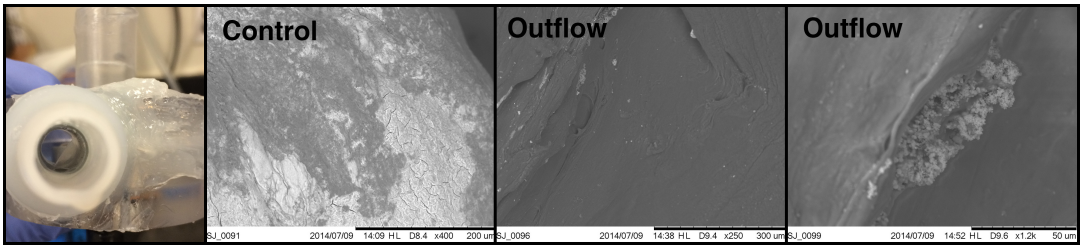

---

5. Experiment 5 (Clot 53)
    a. Experiment Description: Stationary blood clot created from 5mL equine plasma and $CaCl_2$ solution in a glass test tube.
    b. Data Collected:
        i. Cassette 1: Control
        ii. Cassette 2: Pieces found floating in liquid in VAD chamber
        iii. Cassette 3: Specimen from the outflow track

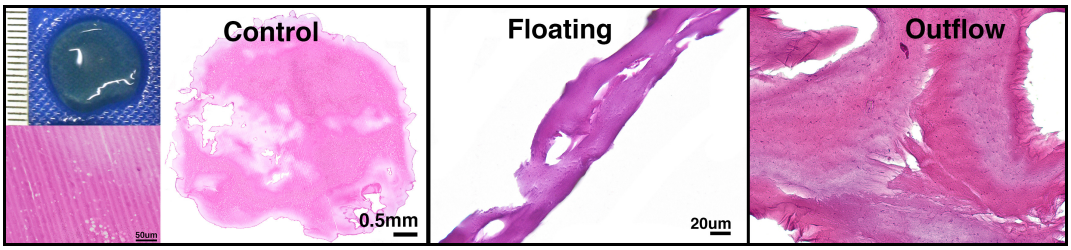

---

6. Experiment 6 (Clot 53)
    a. Experiment Description: Remaining sections of Clot 53 were subjected to the VAD flow loop after condensing for less than 24 hours.
    b. Data Collected:
        i. Cassette 4: Control
        ii. Cassette 5: Specimen from the outflow track
        iii. Cassette 6: Floating specimens

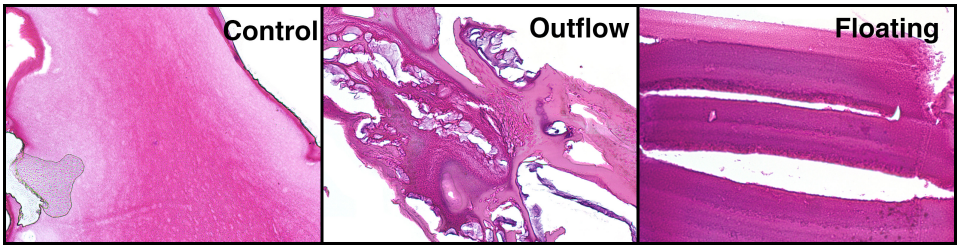

Centrifugal Flow Mock-VAD Design Version 2.0 (used in remaining centrifugal flow experiments):

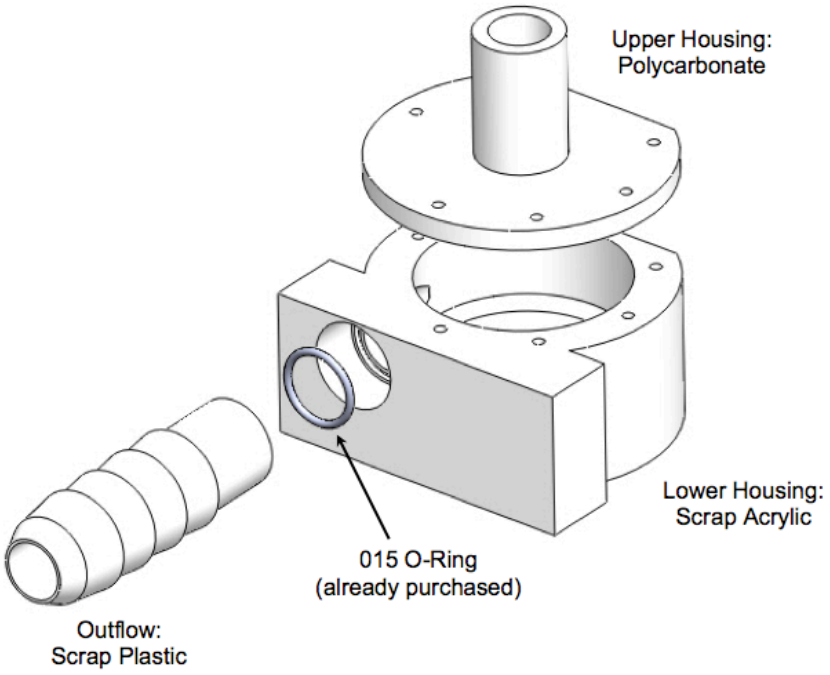

7. Experiment 7 (Clot 54)
    a. Experiment Description: 5mL of equine plasma and the $CaCl_2$ solution were added to a petri dish (50mm diameter) lined with aluminum foil. A second petri dish (38mm diameter) was affixed to a rotational motor capable of 75 RPM. The petri dish applied a rotational force to the plasma as it clotted. The clot formed in a circular shape under the rotating surface as the motor ran for 6.5 hours. Clot was sectioned into 4 pieces. One section was put into formalin and saved as a control. The second was inserted into the flow loop and disintegrated upon contact with the impeller. Fragments were too small to collect for histological evaluation.
    b. Data Collected:
        i. Cassette 1: Control

8. Experiment 8 (Clot 54)
    a. Experiment Description: Remaining section of Clot 54 after sitting in DI water for less than 24 hours.
        i. Cassette 3: Specimen adhered to the lower housing
        ii. Cassette 4: Control

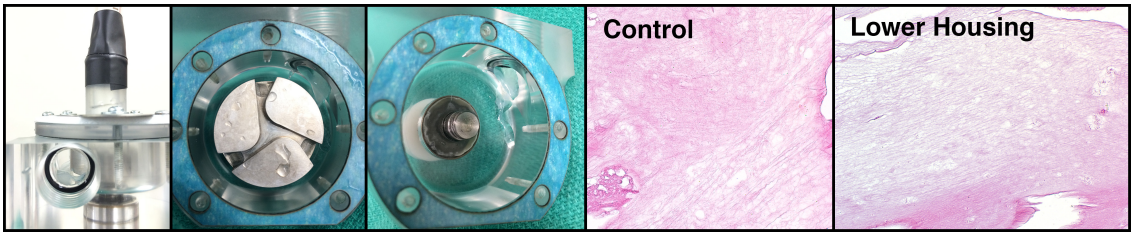

---

9. Experiment 9 (Clot 55)
    a. Experiment Description: Stationary blood clot created from 5mL equine plasma and $CaCl_2$ solution in a glass test tube.
    b. Data Collected:
        i. Cassette 1: Control
        ii. Cassette 2A: Pieces filtered out of flow loop
        iii. Cassette 2B: Piece adhered to the lower housing

---

10. Experiment 10 (Clot 55)
    a. Experiment Description: Remaining section of Clot 55 administered to the flow loop with the motor for the VAD set at a lower power setting (6V instead of 12V).
    b. Data Collected:
        i. Cassette 3: Specimens collected via filtration

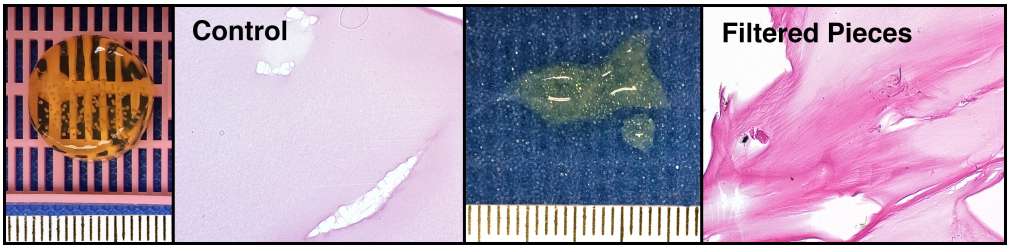

---

11. Experiment 11 (Clot 55)
    a. Experiment Description: Final section of Clot 55 administered to the flow loop 48 hours after clot was created.
    b. Data Collected:
        i. Cassette 4: Specimens collected via filtration

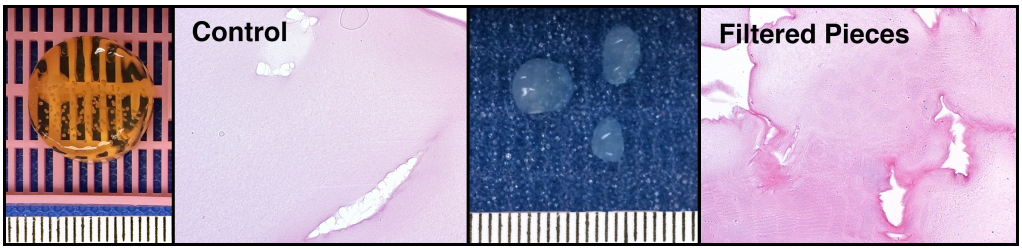

Setup for Experiments 12-22: (See Figure 34 in Section 8)

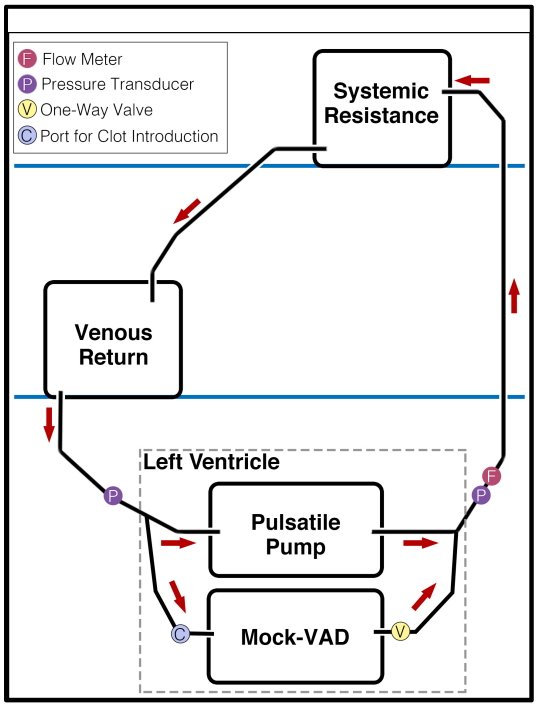

12. Experiment 12 (Clot 58)
    a. Experiment Description: Stationary blood clot created from 5mL equine plasma and $CaCl_2$ solution in a glass test tube. Clot was administered to the flow loop 16 days after $CaCl_2$ solution was added to the plasma. The fluid in the flow loop was water. The clot entered the VAD approximately 8-9 seconds after data collection began. After the clot entered the VAD there were loose pieces in the tubing and a piece on the impeller.
    b. Data Collected:
        i. Cassette 1: Control
        ii. Cassette 2: Loose pieces collected via filtration
        iii. Cassette 3: Piece on impeller

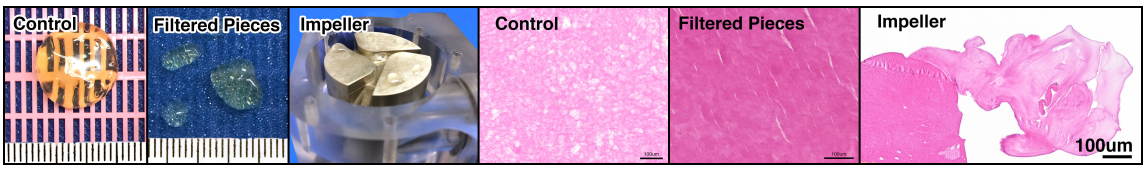

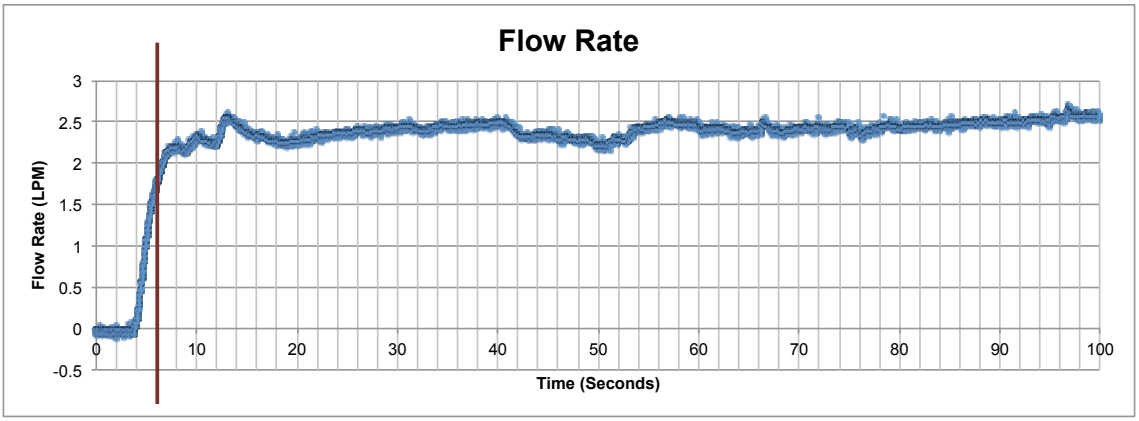

13. Experiment 13 (Clot 58)
    a. Experiment Description: Section 2 from Clot 58 was administered to the VAD approximately 17 days after clot creation. The clot entered the VAD approximately 3 seconds after data collection began. After the clot interacted with the VAD, there were loose pieces in the tubing and a small deposit on the inferior surface of the impeller.
    b. Data Collected:
        i. Cassette 4: Loose pieces in tubing
        ii. Cassette 5: Small deposit on inferior surface of impeller

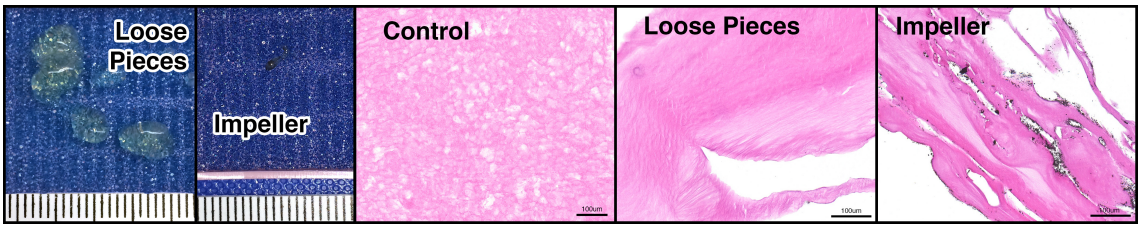

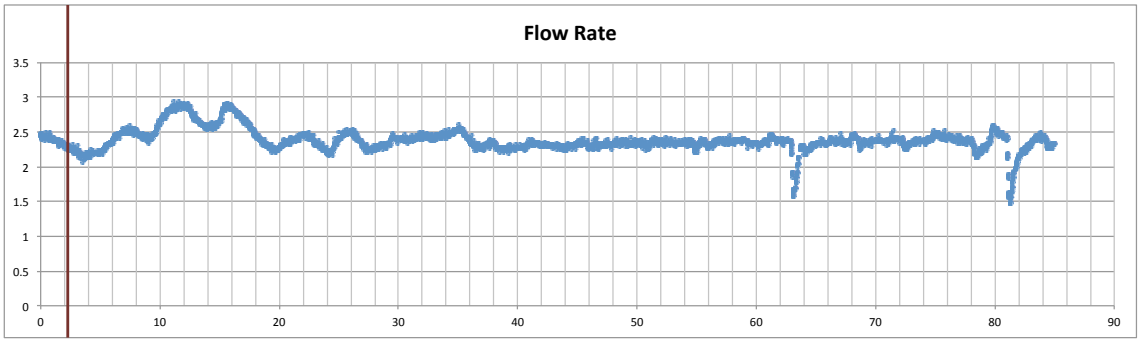

14. Experiment 14 (Clot 58)
    a. Experiment Description: The fibrous section of Clot 58 was inserted into the flow loop approximately 30 days after clot creation. The clot entered the VAD approximately 19 seconds after data collection began.
    b. Data Collected:
        i. Cassette 6: Control
        ii. Cassette 7: Deposit on impeller

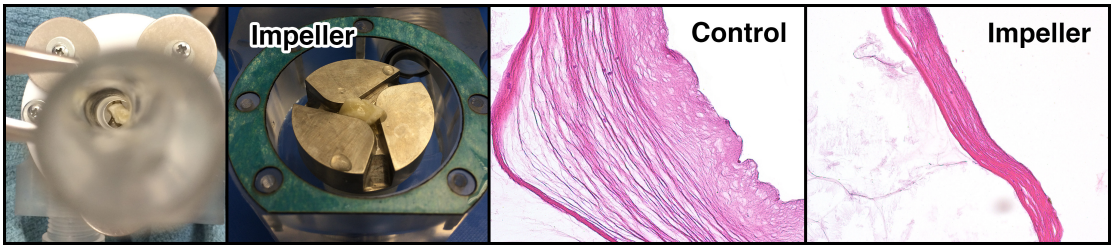

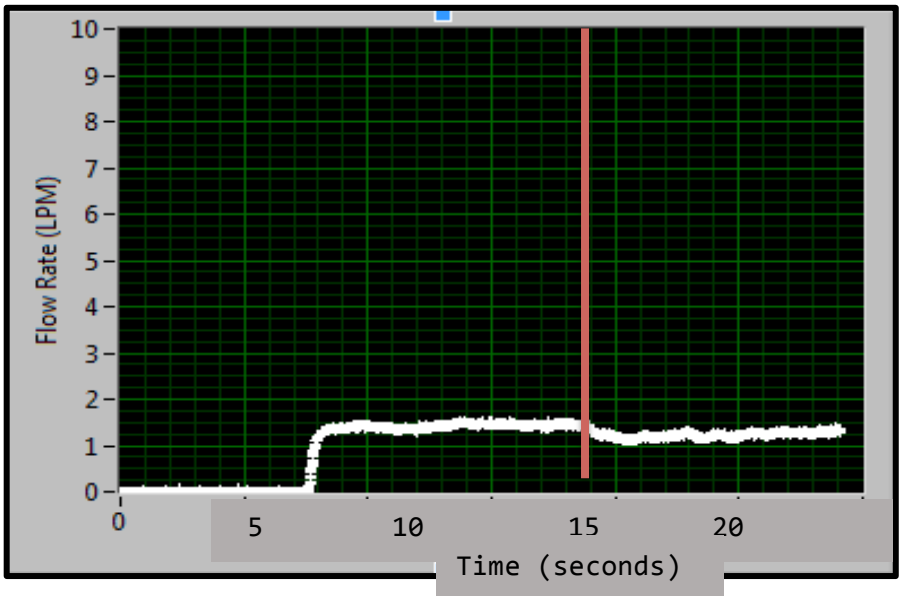

---

15. Experiment 15 (Clot 59)
    a. Experiment Description: Stationary blood clot created from 5mL equine plasma and $CaCl_2$ solution in a glass test tube. Clot was sectioned into 3 sections and administered to the flow loop on two separate dates approximately 30 days after clot creation. The fluid in the loop was water.
    b. Data Collected:
        i. Cassette 1: Control

ii. Cassette 2: Floating pieces
iii. Cassette 3: Impeller pieces

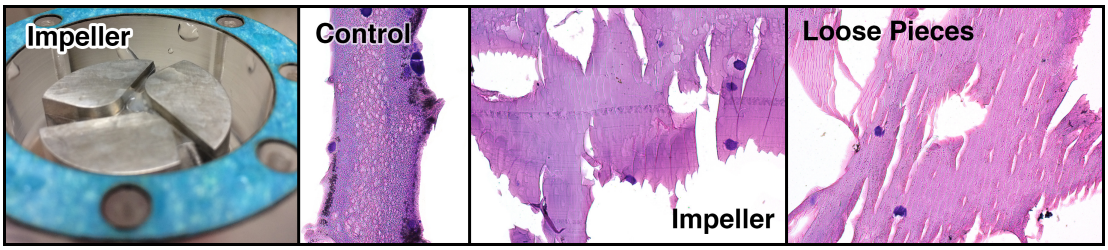

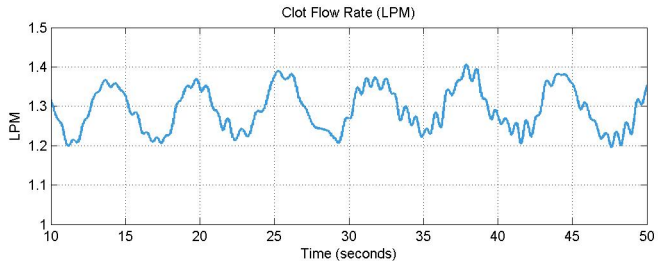

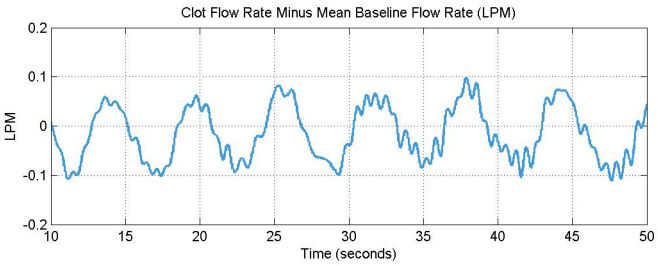

---

16. Experiment 16 (Clot 59)
    a. Experiment Description: Section 2 from Clot 59 was inserted into the flow loop. The fluid in the loop was water.
    b. Data Collected:
        i. Cassette 4: Control
        ii. Cassette 5: Pieces from VAD
        iii. Cassette 6: Pieces from VAD

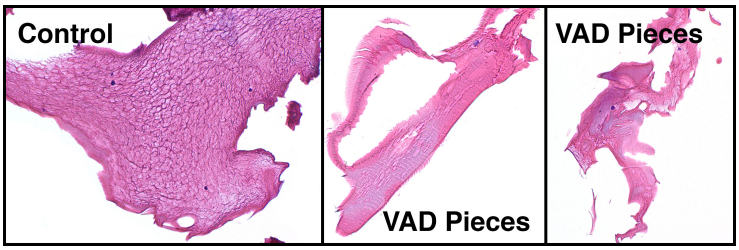

17. Experiment 17 (Clot 59)
    a. Experiment Description: Section 3 from Clot 59 was inserted into the flow loop approximately 30 days after clot creation. Clot went into the VAD at 43 seconds. The fluid in the loop was water.
    b. Data Collected:
        i. Cassette 7: Floating pieces
        ii. Cassette 8: Pieces from the lower housing
        iii. Cassette 9: Piece from the outflow
        iv. Cassette 10: Pieces from the impeller

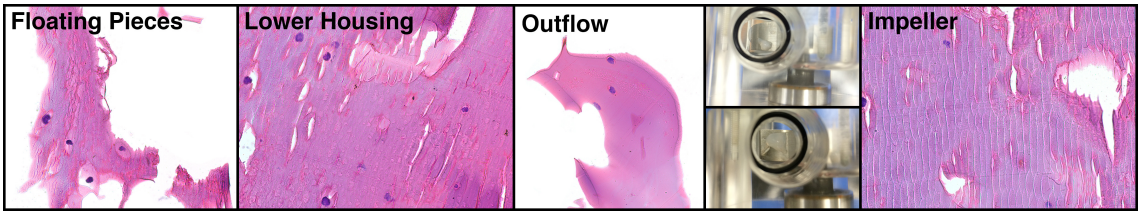

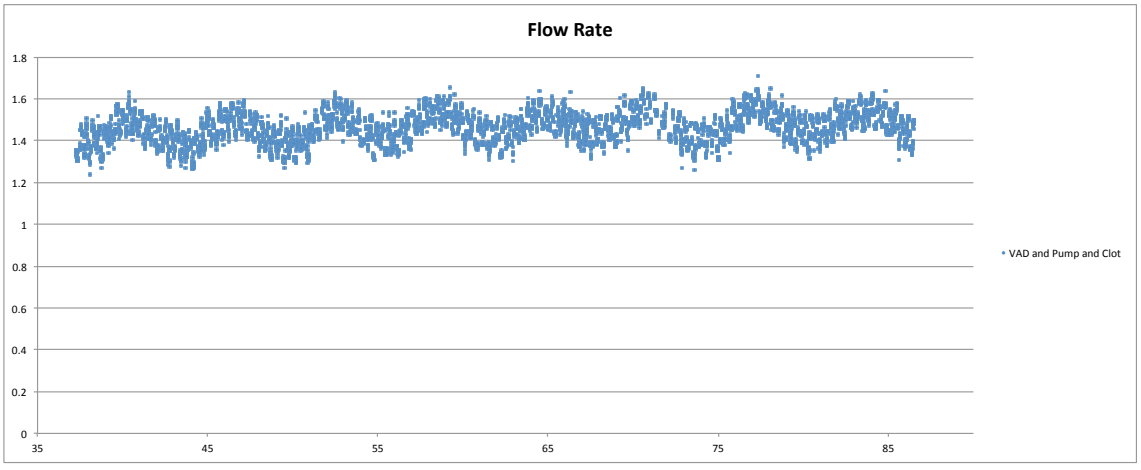

18. Experiment 18 (Clot 63)
    a. Experiment Description: Stationary blood clot created from 5mL equine plasma and $CaCl_2$ solution in a glass test tube. Clot was sectioned into 2 sections and administered to the flow loop approximately 30 years after clot creation. The fluid within the flow loop was a water/glycerin mixture. The temperature of the fluid was set to 38°C to simulate normal temperature of equine specimens. The pulsatile pump was set to higher flow rates to simulate normal heart flow.
    b. Data Collected:
        i. Cassette 1: Control
        ii. Cassette 2: Floating pieces in the reservoir

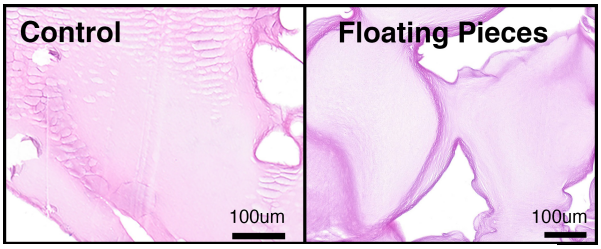

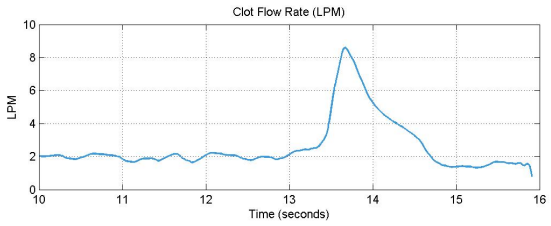

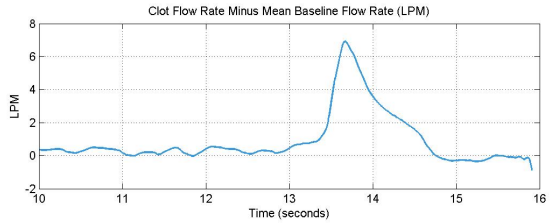

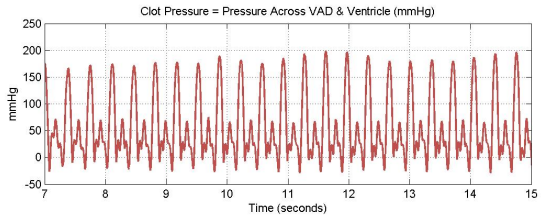

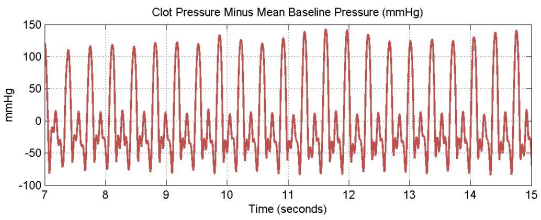

---

19. Experiment 19 (Clot 63)
    a. Experiment Description: Section 2 from Clot 63. This section was larger than previous samples. The clot went through the VAD after 6.56 seconds of data collection. The fluid within the flow loop was a water/glycerin mixture. The temperature of the fluid was set to 38°C to simulate normal temperature of equine specimens. The pulsatile pump was set to higher flow rates to simulate normal heart flow.
    b. Data Collected:

i. Cassette 3: Floating pieces
ii. Cassette 4: Pieces most near VAD (one floating, two in one-way valve)

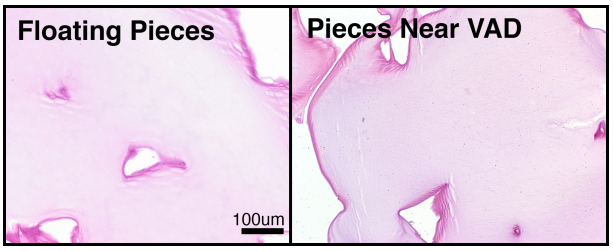

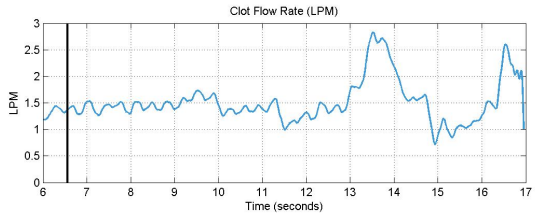

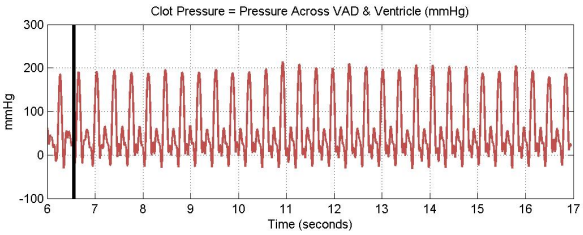

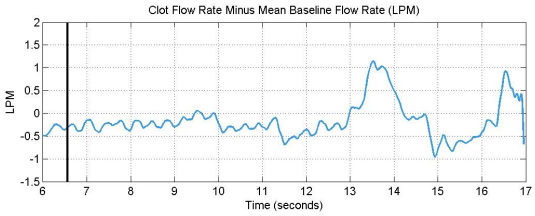

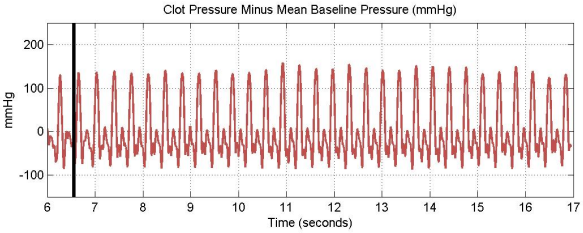

20. Experiment 20 (Clot 64)
    a. Experiment Description: Stationary blood clot created from 5mL equine plasma and $CaCl_2$ solution in a glass test tube. Clot was sectioned into 2 sections and administered to the flow loop. The fluid within the flow loop was a water/glycerin mixture. The temperature of the fluid was set to 38°C to simulate normal temperature of equine specimens. The pulsatile pump was set to lower flow rates to simulate heart failure. The clot went through the VAD at 16.40 seconds.
    b. Data Collected:
        i. Cassette 1: Floating pieces
        ii. Cassette 2: Floating pieces

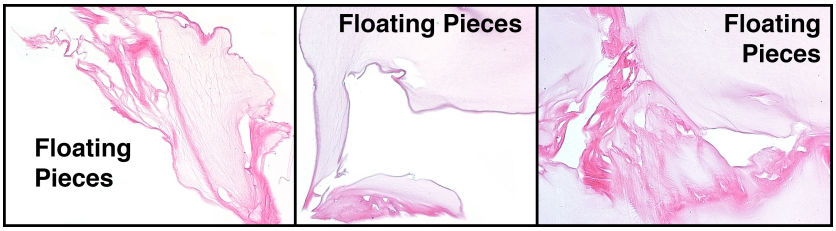

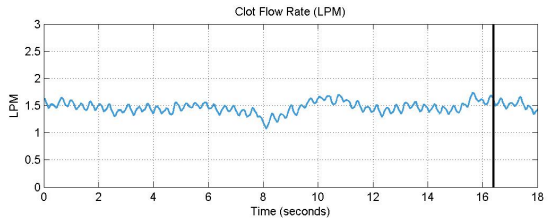

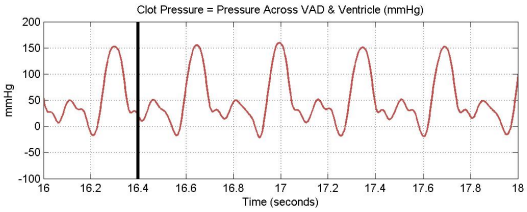

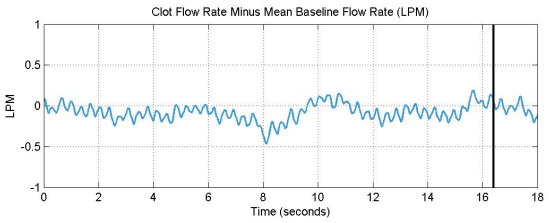

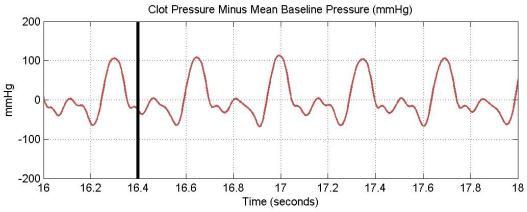

---

21. Experiment 21 (Clot 64)
    a. Experiment Description: Section 2 from Clot 64 was inserted into the flow loop. The fluid within the flow loop was a water/glycerin mixture. The temperature of the fluid was set to 38°C to simulate normal temperature of equine specimens. The pulsatile pump was set to lower flow rates to simulate heart failure. The clot went through the VAD at 13.01 seconds.
    b. Data Collected:
        i. Cassette 3: Floating pieces
        ii. Cassette 4: Floating pieces
        iii. Cassette 5: Floating pieces

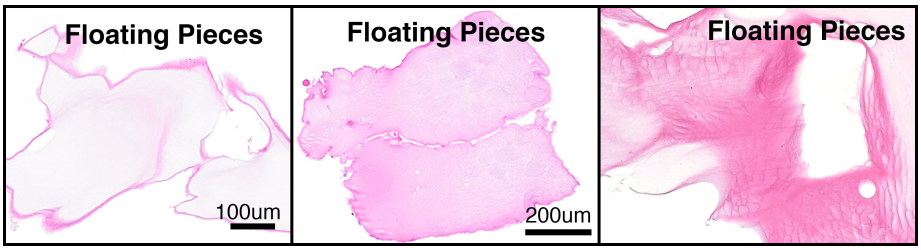

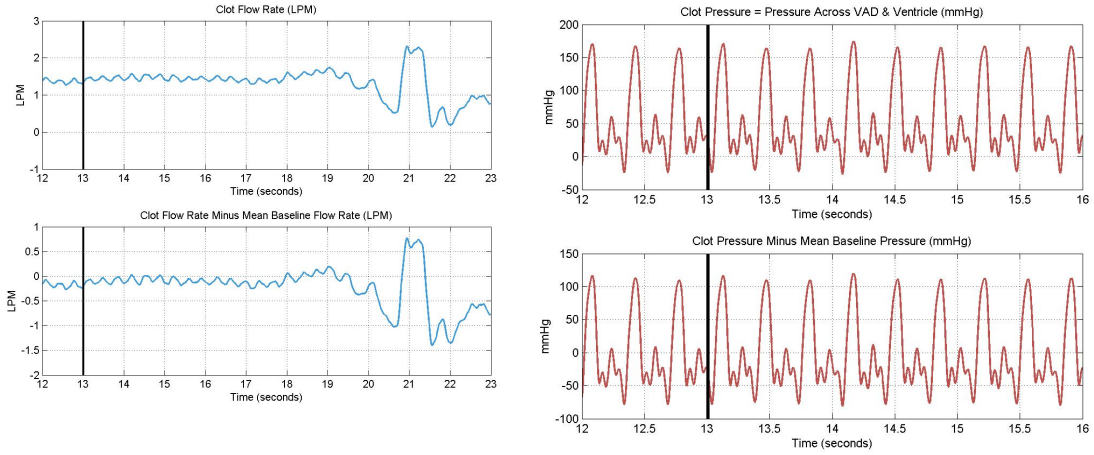

---

22. Experiment 22 (Clot 65)
    a. Experiment Description: Stationary blood clot created from 5mL equine plasma and $CaCl_2$ solution in a glass test tube. Clot was administered to the flow loop. The clot went through the VAD at 13.9 seconds. The fluid within the loop was a water/glycerin mixture. The temperature of the fluid was set to 38°C to simulate normal temperature of equine specimens. The pulsatile pump was set to lower flow rates to simulate heart failure.
    b. Data Collected:
        i. Cassette 1: Specimen within VAD
        ii. Flow and pressure data: Clot 65 take 2

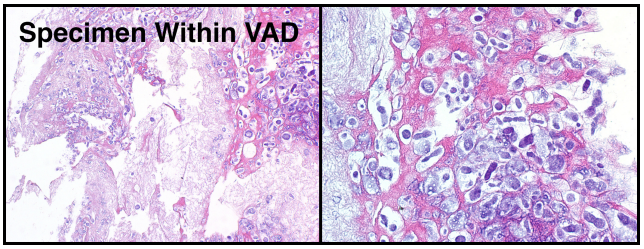

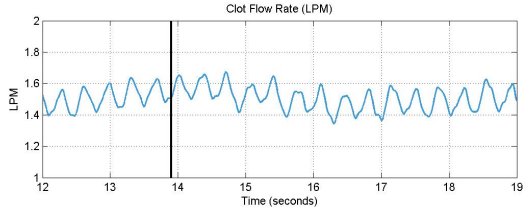
Clot Flow Rate (LPM)
LPM
Time (seconds)

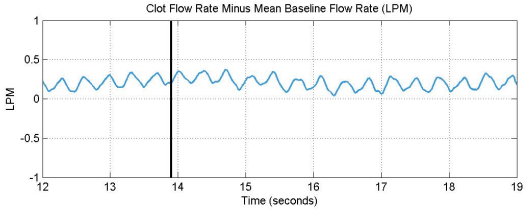
Clot Flow Rate Minus Mean Baseline Flow Rate (LPM)
LPM
Time (seconds)

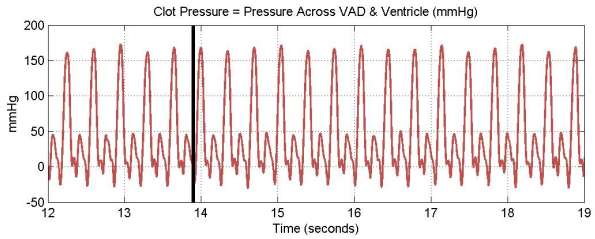
Clot Pressure = Pressure Across VAD & Ventricle (mmHg)
mmHg
Time (seconds)

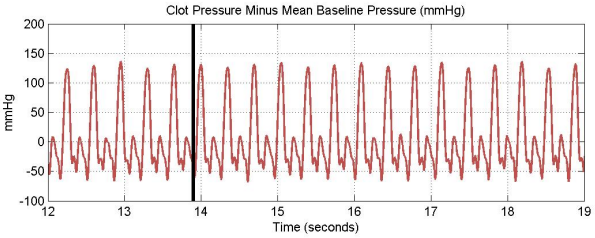
Clot Pressure Minus Mean Baseline Pressure (mmHg)
mmHg
Time (seconds)

Axial Flow Experiments

Axial Flow Mock-VAD Design (used in following experiments):

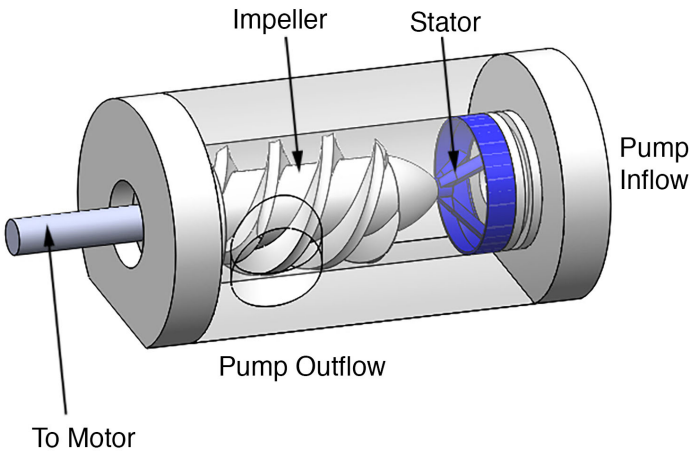

1. Experiment 1 (Axial Test Clot)
    a. Experiment Description: Stationary blood clot created from 5mL of feline packed red blood cells and $CaCl_2$ solution in a glass test tube. Clot was administered to the flow loop approximately 30 days after clot creation. The fluid within the loop was water at room temperature. The pulsatile pump was set to lower flow rates to simulate heart failure.
    b. Data Collected:
        i. Cassette 1: Pieces around stator/bearing/impeller
        ii. Cassette 2: Control

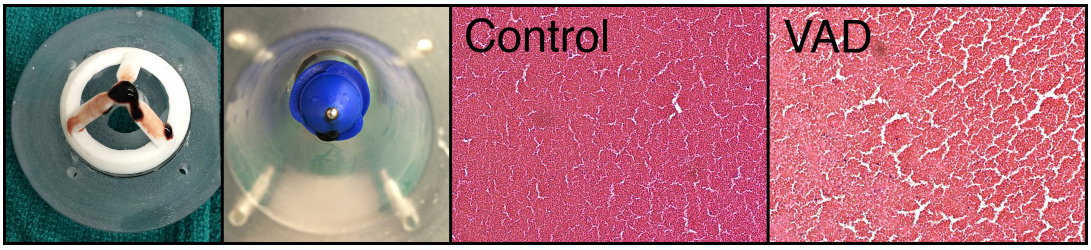

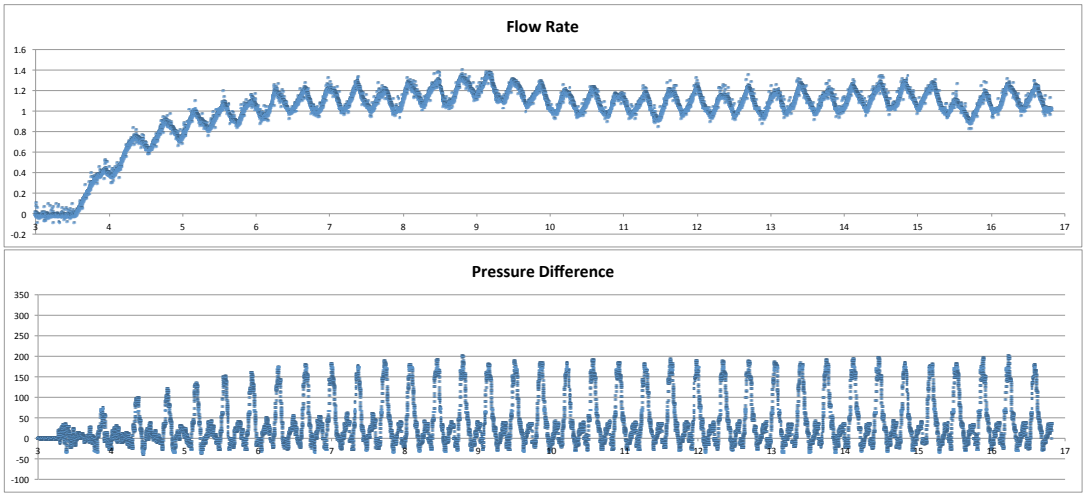

---

2. Experiment 2 (Clot 66)
    a. Experiment Description: Stationary blood clot created from 5mL of gently centrifuged bovine plasma and $CaCl_2$ solution in a glass test tube. Clot was administered to the flow loop approximately 14 days after clot creation. The fluid within the loop was water at room temperature. The pulsatile pump was set to higher flow rates to simulate normal heart function. The clot remained in the stator after it entered the VAD.
    b. Data Collected:
        i. Cassette 1: Control
        ii. Cassette 2: Clot in stator

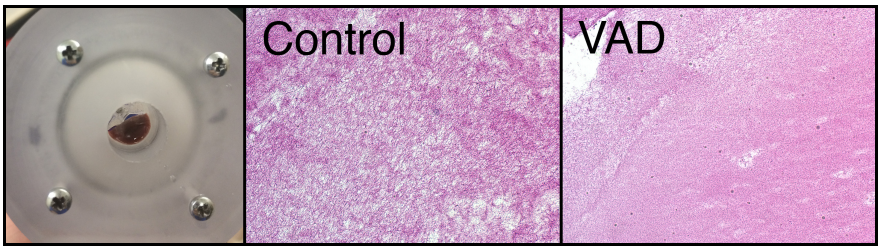

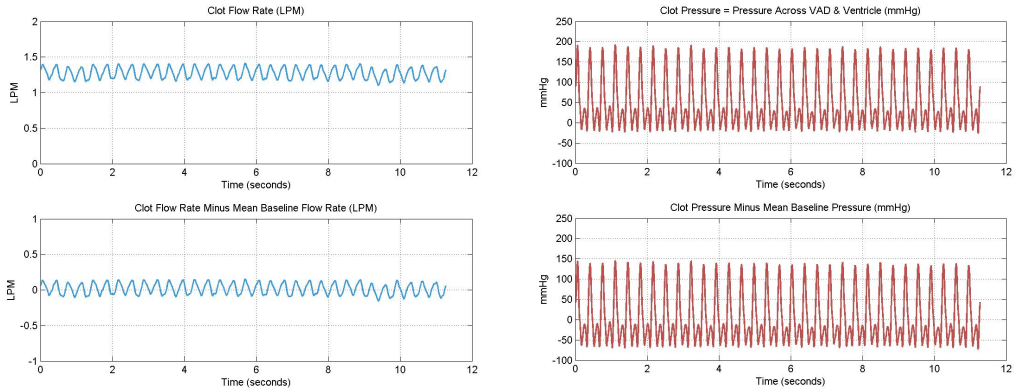

---

3. Experiment 3 (Clot 66)
    a. Experiment Description: Stationary blood clot created from 5mL of gently centrifuged bovine plasma and $CaCl_2$ solution in a glass test tube. Clot was administered to the flow loop approximately 14 days after clot creation. The fluid within the loop was water at room temperature. The pulsatile pump was set to higher flow rates to simulate normal heart function. The clot remained in the stator after it entered the VAD.
    b. Data Collected:
        i. Cassette 3: Clot in stator

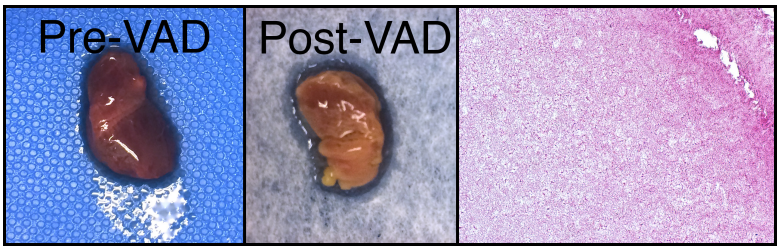

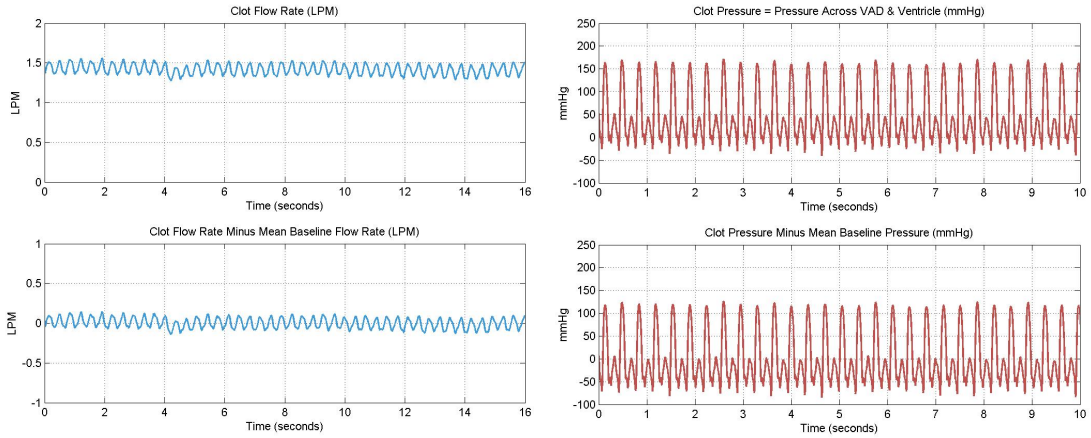

4. Experiment 4 (Clot 67)
    a. Experiment Description: Stationary blood clot created from 5mL of bovine plasma and $CaCl_2$ solution in a glass test tube. Clot was administered to the flow loop approximately 31 days after clot creation. The fluid within the loop was water at room temperature. The pulsatile pump was set to lower flow rates to simulate heart failure. The clot went into the VAD quickly after data collection began.
    b. Data Collected:
        i. Cassette 1: Control
        ii. Cassette 2: Stator/impeller interface material

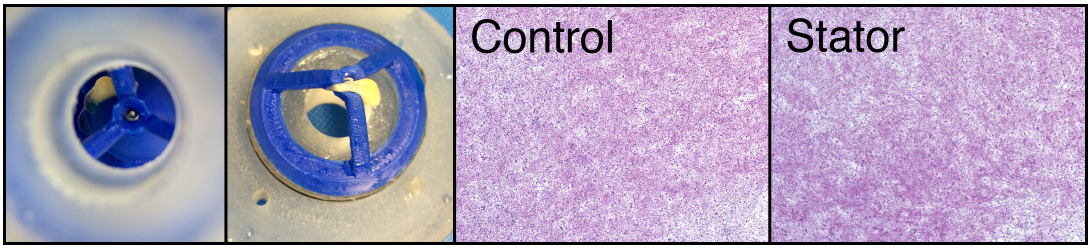

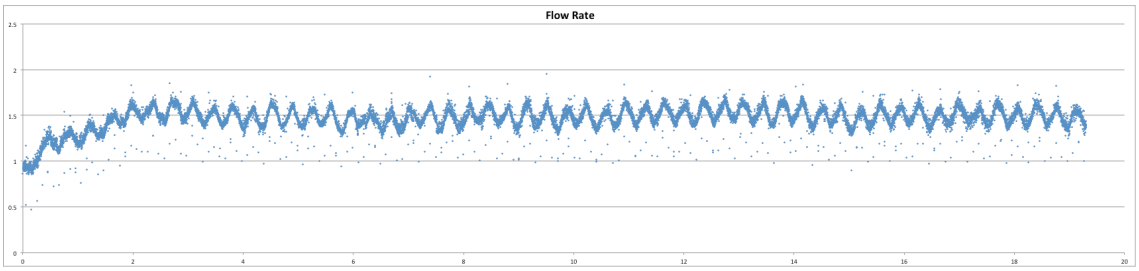

---

5. Experiment 5 (Clot 67)
    a. Experiment Description: Stationary blood clot created from 5mL of bovine plasma and $CaCl_2$ solution in a glass test tube. Clot was administered to the flow loop approximately 35 days after clot creation. The fluid within the loop was water at room temperature. The pulsatile pump was set to higher flow rates to simulate normal heart function. The clot broke into several pieces before entering the VAD.
    b. Data Collected:
        i. Cassette 3: Impeller piece
        ii. Cassette 4: Stator piece

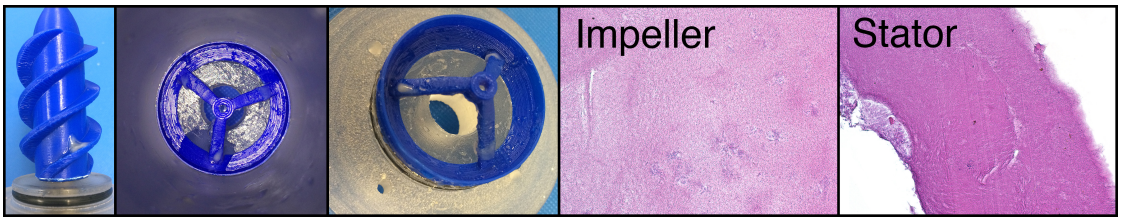

---

6. Experiment 6 (Clot 67)
    a. Experiment Description: Stationary blood clot created from 5mL of bovine plasma and $CaCl_2$ solution in a glass test tube. Clot was administered to the flow loop approximately 35 days after clot creation. The fluid within the loop was water at room temperature. The pulsatile pump was set to higher flow rates to simulate normal heart function. The clot broke into several pieces before entering the VAD.
    b. Data Collected:
        i. Cassette 5: Stator piece

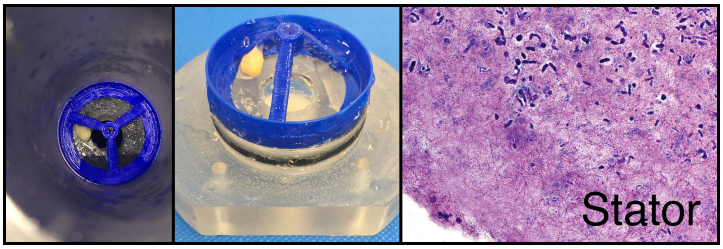

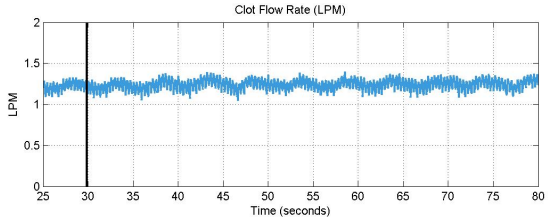

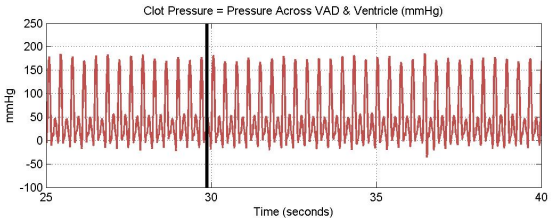

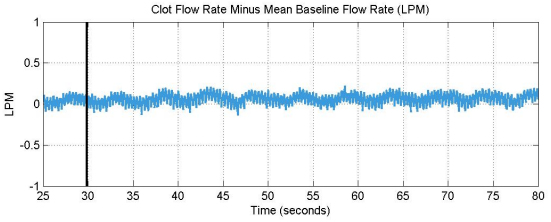

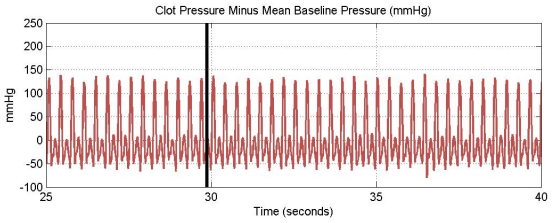

7. Experiment 7 (Clot 68)
    a. Experiment Description: Stationary blood clot created from 5mL of gently centrifuged bovine plasma and $CaCl_2$ solution in a glass test tube. Clot was administered to the flow loop approximately 15 days after clot creation. The fluid within the loop was water at room temperature. The pulsatile pump was set to lower flow rates to simulate heart failure. The clot broke into several pieces that entered the VAD at different times. After clot entered the VAD, there were several floating pieces noticed in the chamber, several pieces collected from the stator arms, and one piece from the stator/bearing ball interface.
    b. Data Collected:
        i. Cassette 1: Multiple small pieces from lower reservoir
        ii. Cassette 2: 2 pieces of silicone sealant with sections of clot
        iii. Cassette 3: ~6 small pieces from top reservoir and 2 larger pieces from stator arms
        iv. Cassette 4: 1 small piece from stator/bearing ball interface

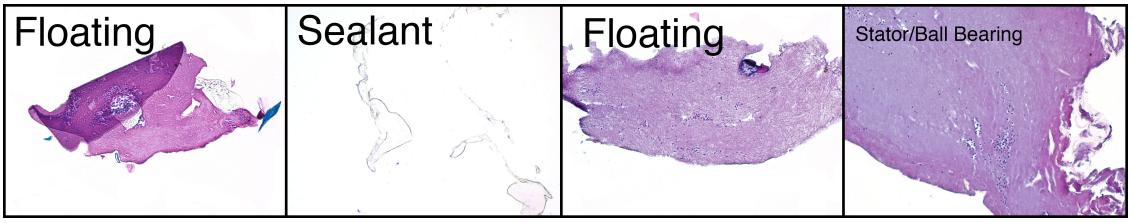

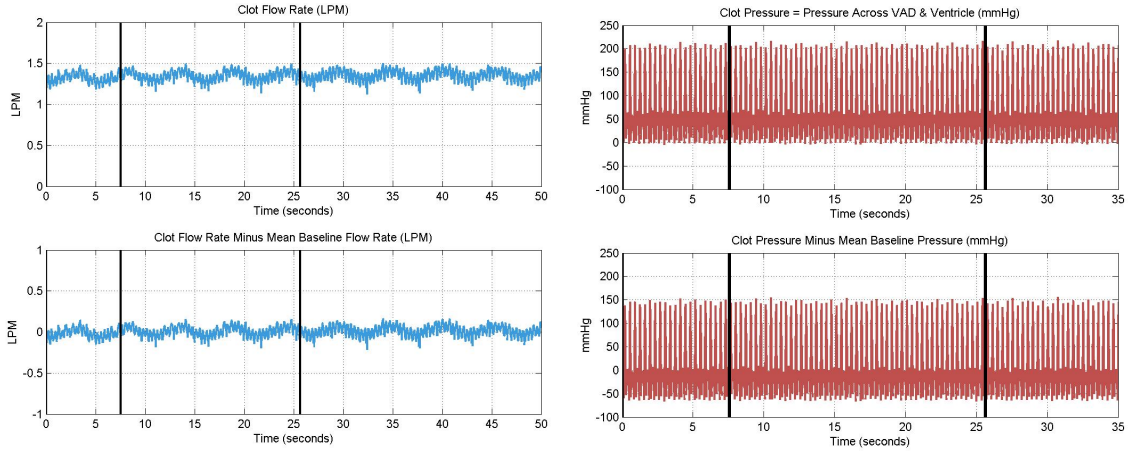

8. Experiment 8 (Clot 68)
    a. Experiment Description: Stationary blood clot created from 5mL of gently centrifuged bovine plasma and $CaCl_2$ solution in a glass test tube. Clot was administered to the flow loop approximately 28 days after clot creation. The fluid within the loop was water at room temperature. The pulsatile pump was set

to higher flow rates to simulate normal heart function. After the VAD and pulsatile pump were turned off, a piece of the clot was noted in floating in the chamber and two small pieces were noted on the stator.

b. Data Collected:
    i. Cassette 5: Control
    ii. Cassette 6: 2 small pieces on stator
    iii. Cassette 7: Large piece in unit (floating)

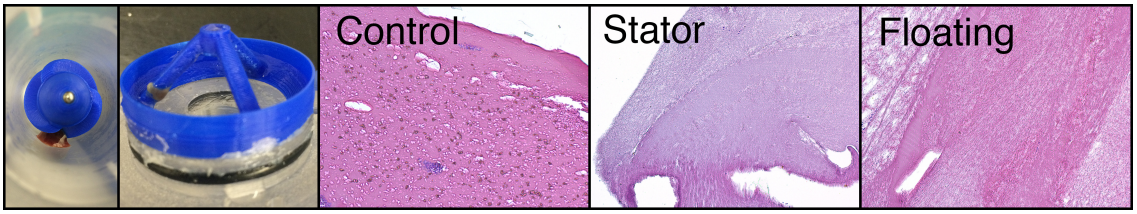

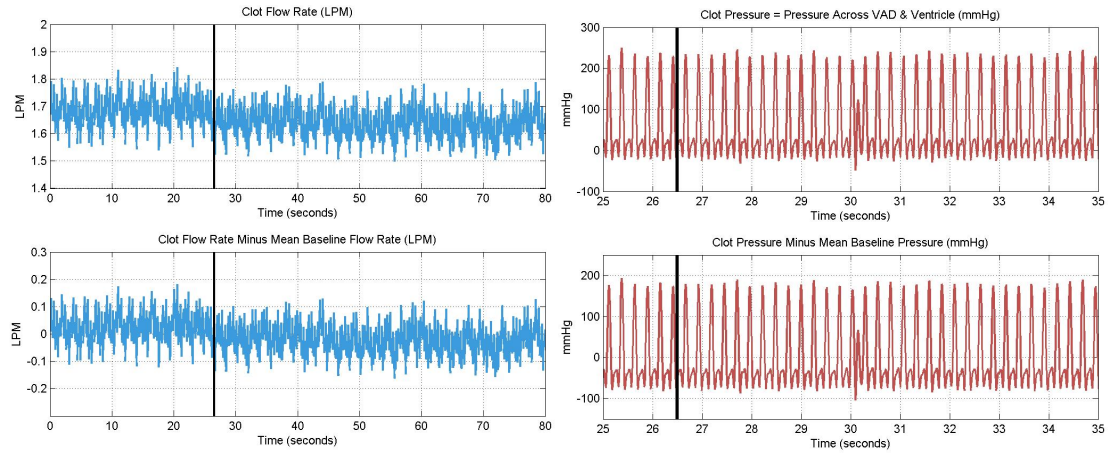

---

9. Experiment 9 (Clot 70)
    a. Experiment Description: Stationary blood clot created from 5mL of bovine plasma and $CaCl_2$ solution in a glass test tube. Clot was administered to the flow loop approximately 56 days after clot creation. The fluid within the loop was a water/glycerin mixture at room temperature. After the VAD and pulsatile pump were turned off, several pieces of the clot were noted floating in the chamber and small pieces were noted on the stator and impeller.
    b. Data Collected:
        i. Cassette 1: Control
        ii. Cassette 2: 11 small pieces, 1 large piece
        iii. Cassette 3: 7 small pieces, 2 medium pieces, 1 large piece

iv. Cassette 4: 1 from bottom of impeller, 2 from stator

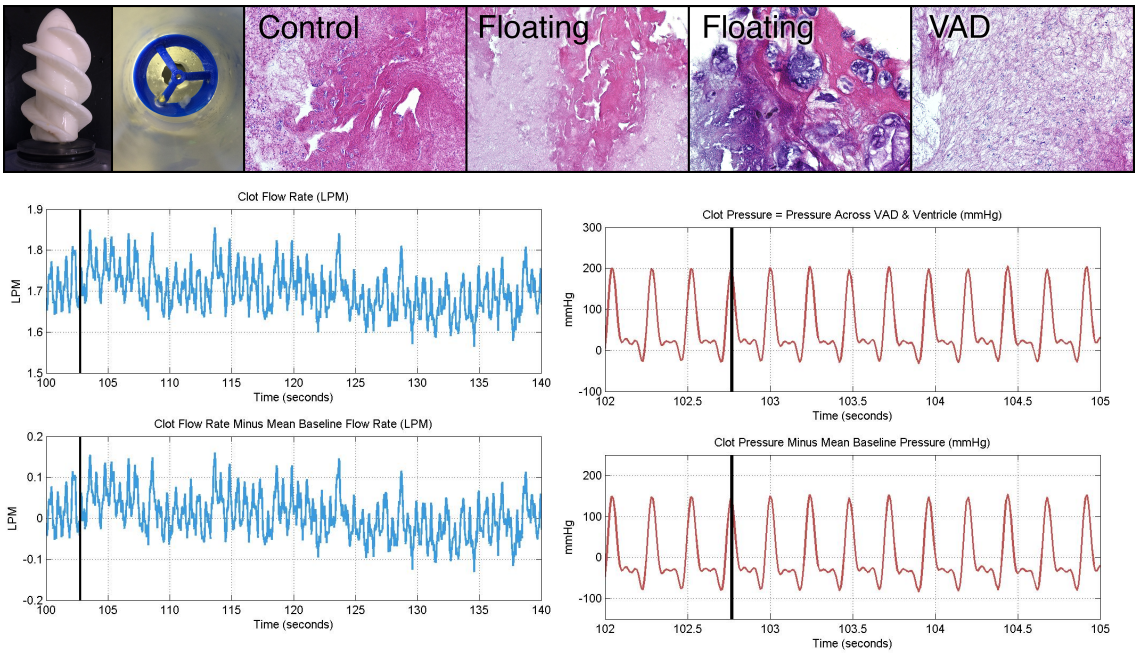

---

10. Experiment 10 (Clot 70)
    a. Experiment Description: Stationary blood clot created from 5mL of bovine plasma and $CaCl_2$ solution in a glass test tube. Clot was administered to the flow loop approximately 70 days after clot creation. The fluid within the loop was a water/glycerin mixture at room temperature. The pulsatile pump was set to lower flow rates to simulate heart failure. After the VAD and pulsatile pump were turned off, one small piece was filtered from the flow loop.
    b. Data Collected:
        i. Cassette 5: Control
        ii. Cassette 6: 1 small filtered piece

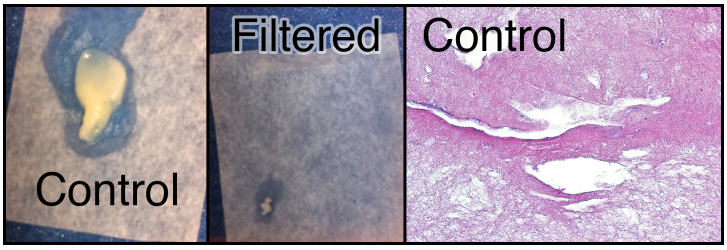

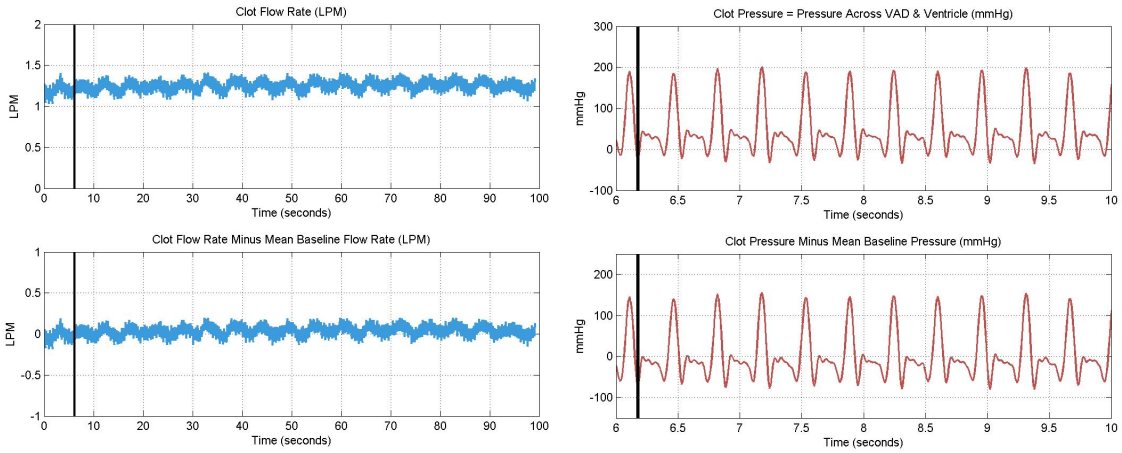

---

11. Experiment 11 (Clot 72)
    a. Experiment Description: Stationary blood clot created from 5mL of bovine plasma and $CaCl_2$ solution in a glass test tube. Clot was administered to the flow loop approximately 56 days after clot creation. The fluid within the loop was a water/glycerin mixture at 43°C. The pulsatile pump was set to higher flow rates to simulate normal heart function. After the VAD and pulsatile pump were turned off, the clot remained on one of the impeller blades.
    b. Data Collected:
        i. Cassette 1: Control
        ii. Cassette 2: Clot from chamber

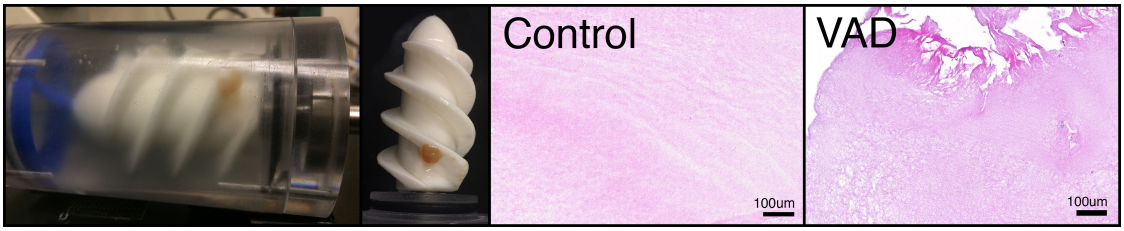

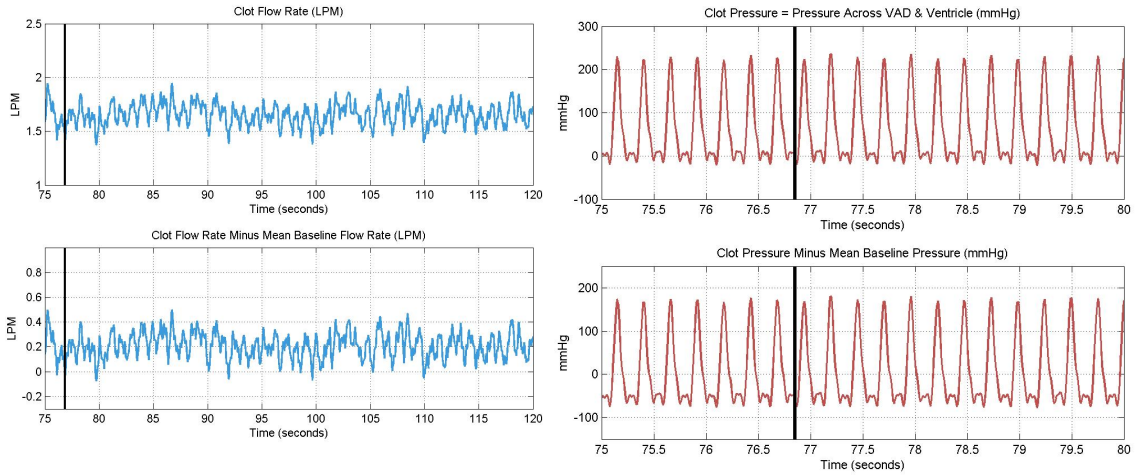

12. Experiment 12 (Clot 72)
    a. Experiment Description: Stationary blood clot created from 5mL of bovine plasma and $CaCl_2$ solution in a glass test tube. Clot was administered to the flow loop approximately 56 days after clot creation. The fluid within the loop was a water/glycerin mixture at 38°C. The pulsatile pump was set to higher flow rates to simulate normal heart function. After the VAD and pulsatile pump were turned off, the clot remained on one of the stator struts.
    b. Data Collected:
        i. Cassette 3: Clot

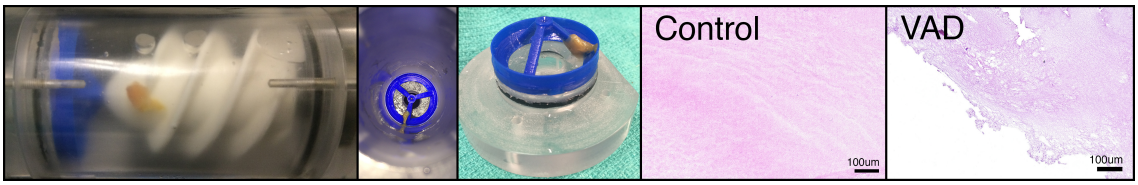

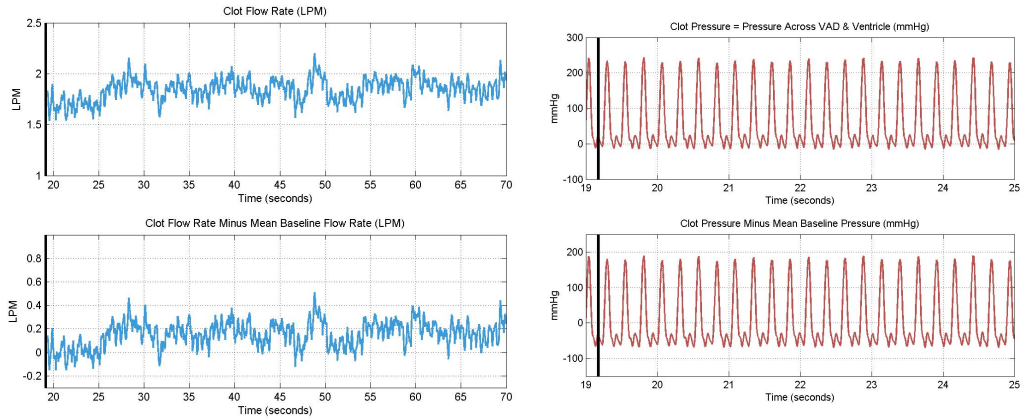

13. Experiment 13 (Clot 73)
    a. Experiment Description: Stationary blood clot created from 5mL of gently centrifuged bovine plasma and $CaCl_2$ solution in a glass test tube. Clot was administered to the flow loop approximately 63 days after clot creation. The fluid within the loop was a water/glycerin mixture at 43°C. The pulsatile pump was set to lower flow rates to simulate heart failure. After the VAD and pulsatile pump were turned off, the clot remained within the VAD casing.
    b. Data Collected:
        i. Cassette 1: Control
        ii. Cassette 2: Clot

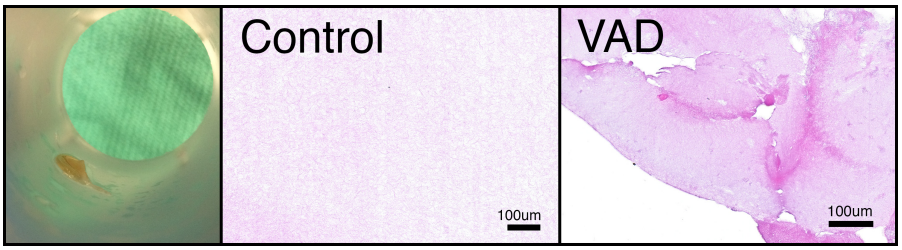

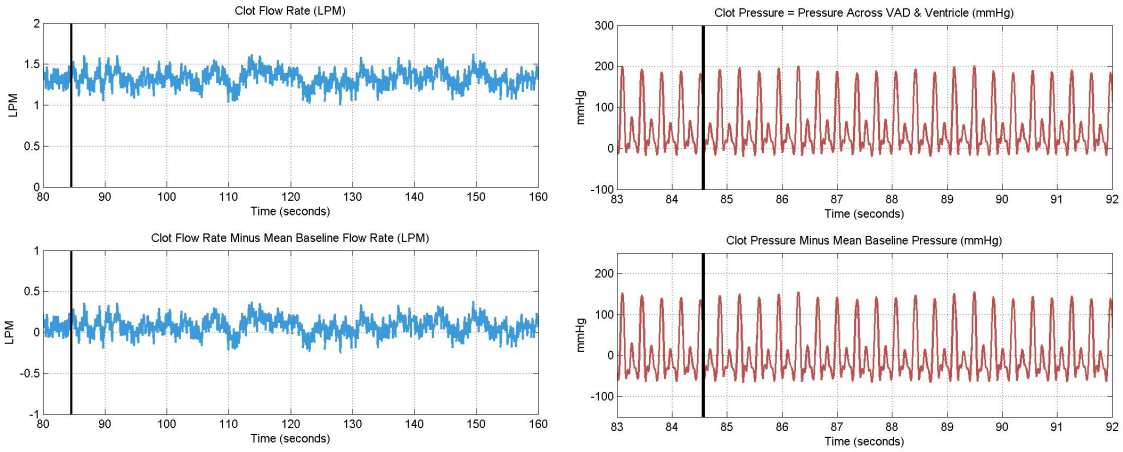

14. Experiment 14 (Clot 73)
    a. Experiment Description: Stationary blood clot created from 5mL of gently centrifuged bovine plasma and $CaCl_2$ solution in a glass test tube. Clot was administered to the flow loop approximately 63 days after clot creation. The fluid within the loop was a water/glycerin mixture at 38°C. The pulsatile pump was set to lower flow rates to simulate heart failure. After the VAD and pulsatile

pump were turned off, the clot had broken into several pieces floating within the fluid and lightly adhered to the casing wall and stator struts.

b. Data Collected:
    i. Cassette 3: Floating pieces
    ii. Cassette 4: 1 small piece from wall, 2 cylindrical pieces from stator